



University
of Glasgow

Hasoo, Manhl (2013) *Regulation of liver X receptors by microRNA-155 in pulmonary fibrosis*. PhD thesis.

<http://theses.gla.ac.uk/4563/>

Copyright and moral rights for this thesis are retained by the author

A copy can be downloaded for personal non-commercial research or study

This thesis cannot be reproduced or quoted extensively from without first obtaining permission in writing from the Author

The content must not be changed in any way or sold commercially in any format or medium without the formal permission of the Author

When referring to this work, full bibliographic details including the author, title, awarding institution and date of the thesis must be given

**Regulation of Liver X Receptors by MicroRNA-155
in pulmonary fibrosis**

Manhl Khuder Hasoo

MSc

**Submitted in fulfilment of the requirements for the
degree of Doctor of Philosophy**

**College of Medicine, Veterinary and Life Sciences
University of Glasgow**

2013

I Abstract

Introduction: Liver X receptors (LXR α and LXR β) are members of the nuclear receptor superfamily of ligand-activated transcription factors that regulate many biological and physiological processes. LXRs are important regulators of cholesterol and lipid metabolism and this is mediated by regulating a wide range of genes such as ABCA1 and ABCG1 that are involved in lipogenesis, cholesterol efflux and absorption, and bile acid synthesis. Since there is a relationship between chronic inflammatory diseases and lipid metabolic dysfunction, the role of LXRs has been investigated in different inflammatory diseases and disease models. Generally, LXRs have an anti-inflammatory effector function, however occasionally pro-inflammatory effects have also been reported.

MicroRNAs (MiRNAs) are small, evolutionary conserved, single-stranded, non-coding RNA molecules with 20- 22 nucleotide base pairs. They regulate mRNA translation by fine tuning the production of proteins involved in the initiation or maintenance of inflammation. MiR-155 is one of the most studied members of miRNAs, and it has a regulatory role in certain inflammatory diseases such as collagen induced arthritis, lung fibrosis, and cardiovascular diseases.

Idiopathic pulmonary fibrosis (IPF) is a devastating inflammatory disease of unknown aetiopathogenesis characterised by progressive breathlessness. IPF is characterised by approximately 50% survival of around 3 years after diagnosis, and there is no effective treatment. The main imperative for pulmonary fibrosis research is to identify potential causal inflammatory and remodelling pathways that contribute to IPF initiation and progression in order to determine possible candidate pathways for therapeutic intervention.

Hypothesis: LXRs play an important role in lipid metabolism and cholesterol homeostasis and because there is a strong relationship between metabolic disease and chronic inflammatory and fibrotic diseases, e.g. LXR agonists may be beneficial for the treatment of RA. We proposed the following hypothesis " Liver X Receptors can modulate bleomycin-induced pulmonary fibrosis and therapeutic intervention with LXR agonists may be beneficial for the treatment of pulmonary fibrosis'.

Methods & Results: Administration of the LXR agonist GW3965 to LXR $\alpha^{-/-}\beta^{-/-}$ or LXR $\alpha\beta$ wild type mice given bleomycin to induce pulmonary fibrosis significantly exacerbated the severity of the disease only in LXR $\alpha\beta$ wild type mice. The worsening of disease was seen as enhanced loss of body weight, increased inflammatory and fibrotic pathomorphological changes in the lung, increased inflammatory cells in the bronchoalveolar lavage, increased concentrations of several pro-inflammatory and pro-fibrotic mediators, and increased expression of genes that regulate inflammation and fibrosis, such as collagen and TGF β , increased lung collagen content, and finally up-regulation of the expression of the alternative activated macrophages (M2) markers arginase 2 and IL-13 receptor.

The effect of the LXR agonist was mediated specifically by LXRs because the severity of disease did not change in $LXR\alpha^{-/-}\beta^{-/-}$ mice given bleomycin and treated with GW3965, nor on similarly treated single $LXR\alpha$ or $LXR\beta$ gene-deleted mice. Furthermore, similar activation of LXRs in primary human or murine fibroblasts demonstrated up-regulation of the expression of collagen. The function of LXR agonist was directly on collagen gene expression and did not require *de novo* protein synthesis as demonstrated by the addition of cycloheximide as a translation inhibitor to murine primary fibroblasts activated with LXR agonist. This suggested that the LXR may have acted directly on the promoter region of the collagen gene. Also I investigated if the collagen genes have response elements for LXR in their promoter regions using a cell reporter system. I demonstrated that the collagen genes have response elements for LXR in their promoter regions.

In a parallel set of experiments, administration of bleomycin or PBS to $miR-155^{-/-}$ and $miR-155$ wild type mice demonstrated a significantly stronger inflammatory and fibrotic process in the $miR-155$ gene-deleted mice. This worsening of disease was seen as an enhanced loss of body weight, increased inflammatory and fibrotic pathomorphological changes in the lung, increased inflammatory cells in the bronchoalveolar lavage, increased concentration of several pro-inflammatory and pro-fibrotic mediators, and increased expression of genes that regulate inflammation and fibrosis; such as collagen and $TGF\beta$, increased lung collagen content, and finally up-regulation of the expression of the alternative activated macrophages (M2) markers arginase 2 and IL-13 receptor. The effect was mediated specifically by $miR-155$ because the severity of disease was increased in $miR-155^{-/-}$ mice compared with $miR-155$ wild type mice given bleomycin. Also no differences were observed in $miR-155^{-/-}$ and $miR-155$ wild type mice given PBS.

Conclusion: My results demonstrate that both the LXR and $miR-155$ have an important impact on the progression and extent of murine pulmonary fibrosis. Since completing the work for this thesis some of my additional pilot work has shown that LXR is a target for $miR-155$ and therefore both may have an important role in lung homeostasis.

My results suggest the therapeutic approaches for IPF might include targeting the LXRs or LXR-regulated pathways, including potential fine tuning levels of $LXR\alpha$ with $miR-155$ antagonists. The aim would be to prevent excessive remodelling. Furthermore, any such therapeutic intervention would need to be done in a very careful way because LXRs are involved in many other physiological processes. Therefore, more targeted therapy perhaps controlling $miR-155$ may be of clinical relevance for therapeutic strategies.

II TABLE OF CONTENTS

I Abstract.....	2
II Table of content.....	4
III List of tables.....	7
IV List of figures.....	8
V Acknowledgements.....	12
VI Author's declaration.....	14
VII Abbreviations.....	15
1. Introduction.....	18
1.1 Nuclear Receptors.....	19
1.1.1 Introduction to nuclear receptors.....	19
1.1.2 Categorisation of nuclear receptors	20
1.1.3 Structure of nuclear receptors.....	21
1.1.4 Liver X Receptors (LXRs).....	22
1.1.4.1 Structure and Function.....	22
1.1.4.2 Liver X Receptor alpha (LXR α).....	23
1.1.4.3 Liver X Receptor beta (LXR β).....	23
1.1.4.4 LXR ligands.....	23
1.1.4.5 LXR regulation and expression.....	26
1.1.5 LXR in physiology, inflammation and disease.....	29
1.1.5.1 The role of LXR in obesity.....	29
1.1.5.2 The role of LXR in atherosclerosis.....	29
1.1.5.3 The role of LXR in inflammation.....	32
1.2 Micro RNA.....	35
1.2.1 Introduction to microRNAs.....	35
1.2.2 MicroRNA expression and function.....	35
1.2.3 MicroRNA biogenesis.....	36
1.2.4 MicroRNA mechanism of action.....	37
1.2.5 MicroRNA-155.....	38
1.2.6 Regulation of immunity and inflammation by miR-155.....	39
1.3 Pulmonary fibrosis.....	42
1.3.1 Introduction: idiopathic pulmonary fibrosis (IPF).....	42
1.3.2 Aetiology of IPF.....	42
1.3.3 Pathogenesis of IPF.....	43
1.3.4 Collagen and pulmonary fibrosis.....	45
1.3.5 Fibroblasts and pulmonary fibrosis.....	46
1.3.6 Pulmonary immune and inflammatory cells in the lung.....	48
1.3.7 Inflammatory mediators in IPF.....	49
1.3.8 Symptoms and Diagnosis.....	50
1.3.9 Treatment.....	51
1.3.10 Animal models of pulmonary fibrosis.....	52
1.3.11 IPF: The clinical unmet need.....	54
1.4 Hypothesis and Aims.....	55
2. Materials and Methods.....	56
2.1 General materials.....	57
2.2 General buffers and reagents.....	57
2.3 <i>In vivo</i> work.....	58
2.3.1 Animal housing.....	58
2.3.2 Mice.....	58
2.3.3 Administration of PBS or bleomycin in C57BL/6 mice.....	59
2.3.4 Administration of different doses of LXR agonist GW3965 or vehicle Cremophor in C57BL/6 mice given bleomycin.....	60

2.3.5	Experimental detail of bleomycin-induced pulmonary fibrosis in LXR $\alpha^{-/-}$ $\beta^{-/-}$ double knockout and LXR $\alpha\beta$ wild-type mice.....	60
2.3.6	Experimental detail of bleomycin-induced pulmonary fibrosis in LXR $\alpha^{-/-}$ knockout and LXR $\beta^{-/-}$ knockout mice.....	61
2.3.7	Experimental detail of bleomycin-induced pulmonary fibrosis in MicroRNA-155 $^{-/-}$ and MicroRNA-155 wild-type mice.....	62
2.3.8	Clinical observation of mice.....	62
2.4	Cytological evaluation of bronchoalveolar lavage.....	62
2.5	Lung tissue preparation.....	63
2.5.1	Preparation of lungs for histology.....	63
2.5.1.1	Tissue processing, embedding and sectioning.....	63
2.5.1.2	Haematoxylin and Eosin staining (H&E).....	64
2.5.1.3	Gomori's Trichrome stain.....	65
2.5.2	Histological evaluation of lung inflammation and fibrosis.....	66
2.6	Measurement of total lung collagen.....	68
2.7	Serum and bronchoalveolar lavage fluid analysis.....	69
2.7.1	Measurement of cytokines using a Luminex multiplex assay.....	69
2.7.2	TGF- β 1 ELISA assay.....	70
2.8	Investigation of gene expression.....	72
2.8.1	Extraction of RNA from tissue.....	72
2.8.1.1	TRIZOL homogenization for tissue.....	72
2.8.1.2	RNA extraction from cells.....	72
2.8.2	Complementary DNA (cDNA) synthesis.....	73
2.8.3	SYBR Green reverse transcriptase-polymerase chain reaction (QRT-PCR).....	75
2.9	<i>In vitro</i> work.....	76
2.9.1	Generation of murine fibroblast cell lines.....	76
2.9.2	Generation of primary human fibroblast line.....	76
2.9.3	Fibroblast stimulation with LXR agonist.....	77
2.9.4	Fibroblast stimulation with LXR agonist and cyclohexamide.....	77
2.10	Promoter analysis of murine collagens 1 and 3.....	77
2.10.1	<i>In silico</i> analysis of murine collagens 1 and 3.....	77
2.10.2	Amplification of putative LXR/RXR binding sites.....	78
2.10.3	Agarose gel electrophoresis.....	79
2.10.4	Cloning of PCR amplified DNA fragments.....	79
2.10.4.1	TOPO cloning PCR products.....	79
2.10.4.2	DNA transformation into competent <i>E.coli</i>	80
2.10.4.3	Plasmid DNA purification.....	81
2.10.4.4	Restriction endonuclease digestion of plasmid DNA.....	82
2.10.4.5	Gel purification of DNA fragments from agarose gel.....	82
2.10.4.6	DNA ligation.....	82
2.10.5	Construction of pGL3-promoter plasmids.....	83
2.10.6	Cell transfection.....	84
2.10.7	Luciferase reporter assay.....	84
2.11	Statistical analysis.....	85
3.	Results and discussion.....	86
3.1	Relationship between activation of Liver X Receptor and pulmonary fibrosis in a murine pulmonary fibrosis model.....	89
3.1.1	Introduction and Aims.....	89
3.1.	Justification of the bleomycin-induced pulmonary fibrosis model <i>in vivo</i>	90
3.1.2.1	The time course of bleomycin-induced inflammation suggests	

maximum inflammatory and fibrotic changes at day 18 after administration.....	90
3.1.2.2 Selection of the dose of LXR agonist (GW3965) required to investigate its role in the severity of the murine model of bleomycin-induced pulmonary fibrosis.....	98
3.1.2.3 Treatment with LXR agonist (GW3965) had no effects on C57BL/6 mice given PBS.....	104
3.1.2.4 Validation of LXR agonist function on LXR $\alpha^{-/-}\beta^{-/-}$ mice....	110
3.1.3 Discussion and Conclusion.....	112
3.2 Exacerbation of pulmonary fibrosis is associated with the activation of Liver X Receptor.....	117.
3.2.1 Introduction and Aims.....	117
3.2.2 LXR $\alpha^{-/-}\beta^{-/-}$ double knockout mice.....	117
3.2.3 LXR $\alpha^{-/-}\beta^{-/-}$ mice develop less bleomycin-induced pulmonary fibrosis than LXR $\alpha\beta$ wild type mice; both given LXR agonist (GW3965) .	118
3.2.3.1 Specific effect of LXR agonist in LXR $\alpha\beta$ but not LXR $\alpha^{-/-}\beta^{-/-}$ mice in murine bleomycin-induced pulmonary fibrosis.....	119
3.2.3.2 Mechanisms of LXR involvement in fibrosis.....	131
3.2.3.2.1 LXR modulation of macrophage phenotype.....	131
3.2.3.2.2 LXR modulation of fibroblast function.....	132
3.2.3.2.3 LXR directly targets collagen type I and III expression in murine fibroblast.....	134
3.2.3.2.4 Activation of LXR directly targets the promoters of collagen type I and III in the murine fibroblast cell line T1317.....	135
3.2.4 Discussion and Conclusion.....	137
3.3 Requirement of LXRα and LXRβ for fibrosis-enhancing effects of the LXR agonist.....	142
3.3.1 Introduction and Aims.....	142
3.3.2 LXR $\alpha^{-/-}$ and LXR $\beta^{-/-}$ mice.....	143
3.3.3 LXR activation had no effect on the augmentation of bleomycin induced pulmonary fibrosis in single LXR $\alpha^{-/-}$ or LXR $\beta^{-/-}$ mice compared with wild-type mice.....	143
3.3.4 Discussion and Conclusion.....	155
3.4 Potential involvement of MicroRNA-155 in the development of pulmonary fibrosis in a murine model.....	158
3.4.1 Introduction and Aims.....	158
3.4.2 MiR-155 $^{-/-}$ mice develop worse bleomycin-induced pulmonary fibrosis in comparison with miR-155 wild type mice.....	158
3.4.3 The macrophages in the miR-155 $^{-/-}$ mice had a different phenotype compared with the wild-type littermates; both given bleomycin.....	170
3.4.4 Discussion and conclusion.....	172
3.5 General Discussion and Conclusion.....	175
VIII References.....	183
IX Publications.....	196

III List of tables

Table 2.1 Typical samples collected on a cull day.....	60
Table 2.2 Illustrative examples of the lung inflammation used to describe a scoring system for assessing inflammatory changes associated with murine bleomycin-induced pulmonary fibroses.....	67
Table 2.3 Illustrative examples of the lung fibrosis used to describe a scoring system for assessing changes associated with murine bleomycin-induced pulmonary fibroses.....	68
Table 2.4 Protocol for activation of latent form of mouse TGF- β 1 in the serum and bronchoalveolar lavage to enable their measurement.....	71
Table 2.5 Primers Used for Real-Time qPCR.....	76
Table 2.6 Amplification products were examined by agarose gel electrophoresis.....	78
Table 2.7 Primers used for producing PCR gene products.....	79
Table 2.8 Recipe for 50x TAE buffer.....	79
Table 2.9 DNA ligation components.....	83
Table 3.1 Mice number for the optimisation of the course length of the bleomycin-induced pulmonary fibrosis model in C57BL/6 mice.....	91
Table 3.2 Inflammatory and fibrotic mediators in the serum of WT and LXR $\alpha^{-/-}\beta^{-/-}$ mice given bleomycin and treated with LXR agonist or vehicle.....	127
Table 3.3 Inflammatory and fibrotic mediators in the BAL of WT and LXR $\alpha^{-/-}\beta^{-/-}$ mice given bleomycin and treated with LXR agonist or vehicle.....	128
Table 3.4 Inflammatory and fibrotic mediators in the serum of WT, LXR $\alpha^{-/-}$ and LXR $\beta^{-/-}$ mice given bleomycin and treated with either LXR agonist or vehicle.....	151
Table 3.5 Inflammatory and fibrotic mediators in the BAL of WT, LXR $\alpha^{-/-}$ and LXR $\beta^{-/-}$ mice given bleomycin and treated with either LXR agonist or vehicle.....	152
Table 3.6 Inflammatory and fibrotic mediators in the serum of miR-155 $^{-/-}$ and WT mice given PBS or bleomycin.....	166
Table 3.7 Inflammatory and fibrotic mediators in the BAL of miR-155 $^{-/-}$ and WT mice given PBS or bleomycin.....	167

IV List of figures

Figure 1.1 Activation of the nuclear receptor LXR by natural and synthetic agonists.....	20
Figure 1.2 Human nuclear receptor superfamily classification, the classification depends on their physiological ligands and potential functions.....	21
Figure 1.3 General structure of a putative nuclear receptor.....	22
Figure 1.4 Structures of cholesterol and most common oxysterols.....	24
Figure 1.5 Regulation and transcription of LXR.....	28
Figure 1.6 Regulation of ABCA1 gene expression and cholesterol efflux by LXR as result of lipid loading.....	30
Figure 1.7 Mechanisms involved in antidiabetic effect of LXR agonists.....	33
Figure 1.8 The biogenesis of miRNAs.....	37
Figure 1.9 MiRNA biogenesis pathway and mechanisms of action.....	38
Figure 1.10 Stages of the wound healing process.....	45
Figure 1.11 Main components involved in the IPF pathogenesis.....	45
Figure 1.12 Main cells involve in pulmonary fibrosis.....	47
Figure 1.13 Major pro-inflammatory and pro-fibrotic mediators that participate in fibrosis.....	50
Figure 2.1 Map of pCR2.1 TOPO.....	80
Figure 2.2 pGL3-promoter plasmid.....	83
Figure 2.3 Cell transfection pRL-TK.....	84
Figure 3.1 Experimental timeline for the optimisation of the time course of the bleomycin –induced pulmonary fibrosis model in C57BL/6 mice.....	91
Figure 3.2 Daily body weight changes in mice given bleomycin or PBS.....	92
Figure 3.3 Histological inflammatory and fibrotic changes in the lung of mice given bleomycin or PBS.....	93
Figure 3.4 Lung inflammation score of the mice given bleomycin or PBS.....	94
Figure 3.5 Lung fibrosis score of the mice given bleomycin or PBS.....	94
Figure 3.6 Total BAL cell count in the BAL of mice given bleomycin or PBS.....	95
Figure 3.7 Macrophage cell count in the BAL of mice given bleomycin or PBS....	96
Figure 3.8 Lymphocyte cell count in the BAL of mice given bleomycin or PBS....	97
Figure 3.9 Daily body weight changes in mice given bleomycin and treated with different concentration doses of LXR agonist or vehicle.....	99
Figure 3.10 Histological inflammatory and fibrotic changes in the lung of mice given bleomycin and treated with different concentration doses of LXR agonist or vehicle.....	100
Figure 3.11 Lung inflammation score of the mice given bleomycin and treated with different concentration doses of LXR agonist or vehicle.....	101
Figure 3.12 Lung fibrosis score of the mice given bleomycin and treated with different concentration doses of LXR agonist or vehicle.....	101
Figure 3.13 Total BAL cell count in the BAL of mice given bleomycin and treated with different concentration doses of LXR agonist or vehicle.....	102
Figure 3.14 Macrophage cell count in the BAL of mice given bleomycin and treated with different concentration doses of LXR agonist or vehicle.....	103

Figure 3.15 Lymphocyte cell count in the BAL of mice given bleomycin and treated with different concentration doses of LXR agonist or vehicle.....	104
Figure 3.16 Daily body weight changes in mice given PBS and treated with different concentration doses of LXR agonist or vehicle.....	105
Figure 3.17 Histological inflammatory and fibrotic changes in the lung of mice given PBS and treated with different concentration doses of LXR agonist or vehicle.....	106
Figure 3.18 Lung inflammation score of mice given PBS and treated with different concentration doses of LXR agonist or vehicle.....	107
Figure 3.19 Lung fibrosis score of mice given PBS and treated with different concentration doses of LXR agonist or vehicle.....	107
Figure 3.20 Total BAL cell count in the BAL of mice given PBS and treated with different concentration doses of LXR agonist or vehicle.....	108
Figure 3.21 Macrophage cell count in the BAL of mice given PBS and treated with different concentration doses of LXR agonist or vehicle.....	109
Figure 3.22 Lymphocyte cell count in the BAL of mice given PBS and treated with different concentration doses of LXR agonist or vehicle.....	110
Figure 3.23 ABCA1, LXR α , and LXR β gene expression in lung of mice treated with vehicle or LXR agonist.....	111
Figure 3.24 Daily body weights changes in WT and LXR $\alpha^{-/-}\beta^{-/-}$ mice given bleomycin and treated with either LXR agonist or vehicle.....	119
Figure 3.25 Histological inflammatory and fibrotic changes in the lung of WT and LXR $\alpha^{-/-}\beta^{-/-}$ mice given bleomycin and treated with LXR agonist or vehicle.....	121
Figure 3.26 Lung inflammation score of WT and LXR $\alpha^{-/-}\beta^{-/-}$ mice given bleomycin and treated with LXR agonist or vehicle.....	122
Figure 3.27 Lung fibrosis score of WT and LXR $\alpha^{-/-}\beta^{-/-}$ mice given bleomycin and treated with LXR agonist or vehicle.....	122
Figure 3.28 Total BAL cell count in the BAL of WT and LXR $\alpha^{-/-}\beta^{-/-}$ mice given bleomycin and treated with LXR agonist or vehicle.....	123
Figure 3.29 Macrophage cell count in the BAL of WT and LXR $\alpha^{-/-}\beta^{-/-}$ mice given bleomycin and treated with LXR agonist or vehicle.....	124
Figure 3.30 Lymphocyte cell count in the BAL of WT and LXR $\alpha^{-/-}\beta^{-/-}$ mice given bleomycin and treated with LXR agonist or vehicle.....	125
Figure 3.31 Neutrophil cell count in the BAL of WT and LXR $\alpha^{-/-}\beta^{-/-}$ mice given bleomycin and treated with LXR agonist or vehicle.....	126
Figure 3.32 TGF β 1 gene expression in lung of WT and LXR $\alpha^{-/-}\beta^{-/-}$ mice given bleomycin and treated with LXR agonist or vehicle.....	129
Figure 3.33 Collagen gene expression in lung of WT and LXR $\alpha^{-/-}\beta^{-/-}$ mice given bleomycin and treated with LXR agonist or vehicle.....	130
Figure 3.34 Soluble collagen content in lungs of WT and LXR $\alpha^{-/-}\beta^{-/-}$ mice given bleomycin and treated with LXR agonist or vehicle.....	131
Figure 3.35 Expression levels of macrophage phenotype markers in the lungs of WT and LXR $\alpha^{-/-}\beta^{-/-}$ mice given bleomycin and treated with LXR agonist or vehicle.....	132
Figure 3.36 Collagen gene expression in primary mouse lung fibroblasts from WT	

and LXR $\alpha^{-/-}\beta^{-/-}$ mice given bleomycin and treated with LXR agonist or vehicle...	133
Figure 3.37 Collagen gene expression in primary human fibroblast treated with LXR agonist or vehicle.....	134
Figure 3.38 LXR agonist directly increased collagen gene expression in primary mouse lung fibroblasts.....	135
Figure 3.39 The effect of LXR agonist on luciferase activity indicating collagen gene expression in transfected mouse primary fibroblasts.....	136
Figure 3.40 Daily body weight changes in WT, LXR $\alpha^{-/-}$ and LXR $\beta^{-/-}$ mice given bleomycin and treated with either LXR agonist or vehicle.....	144
Figure 3.41 Histological inflammatory and fibrotic changes in the lung of the WT, LXR $\alpha^{-/-}$ and LXR $\beta^{-/-}$ mice given bleomycin and treated with either LXR agonist or vehicle.....	145
Figure 3.42 Lung inflammation score of the WT, LXR $\alpha^{-/-}$ and LXR $\beta^{-/-}$ mice given bleomycin and treated with either LXR agonist or vehicle.....	146
Figure 3.43 Lung fibrosis score of the WT, LXR $\alpha^{-/-}$ and LXR $\beta^{-/-}$ mice given bleomycin and treated with either LXR agonist or vehicle.....	147
Figure 3.44 Total BAL cell count in the BAL of WT, LXR $\alpha^{-/-}$ and LXR $\beta^{-/-}$ mice given bleomycin and treated with either LXR agonist or vehicle.....	148
Figure 3.45 Macrophage cell count in the BAL of WT, LXR $\alpha^{-/-}$ and LXR $\beta^{-/-}$ mice given bleomycin and treated with either LXR agonist or vehicle.....	149
Figure 3.46 Lymphocyte cell count in the BAL of WT, LXR $\alpha^{-/-}$ and LXR $\beta^{-/-}$ mice given bleomycin and treated with either LXR agonist or vehicle.....	150
Figure 3.47 TGF β 1 gene expression in lungs of WT, LXR $\alpha^{-/-}$ and LXR $\beta^{-/-}$ mice given bleomycin and treated with either LXR agonist or vehicle.....	153
Figure 3.48 Collagen gene expression in lungs of WT, LXR $\alpha^{-/-}$ and LXR $\beta^{-/-}$ mice given bleomycin and treated with either LXR agonist or vehicle.....	153
Figure 3.49 Soluble collagen content in lungs of WT, LXR $\alpha^{-/-}$ and LXR $\beta^{-/-}$ mice given bleomycin and treated with either LXR agonist or vehicle.....	154
Figure 3.50 Daily body weights changes for miR-155 $^{-/-}$ and miR-155 wild type mice given PBS or bleomycin.....	159
Figure 3.51 Histological inflammatory and fibrotic changes in the lung of the lung of miR-155 $^{-/-}$ and miR-155 wild type mice given PBS or bleomycin.....	161
Figure 3.52 Lung inflammation score of the miR-155 $^{-/-}$ and miR-155 wild type mice given PBS or bleomycin.....	162
Figure 3.53 Lung fibrosis score of the miR-155 $^{-/-}$ and miR-155 wild type mice given PBS or bleomycin.....	162
Figure 3.54 Total BAL cell count in the BAL of miR-155 $^{-/-}$ and miR-155 wild type mice given PBS or bleomycin.....	163
Figure 3.55 Macrophage cell count in the BAL of miR-155 $^{-/-}$ and miR-155 wild type mice given PBS or bleomycin.....	164
Figure 3.56 Lymphocyte cell count in the BAL of miR-155 $^{-/-}$ and miR-155 wild type mice given PBS or bleomycin.....	165
Figure 3.57 TGF β 1 gene expression in lungs of miR-155 $^{-/-}$ and miR-155 wild type mice given PBS or bleomycin.....	168
Figure 3.58 Collagen gene expression in lungs of miR-155 $^{-/-}$ and miR-155 wild type	

mice given PBS or bleomycin.....	169
Figure 3.59 Soluble collagen content in lungs of miR-155 ^{-/-} and miR-155 wild type mice given PBS or bleomycin.....	170
Figure 3.60 Expression levels of macrophage phenotype markers in the lungs of miR-155 ^{-/-} and miR-155 wild type mice given PBS or bleomycin.....	171

V Acknowledgements

PhD research often appears a solitary undertaking. However, it is impossible to maintain the degree of focus and dedication required for its completion without the help and support of many people.

First I would like to thank Professor Iain McInnes and Dr Charles McSharry for being my supervisors and for their help and support through my time as a PhD student and for that I am extremely grateful.

Professor Iain McInnes has provided much support and has allowed me to join his group to develop my career. He is an inspiring clinical and scientific mentor and has always tried to help developing my career in the best possible ways.

Dr Charles McSharry has given invaluable support and patience throughout my time as a PhD student. Without his constructive critiques and recommendations, this thesis would not have been the same.

I think I can honestly say through all the ups and downs, scientific and otherwise, I have never regretted the decision to embark on a PhD (or not much anyway!). This is almost entirely due to the people I've met along the way.

This thesis would not have been possible without the help and support from my laboratory and clinical colleagues. There were always plenty of people ready and willing to give advice and support.

Dr Derek Gilchrist has been a source of wealth of knowledge in molecular biology. I am grateful for his patience in teaching me all the techniques that I needed to conduct my molecular work.

Dr Mariola Kurowska-Stolarska has always been enthusiastic about my study and has provided scientific input through the course of my PhD. She also provided the miR-155^{-/-} mice.

Dr Darren Asquith for his guidance throughout beginning of my study. Also for his kindness of generating of LXR α ^{-/-} β ^{-/-} mice which was a great help.

Dr Neil Millar for his support and donating of human fibroblast.

Jim Riley, Shauna Kerr, and Ashley Gilmour for making me feel welcome and assisting me in different ways within the laboratory.

Dr Mousa Komai-Koma for his invaluable support and advice throughout this study and during the whole time that I was doing my PhD study.

I would like to thank all previous and current members in the CRD lab group for their continuous support and encouraging since the beginning of my career and who were always a great advice.

I would like to thank the staff at the University of Glasgow's Biological services, especially Maurice Dixon who have all been a great help and support.

I gratefully acknowledge the funding sources that made my PhD work possible. I was funded by the Iraqi Ministry of Higher Education and Scientific Research.

Special thanks also to my family, I am grateful to my parents who have loved me unconditionally and believed in me always and to God the voice in my head urging me on and keeping me focused.

VI Author's declaration

I declare that, except where referenced to others, this thesis is the product of my own work and has not been submitted for any other degree at the University of Glasgow or any other institution.

Signature _____

Printed name ____Manhl Khuder Hasoo__

VII Abbreviations

ABCA1	ATP Binding Cassette A1
AF1/2	Activation Function Domains1/2
APO	Apolipoprotein
AR	Androgen Receptor
Arg2	Arginase 2
BAL	Bronchoalveolar lavage
BIC	B-cell Integration Cluster
COX	Cyclooxygenase
CTE	Constitutive Transport Element
CYP7A1	Cholesterol 7 α -hydroxylase A1
DBD	DNA-Binding Domain
DEPC	Diethyl Pyrocarbonate
ECM	Extracellular Matrix
FCS	Foetal Calf Serum
FGF basic	Basic Fibroblast Growth Factor
GM-CSF	Granulocyte Macrophage Colony-Stimulating Factor
GR	Glucocorticoid Receptor
HRCT	High-Resolution Computed Tomography
HDL	High Density Lipoproteins
IPF	Idiopathic Pulmonary Fibrosis
IL	Interleukin
iNOS	Inducible Nitric Oxide Synthase
LBD	Ligand Binding Domain
LPS	Lipopolysaccharide
LXR	Liver X Receptor
LDL	Low Density Lipoprotein

LXRE	LXR Response Element
MCSF	Macrophage Colony Stimulating Factor
MIP	Macrophage Inhibitory Protein
MCP	Monocyte Chemotactic Protein
MMP	Matrix Metalloproteinase
miRNA	MicroRNA
miRISC	MiRNA-Induced Silencing Complex
MR	Mineralocorticoid Receptor
NF- κ B	Nuclear Factor kappa-light-chain-enhancer of activated B cells
NR	Nuclear Receptor
PLTP	Phospholipid Transfer Protein
PDGF-A	Platelet-Derived Growth Factor-A
PPAR	Peroxisome Proliferator-Activated Receptor
PR	Progesterone Receptor
RA	Rheumatoid Arthritis
RLD-1	Rat Liver Digest extract 1
RXR	Retinoid X Receptor
SMA	Smooth Muscle Actin
SHIP1	Src Homology-2 domain-containing Inositol 5- Phosphatase 1
SREBP-1c	Sterol Regulatory Element-Binding Protein 1c
TBP	TATA Binding Protein
TLR4	Toll Like Receptor 4
TMB	Tetramethylbenzidine
TNF α	Tumour Necrosis Factor α
UR	Ubiquitous Receptor
UTR	Untranslated Rregion

VEGF

Vascular Endothelial Growth Factor

1. Introduction

1.1 Nuclear Receptors

1.1.1 Introduction to nuclear receptors

Nuclear receptors (NRs) are a family of ligand-activated transcription factors that regulate many biological and physiological processes, including lipid and glucose metabolism and homeostasis, drug detoxification, cellular differentiation, inflammation, fibrosis, regeneration, embryonic development and organ physiology [1, 2]. There are currently about 48 nuclear receptors described in humans [2, 3], and 49 in mice [3].

Nuclear receptors are characterised by their ability to act as initiators of gene transcription by binding to their response elements which are located in the promoters of appropriate genes. Nuclear receptors can act as monomers, or can assemble into different isoforms such as homodimers, and heterodimers with other nuclear receptors before binding to their response elements; for example ligand activation of the Liver X Receptor (LXR) requires forming a heterodimer with the Retinoid X Receptor (RXR), is a nuclear receptor; it has three isoforms RXR α , RXR β , and RXR γ . It participate in many physiological processes for example cell differentiation and homeostasis, it can make either homodimers or heterodimer with other receptors such as LXRs [4]. LXR/RXR heterodimer followed by binding of the ligand LXR/RXR complex to its response elements thereby increasing the range and regulation options of target gene promoters [5]. This process is illustrated in (Figure 1.1).

The activated nuclear receptor acts either as an up-regulator of target gene expression through positive hormone response elements, or as a repressor of target gene expression through negative hormone response elements. Some of the nuclear receptors can recognise and bind to the same response elements, for example steroid hormone receptors such as the progesterone receptor (PR), androgen receptor (AR), mineralocorticoid receptor (MR), and glucocorticoid receptor (GR) bind to response elements that contain the AGAACA motif [6].

Since their first recognition, NRs had been identified separately by different research groups; therefore, several names were often used for the same receptor. To resolve this, a new scientific nomenclature of NRs was established in 1999. This classification was based on Nuclear Receptor (NR)xyz rules, for example, Liver X receptor alpha (LXR α) is classified as Nuclear Receptor subfamily I, group H and third gene in the group therefore it named as NR1H3. The Liver X receptor beta (LXR β) is NR1H2 [7].

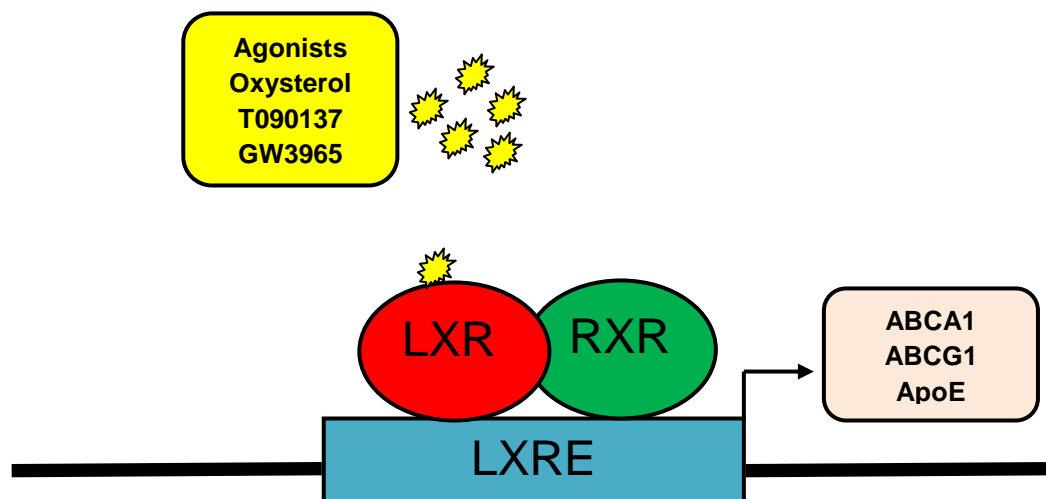


Figure 1.1 Activation of the nuclear receptor LXR by natural and synthetic agonists
 Activation of the nuclear receptor LXR by its natural oxysterol (oxidised cholesterol metabolites) and synthetic (T090137 and GW3965) agonists leads to formation of heterodimer with RXR followed by binding to the Liver x Receptor response elements (LXRE) resulting in expression of target genes involved in lipid metabolism.

1.1.2 Categorisation of nuclear receptors

The nuclear receptor superfamily is classified according to the physiological ligands and potential function. These form three sub-groups as illustrated in (Figure 1.2). The sub-groups are as following:

I- Endocrine receptors: characterized by high affinity for fat-soluble hormones and vitamins. They are important for endocrine and homeostatic control. This subgroup contains steroid receptors and heterodimeric receptors.

II- Adopted orphan receptor: characterised by low affinity for lipids and xenobiotics. This subgroup contains lipid sensor receptors which control synthesis, uptake, storage or clearance of lipids and glucose homeostasis. This subgroup also contains enigmatic orphan receptors which have identified ligands, but the nature of the ligand-dependent regulation in physiology is still not demonstrated.

III- Orphan receptors: This sub-group contains nuclear receptors that have as yet unidentified ligands [8].

Human Nuclear Hormone Receptor Super Family

Endocrine Receptors	Adopted Orphan Receptors	Orphan Receptors
<p style="text-align: center; margin: 0;"><u>Steroid Receptors</u></p> <p>GR glucocorticoid</p> <p>MR mineralocorticoid</p> <p>PR progesterone</p> <p>AR androgen</p> <p>ERα,β estrogen</p>	<p style="text-align: center; margin: 0;"><u>Lipid sensors</u></p> <p>RXRα,β,γ 9cRA</p> <p>PPARα,δ,γ fatty acids</p> <p>LXRα,β oxysterol</p> <p>FXR bile acids</p> <p>PXR xenobiotics</p>	<p>SHP ?</p> <p>DAX-1 ?</p> <p>TLX ?</p> <p>PNR ?</p> <p>GCNF ?</p> <p>TR2,4 ?</p> <p>NR4Aα,β,γ ?</p> <p>Rev-erbα,β ?</p> <p>COUP-TFα,β,γ ?</p>
<p style="text-align: center; margin: 0;"><u>Heterodimeric Receptors</u></p> <p>TRα,β thyroid hormone</p> <p>RARα,β,γ retinoic acid</p> <p>VDR vitamin D (bile acid)</p>	<p style="text-align: center; margin: 0;"><u>Enigmatic Orphans</u></p> <p>CAR androstane</p> <p>HNF-4α,γ fatty acids</p> <p>SF-1/LRH-1 phospholipids</p> <p>RORα,β,γ < cholesterol</p> <p>ERRα,β,γ retinoic acid</p> <p>ERRα,β,γ estrogen?</p>	

Figure 1.2 Human nuclear receptor superfamily classification, the classification depends on their physiological ligands and potential functions (copied from [8] with permission).

1.1.3 Structure of nuclear receptors

Nuclear receptors can be found in both the cell cytoplasm and nucleus. These receptors are activated by ligands that freely cross cell membranes such as lipids, vitamins, thyroid hormones and steroid molecules. Binding leads to aggregation of these receptors and their active transport into the cell nucleus where they act by binding to specific recognition sites on DNA called response elements, enabling regulation of gene transcription in response to ligand activation. Generally all nuclear receptor structures consist of one homology polypeptide of five to six domains; designated A to F, from the N-terminal to the C-terminal end on the basis of regions of conserved sequence and function (Figure 1.3).

Nuclear receptors contain two important regions; 1. The DNA-binding domain (DBD, region C), and 2. The ligand-binding domain (LBD, region E). The DNA binding domain consists of approximately 70 amino acids and contains two highly conserved zinc finger proteins which differentiate the nuclear receptors from other DNA-binding proteins. The DBD (N-terminal) acts as a target receptor to specific DNA sequences known as nuclear receptor response elements, for example, hormone response elements. These response elements are located in the promoter regions of genes relevant to the biological response to the ligand, and binding of the nuclear receptor can therefore regulate gene transcription. The LBD (C-terminal) consists of approximately 250 amino acids and is configured for ligand recognition and binding. The ligand recognition site is characterised by its high specificity and selectivity to recognise appropriate ligands [2, 8-11].

Nuclear receptors contain two transcription activation function domains AF-1 and AF-2 that, act as coactivators of the nuclear receptor. AF-1 is located at the N-terminal region and consists of the A/B domains. Its function is ligand-independent activation. The AF-2 domain is located at the C-terminal region within the LBD and its function is ligand-dependent activation [11, 12]. Synergy between these two domains is required to achieve full transcriptional activity.

The NR contains a hinge region located in region D, which connects the DBD and LBD. This is associated with a constitutive transport element (CTE) which is involved in the trafficking and distribution of the NR.

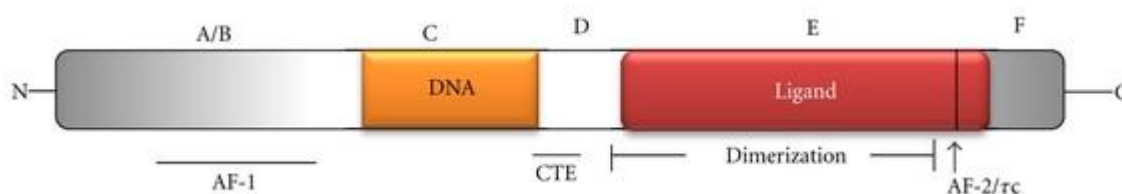


Figure 1.3 General structure of a putative nuclear receptor

The nuclear receptor consists of 6 domains (A, B, C, D, E and F). The DNA binding domain is located in the C domain and the ligand binding domain is located in the E domain. Nuclear receptors also contain a constitutive transport element (CTE), and two transcription activation function domain AF-1 and AF-2 (copied from [2] with permission).

1.1.4 Liver X Receptors (LXRs)

1.1.4.1 Structure and Function

Liver X receptors (LXRs) are member of the nuclear receptor superfamily. They were first identified in 1994 and were initially named RLD-1 (see section 1.4.1.1. below for details) [13]. RLD-1 had the features of a nuclear receptor and was able to interact with RXR, therefore was classified as LXR. The LXRs consist of two isoforms; LXR α (NR1H3) and LXR β (NR1H2) which are both ligand-activated transcription factors [14]. The two LXRs (α and β) are highly conserved; with 78% shared identity of amino acid sequence in both the DBD and LBD domains [15].

Despite the structural similarity and conservation between LXR α and LXR β they are located in different chromosomes and encoded by different genes; human LXR α by HR1H3 on chromosome 11p11.2 and LXR β by NR1H2 on chromosome 19q13.3. LXRs were first identified as orphan receptors before the recognition of their natural ligand. As with the other nuclear receptors, the LXR molecule consists of four domains; two conserved domains (DBD & LBD), and two transcription activation function domains (AF1 and AF2) (Figure 1.2) [16].

1.4.1.2 Liver X Receptor alpha (LXR α)

The Liver X receptor alpha (LXR α) was first identified as RLD-1 (from Rat Liver Digest extract 1). It was described in 1994 using Western blot analysis of rat's liver extract which showed that RLD-1 formed a heterodimer structure with the Retinoid X Receptor (RXR), and was therefore recognised as a novel member of the nuclear receptor family. This new receptor consisted of 445 amino acids. The name of the Liver X receptor came from its conspicuously high expression in the liver [13] and the absence of an identified ligand was replaced by the letter X [17].

The tissue distribution of LXR α expression varies; it's abundantly expressed in liver, spleen, kidney, lung, intestine, pituitary and adipose tissue [13-15, 17]. Many inflammatory cells also express LXR α including T lymphocytes, dendritic cells and monocytes / macrophages [18-20].

1.1.4.3 Liver X Receptor beta (LXR β)

Liver X receptor beta (LXR β) is the second isoform of LXR and was discovered in 1994. It was named initially as a ubiquitous receptor (UR) because both the protein and mRNA for UR were identified in many cell types and functionally the rat UR was found to heterodimerise with human Retinoid X Receptor alpha [21]. High structural similarity between UR protein with LXR α was identified, therefore, a new name was given to this new receptor; LXR β . There was 77% similarity in amino acid sequences in both DBD and LBD for LXR α and LXR β [17]. Generally, LXR β heterodimerise with the Retinoid X receptor (RXR). LXR β is expressed more ubiquitously than LXR α and can be observed in most tissues and cells [14, 15, 22]

1.1.4.4 LXR ligands

The Liver x Receptor was initially identified as an orphan nuclear receptor because neither a physiological nor synthetic ligand was recognised. Subsequently, metabolites of cholesterol and derivative oxysterols were discovered as potential endogenous physiological ligands for these receptors with the ability to activate them [23]. Cholesterol and common oxysterol structures are illustrated in (Figure 1.4). Activated Liver X receptors form a heterodimer with the Retinoid X receptor (RXR). Then the LXR/RXR complex binds to its response elements thereby increasing the range and regulation options of target gene promoters [5].

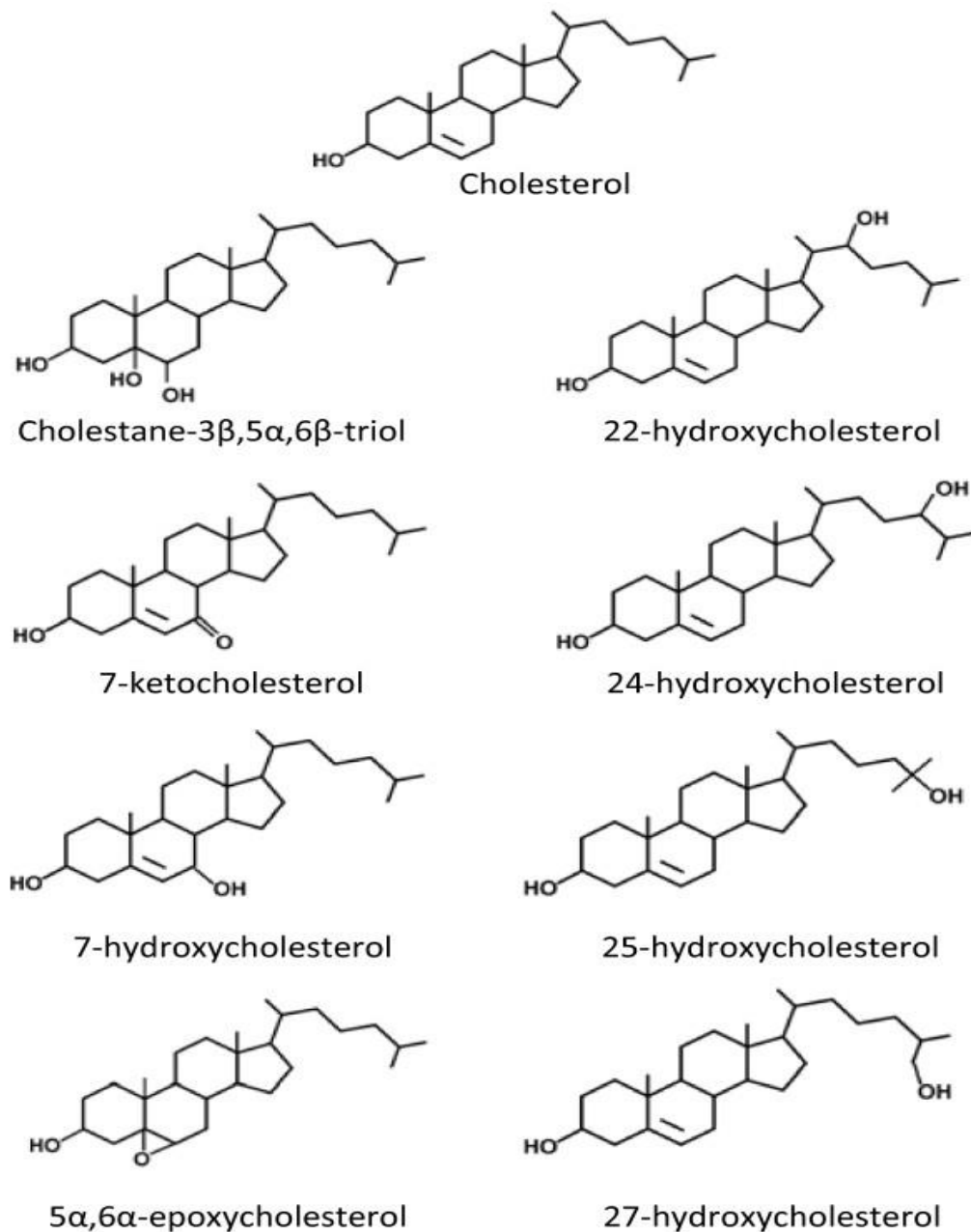


Figure 1.4 Structures of cholesterol and most common oxysterols (copied from [24] with permission).

Liver X receptors are important regulators of cholesterol and lipid metabolism. They control the regulation of genes involved in lipogenesis, cholesterol efflux in macrophages, bile acid synthesis in liver and intestinal cholesterol absorption. For example, LXRs regulate the Cholesterol 7 α -hydroxylase A1 (CYP7A1) gene encoding cholesterol 7 α -hydroxylase which is the rate-limiting enzyme in the conversion of cholesterol to bile acids in the liver [25]. Also activation of macrophage LXR α and LXR β results in increased expression of genes involved in lipid metabolism and transportation such as Apolipoprotein E (APOE), ATP binding cassette A1 (ABCA1), ATP binding cassette G1 (ABCG1), ATP binding cassette G5 (ABCG5), and ATP binding cassette G8 (ABCG8), as well as CCL24 and Toll Like receptor 4 (TLR4) in the case of macrophage activation [19, 20, 26-28].

These proteins, for example ABCA1 has been determined in macrophages as an engulfment receptor which plays a potential role in the treating of cellular lipids by enhancing the effluxes of cellular cholesterol and phospholipids to lipid-poor apolipoproteins. ABCA1 controls the process of reverse cholesterol transport including synthesis of high-density lipoproteins (HDL). Mutations in ABCA1 lead to development of Tangier disease, a severe HDL deficiency disease manifested by accumulation of cholesterol in tissue macrophages and atherosclerosis [29, 30].

Oxysterols are oxidized derivatives of cholesterol and several have been identified as potent natural ligands for LXRs. These include, 20(S)-hydroxycholesterol, 22(R)-hydroxycholesterol, 24(S)-hydroxycholesterol, 27-hydroxycholesterol, and 24(S),25-epoxycholesterol; with the last being the most potent ligand having the highest binding affinity towards both isoforms of LXR [31]. Bile acids are steroid acids that facilitate fat emulsification and digestion in the intestine. They are also identified as natural physiological ligand for LXRs. Bile acids such as 6 α -hydroxylated bile acids were able to activate LXR α specifically and selectively but higher concentration of 6 α -hydroxylated were required to activate LXR β [32].

The liver is the main tissue for LXR function because it has both LXR α and LXR β isoforms and because the important role of LXRs in regulation of lipid metabolism and cholesterol homeostasis occurs mainly in the liver. In addition, the liver is the primary organ responsibility for producing glucose. Glucose is another metabolite of particular importance [33]. Both glucose and d-glucose-6-phosphate are direct agonists for LXRs with higher affinity binding with LXR α than with LXR β . These two forms of glucose were able to bind and activate the receptors resulting in expression of LXR target genes [34]. Physiological concentration of glucose were able to activate LXR except in liver; this observe when a significant glucose influx accompanied by disturbances in insulin regulation function [34].

Some LXR ligands can selectivity activate either LXR α or LXR β . One example is a phenethylphenyl phthalimide derivative which is a potent and selective agonist for LXR α [35]. Whereas another group of synthetic LXRs ligands; the N-acylthiadiazolines have a high selectivity for LXR β but with modest activation potency. A study of macrophages derived from LXR mutant mice confirmed the selectivity of the ligand for LXR β and the activity was confirmed by the ability of the compound to activate macrophages to induce apolipoprotein A1 (APOA1) dependent cholesterol efflux [36].

Investigating different sources of LXR agonists including plant biological products discovered that sterols and stanols were able to activate LXRs [37]. The study demonstrated that sitosterol and sitostanol activated LXR α and LXR β resulting in an increase in ABCA1 expression accompanied by a decrease in the concentration of LDL cholesterol and decreased intestinal absorption of cholesterol [37].

The most commonly used synthetic LXRs ligands bind both LXR α and LXR β with high efficiency and potency are T1317 and GW3965 [38, 39]. T1317 is short for

T0901317 which is (N-(2,2,2-trifluoro-ethyl)-N-[4-(2,2,2-trifluoro-1-hydroxy-1-trifluoromethyl-ethyl)-phenyl]-benzenesulfonamide. It is characterised by its specificity demonstrated by using transient transfection assays in HEK293 cells. The ligand was able to activate LXR α and LXR β , but with a 35 fold higher potency for activating LXR α (35 fold) than LXR β (15 fold) [40]. GW3965 is a nonsteroidal LXR ligand that was synthesized and introduced by the pharmaceutical company GlaxoSmithKline in the USA. It is characterised by its high potency and selectivity to induce the expression of ABCA1 *in vitro* and *in vivo* in mice after oral administration [41]. The specificity of GW3965 to human and murine LXR α and LXR β was demonstrated. A study had shown this specificity by using of a luciferase-based functional assay. The LBDs of human LXR α , human LXR β , mouse LXR α , and mouse LXR β were cloned and inserted into the pM2-GAL4 vector to create LBD/GAL4 'chimeric' receptors. Cells were transfected with the vector and activated with LXR agonist GW3965 resulted in expression of the reporter genes [42]. I acknowledge that the specificity of any chemical ligand is incomplete and I was aware that other molecules could be affected by the compound.

LXRs can also be activated as an indirect consequence of activation of other nuclear receptors activation by their own specific ligands, followed by an obligatory heterodimerisation with LXR. Example of these include activation of Retinoid X receptors (RXRs) by its specific ligand retinoids (e.g. LG268) results in RXR/LXR heterodimerisation and ABCA1 transcription [40].

Also activation of Peroxisome proliferator-activated receptors (PPARs), nuclear receptor contains three subtypes PPAR α , PPAR γ and PPAR δ had been shown correlation with LXR expression. A study had been shown that activation of PPAR α or PPAR γ with unsaturated fatty acids and synthetic PPAR ligands can lead to the induction of expression of LXR α resulting in stimulation of ABCA1 expression and enhance cholesterol efflux to APOA. This was confirmed using human primary monocyte-derived macrophages and in macrophage-derived foam cells [43]. This was supported by another study carried out rats demonstrated that rat fed a high-fat diet rich in unsaturated fatty acids, or PPAR α agonist such as Wy 14.643 results in an induction in LXR α mRNA and protein level expression by 3 folds. This was confirmed *in vitro* cultured hepatocytes. This indicated a direct induction of LXR α gene transcription via PPAR α interacting with several PPREs in the LXR α promoter [44].

1.1.4.5 LXR regulation and expression

The LXRs are considered as members of a class of receptors called ligand-activated nuclear receptors and transcription factors that move between the nucleus and cytoplasm. LXRs vary in their localisation inside the cell; LXR α tends to be localised in the nucleus and LXR β is detected in nucleus and cytoplasm [45].

Activation of LXRs results in their binding with DNA response elements which in turn can regulate transcription of appropriate genes.

These two LXR isoforms are expressed constitutively across a broad distribution of tissues. Different signalling pathways can be involved in the induction of LXR expression; these include specific endogenous and exogenous ligands which modulate LXR synthesis. The topic of what regulates LXR expression is unresolved. Many factors may be involved in the regulation of LXR expression but more work still needs to be done to understand the relative participation of many different pathways. For example, analysis of the LXR promoters demonstrated binding sites for different transcription factors such as Specificity Protein 1 (SP1), nuclear factor kappa-light-chain-enhancer of activated B cells (NF- κ B) and 7 members of E-twenty six family transcription protein (Ets-protein). Different mechanisms therefore can be involved in the regulation of LXR expression. The promoter regions for both LXR α and LXR β are characterised by their abundant of GC and their numerous binding sites (response elements) for the SP1 transcription factor which is responsible for basal expression levels of LXR α and LXR β [46].

LXR expression can be up-regulated or down-regulated by hormones. A recent study has shown that the thyroid hormone (T3) up-regulates the expression of LXR α but not LXR β in mice. This was due to the LXR α and thyroid hormone receptors sharing or competing for the same DNA response elements which have similar geometry and polarity. Moreover, reporter assays demonstrated that the thyroid hormone receptor β 1 could regulate the transcription of the mouse LXR α gene [47]. Different hormones may lead to down-regulation of LXR expression, for example, treating mice with oestrogen (17 β -estradiol) lead to down-regulation of expression of LXR α and its target genes, e.g. ATP-binding cassette A1 (ABCA1), ATP-binding cassette G1 (ABCG1), apolipoprotein E (APOE), sterol regulatory element-binding protein 1c (SREBP-1c), and phospholipid transfer protein (PLTP) [48].

LXR regulation and expression can be induced indirectly through the activation of other receptors. One study demonstrated that in human macrophages LXR α can be regulated and expressed using specific ligands for peroxisome proliferator-activated receptor γ (PPAR γ) e.g. rosiglitazone or GW7845, because the response element for this receptor is found in the LXR 5'-flanking region [49].

A gene expression profile microarray analysis demonstrated a 40-fold up-regulation of LXR α expression during Granulocyte macrophage colony-stimulating factor (GM-CSF) induced differentiation of human monocytes to macrophages [50]. Activation of the LXR in human macrophage cell lines by endogenous or synthetic ligands resulted in an induction of LXR α expression [49, 51]. This auto-regulation ability of LXR α was confirmed by its disappearance in the rare case of a deletion or mutation inside the LXR α promoter region. This lead to the conclusion that the auto-regulation process is specifically associated with LXR α expression

and it was cell specific because it was seen in human macrophages but not in hepatocytes. This auto-regulation of LXR α resulting in an increased LXR α expression may perhaps explain why macrophages generally have higher expression levels of ABCA1 in comparison to hepatocytes.

Cholesterol and its derivative oxysterols have been described as potential endogenous physiological agonists of LXR (22). The classical pathway of LXR activation can be summarised as follows:

Firstly, binding between the LXR agonist and the LXR occurs in the cytoplasm or nucleus and this leads to the formation of a heterodimer of the LXR with another nuclear transcription factor called the retinoid X receptor (RXR), which is necessary for LXR function.

Secondly, the LXR/RXR heterodimer transport to bind to the LXR response elements (LXREs) which are located in the promoters of certain genes. The transportation and trafficking is mediated via constitutive transport elements (CTE) within the NR.

Third, when bound to the LXRE, a conformational changes occur in the LXR/RXR complex with the release of transcriptional corepressors allowing transcriptional coactivator function, this is followed by switching on the promoters of target genes followed by their expression e.g. ABCA1 (Figure 1.5) [52].

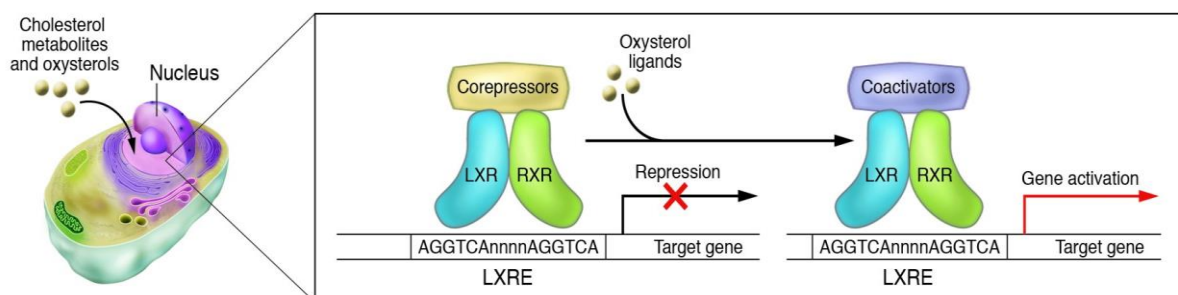


Figure 1.5 Regulation and transcription of LXR

Cholesterol metabolites; oxysterols bind to LXR followed by formation of LXR/RXR heterodimer which in turn binds to the LXREs located in the target gene promoters. Ligand binding induces the conformational change of the LXR/RXR complex inducing the release of transcriptional corepressors which exchange into transcriptional coactivator, switching on the promoters of target genes followed by their expression e.g. ABCA1. (copied from [52] with permission).

1.1.5 LXR in physiology, inflammation and disease

1.1.5.1 The role of LXR in obesity

Fat is the main energy reserve in mammals. Fat accumulation occurs in all parts of the body especially in the abdominal and pelvic cavity in the form of white adipose tissue. This consists mainly of mature adipocytes originating from undifferentiated pre-adipocytes through a differentiation process controlled by transcription factors and hormones [53, 54]. Obesity is characterised by excessive deposition of fat in the tissues resulting in alteration in adipose tissue metabolism accompanied by excessive release of fatty acids and pro-inflammatory mediators. There is a strong relationship between chronic inflammatory diseases and obesity related metabolic dysfunctions, for example there is a strong relationship between obesity and hypertension and dyslipidaemia [55].

LXR α and LXR β are expressed in human and murine adipocytes. Studies have shown increased LXR α expression in mature human and murine adipocytes during lipogenesis. This was accompanied by increased lipid accumulation and fatty acid synthesis, and increased expression of LXR target genes sterol regulatory binding protein-1 (SREBP-1) and peroxisome proliferator-activated receptor gamma (PPAR γ) [53, 54]. Mice that were given the LXRs agonist T0901317 had up-regulation of expression of adipogenic and lipogenic genes in the liver and fat tissue. Interestingly, small interfering (si)RNA that silenced LXR α lead to suppression of adipocyte differentiation [54]. Macrophages are involved in metabolism and inflammation. The involvement of the macrophages in LXR glucose tolerance or obesity stimulated by a high-fat diet was investigated. The study found that transfer of LXR $\alpha\beta^{-/-}$ bone marrow into wild-type recipients mice had no effect on the glucose tolerance or obesity [56].

Macrophages express both LXR α and LXR β and are distributed in all tissues including adipose tissue. The number and size of adipose tissue macrophages increase in obesity, and these are the source of all the Tumour Necrosis Factor α (TNF- α) and most of the inducible nitric oxide synthase (iNOS) and IL-6 expression in adipose tissue [57]. Because of the strong association between obesity and cardiovascular and inflammatory diseases, there may be an important role for LXRs in the regulation of lipid metabolism and transportation. This is due to the ability of LXRs to regulate a wide range lipid-controlling genes such as ABCA1 and ABCG1 that may act as a control method on the development of obesity that may have a beneficial effect for the treatment of cardiovascular diseases and inflammation.

1.1.5.2 The role of LXR in atherosclerosis

Atherosclerosis is a chronic inflammatory disease characterised by progressive thickening of the inner lining of the medium and large artery walls as a result of the

accumulation of lipid deposits. The hallmark feature of these lesions is the presence of lipid-filled cells in the intima [58]. This observation suggests that the pathogenesis of the disease includes abnormalities in cholesterol metabolism. Furthermore, cholesterol and its derivatives are the physiological endogenous ligands for LXRs, and activation of LXR regulates genes involved in lipid metabolism and transportation which normally control the efflux of lipids out of foam cells [19, 20, 23]. Therefore, this suggests a potential role for LXRs in atherosclerosis.

In the early stage of the development of atherosclerosis, local inflammation results in the generation of reactive oxygen species and cholesterol esters which are then bound by low density lipoproteins (LDL) present in the artery wall. These oxidised-(ox)LDLs are then bound and removed by macrophages via their scavenger receptors. These are a wide family of receptors including CD36 that remove a range of waste material due to their broad ligand specificity. In the context of atherosclerosis, locally produced oxLDL are taken up by the macrophage and can accumulate in lysosomes to form lipid-laden 'foamy' macrophages.

The physiological response to this intracellular accumulation of oxLDL is that cholesterol is regenerated and secreted from the cell. This process is called reverse cholesterol transportation or efflux; a process in which cholesterol and phospholipid excretion is regulated by LXRs [58]. The mechanism was described in one study demonstrating that stimulation of mouse macrophages and fibroblast cell lines with an LXR agonist up-regulated the expression of the ABCA1 gene by ~ 30 fold [59]. The process is illustrated in (Figure 1.6).

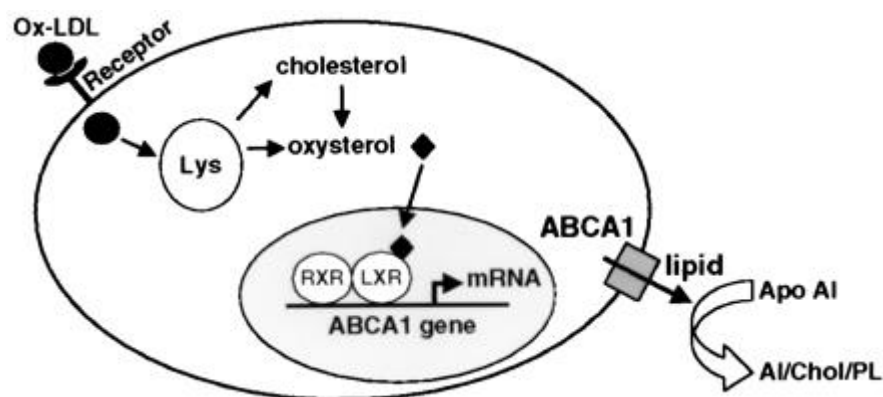


Figure 1.6 Regulation of ABCA1 gene expression and cholesterol efflux by LXR as result of lipid loading

Binding of oxLDL to scavenger receptors is followed by internalization and degradation in lysosomes. Then cholesterol and oxysterols enter the nucleus and activate the LXR/RXR heterodimer activating target genes for example ABCA1. Synthesis of ABCA1 protein leads to an increased efflux of cholesterol and/or phospholipids to apoAI (copied from [59] with permission).

Apolipoprotein E is another target gene for LXRs that participates in lipid transportation [40]. Accumulation of lipids inside macrophages is sufficient to activate LXRs resulting in increased expression of the ABCA1 and apolipoprotein E (ApoE) genes which are involved in cholesterol efflux. Experimental models demonstrate that LXR α is the key regulator of cholesterol efflux. LXR α ^{-/-} mice developed severe atherosclerosis when fed a diet rich in cholesterol in comparison with LXR β ^{-/-} and wild type mice [49, 60, 61].

To understand whether the cholesterol and phospholipid efflux process is controlled by ABCA1 or in cooperation with ApoE, a study was performed using apolipoprotein-E gene-deleted mice. This demonstrated that agonists of LXR and RXR were still able to activate LXRs and to initiate expression of ABCA1 in macrophages resulting in cholesterol efflux but not in LXR $\alpha\beta$ gene-deleted mice [60]. They concluded that cholesterol efflux is mediated through direct expression of ABCA1 in response to LXR activation. These studies therefore suggest that the development of agonists that specifically activate LXR is beneficial for activation of LXRs resulting in regulation of body cholesterol.

The development of atherosclerotic plaques is correlated with chronic inflammation and recently targeting LXRs have been suggested as a potential anti-inflammatory candidate for therapy. It has been suggested that LXR agonists may suppress atherosclerosis. ApoE^{-/-} mice treated with the LXR agonist T1317 had a reduction in the expression levels shown by microarray gene analysis in hepatic cells of the pro-inflammatory cytokines IL-1 and IL-6 as well as serum concentrations [62].

LXRs can participate in the modulation of atherosclerosis by affecting macrophage up-take of oxLDL resulting in decreased cholesterol accumulation. This was shown experimentally by stimulating human monocyte-derived macrophages with either of the LXR agonists T0901317 or 22(R)-hydroxycholesterol, followed by incubation with oxLDL. This resulted in decreased oxLDL uptake. This was due by the ability of LXRs to down-regulate macrophage pinocytosis of oxLDL [63]. This mechanism could be another preventative mechanism by which LXRs can control macrophage foam cell formation.

Some anti-oxidant extracts e.g. curcumin, a potent antioxidant extracted from *Curcuma longa* may participate in the modulation of cholesterol accumulation in macrophages by modulating oxLDL uptake. Cells treated with curcumin show increased expression of ABCA1 protein. Curcumin increased up-regulation of ABCA1 expression through calmodulin (calcium-modulated-protein) for LXR α dependent transcriptional regulation [64].

LXR agonists participate in the regulation of gene expression that regulate lipid metabolism; therefore, they may have potential antiatherogenic effect. One study using New Zealand white rabbits showed that administration of the LXR agonist T0901317 resulted in an increase in plasma LDL level, accompanied by an

increase in the activity of plasma cholesterol ester transfer protein (CETP), ABCA1 and ABCG1, resulting in down-regulation of inflammatory gene expression [65]. LXRs also participate in the metabolism of phospholipid and triglycerides (TG). Oral administration of synthetic LXR agonists T0901317 to mice resulted in an increased concentration in plasma phospholipid and TGs and this lipogenic effect is mediated through the increased induction of fatty acid synthase (FAS), sterol regulatory element binding protein 1c (SREBP-1c) expression, and induced hypertriglyceridaemia [66].

Generally, LXRs have a potential role in regulation of cholesterol metabolism, thus preventing over-accumulation which might lead to atherosclerosis.

1.1.5.3 The role for LXR in inflammation

LXRs can modulate inflammation because of their involvement in cholesterol metabolism and homeostasis. Since the relationship between chronic inflammatory diseases and lipid metabolic dysfunction has been observed, therefore, the role of LXRs in different inflammatory diseases has been investigated. LXRs are distributed across all tissues and cells, including T lymphocytes, dendritic cells, neutrophils and monocytes / macrophages [14, 15, 67]. Generally, an anti-inflammatory effector function for LXRs had been observed but pro-inflammatory effects have also been observed.

The role of LXR in inflammation can be demonstrated by either stimulating or inhibiting the expression of genes for certain pro-inflammatory mediators such as $\text{TNF}\alpha$, IL-1, IL-6, cyclooxygenase (COX)-2 and inducible nitric oxide synthase (iNOS) [68, 69]. The effect of LXR agonist on inflammation may be mediated by the effect on Nuclear Factor kappa-light-chain-enhancer of activated B cells (NF- κ B), which is the central transcriptional regulator of the innate immune response. Many of the genes inhibited by LXR are established target inflammatory genes of NF- κ B signalling. Both of iNOS and COX-2 gene promoters demonstrated that down-regulation of these genes by LXR was mediated through antagonism of NF- κ B. This study demonstrated that there is a relationship between immune response and lipid metabolism involving LXR.

LXRs are also involved in the regulation of genes which participate in innate immunity. For example experimental knockdown of the $\text{LXR}\alpha$ gene in human keratinocytes in culture resulted in significant down-regulation of genes coding for peroxisome proliferator-activated receptor-gamma (PPAR- γ), catalase and vitamin D receptor (VDR), and significant up-regulation of genes coding for interferon-gamma (IFN- γ), c-myc, interleukin-6 (IL-6) and interleukin-8 (IL-8) [52, 70]. In addition, LXRs have been shown to have anti-proliferative properties. Activation of LXRs during T-cell activation leads to suppression of mitogen driven expansion in contrast T-cells which lack $\text{LXR}\beta$ were mitogen stimulation has a synergistic proliferative effect. Furthermore, these mice lacking $\text{LXR}\beta^{-/-}$ had an increase in

their response to antigenic challenge accompanied by lymphoid hyperplasia [71]. These anti-inflammatory and anti-proliferative effects of LXR may be considered as characteristic functional effects for activation of LXR.

LXRs have an involvement in the regulation of innate immune response. $LXR\alpha^{-/-}$ mice exhibited increased susceptibility to intracellular infection by *Listeria monocytogenes*, associated with an increase in macrophage apoptosis after bacterial infection [72]. The activation of LXRs also caused an increased expression of TLR4 in human, but not in mouse, macrophages resulting in an enhanced lipopolysaccharide response [27]. During inflammation several factors affect the expression of LXRs; for example, one study demonstrated down-regulation of $LXR\alpha$ and $LXR\beta$ expression in response to administration of Lipopolysaccharide (LPS) or pro-inflammatory cytokines such as $TNF\alpha$. The inhibitory effect of LPS was mediated by the ability of $TNF\alpha$ to suppress the LXR response elements [73].

LXRs may have an important role in inflammatory disorders of the nervous system e.g. Alzheimer's disease (AD). Activation of the LXRs protect cholinergic neurons and decrease the inflammatory response in an experimental model of AD in amyloid precursor protein (APP)/PS1 transgenic mice [69]. In another inflammatory disease model, LXRs have a positive regulatory effect on diabetic states; anti-diabetic effects were demonstrated in type 2 diabetic rodent models due to the ability of LXRs to increase peripheral glucose uptake, enhance insulin sensitivity, and thereby normalise glycemia [14]. The antidiabetic effect of LXR agonists is suggested to result predominantly from inhibition of hepatic gluconeogenesis. The potential mechanism of the anti-diabetic effect of LXR agonists is illustrated in Figure (1. 7).

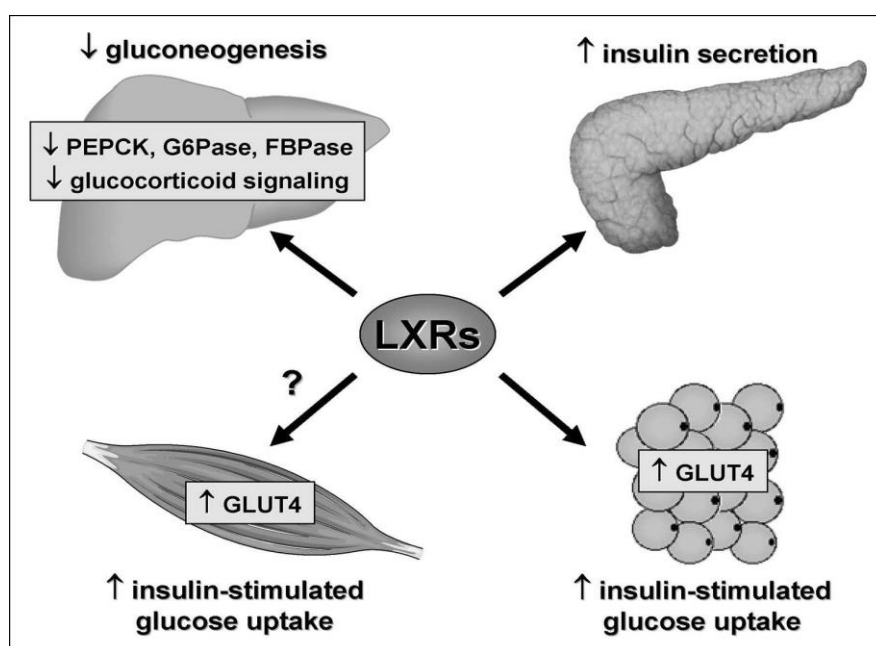


Figure 1.7 Mechanisms involved in antidiabetic effect of LXR agonists (copied from [59] with permission).

In a common murine collagen-induced arthritis model, one recent study demonstrated that activation of LXR with T1317 and GW3965 agonists resulted in exacerbation of the inflammatory response, with excessive cartilage destruction [74].

LXRs may also participate in the regulation of pulmonary inflammation and host defence. They are expressed by murine alveolar macrophages, alveolar epithelial type II cells and neutrophils. A study confirmed that stimulation of LXRs with the synthetic agonist TO-901317 (T1317) reduced the influx of neutrophils into the lung after several different challenge models; either with inhaled LPS, or intra-tracheal administered of KC chemokine (Keratinocyte-derived Cytokine, a counterpart of human GRO protein), or intra-tracheal *Klebsiella pneumoniae*, and impairs pulmonary host defences. One putative underlying mechanism was the impairment of the neutrophil motility due to inhibition of chemokine-induced RhoA activation [67].

Previous work has shown that activation of LXR in mouse primary hepatic stellate cells lead to cell activation and suppression of fibrosis markers such as collagen $\alpha 1(I)$. Mice selectively deleted of the two LXR genes $LXR\alpha\beta^{-/-}$ had increased susceptibility to liver fibrosis and this was reflected by increased production of inflammatory mediators and expression of fibrogenic genes in their stellate cells [75].

Further work is required to determine the nature and diversity in the pro- or anti-inflammatory and pro- or anti-fibrotic responses of the LXR in different disease models. Studies are needed to investigate the control of the inflammatory and fibrotic responses at the level of LXR activation because targeting the LXR in vivo is of potential risk because of the involvement of these receptors in many physiological processes. It is possible that there are different endogenous physiological LXR ligands because there is a strong association between the metabolic diseases and the inflammatory and fibrotic diseases. Improved understanding of LXR in this context may therefore be of considerable clinical importance.

1.2 MicroRNA

1.2.1 Introduction to microRNA

MicroRNAs (miRNAs) are small, evolutionary conserved, single-stranded, non-coding RNAs consisting of 20- 22 nucleotide bases. MiRNAs are endogenous regulators of mRNA translation. They do this by formation of an miRNA-induced silencing complex (miRISC) which provides a molecular structure in which the miRNA bind by Watson and Crick binding to complementary recognition elements within the 3' untranslated region (UTRs) of target mRNA resulting in translational repression or enhanced degradation of the mRNA [76-78].

The first indication of the importance of these small non-coding miRNAs was identified by Lee and colleagues in 1993, who were investigating the role of the lin-4 gene in the timing control of larval development of the worm *Caenorhabditis elegans*. Lin-4 function was characterised by its ability to negatively control the level of LIN-14 gene product, an important protein in larval stage development. They found that the lin-4 gene produces two small lin-4 transcripts of approximately 22 and 61 nucleotides RNAs that do not code for protein [79]. These nucleotides bind and repress the translation of the LIN-14.

In human, there have been approximately 533 miRNA loci identified [80], and more than 1000 miRNAs are predicted to function in humans with the possibility to regulate approximately 60% of human genes [78], with an estimated total of more than 45000 miRNA target sites [81].

1.2.2 MicroRNA expression and function

Both animals and plants express miRNAs. They are associated with the regulation of a major part of the protein-coding transcriptome with important roles in development, stress adaptation and hormone signalling [82]. In addition, miRNA networks regulate a wide range of biological processes such as cell proliferation, differentiation, migration, and apoptosis [78, 80].

The expression levels of miRNAs are different in different tissues to reflect their function. For example, the expression of miRNAs in mouse embryonic stem (ES) cells during differentiation. Some of miRNAs were suppressed during the differentiation of ES cells into embryoid bodies, and these became undetectable in adult mouse organs. This was in contrast to other miRNAs for which the expression was constant or increased during and after differentiation [83].

MiRNAs can also be characterised by their involvement in the outcome of normal and pathogenic immune responses. MiRNAs play an important role in modulating immune cell function. For example, stimulation of innate immune cells with LPS up-regulated miR-146a expression. This in turn inhibited the expression of TRAF6

and IRAK1, which are positive regulators involved in the Toll-like receptor 4 (TLR4) signalling pathways. This in turn inhibited the LPS-controlled TLR4 signal [84]. Also, in cancers of cells of immunological origin there is reduced expression of miRNAs with tumour suppressive function [85].

1.2.3 MicroRNA biogenesis

MicroRNAs (MiRNAs) originated from genome-encoded precursors which fold into imperfect hairpin structures. MiRNA genes transcribed by RNA polymerase II (PolII) into primary miRNA (pri-miRNA), a long hairpin structure consisting of 60–80 nucleotides and may include one or more miRNAs embedded in a stem loop [86].

The pri-miRNA is then processed by RNase III Drosha and DiGeorge syndrome critical region gene (DGCR8) to form ~70-nucleotide-long precursor miRNA (pre-miRNA) (Figure 1.1). The pre-miRNA is exported from the nucleus into the cytoplasm, and then it undergoes cleavage by the cytoplasmic endonuclease enzyme called Dicer into short-lived double-stranded duplexes. These duplexes then separate into one single strand mature functional miRNA, while the other strand undergoes degradation. The mature miRNAs are incorporated into effector complexes containing the argonaute protein. These are called miRISC (miRNA-containing RNA-induced silencing complex). The miRNA then guides the RISC to its target 3' UTRs, leading to inhibition of mRNA translation or cleavage of mRNA (Figure 1.8) [85, 87].

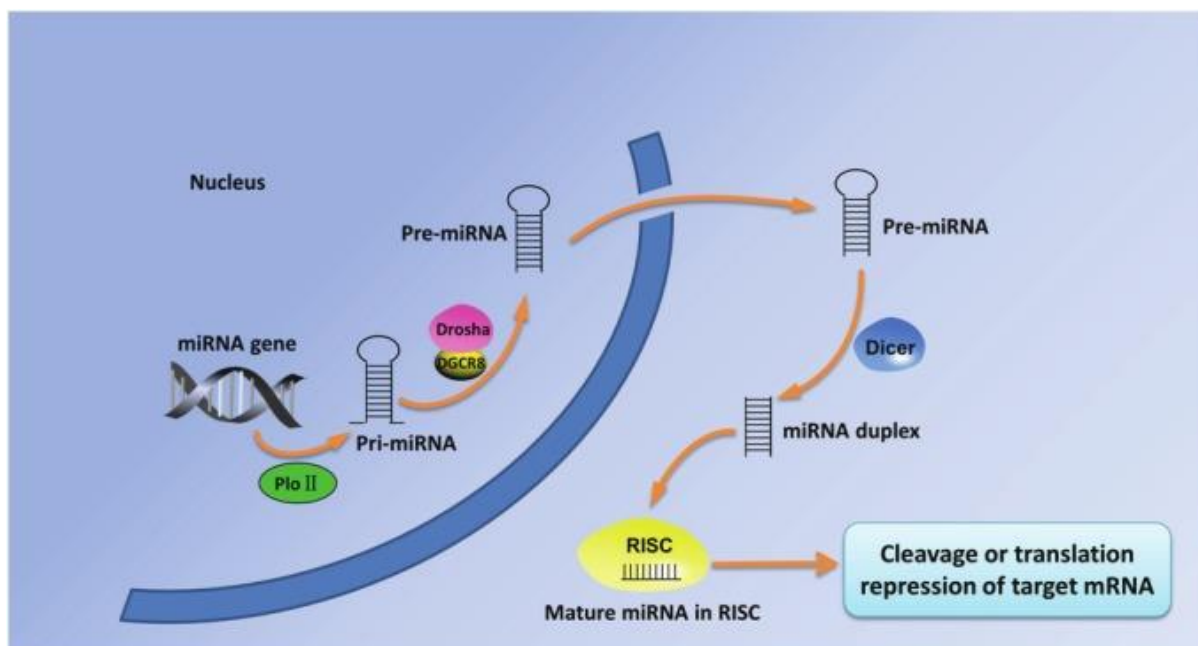


Figure 1.8 The biogenesis of miRNAs

Transcription of miRNA genes occur by RNA polymerase II (PolII) enzyme into primary miRNA (pri-miRNA). Then pri-miRNA followed by further processing by Drosha and DGCR8 resulting in production of precursor miRNA (pre-miRNA) which exported from nucleus into cytoplasm. The pre-miRNA is cleaved by a Dicer enzyme to form a mature miRNA. Then the mature miRNA is loaded into RNA-induced silencing complex (RISC) resulting in mRNA translation repression or cleavage (copied from [87] with permission).

1.2.4 MicroRNA mechanisms of action

MiRNAs perform their inhibitory function by enhanced mRNA degradation or by inhibition of mRNA translational [88]. The exact mechanism by which a miRNA can identify and inhibit or facilitate cleavage a specific mRNA transcript is still not fully determined [76]. Therefore, using prediction algorithms of bases sequences is a reasonable method to predict whether a specific gene can be targeted by a specific miRNA.

Generally, the ability of miRNAs to inhibit or catabolise its specific target mRNA can start when at least 6-8 of the nucleotides in the miRNA 5' end (seed region) bind (even imperfectly) with base sequences in the 3' untranslated region of target gene mRNA [89]. In more detail, the proposed mechanism for miRNA action is that miRNAs target transcripts through imperfect base-pairing to multiple sites in 3' untranslated regions. The 5' end of miRNAs consist of 2–7 nucleotides and are crucial for targeting. Although less important, 3'-end pairing might contribute to target recognition, particularly when sites have weaker miRNA seed matches. The imperfect miRNA–mRNA can hybridise with central bulges (9–12 nucleotide bases). This can lead to target translational inhibition or exonucleolytic mRNA decay. The presence of multiple binding sites in the target mRNA can lead to increased repression [82]. The translation of target mRNA can be blocked or the mRNA can be cleaved as illustrated in (Figure 1.9).

Generally, one imperfect site is required for miRNA-induced cleavage of mRNA. The presence of multiple imperfect sites distinguished by one or more miRNAs is associated with highly effective inhibition of translation [78].

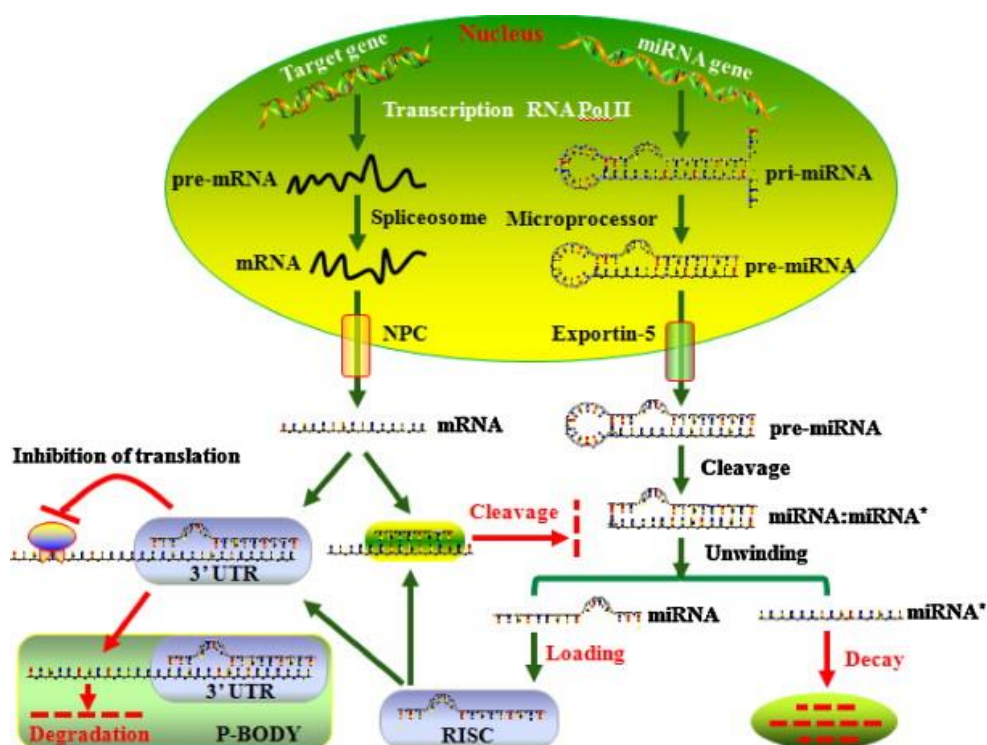


Figure 1.9 MiRNA biogenesis pathway and mechanisms of action
 A schematic shows biogenesis of miRNA and mRNA. The miRNA load into RISC complex then the recognition process for mRNA starts. MiRNA lead to either inhibition of mRNA translation or cleavage of mRNA (copied from [90] with permission).

1.2.5 MicroRNA-155

The gene for microRNA-155 (miR-155) is located in the B-cell Integration Cluster (BIC) which is a 1421 bp long non-coding gene located on chromosome 21. miR-155 is encoded by nucleotides 241–262 of BIC [91]. BIC was demonstrated in the chicken to be a non-coding RNA proto-oncogene [92].

Initially, bic was identified as a gene in the B-cell lymphomas resulted by the avian leucosis virus (ALV). Its transcription can be stimulated by promoter insertion at a retroviral integration site in B-cell lymphomas [93]. MiR-155 is processed from the BIC gene but does not encode for any protein. There are more than 100 gene mRNAs directly targeted by miR-155 [94].

The highest levels of BIC expression are found in the spleen and thymus. There is high homology between human, chicken, and mouse BIC with 78% identity over 138 nucleotides [95]. The miR155 gene is present in only one copy, and miR155

does not share significant sequence homology with other reported miRNAs, therefore, there is little overlapping with other miRNAs [96]. miR155 can be safely targeted for disruption without interfering with the expression of a protein-coding gene or a second transcriptionally-linked miRNA because it is located in an exon of the noncoding gene BIC which does not contain any other miRNAs or conserved RNA [96].

1.2.6 Regulation of immunity and inflammation by miR-155

In humans, bic/miR-155 expression is found in activated mature B and T lymphocytes and activated monocytes, macrophages, and dendritic cells. It can regulate inflammation positively or negatively in mammals [97]. MiR-155 null mice have serious immune defects in both adaptive and innate immunity [97].

O'Connell and colleagues have shown that increased expression of miR-155 can lead to an increase in the number of immature granulocyte *in vivo*, and the proposed mRNA target that participates in this process is called Src homology-2 domain-containing inositol 5-phosphatase 1 (SHIP1). This is an inhibitor of inflammation and this was modulated by the ability of miR-155 to repress SHIP1 [98]. The inflammatory disease model of rheumatoid arthritis (RA) demonstrated an increased expression of miR-155 in synovial membrane and in synovial fluid CD14⁺ cells. The expression levels of miR-155 correlated with the inhibition of the expression of the miR-155 target SHIP-1. Because SHIP-1 is an inhibitor of inflammation, its down-regulation found in synovial tissue CD68⁺ cells and in peripheral blood CD14⁺ cells resulted in an increased production of pro-inflammatory cytokines [99].

Macrophages are involved in inflammation, and an up-regulation in miR-155 expression in macrophages was found in response to infection [100]. Similarly, the expression of miR-155 was increased in murine bone marrow-derived macrophages stimulated with Toll-like receptor (TLR) ligands, e.g. polyribocytidylic acid, or in response to cytokine such as tumor necrosis factor- α (TNF- α) and interferon- β . Different signalling pathways are involved in this process such as TNF- α autocrine/paracrine signalling [101]. This shows the importance of miR-155 in the innate immune response which provides a critical first line of defence against pathogens.

Dendritic cells participate in the initiation of immunity and inflammation. Human monocyte-derived dendritic cells stimulated with LPS demonstrated high expression levels of miR-155. The mechanism of this is suggested to be that miR-155 targets Toll-like receptor/interleukin-1 (TLR/IL-1), which is supported by the observation that gene-deletion or 'knock-down' of miR-155 expression resulted in an increased expression of interleukin-1 β (IL-1 β) [102]. Further evidence of this

interaction is found by the addition of exogenous miR-155 which can suppress the expression of an NF- κ B reporter plasmid in cell lines [102].

T lymphocyte differentiation is associated with functional miR-155. For example, in mice with a gene-deletion of miR-155 (miR-155^{-/-}), the T lymphocyte differentiation is shifted towards T-helper 2 (Th2) lymphocytes, suggesting that miR-155 enhances the T lymphocyte differentiation towards T helper 1 (Th1) cells [85]. MiR-155 is also required for antibody production by B lymphocytes. For example miR-155^{-/-} mice vaccinated with attenuated *Salmonella* showed a switch in the antibody isotype class. Murine B cells lacking miR-155 generated reduced extrafollicular and germinal centre responses and failed to produce high-affinity IgG1 antibodies in comparison with wild type murine B cells [103].

Studies on mice deficient for bic/microRNA-155 demonstrated that these mice were immune-deficient and when challenged with *Salmonella typhimurium* they showed a reduction in survival, cell proliferation, IgG1 production, and IL-2 production, this indicated that miR-155 is required for proper function of T and B lymphocytes and dendritic cells [104]. Of relevance to this thesis, this report also described an age-related increase in lung airway remodelling for which no mechanism was described. Microarray analyses of activated human and murine CD4⁺ Th cells and CD4⁺CD25⁺ regulatory T cells determined an up-regulation of mature miR-155 which suggests that miR-155 is necessary for Treg cell mediated tolerance. The mechanism proposed was that miR-155 regulate the susceptibility of CD4⁺ Th cells to Treg cell-mediated suppression, In more details, CD4⁺ Th cells treated with miR-155 inhibitor demonstrated a much higher susceptibility to Treg-mediated suppression than control CD4⁺ Th cells, this was explained by the ability of miR-155 to mediate of IL-2 expression in CD4⁺ Th cells and induced cell proliferation resulting in that these CD4⁺ Th cells to become insensitive to Treg cell-mediated suppression [105].

MiR-155 is involved in regulation of inflammation and cell survival. Mir-155 has powerful anti-apoptotic function, and high expression of miR-155 in the cells led to suppression in FOXO3a, a gene member of the forkhead family of transcription factors related to cancer. This resulted in cell survival and chemo-resistance to multiple apoptosis inducing agents such as doxorubicin, paclitaxel, and VP-16 [106]. Furthermore, a raised expression level of miR-155 has been demonstrated in Hodgkins lymphoma and in diffuse large B cell lymphomas [107]. Transgenic mice overexpressing miR-155 in B cells develop a pre-leukemic pre-B-cell proliferative disorder resulted in the development of full B-cell lymphomas [108]. The function indicated by this over-expression of miR-155 indicates that it is potentially an oncogene when it is expressed disproportionately.

The expression of miR-155 is increased in breast cancer tissues compared with non-cancer tissues. The expression was positively associated with some clinic-pathological induces such as greater tumor grade, advanced tumor stage and metastases to lymph nodes, whereas it was negatively associated with overall and disease-free survival [109]. One study demonstrated that miR-155 might play a

potential role in TGF β induced epithelial-mesenchymal transition, cell migration and invasion by targeting RhoA. The authors proposed that miR-155 might be a potential therapeutic target for breast cancer intervention [110]. These data support the important role of miR-155 in inflammation, thus targeting miR-155 can be a potential mechanism for treatment of inflammatory diseases.

1.3 Pulmonary fibrosis

1.6.1 Introduction: idiopathic pulmonary fibrosis (IPF)

Pulmonary fibrosis was described in 1868 in a patient with chronic pneumonitis and bulbous fingertips, and this was the first formal recording as idiopathic pulmonary fibrosis (IPF) [111]. IPF is a devastating inflammatory disease of unknown etiopathogenesis characterized by progressive breathlessness [112]. Histologically the disease is characterised by fibrotic changes in the lung with excessive accumulation of fibroblasts and collagen production resulting in decline of alveolar function, and destruction of normal lung architecture [112, 113]; the incidence is increasing and there is no effective therapy [114]. IPF occurs mainly in older adults, the mechanisms that associate IPF with ageing are unknown, but it is proposed that epigenetic changes and abnormal developmental pathways may be involved [115]. IPF is characterised by short survival times of 3-5 years after diagnosis [116]. In the UK, the estimated survival time rate is worse than several types of cancer and increasingly more people will die each year from IPF [117]. Over the last 20 years the mortality rate for pulmonary fibrosis was increasing significantly in the USA [118], with a mortality rate of up to 50.8 per 1,000,000 of the population. The disease is distributed worldwide and affects approximately five million people [119]. Deaths with IPF are due to the consequence of fibrosis, for example respiratory failure, heart failure, ischemic heart disease, infection, bronchogenic carcinoma, and pulmonary embolism; with respiratory failure responsible for more than 80% of all deaths [120, 121].

1.3.2 Aetiology of IPF

The aetiology of idiopathic pulmonary fibrosis is unknown despite extensive investigation of this devastating disease. The development of pulmonary fibrosis appears to be related to several endogenous and exogenous factors, host factors such as age, genetic susceptibility, and family background. For example a genome wide scan study in Finnish families demonstrated a gene with unknown physiological function called engulfment and motility domain containing 2 (ELMOD2) which was a candidate gene for susceptibility to IPF [122, 123]. In addition there is involvement of some external predisposing factors including smoking, autoimmune processes, infection, environmental toxins, antigens and allergen, trauma and drug-induced reactions, metal and wood dust exposure, chemicals such as alkylating agents, pesticides, and ionizing radiation.

The lungs are constantly exposed to the environment and are therefore in contact with aero-environmental risk factors which may cause lung injury. Tobacco smoking is considered one of the high-risk predisposing factors for initiation and progression of IPF; the odds ratio for IPF in smokers compared with non-smokers was 2.3 [124].

Smoking is thought to participate in the development of IPF by increasing oxidative stress, this had been demonstrated in current and former smokers and reflected by lower survival reported for current and former smokers in comparison with non-smokers [125]. For example a study on IPF patients testing the effect of the antioxidant N-acetylcysteine suggested that the cellular redox state had an important involvement in the progression of disease. The suggested mechanism involved activation of growth factors and regulation of matrix metalloproteinases and protease inhibitors [126].

The involvement of genetic factors in IPF has been investigated. There is a family genetic component and development of IPF; approximately 3% of IPF cases are familial [127]. The genetic factor participates in the initiation and progression of IPF and this may be in response to common stressors in the shared familial environmental. Furthermore, heterogeneity of the disease observed within the families was depended on the nature of the stressors among this families [128]. It is highly possible that there is a synergy between genetic factors and environmental factor in disease susceptibility and progression.

Using genome-wide association study analysis, single nucleotide polymorphisms (SNP) have identified relationships with IPF e.g. SNPs in the cyclooxygenase 2 gene (COX2.3050 and COX2.8473) are associated with an increase in IPF by approximately 1.4 fold at age 30 [129]. Latent viral infections, such as the herpes virus family, have been demonstrated in IPF [130]. Examination of lung specimens from 33 IPF patients using PCR analysis demonstrated the presence of at least one of four herpesviruses:- cytomegalovirus (CMV), Epstein-Barr Virus (EBV), human herpesvirus 7 (HHV-7), and human herpesvirus 8 (HHV-8) in almost all patients [131].

Environmental exposures are associated with IPF initiation and progression. Occupational exposure to metal and wood dusts are associated with a significantly increased risk of IPF [132]. Also, exposure to inorganic particles such as silicon and aluminum were possible causes for IPF, shown in an autopsy study where the presence of high concentrations of silicon and aluminium were found in the hilar lymph nodes of IPF patients [133].

1.3.3 Pathogenesis of IPF

The pathogenesis of IPF is unresolved. There are numerous mechanisms suggested to be responsible for the initiation and development of IPF, and it is likely that more than one mechanism is involved. Furthermore, IPF itself may be a diagnosis of overlapping disease syndromes, increasing the difficulty of identifying a simple causal mechanism. Typically, the initiating factors are unknown, but could be considered for the moment as a combination of accumulated environmental and susceptibility factors. It is easier to examine the consequences of these.

Disturbances in the wound healing process leads to development of pulmonary fibrosis; generally the wound healing process include four steps [134].

- (1) Clotting and coagulation;
- (2) Migration of an inflammatory cell;
- (3) Migration, proliferation and activation of fibroblasts; and
- (4) Tissue remodelling and resolution (Figure 1.10)

In addition, the basement membrane of the alveolar–capillary barrier loses its integrity, with the collapse of alveolar structures, fusion of their basement membranes, and hyperplasia of type II epithelial cells and dysregulation of extracellular matrix formation [135].

IPF may be considered as a response to injury that comprises fibrosis and excessive extracellular matrix (ECM) deposition mediated by activation and proliferation of fibroblasts [86]. The histology of IPF is characterised by abnormal lung tissue remodelling accompanied by up-regulation of matrix metalloproteinase-1 (MMP-1), which is the prototype of some of the MMPs capable of degrading fibrillar collagens types I, and III [136]. This study demonstrated that polymorphisms of the MMP-1 promoter correlated with increased risk for IPF and exhibited a putative gene-environment interaction such as with smoking. A relationship between IPF and oxidative stress resulting from smoking was demonstrated [89], therefore, the use of therapeutic antioxidants may restore cellular redox balance, thereby regulating MMPs, growth factors, and protease inhibitors [126]

A proposed mechanism is through epithelial-mesenchymal transition occurring for alveolar type II epithelial cells. The process involves transition of epithelial cells into mesenchymal cells for example fibroblasts and myofibroblasts. For example, Addition of TGF- β 1 to rat alveolar epithelial cells induces cell mesenchymal transition *in vitro*. The process manifested by losing of epithelial cell type specific markers for example E-cadherin and gain mesenchymal cell markers such as an increased expression of α -smooth muscle actin (α -SMA) [137]. This process is accompanied by increasing fibroblast proliferation, extracellular matrix protein deposition, accumulation of inflammatory cells and excessive generation of pro-fibrotic mediators [138]. The main components involved in the pathogenesis of IPF are illustrated in (Figure 1.11).

One causal mechanism proposed for IPF is the disturbances in surfactant protein (SP)-C folding [139]. Mutations in SP-C resulted in protein misfolding and deposition of misfolded aggregated SP-C resulted in abnormal endoplasmic reticulum stress. The consequential increased production of reactive oxygen species then cause DNA damage and contributed to IPF.

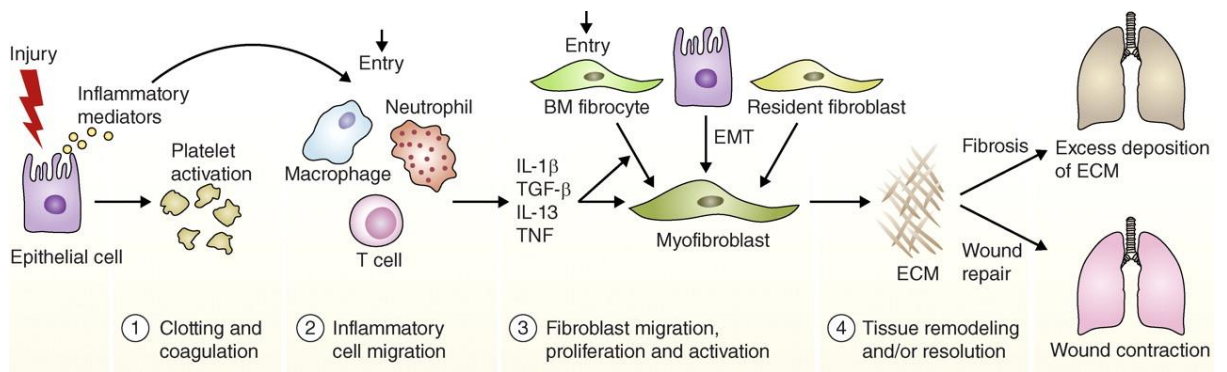


Figure 1.10 Stages of the wound healing process
Wound healing includes four steps; (1) clotting and coagulation; (2) migration of an inflammatory cell; (3) migration, proliferation, and activation of fibroblast; and (4) tissue remodelling and resolution (copied from [134] with permission).

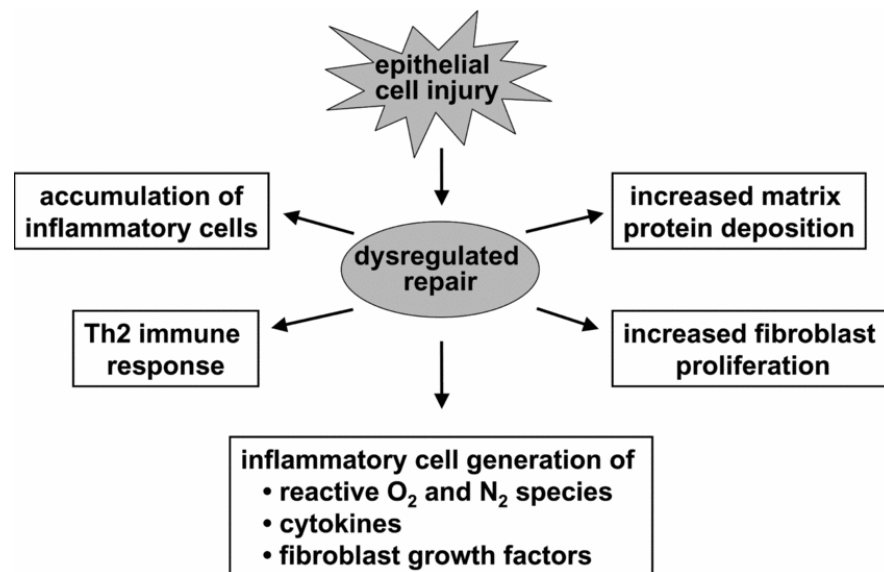


Figure 1.11 Main components involved in the IPF pathogenesis
Dysregulation repair process following epithelial cell injury leads to IPF. The process involves an increase in fibroblast proliferation, an increase in matrix protein deposition, accumulation of inflammatory cell with a Th2 immune response, and excessive production of pro-fibrotic mediators (copied from [138] with permission).

1.3.4 Collagen and pulmonary fibrosis

Collagen is the fibrous protein constituent of bone, cartilage, tendon, and other connective tissue. It is the most abundant tissue protein of mammals. The total

amount of collagen in tissue depends on the balance between collagen synthesis and catabolism. There can be an imbalance between these two regulatory processes in some remodelling diseases in which fibroblasts produce more collagen than is degraded [140]. Collagen types I, III, IV, and V can be demonstrated in healthy and fibrotic human lungs. Generally their localisation in the lung varies, for example collagen type I is mainly found in the interstitium of alveolar septa, collagen type III is more abundant and is found in alveolar septa and a perivascular, collagen type IV is found in alveolar and capillary basement membranes, and collagen type V is found in the interstitium [141].

Collagen is the most abundant protein produced in the lungs and it is produced during the normal growth and repair processes. Excessive deposition in the lung is the main characteristic feature of IPF. Type I collagen (COL1 gene) is considered the main fibrous collagen synthesized by wound fibroblasts during the repair process [142]. During lung fibrosis there is an increased amount of collagen type I in thickened alveolar septa, with a reduced amount of collagen type III. There are no changes in collagen type IV, but an increase in collagen type V was observed in the interstitium and in areas of smooth muscle cell proliferation [141].

Measurement of collagen metabolism is important in evaluating of the fibrosis in IPF patients. Analysis of IPF patients serum demonstrated an increase in the concentration of the 7S domain (7S collagen) of type IV collagen compared with serum from healthy people or people with other non-fibrotic pulmonary diseases [143]. Inhibiting collagen synthesis has a beneficial effect on fibrosis.

Administration of antisense oligonucleotides (AS60) to type I collagen on a human skin organ culture had a protective effect as shown by a reduction in the mRNA expression and translation of collagen type I [144].

1.3.5 Fibroblasts and pulmonary fibrosis

Many cells participate in the progression of pulmonary fibrosis, for example fibrocytes which are bone marrow-derived mesenchymal progenitor cells that can differentiate into fibroblasts, myofibroblasts and adipocytes [145]. Increased numbers of circulating fibrocytes have been found in the peripheral blood of mice in response to the bleomycin injury [146]. Fibrocytes produce proteins and glycoproteins which participate in tissue remodelling including collagen types I and III, vimentin and matrix metalloproteinases. Fibrocytes isolated from wounds of animal models of wound repair expressed mRNA for IL-1 β , IL-10, TNF- α , monocyte chemoattractant protein (MCP), macrophage inhibitory protein-1 α (MIP-1 α), macrophage inhibitory protein-1 β (MIP-1 β), MIP-2, platelet-derived growth factor-A (PDGF-A), TGF- β 1, and M-CSF [147].

It is widely accepted that activation in fibroblast foci and epithelial injury are key regulatory components that trigger a cascade of changes leading to

reorganization of pulmonary tissue compartments [148]. Phenotypic characteristics of pulmonary fibroblasts, for example, their migratory and contractile properties participate in relocation of the lung fibroblast to wound areas resulting in an increase in fibrogenesis [149]. Fibroblasts cooperate with inflammatory cells to regulate fibrosis. Inflammatory cytokines, mediators and growth factors act directly on fibroblasts to induce proliferation and differentiation, therefore, the interaction between fibroblasts, inflammatory cells, parenchymal, and pulmonary epithelial and endothelial cells is important during fibrosis as illustrated in (Figure 1. 12) [150].

Activation of fibrocytes results in their differentiation into fibroblasts. Fibroblasts are key cells involved in wound healing and fibrosis. They are characterised by their ability to produce extra cellular matrix (ECM) and to differentiate into myofibroblasts which participate in the contraction of wound edges and closing the injured tissue [151]. In IPF, the fibroblasts differentiate into myofibroblasts which are characterised by having a greater contractile and stronger pro-fibrotic activity. These myofibroblasts can differentiate from resident lung fibroblasts or they may be derived from epithelial cells through a process of epithelial-mesenchymal transition [152].

Excessive myofibroblast differentiation including production of extracellular matrix components such as collagen I, III and fibronectin results in dysregulation in lung repair and remodelling [153].

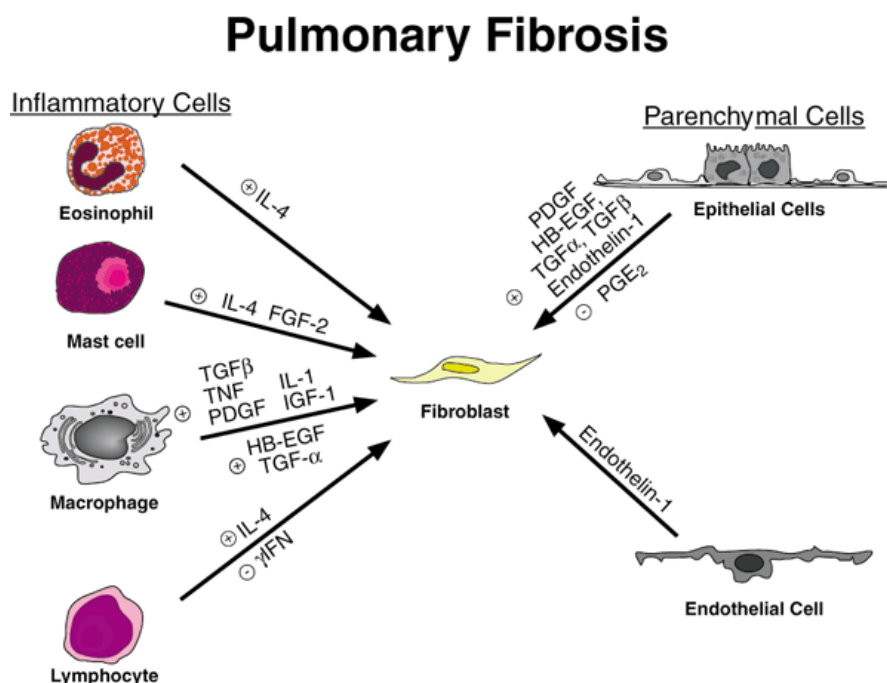


Figure 1.12 Main cells involve in pulmonary fibrosis
Fibroblasts are the central cell in pulmonary fibrosis and their interaction with inflammatory and parenchymal cells is essential in the course of the disease (copied from [150] with permission).

1.3.6 Pulmonary immune and inflammatory cells in the lung

It is unresolved whether inflammation is a necessary and sufficient prerequisite for IPF. However IPF is characterised by the involvement of inflammation and different kinds of immune and inflammatory cells may participate in the initiation and continuation of the disease. These immune and inflammatory cells include macrophages, lymphocytes, dendritic cells, and mast cells [150]. Macrophages are characterized by their production of a wide range of inflammatory mediators in response to stimulation. For example, in experimental models of pulmonary fibrosis stimulated by administration of bleomycin, lung macrophages produce mediators including TGF β 1 and TNF- α [154]. Macrophages are involved in the development of IPF. BAL alveolar macrophages from IPF patients have a reduced apoptotic rate that did not correlate with a reduction in the expression of mediators involved in the apoptotic pathways [155].

Generally, IPF is characterised by an inflammatory response dominated by a helper T-cell (Th2-type) response and a shift to alternatively activated (M2) macrophages that normally control extracellular matrix and wound healing [156]. M2 macrophages are thought to be important for resolving inflammation and in the wound repair process. They produce anti-inflammatory cytokines such as interleukin-1 receptor antagonist (IL-1Ra) and pro-fibrotic cytokines such as TGF β [157]. Also M2 macrophages markedly express tissue inhibitors of metalloproteinase that inhibit MMPs and impair remodelling of excess deposited ECM [158].

There is some controversy concerning the role of T lymphocytes in IPF. Conflicting data suggested they have either a pro-fibrotic, an anti-fibrotic, or a neutral role in pulmonary fibrosis [159]. A recent study has suggested that IPF is an immunologic disease, because they demonstrated that lymphocytes can directly damage the lung tissue [160]. In a screening study of IPF patients, blood CD4 lymphocytes had significant down-regulation of CD28 in response to repeated antigen-driven proliferation *in vitro*, and these cells were characterised by an increased production of pro-inflammatory cytokines and cytotoxic mediators, which were associated with a poor prognosis for the IPF patient. In another study, regulatory CD4+CD25+FOXP3+ T cells (Treg) in the BAL of IPF patients had an impairment of their suppressor effect on helper T-cell type 1 and 2 cytokine secretion [161].

Dendritic cells (DCs) participate in sustaining the chronic inflammation of IPF by producing pro-inflammatory mediators. In lung tissue of IPF patients with advanced disease, there is an accumulation of DCs in the pulmonary parenchyma and in areas of epithelial hyperplasia and established fibrosis [162]. There is an increased absolute count and relative proportion of neutrophils in BAL of IPF patients which is associated with early mortality [163]. Increased numbers of mast cells have been demonstrated in lung tissue sections of IPF patients, but their role in pathogenesis is still unresolved. Studies on human mast cells identified that they are a source of some pro-fibrotic factors for example TGF β and tryptase [164]. However bleomycin can induce fibrotic responses equally in wild type and mast

cell deficient mice strains (our own unpublished data and [165]), suggesting a non-essential role. However, how this observation applies to humans is unknown.

1.3.7 Inflammatory mediators in IPF

Fibrogenic cytokines and growth factors are important mediators involved during the course of IPF. Mediators such as platelet-derived growth factor (PDGF), TNF- α , and TGF β 1 can mediate recruitment and phenotypic modulation of fibrocytes, fibroblasts and myofibroblasts [148]. TGF β 1 is an important mediator in IPF. It regulates the differentiation of pulmonary fibroblasts into myofibroblasts, as seen by their expression of smooth muscle actin (SMA), and by their increased tissue fibrogenesis and migratory activities [142].

IL-1 β is an important pro-inflammatory cytokine. Animal experiment performed on rat models of IL-1 β induced fibrosis demonstrated high expression levels of pro-inflammatory and pro-fibrotic mediators e.g. TNF- α , IL-6, PDGF, and TGF- β 1, associated with progressive fibrotic changes in the lung manifested by accumulation of fibroblasts, myofibroblasts, collagen and fibronectin [166].

TNF- α , a potent pro-inflammatory cytokine with an involvement role in IPF. Animal model of bleomycin-induced pulmonary fibrosis using TNF- α ^{-/-} mice demonstrated intense and persistent inflammation due to reduced apoptosis of inflammatory cells. Administration of exogenous murine recombinant TNF to these mice lead to elimination of inflammatory cells from the bronchoalveolar space by apoptosis and improved tissue repair of damaged lungs [167].

Chemokines and their receptors have been demonstrated in IPF. MCP-1/CCL2 and MIP-1 α /CCL3 are pro-inflammatory chemokines produced by macrophages, lymphocytes and fibroblasts which can regulate monocyte recruitment. CCL2 and CCL3 are up-regulated in BAL fluid of mice with bleomycin-induced lung fibrosis and of IPF patient [168].

The major pro-inflammatory and pro-fibrotic mediators that participate in fibrosis are illustrated in (Figure 1.13).

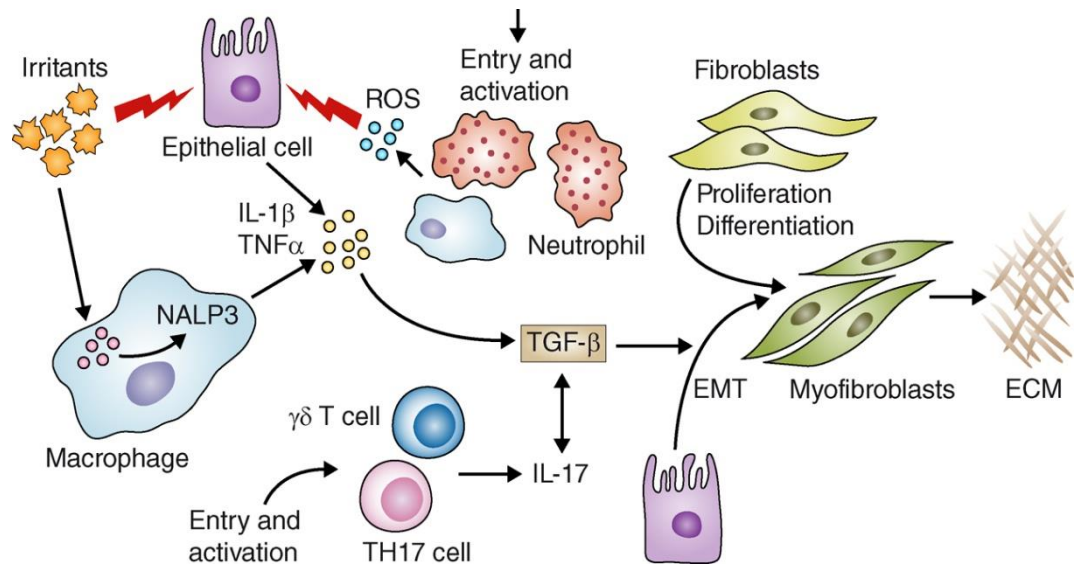


Figure 1.13 Major pro-inflammatory and pro-fibrotic mediators that participate in fibrosis Entry of irritants such as bleomycin lead to injury of lung epithelial cells and this may be detected by the Nalp3 inflammasome in macrophages. Irritants also stimulate the production of inflammatory mediators (cytokines, chemokines, and ROS). These mediators potentiate leukocyte recruitment and activation. For example, IL-1 β can induce the activation of ROS-expressing neutrophils resulting in addition destruction of epithelial cells. IL-1 β also promotes production of TGF β 1 which can 1- Stimulate fibroblast proliferation and differentiation. 2- Stimulate epithelial-mesenchymal transition resulting in the formation of ECM-producing myofibroblasts. 3- Stimulating the differentiation of Th17 resulting in promotion of inflammatory process (copied from [134] with permission).

1.3.8 Symptoms and Diagnosis

The lung has considerable functional reserve and elasticity which helps to compensate for any decrease in oxygen tension or tissue damage. This reserve means that there can be extensive lung damage before symptoms become apparent. During conditions for example in pulmonary fibrosis the lungs lose elasticity because of the deposition of excess collagen, and the consequent thickening or the alveolar walls restricts gas transfer resulting in shortness of breath. The symptoms of IPF include cough and progressive dyspnoea.

As the symptoms and signs of IPF are common symptoms of many forms of respiratory disease, the diagnosis depends on the recognition of a pattern of symptoms and signs followed by more specific tests. Auscultation demonstrates fine end-inspiratory crackles on the basal areas. Lung physiological tests are used to demonstrate decreases in the partial pressure of oxygen in the blood (PaO₂) and an impairment in gas exchange [135]. A tentative diagnosis can be performed using histo-pathological investigation and imaging, for example, high-resolution computed tomography (HRCT) scan [114].

Histo-pathologically, the affected areas are subpleural and in the para-septal parenchyma. Fibrotic lung tissue sections show a heterogeneous appearance with

areas of fibrosis in comparison with the other areas of normal or less affected parenchyma. The fibrotic changes manifested by deposition of dense collagen, and fibrotic foci consist mainly of fibroblasts and myofibroblasts. The inflammatory changes are characterised by an infiltration of lymphocytes, plasma cells, hyperplasia of type 2 pneumocytes and bronchiolar epithelium. HRCT demonstrates these changes as honeycombing; basilar and sub-pleural reticular abnormalities and opacities [114].

Investigating serum biomarkers such as Krebs-van-den-Lungen KL-6, a high MW glycoprotein (MUC1 mucin), has been of diagnostic value. Serological examination performed on IPF patients demonstrated an increase in the level of circulating KL-6. These levels can predict the increased risk of subsequent mortality [169]. Similarly, plasma concentrations of osteopontin (OPN), a fibrogenic cytokine produced by alveolar macrophages has been investigated in IPF patients. Plasma levels of OPN correlate inversely with arterial oxygen tension in IPF patients [170]. Measuring matrix metalloproteinase (MMP) concentration can help in the demonstration of asymptomatic IPF and correlated with prognosis. The analysis of IPF patients exhibited an increase in the level of MMP1 and MMP7 in BAL and plasma [171].

1.3.9 Treatment

There are few specific treatments available for IPF and none that are curative. Since there is no specific treatment, the main goal is to suppress the progression and control the symptoms of the disease. Treatment options depend on the stage and severity of the disease.

Corticosteroids are characterised by their ability to limit acute inflammation. They inhibit lymphocyte and neutrophil migration into the lung and alter alveolar macrophage function. There is no clear long term beneficial effect on IPF patient survival in response to treatment with corticosteroids alone or in combination with other agent. Current evidence suggests that using corticosteroid alone is not indicated in the treatment of IPF [172]. The other main therapy is N-acetylcysteine, as a mucolytic agent which characterised by its anti-oxidant properties. Disturbances in oxidant/anti-oxidant balance may be one of the mechanisms for alveolar cell injury and controlling this by using a high dose of acetylcysteine, a precursor of the antioxidant glutathione, in addition to prednisone and azathioprine, preserves vital capacity and carbon monoxide diffusing capacity (DLCO) in patients with IPF better than single drug standard therapy [173].

Targeting proteins involved in the development of IPF is another therapeutic approach. TGF- β 1 is a powerful pro-fibrotic, pro-inflammatory, and immunomodulatory cytokine. TGF β 1 is involved in the dysregulation of tissue repair resulting in an increase in synthesis of extracellular matrix accompanied by inhibition of matrix degradation. Targeting of inflammatory pathway steps

downstream of TGF- β 1 activation induced c-Abelson (c-Abl), a proto-oncogene and Imatinib, a tyrosine kinase inhibitor and inhibitor of c-Abl, exhibited a beneficial effect preventing pulmonary fibrosis in a murine model of bleomycin induced fibrosis. However, Imatinib was unable to prevent IPF progression in a phase II/III study of patients [135]. Recently, pirfenidone (5-methyl-1-phenyl-2-[1H]-pyridone) a new potential anti-inflammatory, anti-fibrotic and antioxidant drug that acts by inhibiting TGF- β has been tested. A study on IPF patient demonstrated that treatment with pirfenidone may decrease the rate of decline in vital capacity (VC) and may increase the progression-free survival (PFS) time over 52 weeks [174]. Another promising molecule is Galectin-3, a β -galactoside binding lectin highly expressed in fibrotic tissue of diverse diseases. A study of murine bleomycin models of lung fibrosis using galectin-3^{-/-} mice or mice treated with a novel inhibitor of galectin-3, TD139, demonstrated an inhibition of TGF β 1-induced EMT and myofibroblast activation and blocking of collagen production [175].

Recently, more studies have been looking to determine a number of potential molecular therapeutic targets for IPF such as endothelin-1 (ET-1), a vasoconstrictor and mitogenic peptide [176], studies in humans have determined that ET-1 is a mediator in IPF, therefore, targeting of this molecule is beneficial. Bosentan, a nonselective endothelin receptor antagonist approved in the USA and Europe for the treatment of patients with pulmonary arterial hypertension. Recent trial study demonstrated that there was no significant difference between IPF patient treated with treatment with Bosentan and placebo groups for time to death or to IPF worsening [177].

Lung transplantation is the final resort in severe IPF. This procedure has considerable risk in patients over 60 years and since the average age of IPF is around 70 years, therefore, only a small proportion of IPF patient may benefit with the emphasis in treating younger patients [178]. Good supportive care should be provided for IPF patients and this includes oxygen therapy, pulmonary rehabilitation, and use of analgesia.

1.3.10 Animal models of pulmonary fibrosis

The use of experimental animal models of fibrosis provides an opportunity to test the key aspects to improve the understanding of the pathogenesis of human IPF. We recognise that there are differences between IPF in human and animal models of fibrosis, however, using these models is one of the few research opportunities available. Different models have been demonstrated in animals, e.g. administration of bleomycin, fluorescein isothiocyanate, or silica, or by irradiation, or by transgenic expression of pro-fibrotic molecules including by viral vectors, and by adoptive cell transfer [179].

Bleomycin-induced pulmonary fibrosis is the most widely used experimental model in animals. Bleomycin is an antibiotic generated by *Streptomyces verticillus* and

was discovered in 1966. It had limited anti-bacterial activity but had useful anti-tumour ability and was developed for treating different types of tumours [180]. The main side-effect of treatment with bleomycin was the development of interstitial pulmonary fibrosis [181]. Because of this, bleomycin has been used in different species such as mouse, rat, dog, hamsters, rabbits, guinea pigs, and primates using different doses administered via different routes e.g. intraperitoneal, intravenous, subcutaneous, or intra-tracheal resulting in a pathological response that includes alveolar epithelial damage, consolidation of alveoli, fluid and plasma proteins leakage into the alveolar space, formation of hyaline membranes, type I epithelial cells necrosis, and type II epithelial cells metaplasia. Inflammatory infiltrates, and fibrosis develops in sub-pleural regions [179]. The acute inflammation starts within hours of administration followed by fibrosis which develops commonly over a 2 to 3 week period [182].

Fluorescein isothiocyanate (FITC)-induced pulmonary fibrosis is induced after intra-tracheal installation of FITC. This results in development of inflammatory changes for example, infiltration of granulocytes, T lymphocytes in areas of FITC deposition associated with subsequent development of pulmonary fibrosis [183]. One advantage of this model is the ability to visualise areas where deposition occurs by using fluorescence which shows that the fibrotic changes occurred only in areas of FITC deposition and also that the fibrotic response continued for more than 6 months [183].

Silica induced pulmonary fibrosis is another experimental model of pulmonary fibrosis that is considered to replicate occupational fibrosis found in stone masons. The model is induced by instilling silica particles into the lung which causes tissue damage associated with the inability of phagocytes to remove these particles, resulting in sustained inflammatory and fibrotic processes [182]. The use of silica in animals caused the development of a slowly progressive form of pulmonary fibrosis accompanied by granulomatous inflammation. This model requires a longer time period than bleomycin to develop pulmonary fibrosis. Several months were required to develop the same degree of fibrosis as that achieved by bleomycin in weeks. The advantage of this model is from the dependence of this model on macrophages and other mononuclear phagocytes; the fibrosis is demonstrated as fibrotic nodules that develop in areas of silica deposition [184, 185].

Irradiation-induced pulmonary fibrosis is performed by exposure to a single dose of 12.5 Gy irradiation to the thorax resulting in pulmonary fibrosis at 26 weeks [186]. The fibrotic response in animals depends on the irradiation dose and their genetic background [187]. Histological examination of nine strains of mice exposed to irradiation demonstrated differences between strains in the focal fibrosis, the development of hyaline membranes and the fibrin concentration in oedema fluid. The inflammatory and fibrotic processes are characterised by sub-pleural foci of collapsed alveolar walls with collagen deposition, the fibrotic response was stronger in C57 strains than the rest of experimental strains. TGF β and TNF- α have been implicated as important signals in the development of

irradiation-induced fibrosis [188, 189]. One advantage of this model is the different response depending on the genetic background.

Models of pulmonary fibrosis can be induced by transfer of transgenic mediators into laboratory animals. These transgenic models show the importance of the continuous expression and production of the mediators coded by the transgene to the patho-physiological fibrotic changes. An alternative method of transgenic delivery using vectors such as adenoviral vectors provides a more transient production of the mediator potentially involved in the processes of fibrosis. For example adenovirus-mediated gene transfer techniques were used to transfer some of the highly expressed growth factors, cytokines, and chemokines such as TGF β which had been determined to cause a strong fibrotic lung injury in rodents. These viruses are highly tropic for epithelial cells with low transfection efficiency for other cell types found in the lung. Rat lung transfected with replication-deficient adenovirus vectors transferring the cDNA of TGF β 1 resulted in high expression of TGF β 1 accompanied by severe fibrosis and excessive deposition of collagen, fibronectin, and elastin [190]. Using this model helps to determine the effect of a single potentially inducible gene product on fibrosis. However, this model is limited by the immunogenicity of these vectors, thus preventing repeated dosing.

Adoptive transfer of human cells into immune-deficient mice provides another potential model of pulmonary fibrosis. Human fibrocytes passively transferred into the mouse can migrate into the lung after challenge with bleomycin and can be shown to participate in lung remodelling [191]. While none of the animal models mentioned above have the ability to show all of the main characters of usual interstitial pneumonia, the pathologic correlate to IPF, these models are important because they provide an experimental model for understanding the mechanisms involved in the pulmonary fibrosis and also provide an opportunity to test a new therapeutic drug.

1.3.11 IPF: The clinical unmet need

The incidence of IPF is greater than that of ovarian cancer, similar to those of pancreatic cancer and of all leukemias combined, and nearly 30 times that of cystic fibrosis. An estimated 100,000 people are living with IPF in the United States, and more than 30,000 new cases are diagnosed annually. In UK approximately 5000 people are diagnosed annually and the incidence has been rising; from 1 per 100,000 of the population in 1991-5, to 1.5 from 1996-1999, to 2.5 from 2000-2003. Currently the incidence in Scotland is 5.7 per 100,000, making it one of the highest in the world.

There is no effective therapy for IPF and this represents an increasing clinical unmet need. The necessary development of new therapies is limited by our lack of understanding of the disease process. We recognise that there is limited empirical

evidence to support a role for LXR in a fibrotic process; however, we feel that there is sufficient to justify this project. Our approach is novel and will therefore generate new data. We will keep the focus of new findings on the potential benefits to patients.

1.4 Hypothesis and Aims

Hypothesis: We hypothesised that LXRs can modulate bleomycin-induced pulmonary fibrosis.

Aims: To test this hypothesis, I tried to achieve the following aims:-

- 1- My first aim was to validate the model by determining the optimum experimental condition for murine bleomycin-induced pulmonary fibrosis. I aimed to achieve the following:-
 - A- Evaluate the time course require to get the optimum inflammatory and fibrotic changes.
 - B- Select the dose of LXRs agonist GW3965 required to investigate the effects on the severity of the pulmonary fibrosis.
 - C- Understand the effect of LXR agonist GW3965 and the vehicle excipient Cremophor on the wild type mice given PBS.
 - D- Validate the accuracy of gene deletion for LXR $\alpha\beta^{-/-}$ mice.
- 2- Determine the correlation of single or double Liver X Receptors activation and the development of lung fibrosis in murine model of pulmonary fibrosis.
- 3- Demonstrate the role of MicroRNA-155 in the course of pulmonary fibrosis in a murine model of pulmonary fibrosis.

To achieve these aims I used an experimental model of murine pulmonary fibrosis which occurs after administration of bleomycin sulphate. This was tested under different experimental conditions and using a variety of gene-deleted mice strains. These are outlined in the following Material section and in more detail is each Results chapter section.

2. Materials and Methods

2.1 General materials

Chemicals: The chemicals used in these projects were purchased from Sigma (Dorset, UK) unless otherwise mentioned.

Plastics: The plastic ware used in these projects were purchased from Corning and Gibco (Corning, NY, USA) unless otherwise mentioned.

2.2 General buffers & reagents

Complete medium RPMI 1640: Consists of RPMI1640 Invitrogen (Paisley, UK), 10% foetal calf serum, L-Glutamine (2mM), Penicillin (100 units/ml) and Streptomycin (100 µg/ml).

Wash medium: Consists of RPMI1640 (Invitrogen), L-Glutamine (2mM), Penicillin (100 units/ml) and Streptomycin (100 µg /ml).

Complete medium DMEM: Consists of Dulbecco's Modified Eagle's Medium (Sigma), 10% foetal calf serum, L-Glutamine (2mM), Penicillin (100 units/ml) and Streptomycin (100 µg/ml).

Complete medium RPMI: Consists of RPMI 1640 (Invitrogen), 10% heat inactivated foetal bovine calf serum, Penicillin (100 units/ml), Streptomycin (100 µg/ml) and L-Glutamine (2 mM).

Trypsin EDTA: Consist of trypsin EDTA 0.05% (Invitrogen).

Bleomycin: Bleomycin sulphate, from *Streptomyces verticillus* (Sigma) was dissolved in PBS at a stock 1mg/ml. A dose of 0.1mg in 30 µl per 25 g mouse, was used *in vivo* administrated by intranasal installation under anaesthesia.

LXR agonist: GW3965 was synthesised and donated by Schering-Plough Corporation (Hertfordshire, UK) and supplied in 2 g vials. This was dissolved in 5% Cremophor (Sigma)/ PBS as excipient and used in doses for daily administration *in vivo* by intraperitoneal injection. For the *in vitro* work the agonist were dissolved in DMSO Riedel-de Haen (Hanover, Germany).

PBS: Phosphate buffered saline (Invitrogen).

ELISA wash buffer: 0.05% Tween 20 in PBS.

Trypan blue solution: Stock 0.4 g Trypan blue solution (0.4%) was purchased from (Sigma). This was diluted 1:10 with PBS before use.

0.1 M Bicarbonate buffer (100 ml): 0.84 g sodium bicarbonate (NaHCO₃) was dissolved in a final volume of 100 ml dH₂O and stored at 4°C.

1 N HCL (100 ml): 8.33 ml of 12 N HCL was added slowly to 91.67 ml deionised water and mixed well.

1.2 N NaOH/0.5 M HEPES (100 ml): 12 ml of 10 N NaOH was added to 75 ml deionised water to which was added 11.9 g HEPES and mixed well.

2.5 N Acetic Acid/10 M Urea (250 ml): 150.2 g urea was added to 100 ml deionised water and mixed well until dissolved. To this was slowly added 35.9 ml glacial acetic acid then bring the final volume to 250 ml with deionised water.

2.7 N NaOH/1 M HEPES (250 ml): 67.5 ml of 10 N NaOH was added to 140 ml deionised water and mixed well, then 59.5 g HEPES was added and the final volume was brought to 250 ml with deionised water.

Tris-acetate-EDTA (TAE) buffer: 50 X TAE stock solution was made by dissolving of 242 g of Tris base in 750 ml dH₂O. Mixed well then added to 57.1 ml glacial acetic acid and 100 ml 0.5 M EDTA (pH 8.0). The final volume was then made up to 1 litre with dH₂O. The working concentration was made by diluting this buffer 1:50 with dH₂O.

Liquid broth (LB medium, Sigma): Prepared by dissolving 10 g tryptone, 5 g yeast extract, 10 g NaCl, and 15 g agar in one litre of distilled water. This was mixed well until all the components were dissolved completely, then sterilized by autoclave and stored at 4°C until use.

Nutrient agar plates: 10 ml of liquid broth with 100 µg/ml ampicillin was poured into Petri dishes and left to set at room temperature until it solid then stored at 4°C until use.

2.3 *In vivo* work

2.3.1 Animal husbandry

Animals were housed in the Biological Services Joint Research Facility (JRF) at the University of Glasgow. All animals were kept in a pathogen free environment with free access to food and water. The procedures were carried out using an approved personal licence by the United Kingdom Home Office and in accordance with the Animals (Scientific Procedures) Act 1986.

2.3.2 Mice

C57BL/6 mice: Male mice were purchased from Harlan (Blackthorn, UK) and allowed to adapt under quarantine for one week before the procedures were carried out.

LXR null mice: LXR $\alpha^{-/-}\beta^{-/-}$ double knockout mice were bred in house from LXR $\alpha^{-/-}$ and LXR $\beta^{-/-}$ mice and wild-type (WT) littermates on a C57BL/6 background. The single knockout mice were generated by Lexicon (The Woodlands, TX, USA) and supplied by Schering Plough Corporation (UK).

LXR $\alpha^{-/-}\beta^{-/-}$ double knockout mice were generated following a schematic breeding programme which included crossbreeding of LXR $\alpha^{-/-}$ mice with LXR $\beta^{-/-}$ mice resulting in the generation of LXR α/β heterozygotes, which were confirmed by a

PCR demonstrating of genomic DNA for LXR genotype. These heterozygote mice were self-crossed resulting in the generation of $LXR\alpha^{-/-}\beta^{-/-}$ mice of both sexes, which was confirmed by PCR demonstrating the $LXR\alpha$ and $LXR\beta$ genotypes. Other genotypes were identified but they were not of interest for our study. $LXR\alpha^{-/-}\beta^{-/-}$ mice were selected and crossbred to generate more breeding pairs, which were screened by PCR to confirm the absence of both $LXR\alpha$ and $LXR\beta$ before setting up breeding colonies.

Mir-155 null mice: Male microRNA-155^{-/-} knockout mice (miR-155^{-/-}) mice on a C57BL/6 background were purchased from Jackson Laboratories (Bar Harbor, ME, USA). MiR-155^{-/-} mice were backcrossed with C57BL/6 to get WT control littermates. Both strains then were bred in-house in a pathogen-free facility [44]. The absence of miR-155 confirmed by PCR and by experimentation.

Justification of numbers of mice used power analysis: the purpose of a power analysis is to minimise type 1 and type 2 errors. This requires an estimate of variability in the primary end-point which is day 18 fibrosis. There are many publications describing the bleomycin-induced model of lung fibrosis but none to our knowledge which addresses this issue. This is similar to the use of the collagen-induced arthritis model. This suggests that group numbers are decided by pragmatism; based on our experience. We and others find that the bleomycin model is highly variable and our experience is that minimum group numbers of 8 are required to show effects.

2.3.3 Administration of PBS or bleomycin in C57BL/6 mice

Choice of species: I am fully committed to the concept of Replacement, Refinement and Reduction as an ethical and humane framework for conducting scientific experiments using animals. Mice are the least sentient species in which auto-immune and inflammatory models have been developed. Their use is a refinement of the use of higher animals.

Choice of models: Mice don't normally develop interstitial lung disease. This model therefore requires stimulation or disruption of cells or molecules involved in inflammation. Administration of bleomycin is the most commonly used model. We used the most up-to-date refined protocols that are widely accepted by the scientific community to represent human interstitial lung disease.

Minimising animal suffering: We have several measures in place in order to reduce animal suffering, including daily monitoring.

Male C57BL/6 mice were purchased at 7-8 weeks old. On day zero of the experiment the mice were anaesthetised using isoflurane inhalation in an anaesthetic chamber. Mice were then given intranasally (i.n.) either 0.06 mg bleomycin in 30 μ l PBS or 30 μ l PBS as control [192]. The mice were observed daily and body weight were recorded until day 32 in the time course experiments, or more typically on day18 when the mice were culled.

2.3.4 Administration of different doses of LXR agonist GW3965 or vehicle Cremophor in C57BL/6 mice given bleomycin

Different doses of LXR agonist (GW3965 in 5% Cremophor/PBS) or vehicle (excipient 5% Cremophor /PBS) were administered daily to male C57BL/6 mice for 3 days before they were given bleomycin intranasally and then each day thereafter. The mice were divided into three groups (n=10 per group), 10-12 week old and 23-25 g weight. Three days prior the experiment mice were given daily intraperitoneal injections of 3 mg/kg LXR agonist, 30 mg/kg LXR agonist or vehicle which continued until the end of the experiment. On day zero of the experiment all animals were anaesthetised using isoflurane in an inhalation anaesthetic chamber. Then mice were then given intranasally 0.06 mg of bleomycin sulphate in 30 μ l PBS / 25g mouse. The mice were monitored daily for wellbeing and changes in body weight until day 18 when the mice were culled. The following table illustrate the typical samples collected at a cull (Table 2.1).

Sample	Usage
Lung tissue	Histology (H&E and Trichrome stain) Soluble collagen content mRNA expression by PCR
Bronchoalveolar lavage	Cytology (total and differential cell count) Fluid cytokines
Blood	Serum cytokines

Table 2.1 Typical samples collected on a cull day

2.3.5 Experimental detail of bleomycin-induced pulmonary fibrosis in LXR $\alpha^{-/-}\beta^{-/-}$ double knockout and LXR $\alpha\beta$ wild type mice

Bleomycin-induced pulmonary fibrosis is widely used as model for human pulmonary fibrosis. It was first described by Adamson and colleague [193]. 10-12 weeks male LXR $\alpha^{-/-}\beta^{-/-}$ and LXR $\alpha\beta$ wild-type mice were used for bleomycin-induced pulmonary fibrosis.

Mice were allocated to 4 groups (n=19-23 mice per group):-

A- WT treated with vehicle (control)

B- WT treated with LXR agonist

C- LXR α ^{-/-} β ^{-/-} treated with vehicle

D- LXR α ^{-/-} β ^{-/-} treated with LXR agonist

On the day of induction (day zero) mice were anaesthetised using isoflurane inhalation in an anaesthetic chamber. All animals were given bleomycin sulphate (Sigma) intranasally at concentration of 0.06mg in 30 μ l PBS / 25g mouse [192]. Mice were treated with either 30 mg/kg LXR agonist or vehicle. The daily intraperitoneal injection of this treatment started 3 days prior the inductions of the model and continued until the mice were culled. The mice were monitored daily for wellbeing and changes in body weight until day 18 when the mice were culled.

2.3.6 Experimental detail of bleomycin-induced pulmonary fibrosis in LXR α ^{-/-} knockout and LXR β ^{-/-} knockout mice

To determine the role of single LXR KO the following experiment was performed. 10-12 weeks male of LXR α ^{-/-} and LXR β ^{-/-} mice were used for induction of bleomycin pulmonary fibrosis.

Mice were allocated to 4 groups (n=19-23 mice per group):-

A- LXR α ^{-/-} treated with vehicle

B- LXR α ^{-/-} treated with LXR agonist

C- LXR β ^{-/-} treated with vehicle

D- LXR β ^{-/-} treated with LXR agonist

Three days prior the experiment mice were treated with daily injections of LXR agonist or vehicle and this continued until day 18 when the mice were culled. On the day of induction of fibrosis (day zero) animals were anaesthetised using isoflurane inhalation in an anaesthetic chamber. All animals were given bleomycin sulphate intranasally 0.06mg in 30 μ l PBS / animal. The mice were monitored daily for wellbeing and changes in body weight until day 18 when the mice were culled

2.3.7 Experimental detail of bleomycin-induced pulmonary fibrosis in MicroRNA-155^{-/-} and MicroRNA-155 wild-type mice

Bleomycin-induced pulmonary fibrosis was established using miR-155^{-/-} and miR-155 wild-type mice. 10-12 week old male were used, and animals were allocated to four groups (n=7-14 mice per group):-

A- WT given bleomycin

B- WT given PBS

C- MiR-155^{-/-} given bleomycin

D- MiR-155^{-/-} given PBS

On the day of induction of fibrosis (day zero) mice were anaesthetised using isoflurane inhalation in an anaesthetic chamber. Mice were given intranasally either bleomycin sulphate 0.06mg in 30 µl PBS / animal or 30 µl PBS / animal. The mice were monitored daily for wellbeing and changes in body weight until day 18 when the mice were culled.

2.3.8 Clinical observation of mice

The PhD candidate is qualified with a sufficient knowledge and with experience in clinical field. Mice were monitored daily for changes in body weight and general health. The maximum allowance for body weight loss was 20% of the weight on day zero.

2.4 Cytological evaluation of bronchoalveolar lavage

Bronchoalveolar lavage (BAL) was performed to obtain leukocytes from the airway and alveolar spaces. The trachea was opened transversely sufficient to allow entry of a small polyethylene catheter 0.5 cm on the end of a syringe needle and this was located by a knot of surgical ligature. The lungs were washed by aspiration two times with separate 0.8 ml of PBS and the BAL fluid collected. This volume of fluid was chosen because it did not cause distortion affecting subsequent lung histological investigation. The BAL fluids were centrifuged at 1200 rpm for 5 minutes. The supernatant was stored for measurement of airway cytokines measured by enzyme-linked immune-sorbent assay (ELISA). The cell pellet was re-suspended with PBS and the total and differential number of infiltrating leukocytes was quantified as described in [194]. Briefly, the total number of BAL leukocytes was demonstrated by counting leukocytes in a modified Neubauer chamber. Differential counts were obtained from cytopsin (Shandon III)

preparations by determining the percentage of each leukocyte on a slide stained with Giemsa stain.

2.5. Lung tissue preparation

2.5.1 Preparation of lungs for histology

2.5.1.1 Tissue processing, embedding & sectioning

Processing

The whole lung units were excised from mice. The largest lobe (left lob) was separated from the others and preserved in 10 ml of 10% neutral buffered formalin (Sigma) for 24 hours at room temperature. The next day the tissue was incubated in 70% ethanol for two hours at room temperature before further processing by an automated tissue processor (Thermo, Citodel 1000) which transferred the tissues through increasing concentrations of ethanol until they were completely dehydrated and then embedded in wax. The conditions of this process are listed below:

1. 10% neutral buffered formalin 24 hours
2. 70% ethanol 2 hours
3. 90% ethanol 1 hour
4. 95% ethanol 1 hour
5. 100% ethanol 2 hours – this step was repeated 3-fold
6. Xylene 2 hours – this step was repeated 3-fold
7. Paraffin wax 4 hours – this step was repeated 2-fold

Embedding

Wax blocks were prepared immediately after the tissue processing was finished using Thermo scientific histocentre 3 embedding center (Loughborough, UK) followed by cooling of the blocks for 30 minutes. The blocks were stored at 4°C until they were used for sectioning.

Sectioning

Tissue blocks were trimmed using a microtome set at 10 µm to remove the excess wax. The blocks were placed on ice for 1 hour to harden the paraffin wax before further cutting. 4 µm sections were cut and placed in a floating water bath set at

40°C. The sections were separated and placed on a charged frosted microscope slide (Superfrost plus, VWR, Lutterworth, Leicestershire, UK) and placed on a hotplate (Raymond A Lamb Hotplate, Thermo scientific) at 55°C for 1 hour to allow the tissue section to completely dry. The slides were stored at 4°C until required for staining.

2.5.1.2 Haematoxylin and Eosin staining (H&E)

For routine histological analysis the sections were stained using Haematoxylin and eosin (H&E). All the reagents used in the H&E staining were purchased from Sigma. The protocol is listed below and the different ethanol concentrations required were made by diluting 100% ethanol with dH₂O to the required concentration (v/v).

The staining procedure included several stages, softening of the wax by incubation the sections in an oven from GenLab (Cheshire, UK) at 60°C for 35 min followed by removing the wax from the section by immersing the sections in xylene. Rehydration of the sections was carried out by immersing the sections in gradually decreasing concentrations of ethanol to allow rehydration and subsequent staining with water soluble H&E.

The two important components of the H&E are Harris Haematoxylin which stains nuclei and Eosin which stains the cytoplasmic structures. The staining was followed by dehydration of the sections by immersing them in gradually increasing concentrations of ethanol then the sections immersed in xylene before adding mounting fluid and coverslips.

The steps are summarised in the following:

1. Heating sections in oven at 60°C for 35 minutes
2. Dewax in Xylene 3 minutes - repeated 2-times
3. 100% Ethanol 3 minutes - repeated 2-times
4. 90% Ethanol 3 minutes - repeated 2-times
5. 70% Ethanol 3 minutes - repeated 2-times
6. dH₂O 3 minutes
7. Harris Haematoxylin 2 minutes
8. Running water 3 minutes
9. 1% Acid/Alcohol few seconds
10. Rinse under slow running tap water for a quick wash
11. Scott's tap water substitute 30 seconds

12. Rinse under slow running tap water for a quick wash
13. 1% Eosin 2 minutes
14. Running water 2 minutes
12. 70% Ethanol 30 seconds
13. 90% Ethanol 30 seconds
14. 100% Ethanol 30 seconds - repeated 2-times
15. Xylene 3 minutes - repeated 2-times
16. The sections were mounted with one drop of DPX mount (VWR), the drop was placed on the section by Pasteur pipette then a cover slip (VWR) put over the section. The sections were allowed to dry in the hood before it examined under the microscope.

2.5.1.3 Gomori's Trichrome stain

The basic components of the Gomori's Trichrome stain included chromotrope 2R (Sigma), fast green FCF (Thermo Scientific), phosphotungstic acid (Sigma). Different ethanol concentrations were prepared by diluting 100% ethanol with dH₂O to the required concentration (v/v).

Initially, the staining procedure started by softening of the wax by incubating the sections in an oven (GenLab) at 60°C for 35 min followed by removing the wax from the section by immersing them in Xylene. Rehydration of the sections was carried out by immersing the sections in gradually decreasing concentrations of ethanol.

The sections were stained with Harris Haematoxylin which stains nuclei then by washing with dH₂O. The sections were immersed with chromoptrope-green mixture to stain the collagen followed by quick rinse with acetic acid. This staining was followed by dehydration of the sections by immersing them in gradual increasing concentrations of ethanol then the sections were immersed in Xylene before mounting with coverslips.

The steps are summarised as the following:

1. Heating sections in oven at 60°C for 35 minutes
2. Dewax in Xylene 3 minutes - repeated 2-times
3. 100% Ethanol 3 minutes - repeated 2-times
4. 90% Ethanol 3 minutes - repeated 2-times
5. 70% Ethanol 3 minutes - repeated 2-times

6. dH₂O 3 min
7. Harris Haematoxylin 2 minutes
8. Running water 3 minutes
9. dH₂O 5 minutes
10. Chromoptrope-green mixture 20 minutes
11. 0.2% acetic acid few seconds
12. Running water 2 minutes
13. 70% Ethanol 30 seconds
14. 90% Ethanol 30 seconds
15. 100% Ethanol 30 seconds repeated 2 times
16. Xylene 3 minutes repeated 2 times

The sections were mounted with one drop of DPX mount (VWR), and then a cover slip (VWR) was put over the section. The sections were allowed to dry in the fume hood before examination under the microscope.

2.5.2 Histological evaluation of lung inflammation and fibrosis

The severity of the inflammatory changes was assessed in the lungs by two observers blind to the experimental details. Typically 10 different low-power fields were used in the scoring of each tissue section. The parameters used in the scoring of the inflammation reflected the degree of inflammatory cells infiltration, perivascular haemorrhage, and parenchymal and alveolar changes.

After an assessment of the literature and discussion with colleagues, there was an impression was that there is no gold-standard scoring system for murine lung inflammation therefore we designed our own. We used a pragmatic 5-point histological score as described in the following examples (Table 2.2): This was based on the extremes of normal compared with the worst possible (severe-with architectural changes), and then recognising a mild-point (Moderate). Even with brief experience, it became comfortable to score between these as mild and severe.

The overall score for each tissue section was a mean of the measures.

The examples are as follows:

1 = Histologically normal

2 = Mild inflammatory infiltrate

3 = Moderate inflammatory infiltrate

4 = Severe inflammatory infiltrate

5 = Severe inflammatory infiltrate, with loss of lung architecture

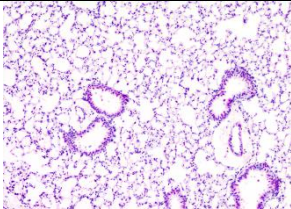
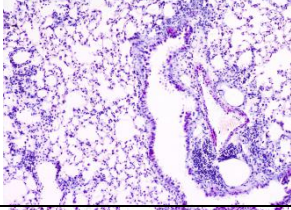
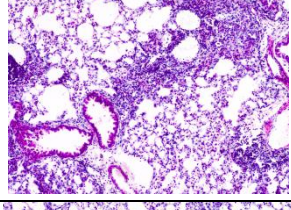
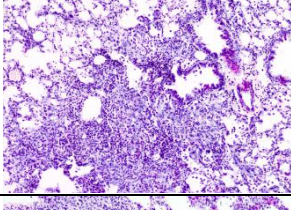
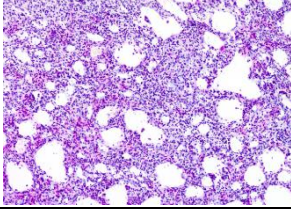
Score	Description	Histological finding
1	Normal	
2	Mild inflammation	
3	Moderate inflammation	
4	Severe inflammation	
5	Severe inflammation and loss of lung architecture	

Table 2.2 Illustrative examples of the lung inflammation used to describe a scoring system for assessing inflammatory changes associated with murine bleomycin-induced pulmonary fibroses.

The severity of fibrosis was assessed in the lung sections by staining with Gomori's Trichrome stain. The sections were scored independently by two observers blinded to the nature of the samples. Each scored the fibrosis in 10 different low-power fields per slide. The assessment of fibrosis was subjective and based on the size and distribution of the collagen deposition across the lung section. We used the arbitrary fibrosis score described below (Table 2.3).

The overall score for each tissue section was a mean of the measures.

1 = Normal

2 = Thin collagen deposition around bronchioles and blood vessels

3 = Patches of collagen deposition across the parenchyma

4 = Collagen deposition all over the tissue section

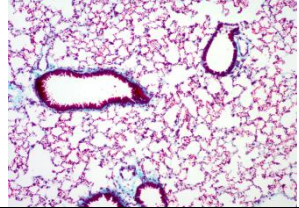
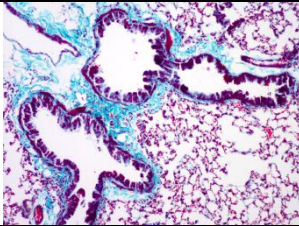
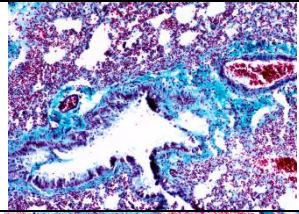
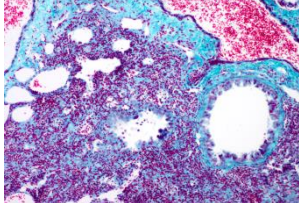
Score	Description	Fibrosis finding
1	Normal	
2	Thin collagen deposition around bronchioles and blood vessels	
3	Patches of collagen deposition across the parenchyma	
4	Collagen deposition all over the tissue section	

Table 2.3 Illustrative examples of the lung fibrosis used to describe a scoring system for assessing changes associated with murine bleomycin-induced pulmonary fibroses.

2.6 Measurement of total lung collagen

The total soluble collagen content of the lung tissues were measured using a commercial kit (Sircol) from Biocolor, (Carrickfergus, UK). Sircol is a dye-binding method for the analysis of acid and pepsin-soluble collagens, the principal of this test is the binding of a dye to collagen. The collagen-bound dye is recovered by centrifugation, eluted with alkali, and measured using a spectrophotometer at 540 nm. The intensity of colour measurement is proportional to the collagen concentration in a sample. All lungs were weighed and the lung tissue was diced and washed twice for one hour each by incubation in cold phosphate buffered saline. The tissue was transferred into 1.5 ml eppendorf tubes and incubated with

1 ml pepsin (Sigma) at a concentration of 0.1 mg/ml in 0.5 M acetic acid at 4°C overnight to remove the terminal non-helical telopeptides, in order to release the collagen into solution.

Specific microcentrifuge tubes supplied with the kit were then used. 100 µl of each test sample was added in duplicate to the tubes and a seven point standard curve was made using recombinant standard collagen dissolved in RPMI complete medium at a concentration of 400 µg/ml followed by five doubling dilutions in duplicate, with two tubes containing only medium as a negative control. 1 ml of sircol dye reagent was added to each tube followed by washing with 750 µl ice-cold acetic-salt wash to remove unbounded dye from the surface of the stained collagen pellet and the inside surface of the tube. To release the collagen from the pellet 250 µl of alkali reagent was added to each tube then 200 µl of the samples and standards were added to 96 micro well plates and the mean intensity was read at 570nm on a microplate reader (Dy nex Technology, Worthing, UK).

The following steps summarise the procedure:

1. 100 mg of diced lung tissue
2. 1 ml pepsin/acetic acid 0.1 mg/ml 0.5 M acetic acid 4°C overnight
3. Collagen standard 400, 250, 100, 50, 10, 5 µg/ml and Blank well with RPMI complete medium.
4. 100 µl of samples and standard in microcentrifuge tubes - repeated 2-times
5. 1 ml of sircol dye reagent 30 minutes with shake
6. Centrifugation 12000 rpm for 10 minutes
7. 750 µl ice-cold acetic-salt wash
8. Centrifugation 12000 rpm for 10 minutes
9. 250 µl of alkali reagent
10. Mixing 5 minutes
11. 200 µl samples and standards in 96 micro well plates
12. Read at 570nm on a microplate reader

2.7 Serum and bronchoalveolar lavage fluid analysis

2.7.1 Measurement of cytokines using a Luminex multiplex assay

The volume of serum retrieved was a limit to the number of soluble mediators that could be analysed. This was optimised by using a system that can simultaneously quantify multiple cytokines and chemokines in the small volumes of mouse serum and bronchoalveolar lavage fluid. Briefly, the principle of the assay was that differentially dual-fluorescent labelled microbeads were purchased pre-coated with antibody to different mediators. (Invitrogen) Depending on the mediator analytes of interest, listed below, a cocktail of beads was incubated with the serum or BAL. After washing off excess fluid the beads were incubated with fluorescent-labelled antibody to the analytes of interest. Analysis was based on the recognition of the characteristic dual-wavelength of the beads that captured a particular analyte, along with the fluorescent signal from the detection antibody which was proportional to the concentration of analyte (Luminex platform; Bio-Plex , Bio-Rad, Hertfordshire, UK). Standards were dissolved in 1 ml of assay diluent to reconstitute each cytokine standard to the required concentration.

The twenty-plex assay was able to analyse the following cytokines, chemokines and growth factors in mouse serum and bronchoalveolar lavage fluids.

Cytokines:

Interleukin (IL)-1 α , IL-1 β , IL-2, IL-4, IL-5, IL-6, IL-10, IL-12p40/p70, IL-13, IL-17, Tumor necrosis factor (TNF) α , and interferon (IFN) γ ,

Chemokines :

CXCL10 (IP-10), CXCL1 (KC), (CCL2) MCP-1, (CXCL9) MIG, and (CCL3) MIP-1 α .

Growth and colony stimulating factors:

VEGF, FGFb, and GM-CSF.

The serum samples were diluted 1:2 with assay diluent and 50 μ l added to each well in duplicate following the manufacturer's protocol. The bronchoalveolar lavage samples were used without dilution and 50 μ l added to each well in duplicate following the manufacturer's protocol.

2.7.2 TGF- β 1 ELISA assay

Mouse TGF β 1 was measured by commercial ELISA (R&D systems, Minneapolis, MN, USA). TGF β 1 is typically found in a latent nonimmunoreactive form, therefore, to be able to measure the actual concentration of TGF- β 1 we treated the samples as in (Table 2.4).

Briefly this ELISA protocol specified using Immunol microtiter plates (Thermo Labsystems). These were coated with 100 μ l of capture antibody in phosphate buffer saline and incubated overnight at 4 $^{\circ}$ C. Before use, the plates were washed by immersion 3 times with 0.05% Tween 20/ PBS, then incubated with 300 μ l of

blocking buffer (5% Tween 20 in PBS with NaN₃) to block non-specific protein binding, and incubated at room temperature for 2 hours. A seven-point standard curve with serial doubling dilutions from 2000 pg/ml was made using standard mouse TGFβ₁ recombinant diluted in reagent diluents (1.4% delipidized bovine serum, Opticlear, Biocell (Compton, CA, USA).

The plates were washed with 0.05% Tween 20/ PBS and 100 µl of sample or standards were added in duplicate to the plate along with two wells containing only reagent diluents then incubated at room temperature for 2 hours. The ELISA plate was then washed three times by immersion with 0.05% Tween 20/ PBS, and the next step was 100 µl of detection antibody diluted in the reagent diluents were added to each well and incubated at room temperature for another 2 hours.

The plates were then washed three times by immersion with 0.05% Tween 20/ PBS and 100 µl of working dilution of streptavidin HRP(R&D) diluted 1:1000 with reagent diluent) was added to each well and the plates were covered and incubated for 20 minutes at room temperature. After washing three times by immersion with 0.05% Tween 20/ PBS, 100 µl of substrate solution (1:1 mixture of H₂O₂ and tetramethylbenzidine (TMB) peroxidase (R&D) was added. The plates were incubated for 20 minutes in darkness at room temperature, and then the reaction was stopped by addition of 50 µl Stop Solution (Biosource, Nottingham, UK) which is 0.16 M sulphuric acid used to terminate the peroxidase/TMB reaction, and the mean intensity was read at 450nm on a microplate reader (Dynex Technology).

Serum	Bronchoalveolar lavage(BAL)
To 0.1 ml sample add 0.1 ml of 2.5 N acetic acid/10 M urea	To 0.5 ml sample add 0.1 ml of 1 N HCL
Mix well	Mix well
Incubation 10 minutes at room temperature	Incubation 10 minutes at room temperature
Add 0.1 ml of 2.7 N NaOH/1 M HEPES for neutralization	Add 0.1 ml of 1.2 N NaOH/0.5 M HEPES for neutralization
Mix well	Mix well
Dilute samples 10 folds with reagent diluents before using in the assay	Used in the assay
Samples value results multiplied by dilution factor 30	Samples value results multiplied by dilution factor 1.4

Table 2.4 Protocol for activation of latent form of mouse TGFβ₁ in the serum and bronchoalveolar lavage to enable their measurement.

2.8 Investigation of gene expression

2.8.1 Extraction of RNA from tissue

2.8.1.1 TRIZOL homogenization for tissue

All lung tissues harvested from the mice were immediately put into RNALater and frozen in liquid nitrogen before being stored at -80°C until they were processed for RNA extraction. One lobe of the lung was homogenized with 1ml TRIZOL RNA stabilisation reagent (Invitrogen) in a homogeniser tube (Precellys Kit CK28, Stretton, UK) followed by homogenisation in a Precellys homogeniser set at 2 X 10 sec at 6500 rpm.

To each sample tube 200 µl of chloroform was added and vortexed until mixed well before being transferred into a new RNase-free eppendorf tube, then followed by centrifugation at 13,000 rpm for 20 min at 4°C. Three fluid phases were obtained and the upper aqueous phase which contained the RNA was transferred into a new RNase-free eppendorf tube. The RNA was precipitated by the addition of 500 µl of propan-2-ol followed by centrifugation at 13,000 rpm for 20 min at 4°C to precipitate the RNA.

The propan-2-ol was removed from the tube and the precipitated RNA pellet was washed by the addition of 300 µl of 70% ethanol followed by centrifugation at 13,000 rpm for 5 minutes. The ethanol was removed from the tubes and the RNA pellet was allowed to dry in air for a few minutes until the ethanol had evaporated before it was dissolved in 100 µl water treated with 0.1% v/v diethyl pyrocarbonate (DEPC) to maintain RNA-free conditions.

RNA quantification was done by comparison of optical density at 260nm and at 200nm using a spectrophotometer (Amersham Biosciences, Amersham, UK) to check for purity and protein contamination. One µl of the RNA was used in this quantification and with this value a stock RNA solution of 200 ng/µl was prepared with Diethyl Pyrocarbonate (DEPC) treated water and stored at -80°C until the cDNA synthesis was performed.

2.8.1.2 RNA extraction from cells

Cells in suspension were prepared for RNA extraction using the RNeasy Mini Kit (Qiagen, Manchester, UK) as described by the manufactures. Adherent cells in culture flasks were removed by addition of 0.05% Trypsin-EDTA (Invitrogen), then washed with PBS and centrifuged to collect cells into a pellet. The cells pellet was resuspended in 350 µl of RLT buffer (lysis buffer for lysing cells and tissues) from Qiagen, mixed gently until complete lysis of the cells occurred. These suspensions were stored at -80°C until they were required for RNA extraction.

RNA extraction was performed by following the manufacture's guidelines:

1. Addition of 350 μ l of 70% ethanol to the sample then transferred into MiniElute spin column. Then centrifugation at 10.000 RPM for 15 seconds.
2. The flow through was discarded.
3. Addition of 80 μ l DNase I followed by an incubation for 15 minutes at room temperature.
4. Addition of 350 μ l of RW1 buffer followed by centrifugation at 10.000 RPM for 15 seconds.
5. The flow through was discarded.
6. Addition of 500 μ l of RPE buffer followed by centrifugation at 10.000 RPM for 15 seconds.
7. The flow through was discarded.
8. Addition of 500 μ l of 80% ethanol followed by centrifugation at 10.000 RPM for 2 minutes.
9. The flow through was discarded.
10. Centrifugation 16.000 RPM for 5 minutes.
11. Addition of 14 ml RNase free water to the pellet then centrifugation at 10.000 RPM for 2 minutes.

RNA quantification was done by using a spectrophotometer (Amersham Biosciences). One μ l of the RNA was used in quantification then the stock of 125 ng/ μ l was prepared with DEPC treated water and stored at -80°C until the cDNA synthesis was performed.

2.8.2 Complementary DNA (cDNA) Synthesis

Complementary DNA (cDNA) was made from the RNA extracted from the mice or cells. The reaction was set in RNase free microcentrifuge tubes (Star lab, Milton Keynes, UK) as described by the manufacture (Qiaqen). The principles of the test are as the following:-

	Tissue	Cells
RNA 1 mg.....	5 μ l	8 μ l
Random hexamers 50 ng/ml.....	1 μ l	1 μ l
dNTP 10mM.....	1 μ l	1 μ l

DEPC water.....	3 µl	0 µl
Final reaction volume	10 µl	10 µl

The reaction components were mixed in the tubes by centrifugation before being placed in the PCR machine for RNA denaturation. The PCR machine was set as the following:

1. 65°C 5 min
2. 0°C 1 min
3. 4°C 10 minutes

Following the manufacture protocol, a second master mix was required to prepare as following:

RT buffer 5X.....	4 µl
MgCl ₂ 50 mM.....	2 µl
DTT 0.1 M.....	2 µl
RNase OUT.....	1 µl
Superscript II RT (200 u/ µl).....	25 µl
DEPC water.....	75 µl
Final reaction volume	10 µl

10 µl from the second master mix were added to each microcentrifuge tube contained the denatured RNA, mixed well by centrifugation, the total volume was 20 µl in each tube. The tubes were placed in PCR machine again for cDNA synthesis using the following programme:

1. 25°C 2 min
2. 42°C 50 min
3. 70°C 15 min
4. 4°C 10 minutes

After the incubation the cDNA was diluted with DEPC water 1:3 then stored at -80°C until required for PCR target genes analysis.

2.8.3 SYBR Green reverse transcriptase-polymerase chain reaction (QRT-PCR)

All QRT-PCR primers and probes were selected on the basis that they crossed intron / exon boundaries to achieve high efficiency of the qRT-PCR.

SYBR Green quantitative reverse transcriptase-polymerase chain reaction (QRT-PCR) was used for genes quantification. The reactions were made in Fast Optical 96-Well Reaction Plate with Barcode (Applied Biosystems). The reactions were performed in triplicate using the final reaction volume of 20 μ l per each well as the following:

cDNA.....	2 μ l
Power SYBR Green Master Mix.....	10 μ l
Primer pairs (Forward & Reverse).....	2 μ l
RNase water.....	6 μ l
Final reaction volume	20 μl

The primers were purchased from Integrated DNA Technology and designed to anneal to adjacent Exons to exclude possible amplification from genomic DNA, all other reagents were purchased from Applied Biosystem (Paisley, UK). To exclude any contamination of the reaction we used two controls with each plate (reaction with no RNA & reaction with water (no template)). After adding all the reaction components in the plate, it was covered with an optical cover and centrifuged at 1000 RPM for 1 minute to mix the contents.

For developing the reaction, the plate was put in the QRT-PCR machine (Applied Biosystems 17900HT/7500) for 40 cycles. The expression of target genes was then quantified relative to the house keeping gene using SDS2.2 software Applied biosystem.

The following human and mouse primers were used for SYBR Green qPCR analysis (Table 2.5).

Mouse	(F)	(R)
TBP	5'-TGC TGT TGG TGA TTG TTG GT-3'	5'-AAC TGG CTT GTG TGG GAA AG-3'
Col1A	5'-AGC TTT GTG GAC CTC CGG CT-3'	5'-ACA CAG CCG TGC CAT TGT GG-3'
Col3A	5'-GTT CTA GAG GAT GGC TGT ACT A AA CAC A-3'	5'-TTG CCT TGC GTG TTT GAT ATT C-3'
TGFβ1	5'-ACC CCC CAT TGCT GTC CCGT-3'	5'-CCT TGG TTC AGC CAC TGC CG-3'
ABCA1	5'-AGT ACC CCA GCC TGG AAC TT-3'	5'-ACG TGT CCT TGG TCA GCT TC-3'
Arg2	5'-ACC AGG AAC TGG CTG AAG TG-3'	5'-TGA GCA TCA ACC CAG ATG AC-3'
LXRα	5'-GGA TAG GGT TGG AGT CAG CA-3'	5'-GGA GCG CCT GTT ACA CTG TT-3'
LXRβ	5'-GCT CAG GAG CTG ATG ATC CA-3'	5'-GCG CTT GAT CCT CGT GTA G-3'
IL13R	5'-TCT GGT ATG AGG GCT TGG AT-3'	5'-GCT GGA GGT AAT CAG CAC ACT-3'
Ym1	5'-CAT GAG CAA GAC TTG CGT GAC-3'	5'-GGT CCA AAC TTC CAT CCT CCA-3'
Nos2	5'-AGA CCT CAA CAG AGC CCT CA-3'	5'-GCA GCC TCT TGT CTT TGA CC-3'
Human		
GAPDH	5'-TCG ACA GTC AGC CGC ATC TTC TTT-3'	5'- ACC AAA TCC GTT GAC TCC GAC CTT -3'
Col1A	5'-CAA TGC TGC CCT TTC TGC TCC TTT-3'	5'- CAC TTG GGT GTT TGA GCA TTG CCT-3'
Col3A	5'-TAT CGA ACA CGC AAG GCT GTG AGA -3'	5'-GGC CAA CGT CCA CAC CAA ATT CTT-3'

Table 2.5 Primers Used for Real-Time qPCR

2.9 In vitro work

2.9.1 Generation of murine fibroblast cell lines

Mouse primary fibroblasts lines were generated from lung tissue. Fresh lung lobes were dissected and chopped into small fragments (~1-2 mm). These were suspended in 10 ml of complete DMEM medium and added to 25-ml tissue culture flasks.

The cultures were incubated for 21 days in standard culture conditions which are at 37°C, 5% CO₂ in a humidified atmosphere. The medium was replaced every week. After 3 weeks the attached fibroblasts were removed using 0.05 Trypsin EDTA, then the cells were washed with DMEM medium, then re-suspended at 5x10⁶ cells/ml in freezing mix (50% FCS and 50% DMSO) before being stored at -70°C for 24 hours then transferred to -80°C freezer until required.

2.9.2 Generation of primary human fibroblast line

Human primary fibroblast lines generated from human tendons were used (Kindly donated by Dr Neil Miller, Immunology, Glasgow University. Tissue obtained with

ethics approval). The human fibroblasts were obtained from 3 different people (n=3). The cells were cultured in 10 ml of RPMI medium in 25 ml tissue culture flasks for 21 days at 37°C, 5% CO₂. The medium was replaced every week. After 3 weeks the attached fibroblasts were removed using 0.05 Trypsin EDTA, then the cells were washed with RPMI medium and stored in freezing mix at -70°C for 24 hours before transferred to -80°C freezer until it required to use.

2.9.3 Fibroblast stimulation with LXR agonist

Fibroblasts were retrieved from frozen stocks by rapid warming of the cryovials to 37°C. The cells were washed three times in complete medium to remove the DMSO and then cultured at 1x10⁵ cells/ml in either complete DMEM (murine fibroblast) or complete RPMI (human fibroblast). Cells were allowed to settle in 6 well plates for 72 hours in standard culture conditions.

The cells were activated with LXR agonist (GW3965) at a final concentration range between 0.125 μM to 0.5 μM or vehicle (DMSO) and incubated at 37°C, 5% CO₂. The cells were cultured for 6, 12 and 24 hours. The supernatants were collected and used for measuring total soluble collagen and the cells were lysed with 350 μl RLT lysing buffer and the RNA was purified and used for qPCR analysis.

2.9.4 Fibroblast stimulation with LXR agonist and cycloheximide

The cells were prepared and cultured in 6 well plates as described above (2.4.3). The cells were activated with LXR agonists (GW3965) at the final concentration of 0.5 μM, vehicle (DMSO), and medium only (DMEM or RPMI), Cycloheximide (Sigma) was added to each well at final concentration of 1 μg/ml. The cells were incubated at 37°C, 5% CO₂ for 24 hours. The cells were lysed with 350 μl RLT lysing buffer then RNA was purified and used for qPCR analysis.

2.10 Promoter analysis of murine collagens 1 and 3

The ability of LXR α/β to directly regulate the expression of collagens 1 and 3 was investigated using a luciferase reporter system. *In silico* analysis identified putative LXR/RXR binding sites in the promoters of mouse collagens.

2.10.1 *In silico* analysis of mouse collagens 1 and 3

In silico analysis was performed using an on-line tool MatInspector, is a software tool that utilizes a large library of matrix descriptions for transcription factor binding

sites to locate matches in DNA sequences (http://www.genomatix.de/online_help/help_matinspector/.html). Putative conserved LXR/RXR binding sites were identified.

2.10.2 Amplification of putative LXR/RXR binding sites

Genomic regions containing the candidate LXR/RXR binding sites were amplified by polymerase chain reaction (PCR) and cloned by TOPO cloning into pCR2.1 TOPO vector (Invitrogen). Primers were designed using Integrated DNA Technologies (IDT) Primer Quest software such that they flanked each LXR/RXR sequence of interest (Table 2.6). Primers were purchased from IDT (Coralville, IA, USA) (Table 2.7). Each region was amplified using Go-Taq master-mix (Promega, Southampton, UK) according to the manufacturer's instructions. A brief description of the reaction used is outlined below:

25 µl of 2x Go-Taq master mix

1.25 µl of 10 µM Forward primer

1.25 µl of 10 µM Reverse primer

2 µl mouse genomic DNA (isolated from NIH3T3 cells)

20.5 µl milli-Q water

Reactions were placed into ABI thermocycler and amplified using the following settings):

	Temperature (°C)	Time	Cycles
Initial Denaturation	95	2 minutes	1
Denaturation	95	15 seconds	35
Annealing	55	15 seconds	
Extension	72	1 minute	
Final Extension	72	7 minute	1

Table 2.6 Amplification products were examined by agarose gel electrophoresis

Gene Name	Species	Primer	Sequence	Product Length
Col (I) A1a	Mouse	5'-AGG CAT GGC CAG GAG GAC CT-3' 5'-CTC TTT GCG GCT GGG GTG GG-3'	F R	509
Col (I) A1b	Mouse	5'-GAG GGA GAC AGC CC GGG AGG-3' 5'-AGT GGG GAT GGA GGC TGC CT-3'	F R	500
Col (I) A1c	Mouse	5'-CCA GCT GAC CTT CCT GCG CC-3' 5'-AAG TGG GCT GGG TGG GAG GG-3'	F R	518
Col (III) A1a	Mouse	5'-TCA ACA GTT GCA GTG CTG TTC CT-3' 5'-GGC TGA AGA AAT ACT GGA ACC AGG G-3'	F R	280

Table 2.7 Primers used for producing PCR gene products

2.10.3 Agarose gel electrophoresis

DNA fragments generated by PCR were examined by agarose gel electrophoresis. DNA samples were prepared for agarose gel electrophoresis by adding 5 μ l of DNA loading buffer (recipe on Table 2.8). 1.5 % (w/v) agarose gels were prepared by dissolving 1.5 grams agarose (Invitrogen) in 100 ml of 1xTAE. Agarose TAE solution was then heated in a microwave until the agarose was completely dissolved. At the same time 10 μ l of 10 mg/ml ethidium bromide (Sigma) (10mg/ml stock solution) was added and mixed by gentle swirling. Molten agarose was then poured into a gel-casting tray along with casting combs and allowed to set. Once set the combs were removed and the gel placed into an electrophoresis tank with enough 1xTAE to just cover the gel. DNA samples were loaded into each well along with 1 Kb plus (Invitrogen) DNA ladder, to allow the size of the DNA fragments to be estimated. Gels were run at 100 V until loading dye had migrated 2/3 the length of the gel. Gels were visualised on a UV trans-illuminator and images recorded using Gel logic 200 imaging system.

Reagent	
Tris base	242 g
Glacial acetic acid	57.1 ml
0.5M EDTA (pH8.0)	100 ml

Table 2.8 Recipe for 50x TAE buffer

2.10.4 Cloning of PCR amplified DNA fragments

2.10.4.1 TOPO cloning of PCR products

Gel purified PCR products were cloned by TOPO cloning into the vector pCR2.1 TOPO (Figure 2.1) (Invitrogen) according to the manufacturer's instructions. This

technique takes advantage of the non-template encoded adenosine nucleotides added to the 3' ends of Taq polymerase amplified fragments. The vector is supplied linearised with 3' thymidine overhangs, topoisomerase I catalyses the ligation of PCR product in the following reaction:

1 μ l of Salt solution

4 μ l of PCR product

1 μ l pCR2.1 TOPO vector

Reactions were amplified at room temperature for 5 minutes, 3 μ l of this reaction was used to transform chemically competent One-shot XLI-Blue E. coli (Invitrogen).

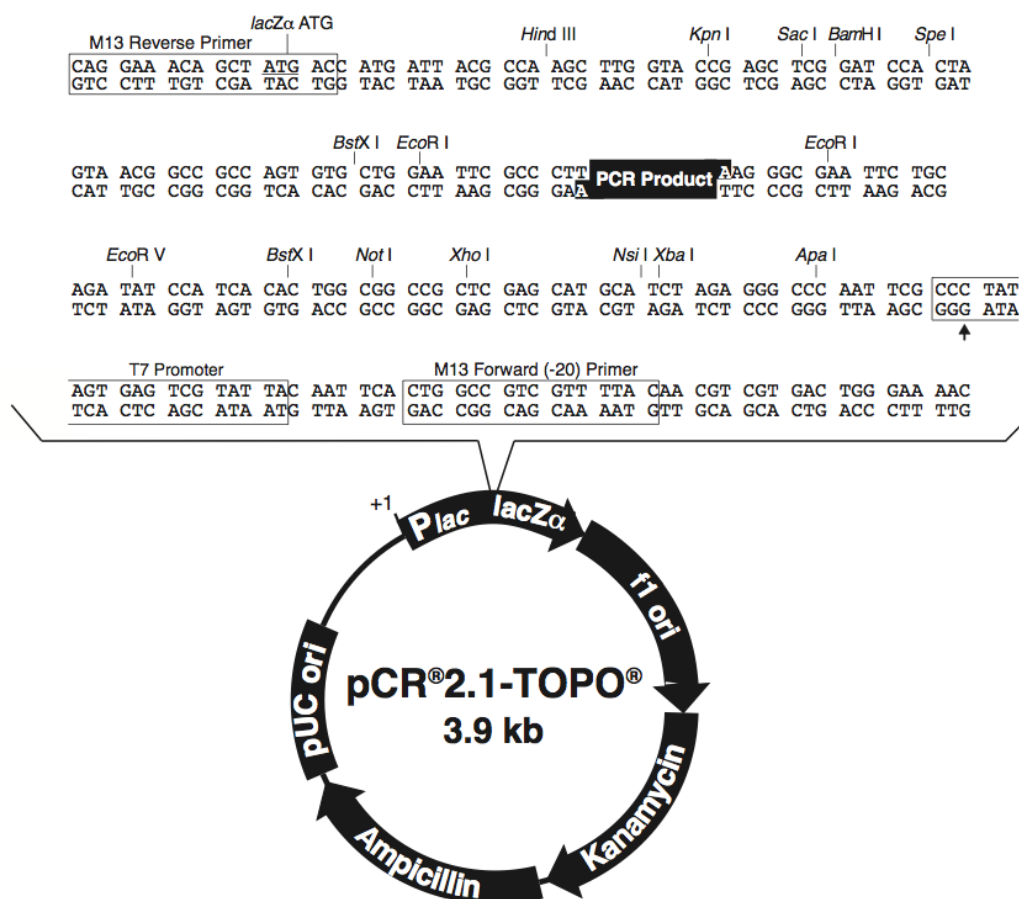


Figure 2.1 Map of pCR2.1 TOPO

2.10.4.2 DNA transformation into competent *E. coli*

Plasmid DNAs were transformed into chemically competent XL1-BLUE cells (Invitrogen) following manufacturer's instructions (described below).

- 1- Competent cells were thawed and kept on ice. 3 μ l of ligation reaction was added to 50 μ l of competent cells, gently mixed together and incubated on ice for 30 minutes.
- 2- Cells were heat-shocked at 42°C for 30 seconds and placed on ice for 2-3 minutes.
- 3- 350 μ l of SOC medium was added to the cells and cells incubated at 37 °C for 45 minutes. 100 μ l of cell suspension was plated onto an LB agar plate containing 50 μ g/ml ampicillin (Sigma).
- 4- Plates were incubated overnight at 37°C. The following day individual colonies were picked into 30 ml universal containers containing 5 ml of LB plus 50 μ g/ml and grown overnight with shaking.

2.10.4.3 Plasmid DNA purification

Plasmid DNA was purified from over-night cultures using QIAprep Spin miniprep kit (Qiagen) following the manufacturer's instructions. A brief description of this is described below.

- 1- 1.5 ml of over-night culture was placed into 1.5 ml eppendorf tube and bacteria were pelleted by centrifugation at 16100 rpm in a microcentrifuge for 3 minutes.
- 2- The supernatant was discarded and the pellet re-suspended in 250 μ l buffer P1.
- 3- 250 μ l of buffer P2 lysis buffer was added to each sample and mixed thoroughly by inverting the tubes 4-6 times.
- 4- 350 μ l of buffer N3 a neutralization buffer was added and mixed thoroughly by inverting the tubes 4-6 times.
- 5- The tubes were centrifuged at 16100 rpm for 10 minutes at room temperature.
- 6- Supernatants were transferred onto QIAprep spin columns and centrifuged at 16100 rpm for 15 seconds. The flow through was discarded.
- 7- 750 μ l of buffer PE were added to each column and centrifuged at 16100 rpm for 15 seconds. The flow through was discarded.
- 8- Columns were then dried by further centrifugation at 16100 rpm for 1 minute.
- 9- The QIAprep spin columns were transferred to fresh collection tubes and 50 μ l of elution buffer (EB) was added to the columns and allowed to stand for 1 minute before being centrifuged at 16100 rpm for one minute. DNA was eluted and quantified by Nanodrop.

2.10.4.4 Restriction endonuclease digestion of plasmid DNA

Plasmid DNA identities were confirmed by restriction endonuclease (RE) digestion. Diagnostic RE digests were chosen according to expected restriction maps generated using the sequence analysis software CloneManager. Restriction enzymes were purchased from a variety of suppliers depending on availability and incubated in the appropriate buffers according to the manufacturer's recommendation.

2.10.4.5 Gel purification of DNA fragments from agarose gel

DNA bands of interest were purified from agarose gel slices using QIAquick gel extraction kit (Qiagen) following manufactures instructions. A brief description of this procedure is outlined below. An excised gel slice is placed into a 1.5 ml Eppendorf tube along with 450 μ l solubilisation buffer QG and incubated at 56°C for 10 minutes. During this time the sample was vortexed every 2 minutes. Once the gel slice had dissolved, 150 μ l of 100% isopropanol was added and the sample was vortexed. The sample was added to a Spin column and centrifuged at 16,100 g for 15 seconds. The flow through was discarded and 750 μ l of PE buffer was added to each column and centrifuged at 16,100 g for 15 seconds. The flow through was discarded. Columns were then dried by further centrifugation at 16,100 g for 1 minute. The spin columns were transferred to fresh collection tubes 50 μ l of elution buffer (EB) were added to the columns allowed to stand for 1 minute before being centrifuged at 16,100 g for one minute. DNA was eluted and quantified by Nanodrop.

2.10.4.6 DNA ligations

DNA inserts were cloned into the appropriate plasmid vectors by ligation. DNA fragments containing compatible ends were ligated together using T4 DNA ligase. For this purpose T4 DNA ligase kit supplied by New England Biolabs was used according to manufacturer's instructions. A typical example of a reaction is shown below (Table 2.9).

Component	Volume (μ l)
Vector	3
Insert	10
Buffer	2
H2O	5
T4 DNA Ligase	1

Table 2.9 DNA ligation components

Ligations mixes were incubated at room temp for 10 minutes, then 3 μ l were added to thawed competent cells and transformed as described in section 2.9.5.2.

2.10.5 Construction of pGL3-promoter plasmids

Genomic regions containing putative LXR response elements from Col1a1 and Col3a1 genes were amplified from mouse genomic DNA, cloned into pCR2.1TOPO. Their presence was confirmed by RE digest and then excised as an KpnI-XhoI fragment before being ligated into the same sites in the pGL3-promoter (Promega) construct (see Figure 2.2). Plasmids containing the correct inserts were initially identified by restriction digest then subsequently confirmed by DNA sequencing. This was performed as a service by MWG Eurofins (A provider of genomic services. Ebersberg, Germany).

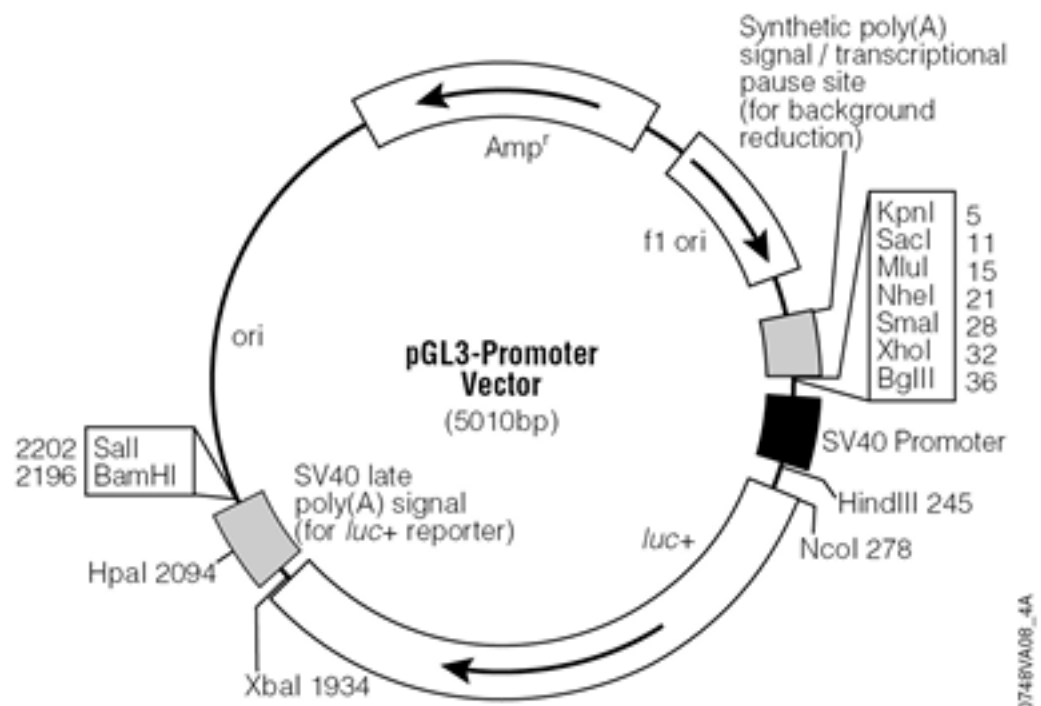


Figure 2.2 pGL3-promoter plasmid

2.10.6 Cell transfection

Endotoxin-free preparations of the various pGL3-promoter constructs plus a normalisation plasmid expressing Renilla, (an internal control reporters used in combination with any experimental reporter vector to cotransfect mammalian cells), were transfected into NIH3T3 cells using the transfection reagent Attractene (Qiagen) as follows:

- 1- 4×10^4 cells/100 μl of DMEM were seeded in a white 96-well plate (Greiner).
- 2- 200 ng of sterile plasmid DNA plus 20 ng of the Renilla-expressing plasmid pRL-TK (Promega) was added to 50 μl of OptiMEM (Invitrogen) and vortexed.
- 3- 2 μl of Attractene was added then vortexed for 2 minutes.
- 4- The transfection complex was incubated at room temperature for 10-15 minutes.
- 5- Complexes were added drop-wise to previously plated cells and incubated overnight 37°C , 5% CO_2 . The process is illustrated below (Figure 2.3).

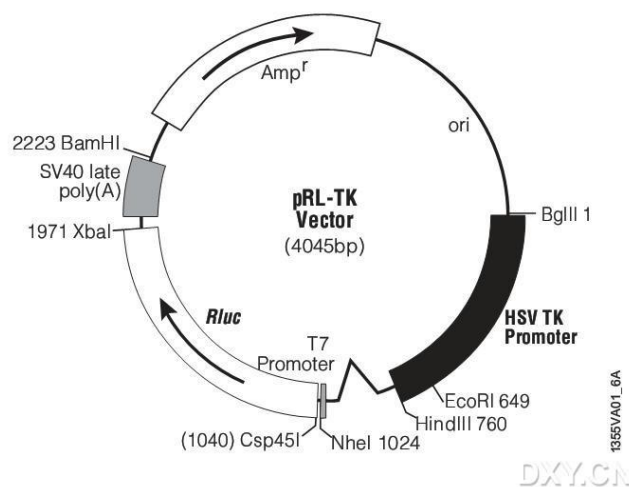


Figure 2.3 Cell transfection pRL-TK

2.10.7 Luciferase reporter assay

Luciferase reporter assays were carried out using the Dual-Glo Luciferase assay system (Promega). The assay was carried out according to the manufacture's guideline as follows:

The medium of the cells transfected with luciferase reporter constructs was removed and replaced with 75 μl of fresh medium. 75 μl of Dual-Glo[®] was added

to each well and incubated at room temperature for 10 minutes. The luminescence produced by each well was measured using a luminometer (Perkin Elmer precisely TLUX 2 DET) at 2-second measurement intervals followed by a 10-second measurement.

Renilla activity was then measured after the addition of 75 μ l Dual-Glo® Stop & Glo® reagent followed by 10 minutes incubation at room temperature.

Luminescence from renilla was measured as above. Luciferase activity was expressed as Relative Light Units (RLU) by normalising luciferase activity to Renilla activity: $RLU = \text{Luciferase activity} / \text{Renilla Activity}$

2.11 Statistical analysis

All results are displayed as Mean \pm Standard error of the mean (SEM) and all statistical analysis were performed by using of students T test, ANOVA test, Mann-Whitney test, and Kruskal-Wallis test as indicated in figure legends, using the Graph Pad Prism 4 software. A p value of < 0.05 was considered statistically significant.

3. Results and Discussion

The Results chapter will include four main parts:

- 3.1** Relationship between activation of Liver X Receptor and pulmonary fibrosis in a murine pulmonary fibrosis model
- 3.2** Exacerbation of pulmonary fibrosis is associated with the activation of Liver X Receptor
- 3.3** Requirement of LXR α and LXR β for fibrosis-enhancing effects of the LXR agonist
- 3.4** Potential involvement of MicroRNA-155 in the development of pulmonary fibrosis in a murine model

Results 3.1 Index:

3.1 Relationship between activation of Liver X Receptor and pulmonary fibrosis in a murine pulmonary fibrosis model

3.1.1 Introduction and Aims

3.1.2 Justification of the bleomycin-induced pulmonary fibrosis model *in vivo*

3.1.2.1 The time course of bleomycin-induced inflammation suggests maximum inflammatory and fibrotic changes at day 18 after administration

3.1.2.2 Selection of the dose of LXR agonist (GW3965) required to investigate its role in the severity of the murine model of bleomycin-induced pulmonary fibrosis

3.1.2.3 Treatment with LXR agonist (GW3965) had no effects on C57BL/6 mice given PBS

3.1.2.4 Validation of LXR agonist function on LXR $\alpha^{-/-}\beta^{-/-}$ mice

3.1.3 Discussion and Conclusion

3.1 Relationship between activation of Liver X Receptor and pulmonary fibrosis in a murine pulmonary fibrosis model

3.1.1 Introduction and Aims

Many attempts have been made to determine the role of LXR in various biological and pathological circumstances beyond their recognised ability to control transcription of genes involved in regulation of high density lipoprotein cholesterol metabolism, hepatic cholesterol catabolism, and intestinal sterol absorption.

Activation of the LXR exhibited diverse effects depending on the experimental model used. The activation of LXR plays an important regulatory role in inflammation, for example in macrophages in response to bacterial infection or LPS stimulation, by inhibiting gene expression of certain inflammatory cytokines including interleukin (IL-1 β), IL-6, inducible nitric oxide synthase (iNOS), cyclooxygenase (COX)-2, granulocyte colony-stimulating factor (G-CSF), chemokines such as monocyte chemoattractant protein-1 (MCP-1, CCL2), (MCP-3, CCL7), macrophage inflammatory protein-1 β (MIP-1 β , CCL4) and interferon-inducible protein-10 (IP-10, CXCL10), and the metalloproteinase MMP-9 [68].

The inhibition of expression of these inflammatory genes occurred by antagonising NF- κ B signalling by LXR ligands. In murine models of atherosclerosis, elimination of LXR activity in bone marrow-derived cells resulted in splenomegaly, aberrant regulation of cholesterol transporter expression, lipid accumulation in macrophages, and increased atherosclerosis [195]. Binding of physiological ligands such as oxysterol to LXR lead to increased expression of genes which participate in lipid metabolism and cholesterol transportation. These include Apolipoprotein E (ApoE), ATP-binding cassette transporter A1 (ABCA1), and ATP-binding cassette transporter G1 (ABCG1) in the case of macrophage activation resulting in cholesterol removal or efflux [196]. The involvement of macrophages in metabolic and inflammatory process lead to investigation of the specific role of LXR. Activation of LXR with synthetic agonists such as GW3965 and T0901317 leads to up-regulation of arginase 2 (Arg 2) expression in macrophages demonstrating that the Arg 2 promoter contains functional LXR response elements [197].

LXR $\alpha^{-/-}\beta^{-/-}$ mice have marked susceptibility to liver fibrosis in a liver injury model and this was reflected by increased production of inflammatory mediators and expression of fibrogenic genes in their stellate cells [75]. One recent study in our lab demonstrated that activation of LXR with T1317 and GW3965 agonists in a murine collagen-induced arthritis model resulted in exacerbation of the inflammatory response with excessive cartilage destruction [74]. The different responses to LXR activation in these two examples of chronic inflammation are difficult to reconcile, however remodelling is clearly affected by LXR in both therefore investigating this apparent difference might be informative of the fibrotic

process in general. We decided to investigate this using an experimental murine model of lung fibrosis caused by administration of bleomycin. The experimental fibrotic response closely mimics the fibrotic response in lungs of patients given this anti-cancer drug therapeutically. It is therefore of potential value in understanding this treatment-limiting factor as well as understanding of the processes of pulmonary fibrosis. Idiopathic pulmonary fibrosis is a fatal disease but the role of LXR in the pathogenesis of this disease has not been investigated.

Aim: Here we aimed to identify the optimal conditions for establishing the murine bleomycin-induced pulmonary fibrosis model and to adapt this model to explore the potential role of LXR in wound healing and tissue repair.

3.1.2 Justification of the bleomycin-induced pulmonary fibrosis model *in vivo*

3.1.2.1 The time course of bleomycin induced inflammation suggests maximum inflammatory and fibrotic changes at day 18 after administration

Introduction and Aim

The murine bleomycin-induced pulmonary fibrosis is a widely used model resembling the fibrosis that can occur in patients taking this antineoplastic drug. Administration of bleomycin in humans and in experimental animals leads to the development of fibrotic lung abnormalities that are similar histologically and pathologically, therefore, the murine model is one of the best models resembling human lung fibrosis [198, 199].

Previous data from our laboratory demonstrated that activation of LXR in a murine collagen induced arthritis (CIA) model leads to severe destructive inflammatory changes in the joints, and the data suggested that LXR-mediated pathways could exacerbate the chronic inflammatory response typical of RA [74]. Therefore, I extended this observation by investigating the role of LXR in another more accessible model of wound healing using bleomycin-induced pulmonary fibrosis.

The aim of this section is to justify the experimental conditions of the model by exploring the most suitable time course of the fibrosis and the optimal dose of the LXR agonist GW3965. My primary end point was checking the histopathomorphological and histo-fibrotic changes in the lung of these mice and also BAL cytology for total and differential cell counts.

Methods: - Two groups of C57BL/6 mice were used for optimising the time course of the development of the bleomycin-induced pulmonary fibrosis; (A) one group given bleomycin (n=30) and (B) one group given PBS (n=15). They were administered by the intranasal route as described in the Materials and Methods (section 2.3.3). On day zero of the experiment all mice were lightly anaesthetised

using isoflurane in an inhalation anaesthetic chamber then the mice were given either PBS or bleomycin sulphate solution 0.06 mg bleomycin in 30 μ l PBS or 30 μ l PBS as control intranasally. The mice were monitored daily for wellbeing and changes in body weight until day 32 when all mice were culled. The experiment time-frame is summarised in Figure (3.1), and the number of mice used in each group (Table 3.1).

PBS (30 μ l / mouse) or Bleomycin (0.06mg in 30 μ l PBS / mouse)



Figure 3.1 Experimental timeline for the optimisation of the time course of the bleomycin – induced pulmonary fibrosis model in C57BL/6 mice

3 groups of C57BL/6 mice were given bleomycin and 3 groups were given PBS at day 0. A group were culled at 3, 18 and 32 days of experiment. Further details in (Materials and Methods section 2.3.3). n= 5-10 mice/group.

Day/Treatment	PBS	Bleomycin
	Used	Used
Day 3	5	10
Day 18	5	10
Day 32	5	10

Table 3.1 Mice number for the optimisation of the course length of the bleomycin-induced pulmonary fibrosis model in C57BL/6 mice

6 groups of C57BL/6 mice male (8 weeks old), and all the mice were given either PBS (30 μ l / mouse) or bleomycin (0.06mg in 30 μ l PBS / mouse) intranasally. n= 5-10 mice/group.

Bleomycin administration is associated with loss of body weight.

Intranasal installation of bleomycin or PBS to the C57BL/6 mice was characterised by a short-lived minor loss of body weight for those given PBS and a more prolonged loss of weight in mice given bleomycin. This difference was significant and maintained although there was a progressive increase in weight thereafter (Figure 3.2).

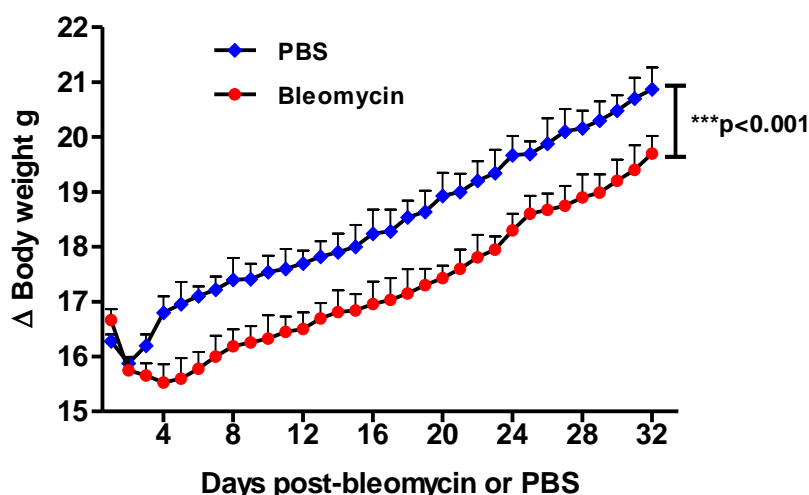


Figure 3.2 Daily body weight changes in mice given bleomycin or PBS

Male C57BL/6 mice (8 weeks old) were randomised to receive either PBS (30 μ l / mouse) or bleomycin (0.06mg in 30 μ l PBS / mouse) intranasally. Systemic inflammation caused by bleomycin administration was associated with a significant loss of body weight $p<0.001$. Bleomycin treated mice lost weight during the first 5 days following bleomycin installation while in the PBS treated group the weight dropped for one day after PBS installation. Thereafter, the mice in both groups started gaining weight normally. Student t-Test; *** $p<0.001$; Mean \pm SEM; n= 5-10 mice/group.

Bleomycin increased the histo-pathological inflammatory and fibrotic changes seen in the mouse lungs

Bleomycin installation caused morphological changes in the normal lung architecture (Figure 3. 3 A and B). Inflammatory and fibrotic changes were observed and were most severe at day 18 after bleomycin installation compared with days 3 and 32. PBS treated mice did not show any changes from normal lung architecture. Lung tissue sections stained with H&E showed a variable infiltration of inflammatory cells, perivascular haemorrhage, and collapse of the alveoli in groups given bleomycin but it was more excessive at day 18 in comparison to day 3 and 32. No significant changes were observed in the lungs of mice given PBS at days 3, 18, and 32 (Figure 3.3 A and Figure 3.4).

Using Gomori's Trichrome stain for visualisation of collagen, there were no changes for collagen in lung tissue observed at day 3 after bleomycin installation or at all times in mice given PBS. Increased collagen deposition was observed in mice given bleomycin by days 18 and 32 (Figure 3.3 B). On day 18 after bleomycin installation, more collagen was deposition than on day 32; the increased collagen was seen as bundles and fibrotic foci distributed mainly around the lung bronchioles and blood vessels, and interstitium (Figure 3.3 B).

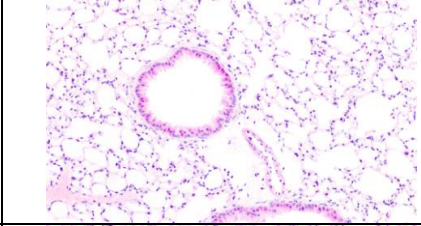
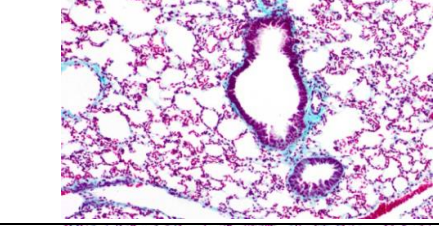
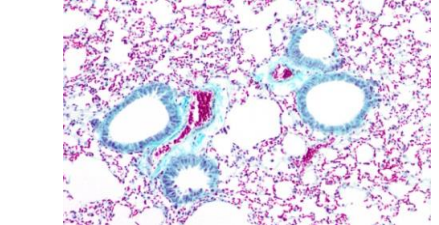
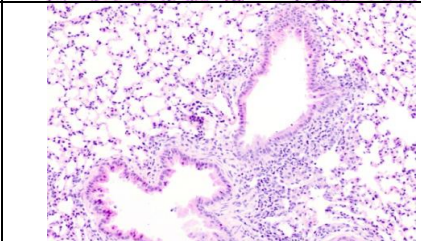
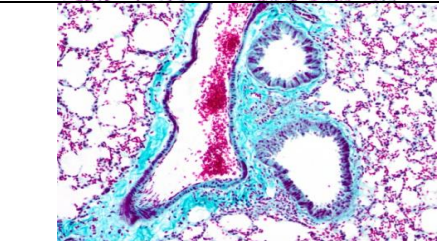
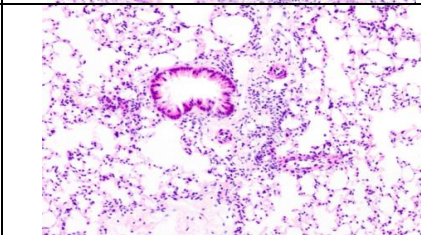
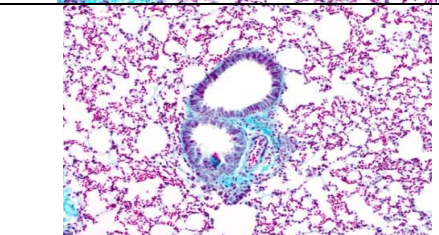
Group	A	B
	H&E	Trichrome
PBS		
Bleomycin day 3		
Bleomycin day 18		
Bleomycin day 32		

Figure 3.3 Histological inflammatory and fibrotic changes in the lung of mice given bleomycin or PBS

(A) Representative images of lung tissue sections showing morphological changes in lung architecture after bleomycin installation, H&E staining shows inflammatory changes in bleomycin treated groups, significantly higher at day 18 than at day 3 and marginally higher than that at day 32. No significant changes were observed in the group given PBS. (B) Images of lung tissue sections showing morphological changes in lung architecture after bleomycin installation, increased collagen deposition in the lung of mice given bleomycin at day 18 and day 32 compared with day 3, and marginally higher at day 18 compared with day 32 ($p=0.025$). There were no significant changes observed at day 18 and 32 compared with day 3 after PBS installation. Gomori's Trichrome stain highlighted collagen patches around bronchioles, blood vessels and in the parenchyma. Sections were viewed under light microscopy (magnification x10).

Lung inflammation score:

H&E stained lung sections were scored for inflammation based on our scoring grade (Materials and Methods section 2.5.2). The lung tissue sections from mice given bleomycin had higher inflammatory scores at day 18 and 32 compared with day 3 or at any time in the PBS treated mice (Figure 3.4). The main characteristic features of inflammation were infiltration of inflammatory cells, perivascular haemorrhage, and collapse of the alveoli. There was a modest but not significant ($p=0.093$) decrease in inflammation score between bleomycin treated mice at day 32 compared with day 18 (Figure 3.4).

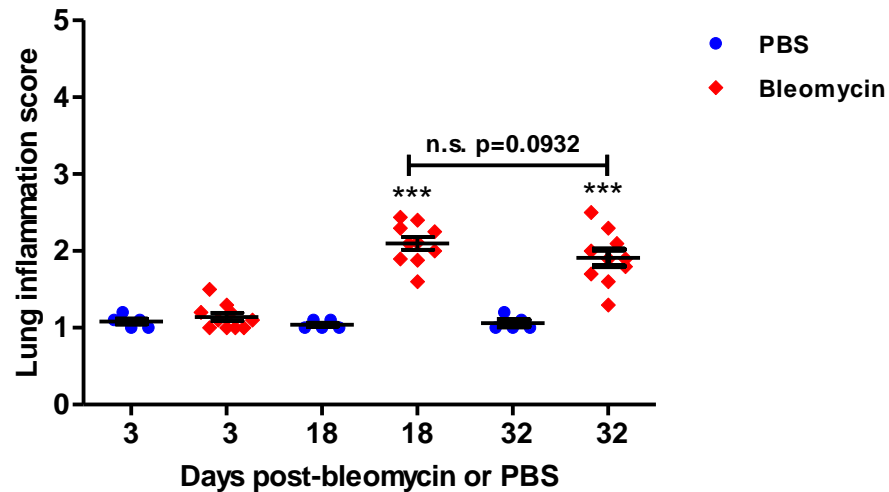


Figure 3.4 Lung inflammation score of the mice given bleomycin or PBS

The lung inflammation was quantified by a histological score described in Materials and Methods (section 2.5.2). A significantly higher score was recorded at day 18 and 32 in mice given bleomycin compared to PBS control groups. One-way ANOVA; n.s. $p > 0.05$; *** $p < 0.001$; bars=mean \pm SEM; n= 5-10 mice/group.

Lung fibrosis score:

The histological assessment of lung fibrosis was quantified and the mice given bleomycin had a highly significant increased score at days 18 and 32 compared with day 3, and higher than mice given PBS. The main features of fibrosis were collagen bundles deposition around bronchioles, blood vessels, and parenchyma. PBS treated mice had no significant changes in the lung fibrosis score (Figure 3.5).

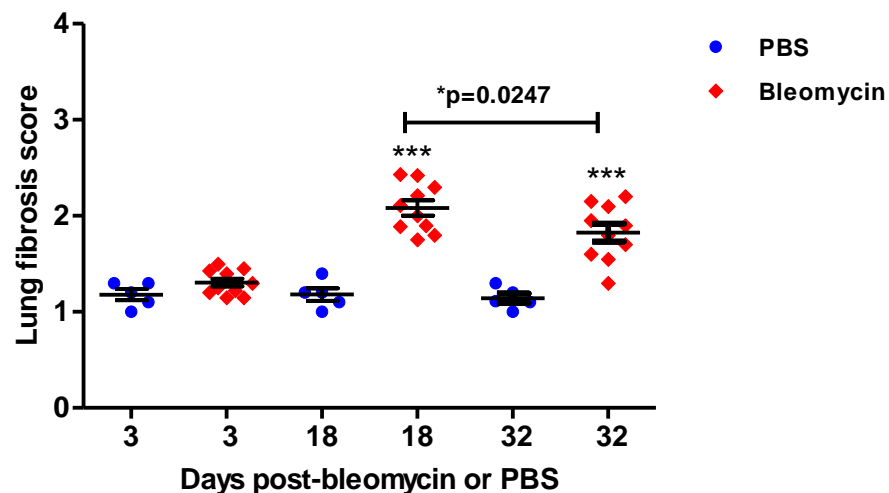


Figure 3.5 Lung fibrosis score of the mice given bleomycin or PBS

Fibrosis was assessed by histological score described in Materials and Methods (section 2.5.2). A highly significant lung fibrosis score was demonstrated for mice given bleomycin at day 18 and 32 compared with day 3. The score was significantly lower at day 32 compared with day 18 for mice given bleomycin ($p = 0.025$). One-way ANOVA; * $p > 0.05$; *** $p < 0.001$; bars=mean \pm SEM; n= 5-10 mice/group.

Bleomycin administration increased the number of inflammatory cells in the lung airspace collected by bronchoalveolar lavage (BAL).

Total cell count:

The cells in the airspace were collected by bronchoalveolar lavage as described in Materials and Methods (section 2.3.9). The total cell counts in fluid obtained by BAL were quantified at 3, 18, and 32 days after PBS or after bleomycin installation. Mice The mean total BAL cell count in the bleomycin treated group at 18 and 32 were significantly higher than bleomycin treated mice at day 3, and all PBS treated groups; day 3, 18, and 32 ($p < 0.001$). The count was significantly lower at day 32 compared with day 18 for mice given bleomycin ($p = 0.0003$).

The mean of total BAL cell counts were as following:-

Mice given bleomycin at days 3	0.23×10^6 ,
Mice given bleomycin at days 18	0.82×10^6 ,
Mice given bleomycin at days 32	0.53×10^6
Mice given PBS at days 3	0.15×10^6 ,
Mice given PBS at days 18	0.16×10^6 ,
Mice given PBS at days 32	0.15×10^6 (Figure 3.6).

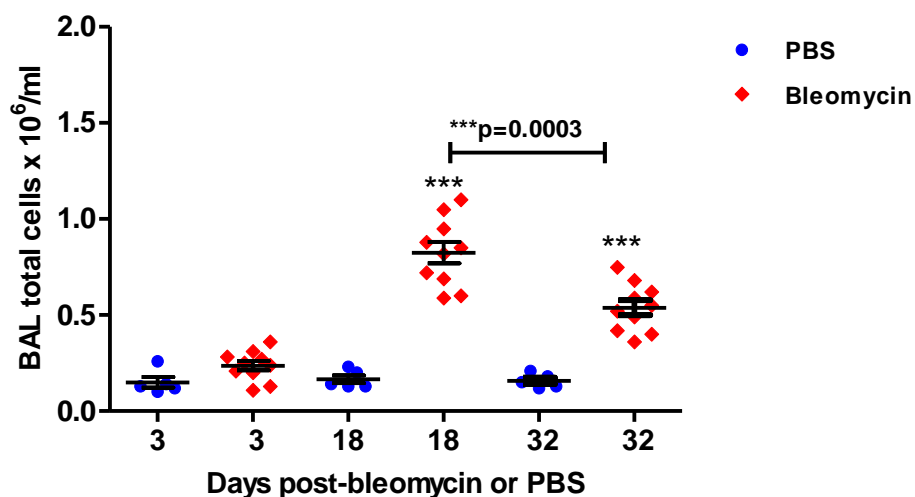


Figure 3.6 Total BAL cell count in the BAL of mice given bleomycin or PBS
The counts from mice given bleomycin at day 18 and 32 were significantly higher compared with the day 3 after bleomycin installation or all PBS treated groups. A significant reduction in cell counts was observed in the mice given bleomycin at day 18 compared with day 32 ($p = 0.001$). One-way ANOVA; *** $p < 0.001$; bars = mean \pm SEM; $n = 5-10$ mice/group.

Macrophage count:

The higher total cell count of the BAL was reflected by changes in the differential cells count (Figure 3.7 and 3.8). The mean total BAL macrophage count in the bleomycin treated group at 18 and 32 were significantly higher than bleomycin treated mice at day 3, and all PBS treated groups; day 3, 18, and 32 ($p < 0.001$). The total BAL macrophage count was significantly reduced at day 32 compared with day 18 after bleomycin ($p < 0.001$) (Figure 3.7).

The mean of total BAL macrophage counts were as following:-

Mice given bleomycin at days 3	0.21×10^6 ,
Mice given bleomycin at days 18	0.64×10^6 ,
Mice given bleomycin at days 32	0.38×10^6
Mice given PBS at days 3	0.13×10^6 ,
Mice given PBS at days 18	0.15×10^6 ,
Mice given PBS at days 32	0.12×10^6 (Figure 3.7).

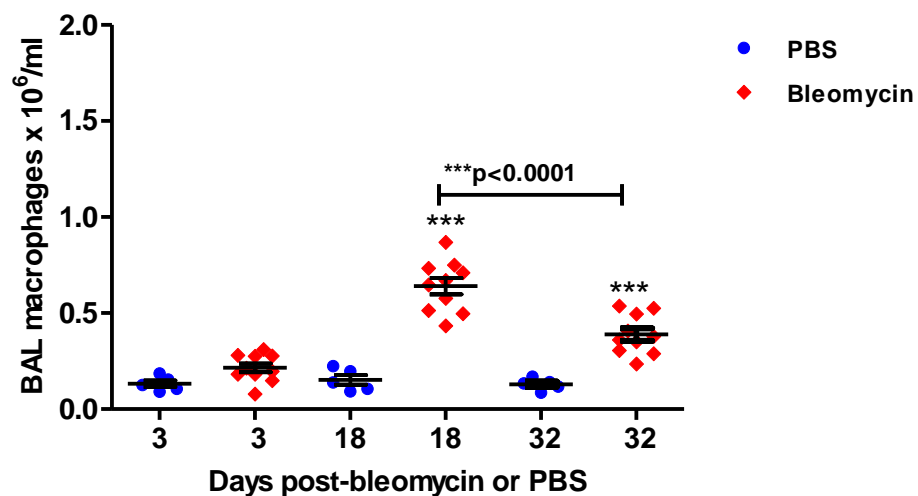


Figure 3.7 Macrophage cell count in the BAL of mice given bleomycin or PBS
The macrophage cell count was significantly higher in the bronchoalveolar lavage fluid retrieved from the bleomycin treated mice at 18 and 32 days in comparison with bleomycin at day 3 or all PBS treated groups. A significant reduction in macrophage count was recorded between the bleomycin treated groups at day 32 compared with day 18. One-way ANOVA; *** $p < 0.001$; bar=mean \pm SEM; n= 5-10 mice/group.

Lymphocyte count:

Lymphocyte cells count demonstrated high significant difference between bleomycin treated group at day 18 and 32 than the day 3 or all PBS treated groups.

The significant differences observed between bleomycin treated mice at day 18 and day32 ($P<0.001$). There was a significant reduction in lymphocyte cell count at day 32 compared with day 18 after bleomycin ($p<0.001$) (Figure 3.8).

The mean of total BAL lymphocyte counts were as following:-

Mice given bleomycin at days 3	0.026×10^6 ,
Mice given bleomycin at days 18	0.17×10^6 ,
Mice given bleomycin at days 32	0.07×10^6
Mice given PBS at days 3	0.007×10^6 ,
Mice given PBS at days 18	0.005×10^6 ,
Mice given PBS at days 32	0.006×10^6 (Figure 3.8).

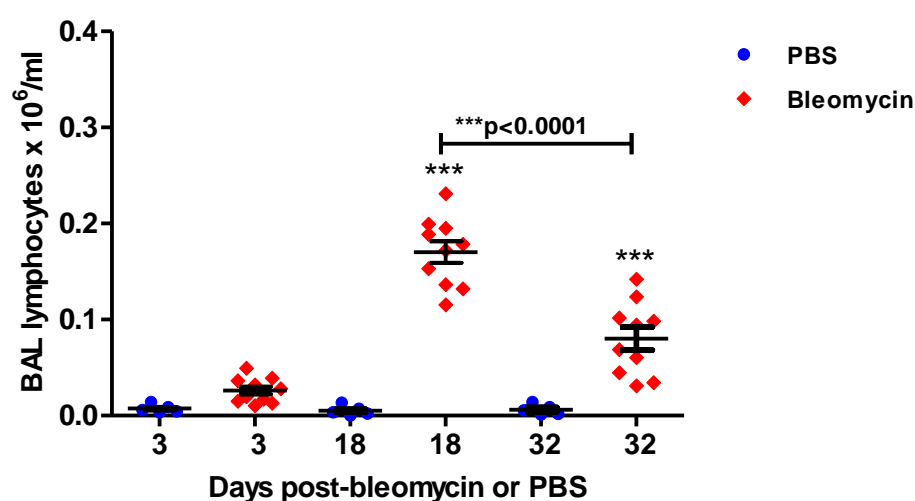


Figure 3.8 Lymphocyte cell count in the BAL of mice given bleomycin or PBS
 The lymphocyte cell count was significantly higher in the bronchoalveolar lavage fluid retrieved from the bleomycin treated mice at 18 and 32 days in comparison with day 3 or all PBS treated groups. A significant reduction was recorded between the bleomycin treated group at day 32 compared with day 18. One-way ANOVA; *** $p<0.001$; bar=mean \pm SEM; n= 5-10 mice/group.

3.1.2.2 Selection of the dose of LXR agonist (GW3965) required to investigate its role in the severity of the murine model of bleomycin-induced pulmonary fibrosis

Introduction and Aim

Many experimental attempts have been made to activate and understand LXR function *in vivo* by using different synthetic agonists, for example GW3965 and T1317. These synthetic compounds used for activating LXR in different models of disease use different doses, time courses, and routes of administration, therefore, it was necessary to determine the most effective dose required for activation of LXR in the murine bleomycin pulmonary fibrosis model. GW3965 was the agonist which was chosen, it has been used in the literature to explore the role of LXRs. GW3965 is a nonsteroidal LXR ligand that was synthesized and introduced by the pharmaceutical company GlaxoSmithKline in the USA. It is characterised by its high potency and selectivity confirmed by its ability to induce the expression of ABCA1 *in vitro* and in the mice intestine after oral dose administration [58]. I selected the high dose 30 mg/kg GW3965 because this dose had previously shown to induce LXR activation, by intraperitoneal (IP) injection [74]. Also I tried to use dose of 3 mg/kg GW3965 to see if there is any sufficient effectively to stimulate LXRs and to avoid using the higher optimised dose.

Methods:- Three groups of male C57BL/6 mice were used (n=10 per group), 10-12 week old and 23-25 grams weight. On day zero all mice were anaesthetised using isoflurane in an inhalation anaesthetic chamber and all were given 0.06mg of bleomycin sulphate in 30 μ l PBS / by intra-nasal application. Three days prior to day zero, the mice were treated with daily intra-peritoneal (IP) injections of either vehicle (5% Cremophor /PBS), 3 mg/kg LXR agonist (GW3965 in 5% Cremophor/PBS) or 30 mg/kg LXR agonist (GW3965 in 5% Cremophor/PBS). The daily intra-peritoneal continued until day 18 were the mice were culled. The mice were monitored daily for wellbeing, changes in body weight.

LXR agonist treatment exacerbated the loss of body weight in mice given bleomycin

The characteristic loss of body weight suggesting systemic characteristics caused by bleomycin administration was evident in all groups of mice (Figure 3.9). The loss of body weight was significantly higher in the group treated with 30 mg/kg LXR agonist compared with the vehicle ($p < 0.001$) or 3 mg/kg LXR agonist ($p = 0.004$).

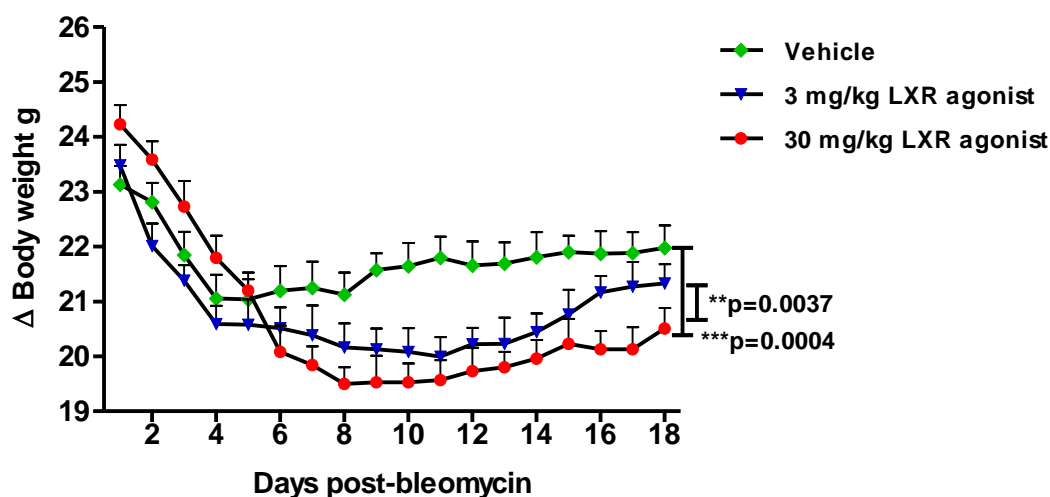


Figure 3.9 Daily body weight changes in mice given bleomycin and treated with different concentration doses of LXR agonist or vehicle
 Three groups of male C57BL/6 mice (8 weeks old) received bleomycin (0.06mg in 30 μ l PBS / mouse) intranasally. Mice groups were treated with daily intra-peritoneal injections of either vehicle (5% Cremophor /PBS), 3 mg/kg LXR agonist (GW3965 in 5% Cremophor/PBS) or 30 mg/kg LXR agonist (GW3965 in 5% Cremophor/PBS). Progressive significant body weight loss was associated with the higher dose of LXR agonist compared with vehicle or 3 mg/kg LXR agonist. Student t-Test; **P<0.01; ***P<0.001; Error bars=mean \pm SEM; n= 10 mice/group.

LXR agonist treatment exacerbated the histopathological inflammatory and fibrotic changes in the lungs of mice given bleomycin

Administration of LXR agonist lead to worsening of the pathomorphological changes in the lung architecture of these mice given bleomycin (Figure 3.10 A and B). The severity of these changes correlated with the concentration of the agonist; daily intraperitoneal administration of 30mg/kg LXR agonist lead to increased severity of the lung inflammatory ($p<0.001$, Figure 3.11) and fibrotic ($p<0.001$, Figure 3.12) changes in comparison with groups treated with 3mg/kg LXR agonist or vehicle (Figure3.10 A and B).

Histological staining of mice lungs with H&E stain demonstrated severe inflammatory changes as shown by an infiltration of inflammatory cells, perivascular haemorrhage, oedema, and collapse of alveoli. This was more pronounced in mice that were treated with 30 mg/kg LXR agonist in comparison with mice treated with 3 mg/kg LXR agonist or vehicle (Figure3.10 A).

Histo-fibrotic changes in lung tissue sections were determined by using Gomori's Trichrome stain. Collagen deposition was seen as bundles and fibrotic foci distributed mainly around bronchioles, blood vessels, and parenchyma. These were observed predominantly in mice that were treated with 30 mg/kg LXR agonist in comparison with mice that were treated with 3 mg/kg LXR agonist or vehicle (Figure 3.10 B).

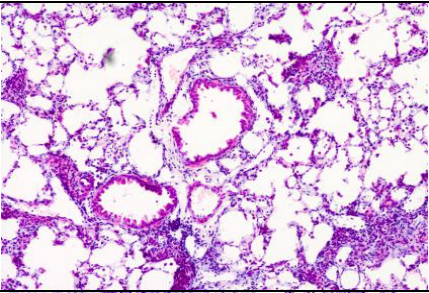
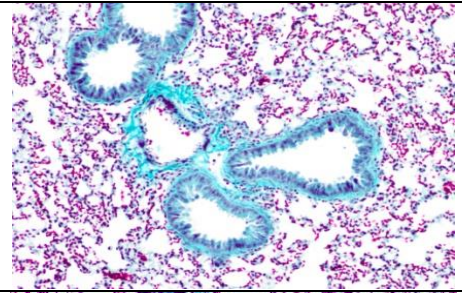
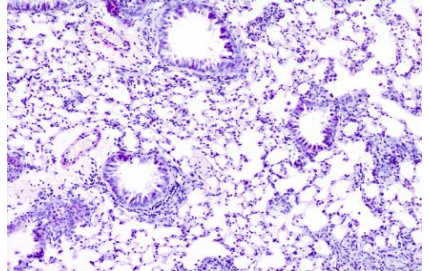
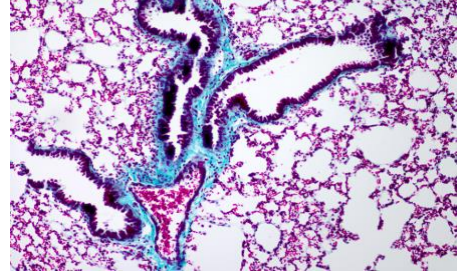
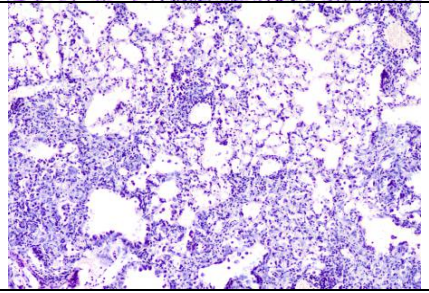
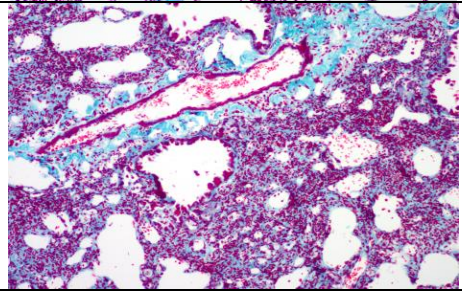
Group	A	B
	H&E	Trichrome
Vehicle		
3 mg/kg LXR agonist		
30 mg/kg LXR agonist		

Figure 3.10 Histological inflammatory and fibrotic changes in the lung of mice given bleomycin and treated with different concentration doses of LXR agonist or vehicle (A) Representative images of stained lung tissue sections showing morphological changes in lung architecture after daily injection of either different doses of LXR agonist or vehicle. H&E staining shows more severe inflammatory changes in the group that was treated with 30 mg/kg LXR agonist, compared with the group that was treated with 3 mg/kg LXR agonist or group that treated with vehicle. (B) Representative images of lung tissue sections stained with Gomori's Trichrome stain showing collagen patches around bronchioles, blood vessels and in the parenchyma. The collagen deposition was more extensive in the lungs of mice given bleomycin and treated with 30 mg/kg LXR agonist, compared with lungs of mice given bleomycin and treated with either 3 mg/kg LXR agonist or vehicle. Sections were viewed under light microscopy (magnification x10).

Lung sections stained with H&E and Gomori's Trichrome stain were scored blind for a semi-quantitative score of inflammation and fibrosis. The scoring was blindly by me and an independent colleague both blind to the origin of the tissue section. There was a significantly higher score ($p < 0.001$) for the lung inflammation in mice given bleomycin and treated with 30 mg/kg LXR agonist compared with those treated with either 3 mg/kg LXR agonist or vehicle (Figure 3.11).

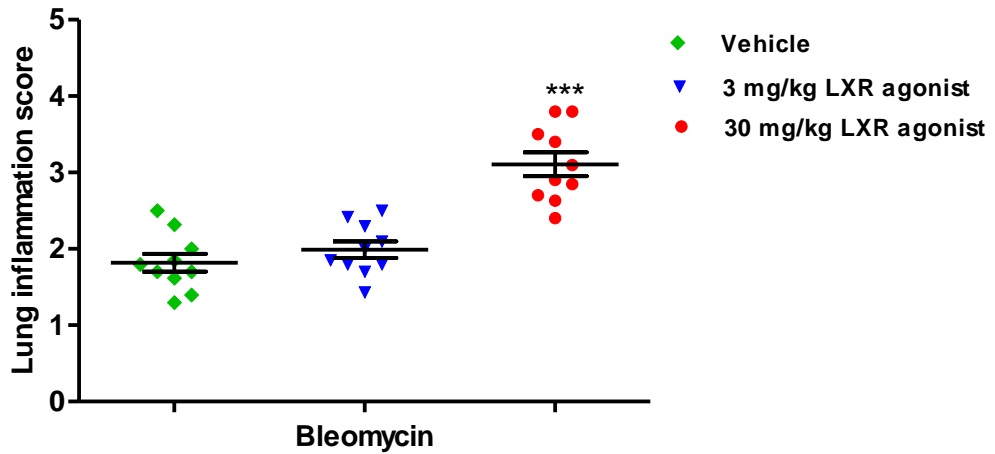


Figure 3.11 Lung inflammation score of the mice given bleomycin and treated with different concentration doses of LXR agonist or vehicle
 Inflammation was assessed by histological score (details are described in the Materials and Methods section 2.5.2). There was a highly significant lung inflammation score in mice given bleomycin and treated with 30 mg/kg LXR agonist compared with groups treated with either 3 mg/kg LXR agonist or vehicle. One-way ANOVA; *** $P < 0.001$; bar=mean \pm SEM; n= 10 mice/group.

The lung tissue fibrosis score was quantified using the Gomori's Trichrome stained lung tissue sections. This demonstrated a highly significant ($p < 0.001$) increase in collagen deposition in the lung of mice given bleomycin and treated with 30 mg/kg LXR agonist compared with those treated with either 3 mg/kg LXR agonist or vehicle (Figure 3.12).

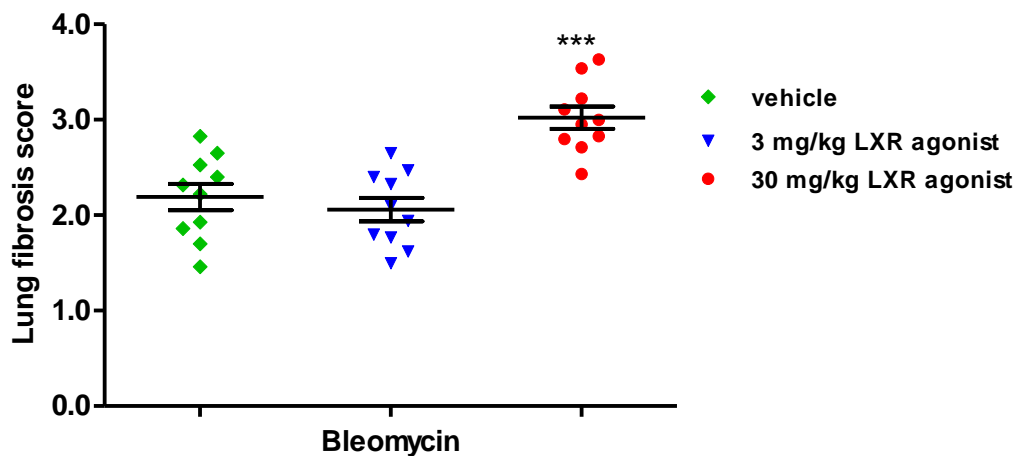


Figure 3.12 Lung fibrosis score of the mice given bleomycin and treated with different concentration doses of LXR agonist or vehicle
 The fibrosis score was assessed by fibrosis score (details are described in the Materials and Methods section 2.5.2). This demonstrated highly significant increase in fibrosis ($p < 0.001$) in lungs of mice given bleomycin and treated with 30 mg/kg LXR agonist compared with those treated with 3 mg/kg LXR agonist or vehicle. One-way ANOVA; *** $P < 0.001$; bar=mean \pm SEM; n= 10 mice/group.

LXR agonist treatment increased the inflammatory cell numbers in the bronchoalveolar lavage (BAL) of mice given bleomycin

Total cell count:

The mean BAL total cells for mice given bleomycin and treated with either 3, 30 mg/kg LXR agonist or vehicle were as follow:

Mice treated with vehicle	0.90 x 10 ⁶ ,
Mice treated with 3 mg/kg LXR agonist	0.87 x 10 ⁶ ,
Mice treated with 30 mg/kg LXR agonist	1.49 x 10 ⁶ ,

The total BAL cell count was significantly higher in the mice received 30 mg/kg LXR agonist than the other groups (p<0.001) (Figure 3.13).

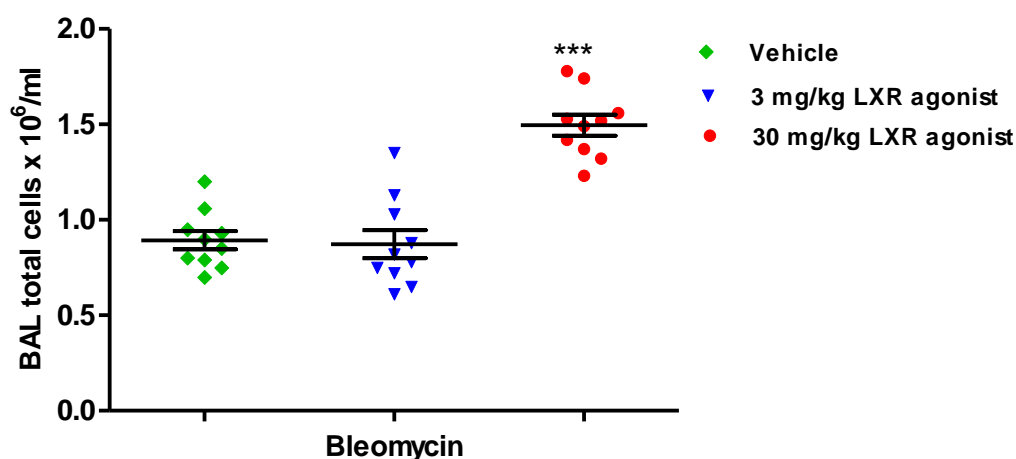


Figure 3.13 Total BAL cell count in the BAL of mice given bleomycin and treated with different concentration doses of LXR agonist or vehicle

The inflammatory cells were retrieved by bronchoalveolar lavage from all bleomycin treated mice. The cell counts were significantly increased in BAL from bleomycin treated mice that received 30 mg/kg LXR agonist compared with 3 mg/kg LXR agonist or vehicle. One-way ANOVA; ***P<0.001; bar=mean ±SEM; n= 10 mice/group.

Macrophage count:

Among of the inflammatory cells that were retrieved from the BAL, macrophages were the dominant cell type. The mean BAL macrophage counts for mice given bleomycin and treated with either 3, 30 mg/kg LXR agonist or vehicle were as follow:

Mice treated with vehicle	0.74 x 10 ⁶ ,
---------------------------	--------------------------

Mice treated with 3 mg/kg LXR agonist 0.69×10^6 ,

Mice treated with 30 mg/kg LXR agonist 1.30×10^6 ,

The mean macrophage count in the mice given bleomycin and with 30 mg/kg LXR agonist was significantly higher ($p < 0.001$) than the mice given bleomycin and treated with either of 3 mg/kg LXR agonist or vehicle (Figure 3.14).

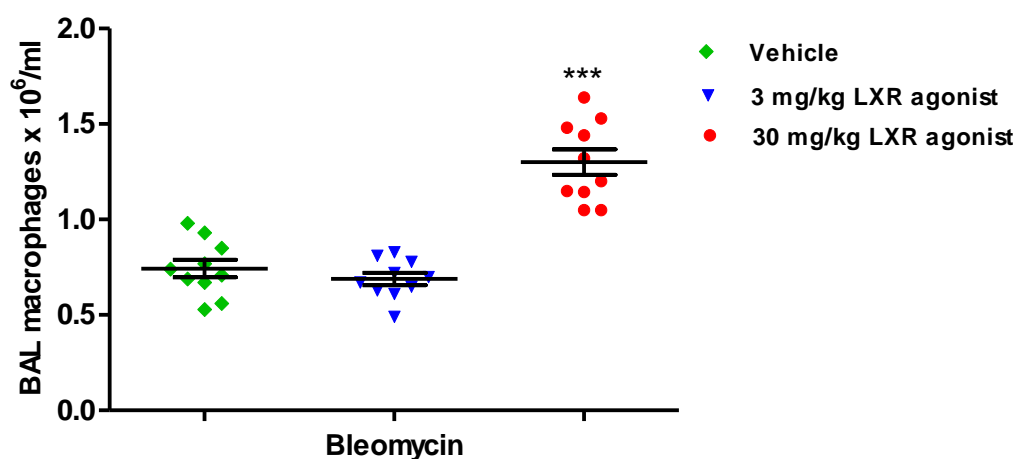


Figure 3.14 Macrophage cell count in the BAL of mice given bleomycin and treated with different concentration doses of LXR agonist or vehicle.

The BAL macrophage cell count was significantly higher in the bronchoalveolar lavage fluid from mice given bleomycin and treated with 30 mg/kg LXR agonist compared with those mice treated with either 3 mg/kg LXR agonist or vehicle. One-way ANOVA; *** $P < 0.001$; bar=mean \pm SEM; n= 10 mice/group

Lymphocyte count:

The mean BAL lymphocyte count revealed that there were no significant differences in the lymphocyte count between all mice given bleomycin and treated with different doses of LXR agonist or vehicle. The mean BAL lymphocyte counts for mice given bleomycin and treated with either 3, 30 mg/kg LXR agonist or vehicle were as follow:

Mice treated with vehicle 0.14×10^6

Mice treated with 3 mg/kg LXR agonist 0.17×10^6 ,

Mice treated with 30 mg/kg LXR agonist 0.19×10^6 , (Figure 3.15).

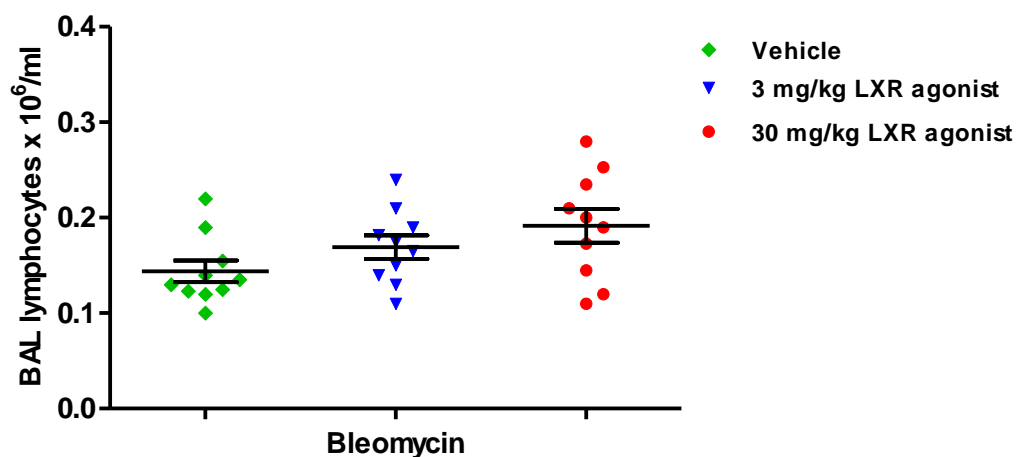


Figure 3.15 Lymphocyte cell count in the BAL of mice given bleomycin and treated with different concentration doses of LXR agonist or vehicle

The lymphocyte cell count exhibited no significant differences between the groups treated with either 30 mg/kg LXR agonist, 3 mg/kg LXR agonist or vehicle. One-way ANOVA; n.s. $P > 0.5$; bar = mean \pm SEM; n = 10 mice/group

3.1.2.3 Treatment with LXR agonist (GW3965) had no effects on C57BL/6 mice given PBS

Introduction and Aim

We had shown above that daily treatment with LXR agonist (GW3965) to C57BL/6 mice given bleomycin resulted in an exacerbation of the pulmonary inflammatory and fibrotic responses. This was shown by an increase in systemic and local inflammatory and fibrotic changes, therefore, it was an important to demonstrate the specificity of this effect by excluding that it was a nonspecific targeting of the LXR agonist.

Methods: - Three groups of male C57BL/6 mice were used (n=10 per group), 10-12 week old and 23-25 g weight. Three days prior the experiment mice were treated with daily intra-peritoneal injection of either vehicle (5% Cremophor/PBS), 3 mg/kg LXR agonist (GW3965 in 5% Cremophor/PBS) or 30 mg/kg LXR agonist (GW3965 in 5% Cremophor/PBS) that continued until day 18 when the mice were culled. On day zero, all mice were anesthetised using isofluorane in an inhalation anaesthetic chamber during which the mice were given intra-nasal 30 μ l PBS. The mice were monitored daily for wellbeing and changes in body weight until day 18 when the mice were culled.

LXR agonist treatment did not affect the body weight in mice given PBS

Daily monitoring of body weight showed no differences in all mice groups tested. All the groups of mice lost weight in the first day due to the procedure of intranasal

administration of PBS but they recovered after that and started growing relatively equally between all groups that treated with different daily intraperitoneal injections of either 3 mg/kg LXR agonist, 30 mg/kg LXR agonist or vehicle, (Figure 3.16).

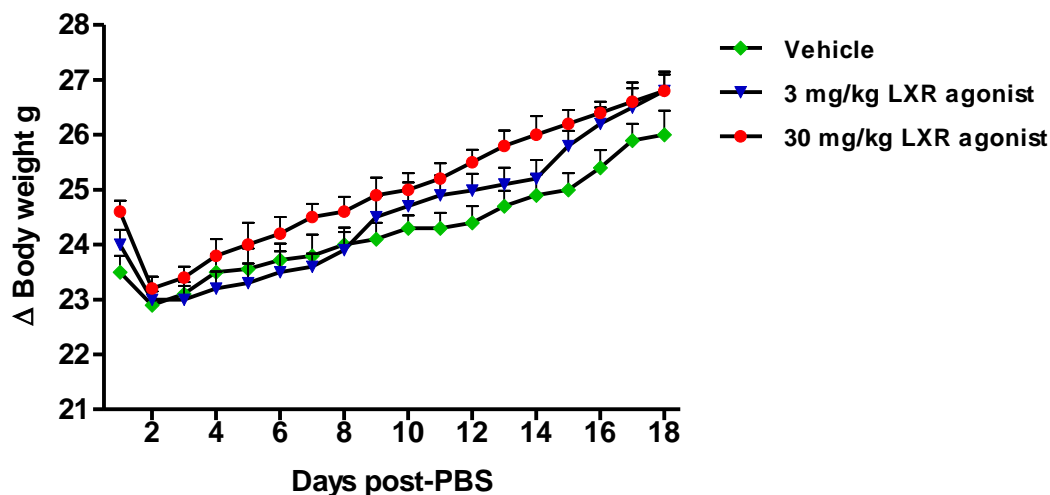


Figure 3.16 Daily body weight changes in mice given PBS and treated with different concentration doses of LXR agonist or vehicle

Daily body weight changes in male C57BL/6 mice (8 weeks old) that received PBS (30 μ l PBS / mouse) intranasally. Mice groups were given daily intra-peritoneal injection of either vehicle (5% Cremophor /PBS), 3 mg/kg LXR agonist (GW3965 in 5% Cremophor/PBS) or 30 mg/kg LXR agonist (GW3965 in 5% Cremophor/PBS). There were no differences in body weight were seen intra-peritoneal. Student t-Test; n.s. $p > 0.05$; bar=mean \pm SEM; n= 10 mice/group.

LXR agonist treatment did not affect histopathological inflammatory and fibrotic outcomes in lungs of mice given PBS

Administration of PBS intra-nasally had no effect on the lung architecture, or caused any significant inflammatory or fibrotic changes from normal mice lungs were observed. Daily administration of the vehicle or 3 mg/kg or 30 mg/kg LXR agonist did not make any significant changes to the normal lung architecture. This was demonstrated by H&E stain and Gomori's Trichrome stain of lung tissue sections of these mice (Figure 3.17 A and B).

Lung section from mice given PBS and treated with vehicle or 3 mg/kg LXR agonist or 30 mg/kg LXR agonist were stained with H&E. This showed normal lung architecture without any inflammatory changes, normal blood vessels, normal alveolar structure and no inflammatory cell infiltration (Figure 3. 17 A).

Gomori's Trichrome stain was used to stain lung section from mice given PBS and treated with vehicle or 3 mg/kg LXR agonist or 30 mg/kg LXR agonist revealed

normal lung collagen content at lung bronchioles, blood vessels and interstitium without any significant fibrotic changes (Figure 3. 17 B).

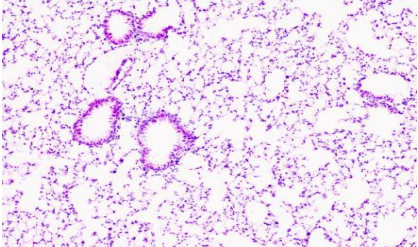
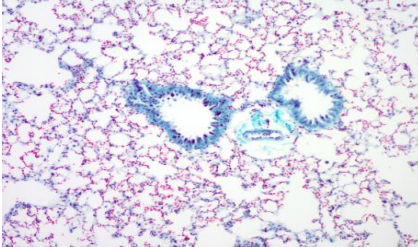
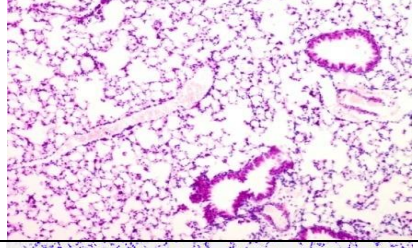
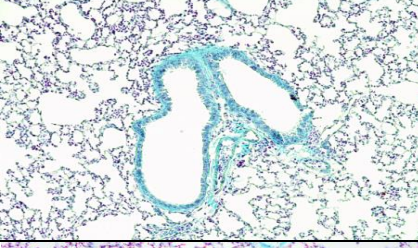
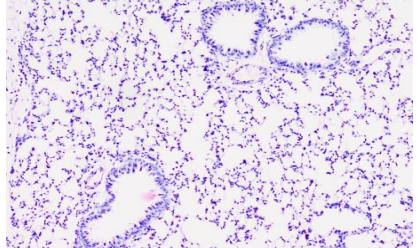
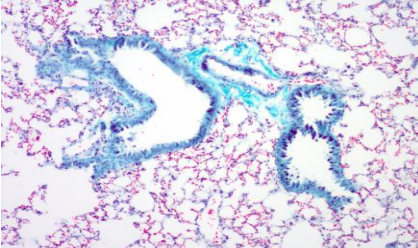
Group	A	B
	H&E	Trichrome
Vehicle		
3 mg/kg LXR agonist		
30 mg/kg LXR agonist		

Figure 3.17 Histological inflammatory and fibrotic changes in the lung of mice given PBS and treated with different concentration doses of LXR agonist or vehicle (A) Representative images of lung tissue sections stained with H&E. Sections demonstrated normal lung architecture without any significant morphological changes after daily injection of either of vehicle or different doses of LXR agonist (3 & 30 mg/kg). (B) Representative images of lung tissue sections stained with Gomori's Trichrome stain. Sections demonstrated normal lung architecture with basal collagen content around lung bronchioles and blood vessels without any significant fibrotic changes after daily injection of either different doses of vehicle or LXR agonist (3 & 30 mg/kg). Sections were viewed under light microscopy (magnification x10).

Quantification of the PBS treated mice lung section stained with H&E and Gomori's Trichrome stain were performed and scored blind for inflammation and fibrosis.

Scoring of H&E stained lung sections from mice given PBS and treated with daily intra-peritoneal injection of either vehicle or 3 mg/kg LXR agonist or 30 mg/kg LXR agonist demonstrated a low score on our inflammation scoring grade described in (Materials and Methods section 2.5.2). There were no significant differences between the groups (Figure 3.18).

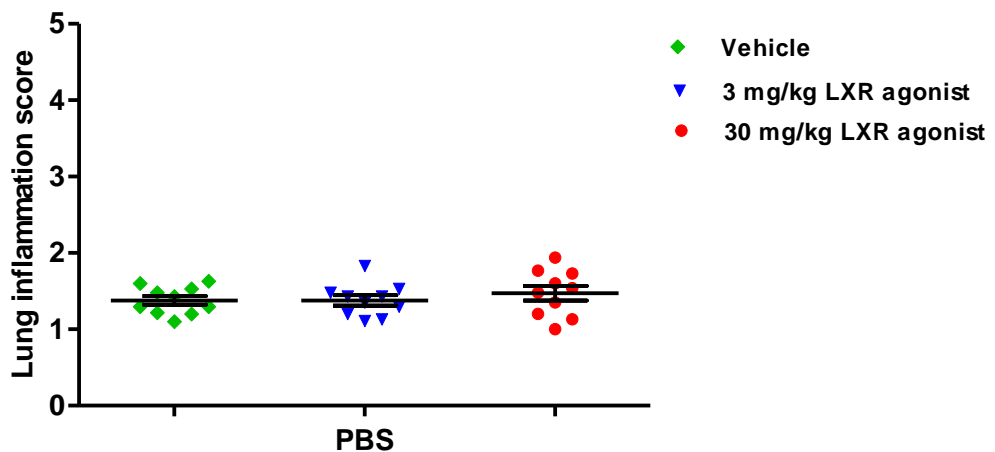


Figure 3.18 Lung inflammation score of mice given PBS and treated with different concentration doses of LXR agonist or vehicle
 Inflammation was assessed by histological score (see Materials and Methods section 2.5.2). No differences were demonstrated between groups treated with either 3, 30 mg/kg LXR agonist or vehicle. One-way ANOVA; n.s. $p > 0.05$; bar = mean \pm SEM; n = 10 mice/group.

Quantifying the tissue fibrosis was carried out on Gomori's Trichrome stained lung tissue sections from groups mice given PBS and treated with vehicle or 3 mg/kg LXR agonist or 30 mg/kg LXR agonist. This demonstrated essentially normal collagen content reflected by a low fibrosis score using our fibrosis grade described in Materials and Methods section 2.5.2 (Figure 3.19).

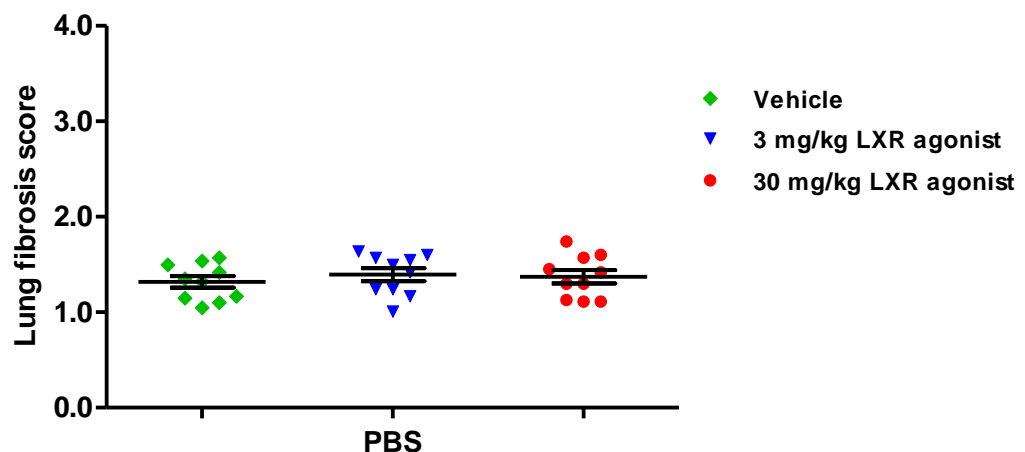


Figure 3.19 Lung fibrosis score of mice given PBS and treated with different concentration doses of LXR agonist or vehicle
 Fibrosis was assessed by fibrosis score (see Materials and Methods section 2.5.2). No differences were shown between the groups. One-way ANOVA; n.s. $P > 0.05$; bar = mean \pm SEM; n = 10 mice/group.

LXR agonist treatment did not affect the inflammatory cell number or phenotype in the bronchoalveolar lavage (BAL) of mice given PBS

Total cell count:

Total BAL cells were counted for mice given PBS and treated with daily intra-peritoneal injections of either vehicle or 3, or 30 mg/kg LXR agonist. The total cell counts did not show any significant differences between these experimental groups. The mean total BAL cells counts were as follows:-

Mice treated with vehicle	0.161 x 10 ⁶ ,
Mice treated with 3 mg/kg LXR agonist	0.170 x 10 ⁶ ,
Mice treated with 30 mg/kg LXR agonist	0.150 x 10 ⁶ (Figure 3.20).

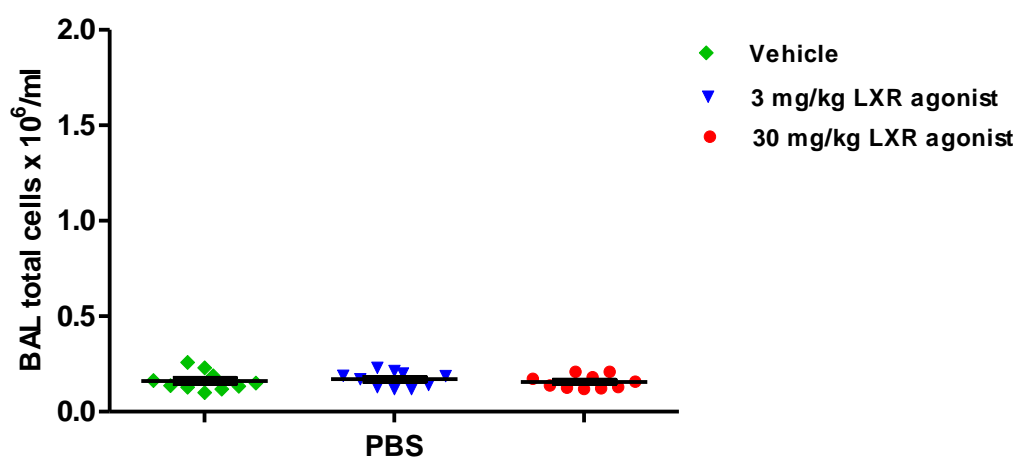


Figure 3.20 Total BAL cell count in the BAL of mice given PBS and treated with different concentration doses of LXR agonist or vehicle

The BAL total cell were retrieved by bronchoalveolar lavage from all mice groups given PBS. The counts showed no significant differences between all experimental groups treated with different daily intra-peritoneal injections of vehicle, 3 mg/kg LXR agonist, or 30 mg/kg LXR agonist. One Way ANOVA; n.s. $P > 0.05$; Mean \pm SEM; n= 10 mice/group.

Macrophage count:

The BAL macrophage differential cell counts for all PBS given animals revealed no significant differences between the experimental groups although they received daily intra-peritoneal injections of either vehicle or 3 mg/kg LXR agonist or 30 mg/kg LXR agonist. The mean macrophage cells counts were as follows:-

Mice treated with vehicle	0.143 x 10 ⁶ ,
Mice treated with 3 mg/kg LXR agonist	0.151 x 10 ⁶ ,

Mice treated with 30 mg/kg LXR agonist 0.129×10^6 (Figure 3.21).

Lymphocyte count:

The BAL lymphocyte differential cell counts for all PBS given animals showed no significant differences between the experimental groups and the mean values were as follows:

Mice treated with vehicle	0.008×10^6 ,
Mice treated with 3 mg/kg LXR agonist	0.007×10^6 ,
Mice treated with 30 mg/kg LXR agonist	0.010×10^6 (Figure 3.22).

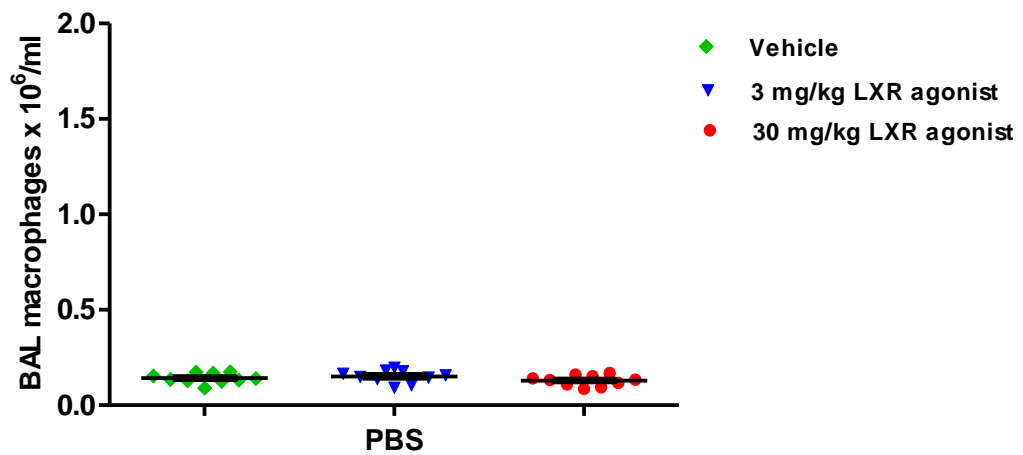


Figure 3.21 Macrophage cell count in the BAL of mice given PBS and treated with different concentration doses of LXR agonist or vehicle

The BAL macrophage cell count showed no significant differences between the groups. One-way ANOVA; n.s. $P > 0.05$; bar = mean \pm SEM; n = 10 mice/group.

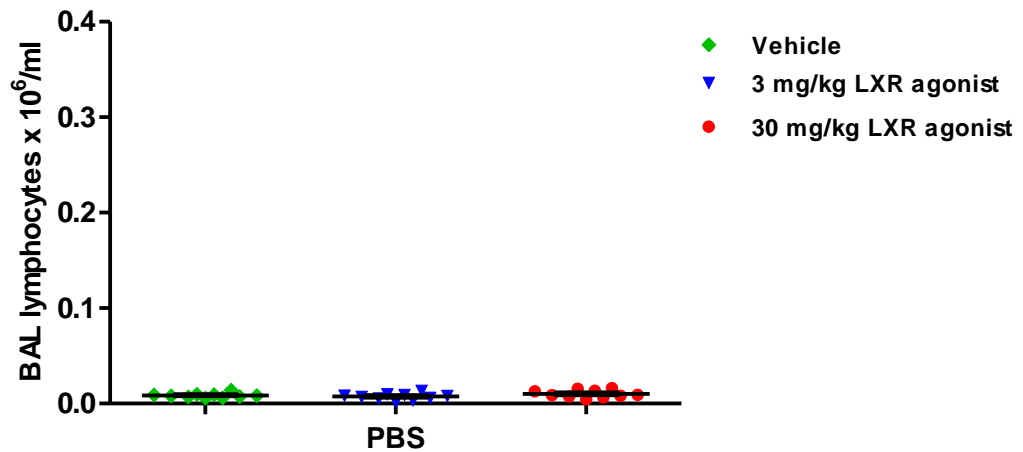


Figure 3.22 Lymphocyte cell count in the BAL of mice given PBS and treated with different concentration doses of LXR agonist or vehicle

The BAL lymphocyte cell count showed no significant differences between the groups. One-way ANOVA; n.s. $P > 0.05$; bar = mean \pm SEM; n = 10 mice/group.

3.1.2.4 Validation of LXR agonist function on $LXR\alpha^{-/-}\beta^{-/-}$ mice

Introduction and aim

The primary gene-target for LXR activation is ABCA1 and expression of this protein can act as a reporter of LXR activation. To validate our $LXR\alpha^{-/-}\beta^{-/-}$ double gene-deleted mice we tried to look on the expression of ABCA1, $LXR\alpha$, and $LXR\beta$ in these mice in response to treatment with LXR agonist (GW3965) or vehicle.

Methods: - Four groups of male mice (two $LXR\alpha^{-/-}\beta^{-/-}$ and two $LXR\alpha^{-/-}\beta^{-/-}$ wild-type) were used (n=5 per group), 10-12 week old and 23-25 g weight. The mice were given either 30 mg/kg LXR agonist (GW3965 in 5% Cremophor/PBS) or vehicle (5% Cremophor /PBS). The mice were allocated in groups as the following:

- A- WT mice treated with LXR agonist
- B- WT mice treated with vehicle
- C- $LXR\alpha^{-/-}\beta^{-/-}$ mice treated with LXR agonist
- D- $LXR\alpha^{-/-}\beta^{-/-}$ mice treated with vehicle

On day zero of the experiment mice were treated with daily intra-peritoneal injection of either vehicle (5% Cremophor /PBS) or 30 mg/kg LXR agonist (GW3965 in 5% Cremophor/PBS) until day 18 were all mice culled and lung sample collected. The mice were monitored daily for wellbeing.

LXR agonist had no effect on ABCA1 expression in lungs of $LXR\alpha^{-/-}\beta^{-/-}$

The expression of $LXR\alpha$, $LXR\beta$ and ABCA1 in RNA extracted from lung tissue after 18 days is shown in (Figure 3.23). There were two important observations from this experiment:

- 1- There was a significant up-regulation of mRNA expression for ABCA1, $LXR\alpha$ and $LXR\beta$ in the WT mice with LXR agonist compare to WT mice treated with vehicle, $P < 0.05$ for $LXR\alpha$ and $p < 0.001$ for $LXR\beta$ and ABCA1 expression.
- 2- The expression of ABCA1, $LXR\alpha$ and $LXR\beta$ were lower than normal in $LXR\alpha^{-/-}\beta^{-/-}$ mice treated with either LXR agonist or vehicle ($P < 0.05$).

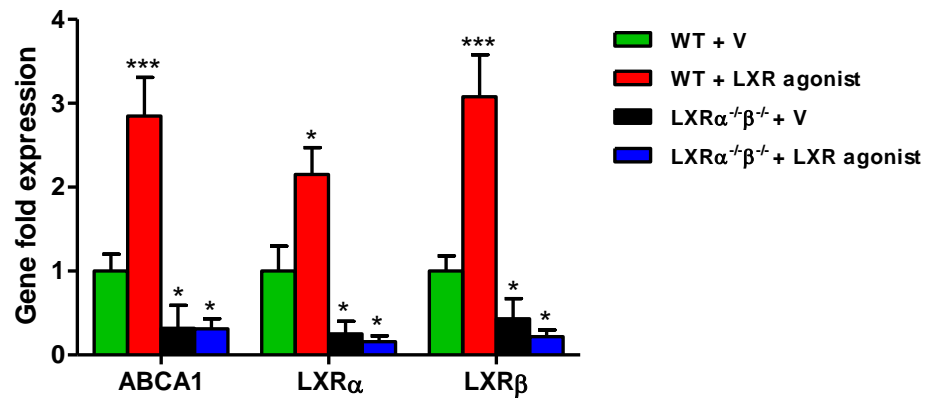


Figure 3.23 ABCA1, $LXR\alpha$, and $LXR\beta$ gene expression in lung of mice treated with vehicle or LXR agonist

ABCA1, $LXR\alpha$, and $LXR\beta$ expression levels in the lungs of four groups of mice treated with LXR agonist or vehicle. ABCA1, $LXR\alpha$, and $LXR\beta$ mRNA expression measured as fold-increase compared with control vehicle-treated mice was significantly higher in the lungs of WT mice treated with LXR agonist than the WT mice treated with vehicle. There was reduced expression of ABCA1, $LXR\alpha$ and $LXR\beta$ observed in $LXR\alpha^{-/-}\beta^{-/-}$ mice treated with vehicle or LXR agonist. One Way ANOVA; * $p < 0.05$; *** $p < 0.001$; Mean \pm SEM; $n = 5$ mice/group.

3.1.3 Discussion and Conclusion

The overall purpose of this study was to explore the role of LXR in the inflammatory process; specifically in inflammatory lung disease. Previous studies identified the involvement of LXR in other inflammatory diseases such as atherosclerosis and rheumatoid arthritis, and their results varies depending on the model, for example, a study performed using apolipoprotein E gene-deleted mice had shown that agonists of LXR and RXR were able to activate LXRs and to initiate expression of ABCA1 from macrophages resulting in cholesterol efflux from ApoE gene deleted mice but not in LXR $\alpha\beta$ gene-deleted mice [60]. This lead to conclusion that cholesterol efflux is mediated through direct expression of ABCA1 in response to LXR activation. Another study in our lab using a murine collagen induced arthritis model demonstrated that activation of LXR with T1317 and GW3965 agonists resulted in exacerbation of the inflammatory response, with excessive cartilage destruction [74]. Also a certain degree of liver fibrosis in the mice treated with LXR agonist (Data not shown), therefore, we tried to understand if LXR is involved in fibrosis and if LXR agonists can modulate the bleomycin-induced pulmonary fibrosis. Our results suggested that administration of LXR agonist can lead to exacerbation in the pulmonary fibrosis which was demonstrated by an active inflammatory and fibrotic processes. I acknowledge the controversy related to LXR activation across different inflammatory model from an anti-inflammatory role in atherosclerosis to a pro-inflammatory role in collagen induced arthritis. This still unresolved for example in atherosclerosis model, activation of LXR reveals an anti-inflammatory effect manifested by removal of the cholesterol from the artery walls but these animals suffer from accumulation of excess amount of fat in their liver.

In this Chapter the initial experiments were justified the conditions of the lung fibrosis model and the dose-response to the intervention drugs, and the characterisation of the gene-deleted mice used. This chapter demonstrated that day 18 after bleomycin administration was a useful time-point to determine the duration of the disease model. This was established by a loss of body weight which was a sign of cachexia and systemic inflammation. This was accompanied by histopathological inflammatory and fibrotic changes with local changes in airway cytology specifically the recruitment of inflammatory immune cells.

These preliminary experiments were to demonstrate the effect of administration of LXR agonist (GW3965) to the bleomycin treated mice. GW3965 is a highly specific LXR agonist. It was used at different doses to determine firstly if the activation of LXR may contribute in the modulation of bleomycin-induced pulmonary fibrosis, and secondly the optimal dose of GW3965 required to sustain the LXR activation was established. Our results suggested that intra-peritoneal administration of 30 mg/kg LXR agonist (GW3965) could augmented the pro-inflammatory and pro-fibrotic process resulting in a more severe loss of body weight, more severe lung histo-pathological inflammatory and fibrotic processes and increased numbers of

local inflammatory cell infiltrate. Compared with this, administration of 3 mg/kg LXR agonist or vehicle (Cremophor) had no significant effect.

Administration of different doses of LXR agonist into PBS treated mice showed no detectable effect on the lungs of PBS treated mice. This suggested that neither of LXR agonist nor vehicle alone affected the normal lung histology and cytology

This suggests that LXR engagement had a dose dependent, profound effect upon bleomycin-induced inflammation and fibrosis. This is the first time to my knowledge that LXR pathway might be involved in lung fibrosis. This knowledge may be informative of the disease process as well as instructive for potential new therapeutic targets.

Using bleomycin for the initiation of lung fibrosis is one of the common ways for establishing an experimental model. Bleomycin has fibrogenic side effects in cancer patients treated with bleomycin as an anticancer therapy. A similar pulmonary fibrosis can be introduced to mice by bleomycin administration suggesting that this is a relevant model.

It was important to determine the time course for the model. We chose an intranasal route of administration of bleomycin to justify getting the drug to the airspace of the lung target.

Determining the peak of the disease is one of the critical points of understanding of the model. A literature search for the optimal time course of the model used by different workers highlighted a lack of consistency. A consensus was that the peak of disease inflammatory and fibrotic features occurred between 14-21 days after bleomycin administration [192, 200, 201]. Based on this, we tried to establish our own time points for the peak of the inflammatory and fibrotic changes in the mice; therefore, we investigated 3 time points after bleomycin administration; on days 3, 18 and 32. We chose day 3 to determine the early inflammatory changes that might determine the subsequent fibrotic response, day 18 an intermediate time point between the most common peak days of the disease remodelling reported in the literature, and day 32 to determining the start of disease resolution.

Body weight changes indicated a systemic inflammatory response that started after bleomycin administration until days 8-11 then the mice started gaining weight (Figure 3.2). Our results are in agreement with other reports which show a similar 20% reduction in body weight in mice given bleomycin [202].

The local airway inflammatory parameters of airway leukocytosis and tissue inflammation and remodelling indicated that day 18 was a useful time point to demonstrate a peak of activity in our model. These results were consistent with a previous study that used Quantitative Image Analysis (QIA) which showed a mild increase in pathomorphological changes during 3-6 days after bleomycin installation while the maximum changes occurred between days 14-21[192].

The pathomorphological changes were accompanied by a significantly higher BAL total cell count; predominantly macrophage and lymphocyte. My results identified that the inflammatory response to bleomycin administration is dominated by macrophage and to lesser extent by lymphocyte infiltration. Alveolar macrophages are characterised by their multi-functional capacity in the lung. After inflammation they have a resolution capacity by their ability to remove apoptotic and necrotic debris through a non-phlogistic pathway resulting in minimisation of inflammation. In tissue fibrosis, macrophages play an important role in enhancing tissue remodelling. Alternatively activated pro-fibrotic (M2) phenotype macrophages have been identified as predominant macrophages in the lung and monocytes from IPF patients in a study that demonstrated an increased in the protein levels of several of (M2) macrophage-associated proteins [203].

Lymphocytes are a minor proportion of cells in normal BAL. That they are increased in BAL from bleomycin treated mice suggest they have an important yet unspecified role in this model. They are one of the inflammatory cell types that can potentially play an important role in initiation, continuing and eventual suppression of the inflammation. Studies have shown an accumulation of lymphocytes and lymphoid follicles with germinal centres in histological analysis of biopsy tissues from patients lung interstitium [204]. Both clinical and laboratory studies have demonstrated a role for different lymphocyte subset in fibrosis; bleomycin-induced pulmonary fibrosis using mouse strains genetically lacking T lymphocytes, or some important T-cell receptors such as CD28 that is required for full T-cell activation, demonstrated an attenuation in the fibrosis, inhibition of fibroblast proliferation and reduction of extra-cellular matrix accumulation. This suggests that T-cells contribute to the pathogenesis. B lymphocyte are an important active inflammatory cell, because of their ability to produce of antibodies, they draw attention because of presence of some auto antibodies such as anti-cytokeratins and anti-vimentin antibodies which act against alveolar epithelial cell antigens were determined in Idiopathic Pulmonary Fibrosis (IPF) patients [204]. Animal model of bleomycin pulmonary fibrosis performed on mouse strain genetically lacking CD19, an essential antigen co-receptor for B lymphocyte function, demonstrated a significant reduction in the susceptibility to bleomycin-induced fibrosis, in contrast, mouse strains that genetically over-express CD19 have enhanced susceptibility to bleomycin-induced fibrosis [205]. This suggests that B-cell activation contributes to pathology by an as yet unresolved mechanism. We did not quantify the lymphocyte subpopulation proportions and we suggest that future studies should include an extensive phenotyping of the airway (BAL) lymphocytes as well as lymphocytes isolated from dispersed interstitial lung tissue and draining thoracic lymph nodes. This could include an investigation of the presence and potential function of innate lymphocytes. These cells can produce type-2 cytokines e.g. IL-13 that is known to promote collagen production and remodelling.

My next preliminary experiment was to determine the most effective dose of the LXR agonist GW3965 required to maintain contentious activation of the receptors. GW3965 is a highly specific and highly potent agonist for LXR and has no off-

target antagonism of other nuclear receptors. The most effective dose was interpreted by monitoring the general and local inflammatory responses in the murine bleomycin-induced pulmonary fibrosis model. The preliminary suggestion of dose was 30 mg/kg based on our experimental observations and observations on previous work which identified this as a sufficient dose to sustain the activation of LXR for 24 hours in murine collagen induced arthritic model CIA model [74].

Using GW3965 at a concentration of 30 mg/kg resulted in worsening of bleomycin-induced inflammation and remodelling (Figure 3.9). The fact that this agonist is selectively and highly specific for LXR strongly supports a role for this receptor in disease outcome. This is supported by additional experiments using LXR^{-/-} mice reported later in this thesis.

Constant with the general systemic inflammatory findings including the reduction of body weight among bleomycin treated mice that received 30 mg/kg GW3965, the pathomorphological findings in the lung demonstrated highly active inflammatory and fibrotic processes (Figure 3.11). Since the effect of the LXR agonist GW3965 is not limited to any specific cell type it is possible that its effect on macrophages and lymphocytes led to an amplification of their normal pro-inflammatory and pro-fibrotic processes. LXR agonism has been shown to slow atherogenesis, but cause hepatic steatosis and dysfunction in C57BL/6 mice. The mechanism is probably that hepatic steatosis resulted from a high expression of sterol regulatory element binding protein 1-c (SREBP1-c), a transcription factor that up-regulates fatty acid synthesis [206].

One of my preliminary experiments was to understand what effect of administration of 3 and 30 mg/kg GW3965 or vehicle to mice that only received PBS intra-nasally. The aim was to demonstrate if there is any inflammatory or fibrotic outcome due to LXR agonism alone using these compounds. Clinical follow-up of these mice did not show any effect on the normal body weight (Figure 3.16). Constant with this finding, an analysis of the pathomorphological changes in lung tissue sections and BAL total and differential cell counts did not reveal any differences among the study groups. These data suggested that there is no specific effect to the administration of this agonist alone in contrast to what was observed when GW3965 was administered at a concentration of 30 mg/kg to mice that received bleomycin. Thus LXR function to exacerbate an inflammatory response triggered by another stimulus.

My last preliminary experiment was to validate our LXR $\alpha^{-/-}\beta^{-/-}$ double gene-deleted mice. This was an important step to provide a strong base for my future work which will contain using of these mice. The validation performed by measuring of the expression level of mRNA for ABCA1, LXR α , and LXR β in these mice in response to treatment with LXR agonist (GW3965) or vehicle. Activation of LXR characterised by up-regulation of ABCA1, LXR α , and LXR β in wild type mice treated with LXR agonist.

Results 3.2 Index:

3.2 Exacerbation of pulmonary fibrosis is associated with the activation of Liver X Receptor

3.2.1 Introduction and Aims

3.2.2 LXR $\alpha^{-/-}\beta^{-/-}$ double knockout mice

3.2.3 LXR $\alpha^{-/-}\beta^{-/-}$ mice develop less bleomycin-induced pulmonary fibrosis than LXR $\alpha\beta$ wild type mice; both given LXR agonist (GW3965)

3.2.3.1 Specific effect of LXR agonist in LXR $\alpha\beta$ but not LXR $\alpha^{-/-}\beta^{-/-}$ mice in murine bleomycin-induced pulmonary fibrosis

3.2.3.2 Mechanisms of LXR involvement in fibrosis

3.2.3.2.1 LXR modulation of macrophage phenotype

3.2.3.2.2 LXR modulation of fibroblast function

3.2.3.2.3 LXR directly targets collagen type I and III expression in murine fibroblast

3.2.3.2.4 Activation of LXR directly targets the promoters of collagen type I and III in the murine fibroblast cell line T1317

3.2.4 Discussion and Conclusion

3.2 Exacerbation of pulmonary fibrosis is associated with the activation of Liver X Receptors

3.2.1 Introduction and Aims

The justification for exploring the LXR in tissue remodelling using the bleomycin model of murine lung fibrosis has been detailed in the Results Chapter 3.1. In that chapter, the main objectives were to optimise the experimental conditions including the bleomycin dose used in the model, the length of the time-course of the model, and providing evidence for the LXRs deletion.

Liver X receptors (LXRs) are cytosolic receptors and transcription factors that participate in lipid transport and anti-inflammatory signalling. A literature search for a novel role in the involvement of LXRs during inflammation suggested that it had mainly an anti-inflammatory effect [52, 68, 69]. However, other literature suggested a pro-inflammatory effect for LXRs [74]. In my previous experiments, LXR agonists caused a worsening of pulmonary fibrosis as demonstrated by potent pro-inflammatory and pro-fibrotic effects. The aim of this chapter is to provide evidence that these pro-inflammatory and pro-fibrotic effects were mediated specifically by the activation of LXRs.

Idiopathic pulmonary fibrosis is a severe interstitial lung disease with no effective treatment. There is very little evidence in the literature for the involvement of LXR and fibrosis. One transcriptome profile study of genes associated with IPF identified that the LXR/RXR was one of the key pathways activated in lungs [207]. Fibrotic lesions in lung biopsies of patients with interstitial lung disease are sometimes associated with lipid-laden or 'foamy' macrophage, in particular in hypersensitivity pneumonitis [208]. Other literature that supports a role for LXR and fibrosis or remodelling includes one report describing hepatic stellate cell activation during chronic liver injury and LXR-mediated fibrotic response [75]. This study revealed that LXRs activation resulted in inhibition in stellate cell activation by suppressing collagen producing genes in primary mouse stellate cells.

The link between LXR and fibrosis is unresolved therefore the aim of this chapter was to determine the association between activation of LXR α and LXR β with GW3965 and the development of lung fibrosis in murine pulmonary fibrosis model by comparing the responses to bleomycin in LXR α ^{-/-} β ^{-/-}, and LXR $\alpha\beta$ wild type mice.

3.2.2 LXR α ^{-/-} β ^{-/-} double knockout mice

The LXR α ^{-/-} β ^{-/-} double knockout mice were generated in our lab by self-cross breeding of LXR α ^{-/-} and LXR β ^{-/-} littermates on a C57BL/6 background. Firstly, the LXR heterozygotes LXR $\alpha\pm/\beta\pm$ were generated from cross breeding of LXR α ^{-/-} and LXR β ^{-/-} littermates [209], these littermates were supplied by Lexicon

Pharmaceuticals (TX, USA). The details of this are provided in the Material and Methods (section 2.3.2).

3.2.3 LXR $\alpha^{-/-}\beta^{-/-}$ mice develop less bleomycin-induced pulmonary fibrosis than LXR $\alpha\beta$ wild type mice; both given LXR agonist (GW3965)

We aimed to demonstrate the specific role of LXRs in murine bleomycin-induced pulmonary fibrosis. The specificity of the role of LXR was confirmed by the use of LXR $\alpha^{-/-}\beta^{-/-}$ mice as control. Our aim was to confirm that the inflammatory and fibrotic response is mediated specifically through direct activation of LXRs and is not because of any off targeting response of the agonist on other nuclear receptor transcription factors or because of the activity of endogenous LXR ligands; to achieve this aim we had to use LXR $\alpha^{-/-}\beta^{-/-}$ mice.

The experiment was performed with male LXR $\alpha\beta$ wild type and LXR $\alpha^{-/-}\beta^{-/-}$ mice (10-12 weeks old and 22-25 grams weight). Animals were divided into 4 groups (n=19-23 mice per group):-

Group A- WT mice treated with vehicle (5% Cremophor in PBS as control)

Group B- WT mice treated with LXR agonist GW3965

Group C- LXR $\alpha^{-/-}\beta^{-/-}$ mice treated with vehicle

Group D- LXR $\alpha^{-/-}\beta^{-/-}$ mice treated with LXR agonist

All mice were given bleomycin intranasally at a dose of 0.06mg in 30 μ l PBS / animal. The mice were treated with daily intraperitoneal (IP) injection of vehicle (5% Cremophor v/v PBS) or LXR agonist GW3965 (30mg / kg dissolved in 5% Cremophor / PBS) according to the classified group.

The daily injection regime was necessary because our pilot data demonstrated that daily IP injection of 30 mg/kg GW3965 is necessary to induce and maintain a 20-fold up-regulation in expression of the ATP-binding cassette transporter (ABCA)1 gene which is the reporter gene of LXR activation [74]. The injections started 3 days prior to the bleomycin challenge to enable the agonist to function, and was continued daily until day 18 when all mice were culled.

3.2.3.1 Specific effect of LXR agonist in LXR $\alpha\beta$ WT but not LXR $\alpha^{-}\beta^{-}$ mice in murine bleomycin-induced pulmonary fibrosis

LXR agonists increase bleomycin induced loss of body weight.

The systemic inflammatory response to bleomycin administration was monitored by a progressive reduction in body weight (Figure 3.24). The weight loss was most evident up to approximately 6-9 days after bleomycin installation for all mice; probably reflecting acute inflammation. The wild-type mice had a typical weight-loss response to bleomycin and the response in LXR $\alpha^{-}\beta^{-}$ mice was not significantly different. There was a significant reduction in the weight loss in the wild-type mice given bleomycin plus LXR agonist compared with wild type mice given bleomycin without the LXR agonist (** $p < 0.0001$). This response was LXR-dependent because there was no exacerbation of weight loss by LXR agonist in the LXR $\alpha\beta^{-}$ mice (Figure 3.24).

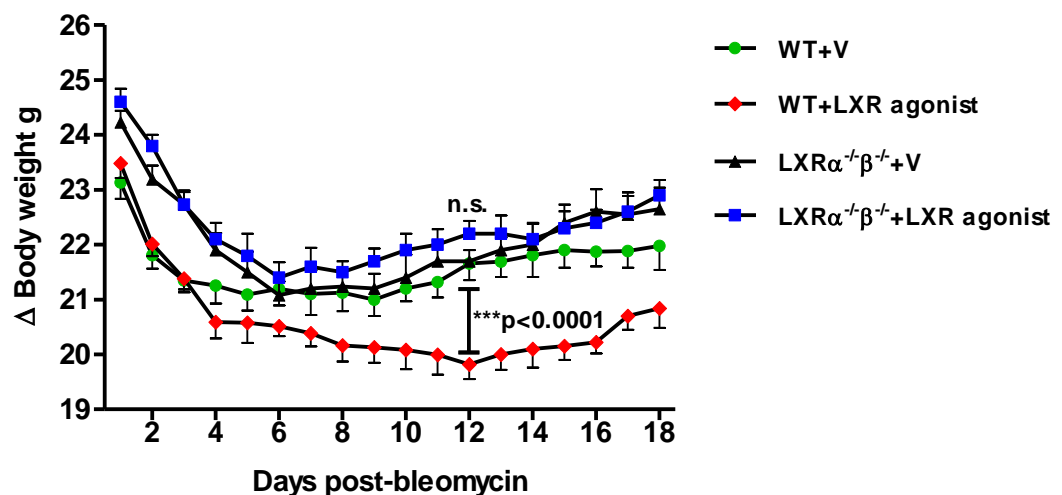


Figure 3.24 Daily body weights changes in WT and LXR $\alpha^{-}\beta^{-}$ mice given bleomycin and treated with either LXR agonist or vehicle

Daily body weights for 10-12 week old, male WT and LXR $\alpha^{-}\beta^{-}$ mice that were given bleomycin. Some mice were treated with daily IP injections of vehicle (5% Cremophor v/v PBS) or LXR agonist GW3965 (30mg/kg dissolved in 5% Cremophor v/v in PBS). Student t-Test; n.s. $p > 0.05$; *** $P < 0.0001$; Mean \pm SEM; $n = 19-23$ mice/group.

LXR agonist treatment increases the histopathological inflammatory and fibrotic changes in the lung of mice given bleomycin

Bleomycin installation caused severe morphological changes to the normal lung architecture demonstrated by inflammatory and fibrotic changes (Figure 3.25 A

and B respectively). Sections stained with H&E showed an infiltration of inflammatory cells, perivascular haemorrhage, and collapse of the alveoli as described in Materials and Methods (2.5.2). This was evident in all experimental groups, but this was more extensive in the WT mice treated with LXR agonist compared to the WT mice treated with vehicle, or in the other control groups; LXR $\alpha^{-/-}\beta^{-/-}$ treated with vehicle and LXR $\alpha^{-/-}\beta^{-/-}$ treated with LXR agonist (Figure 3.25 A).

Collagen was observed in all mice group by using Gomori's Trichrome stain. The collagen bundles and fibrotic foci distribution were mainly around the lung bronchioles and blood vessels but it was more extensive in the WT mice treated with LXR agonist (Figure 3.25 B). The deposition of the collagen was extensive in the lung lobes resulting in severe loss of normal lung architecture.

Quantification of the extent of the inflammation and fibrosis was performed on the lung sections of the WT and LXR $\alpha^{-/-}\beta^{-/-}$ mice. The sections were labelled by an independent colleague who was unaware of the details of the experiment. The slides were then scored using an inflammation scoring scale described in Materials and Methods (section 2.5.2) by two independent observers thus the quantification for inflammation and fibrosis was performed blind to the origin of the samples. Scoring of H&E stained lung sections for WT mice given bleomycin and daily intraperitoneal injection of LXR agonist revealed moderate to severe inflammation which was significantly greater ($p < 0.001$) than the score for the other groups; WT mice given vehicle, LXR $\alpha^{-/-}\beta^{-/-}$ given LXR agonist, and LXR $\alpha^{-/-}\beta^{-/-}$ given vehicle alone (Figure 3.26). There was no significant difference between these last groups.

The quantitative score of fibrosis was performed blind on all mice groups given bleomycin. There was a significantly higher score for WT mice treated with LXR agonist ($p < 0.001$) in comparison with all other experimental groups; WT treated with vehicle, LXR $\alpha^{-/-}\beta^{-/-}$ treated with LXR agonist, and LXR $\alpha^{-/-}\beta^{-/-}$ treated with vehicle (Figure 3.27).

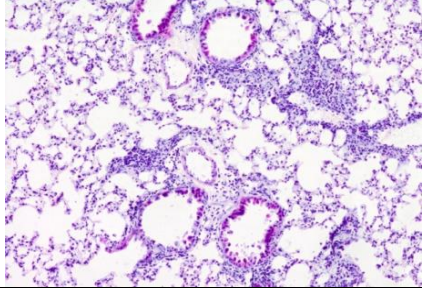
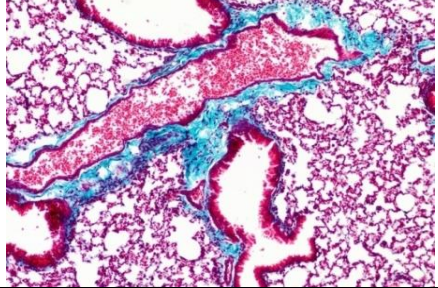
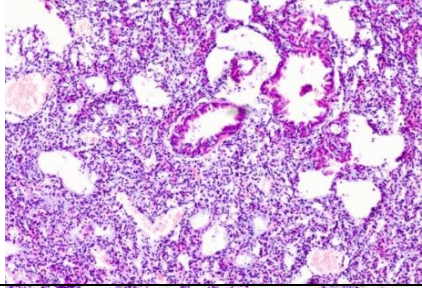
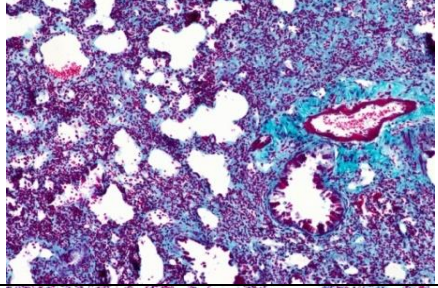
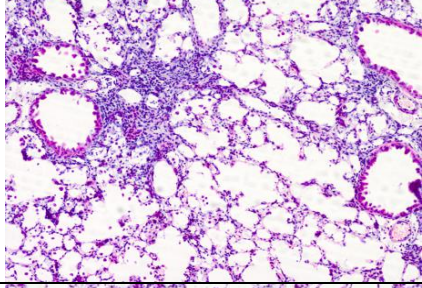
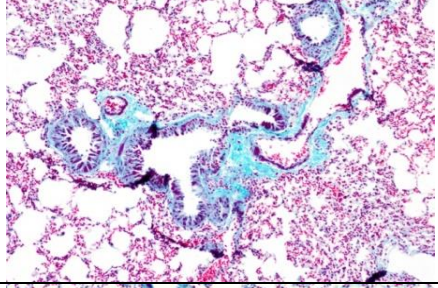
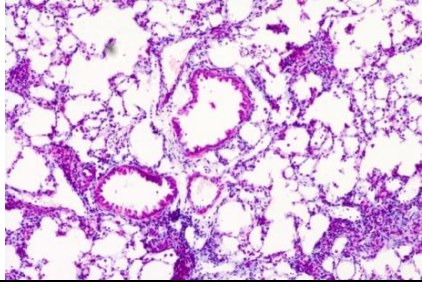
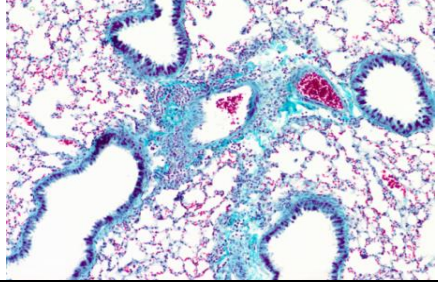
Group	A	B
	H&E	Trichrome
WT + Vehicle		
WT + LXR agonist		
LXR $\alpha^{-/-}\beta^{-/-}$ + Vehicle		
LXR $\alpha^{-/-}\beta^{-/-}$ + LXR agonist		

Figure 3.25 Histological inflammatory and fibrotic changes in the lung of WT and LXR $\alpha^{-/-}\beta^{-/-}$ mice given bleomycin and treated with LXR agonist or vehicle
(A) Representative images of lung lobe sections showing morphological changes in lung architecture after bleomycin installation, H&E staining shows severe inflammatory changes in all the mice groups which were greater in the WT mice treated with LXR agonist. **(B)** Collagen deposition in the lung of WT mice given bleomycin and treated with LXR agonist compared with the other groups. Gomori's Trichrome stain demonstrated large collagen patches around bronchioles, blood vessels and in the parenchyma. Sections viewed under light microscope (magnification x10).

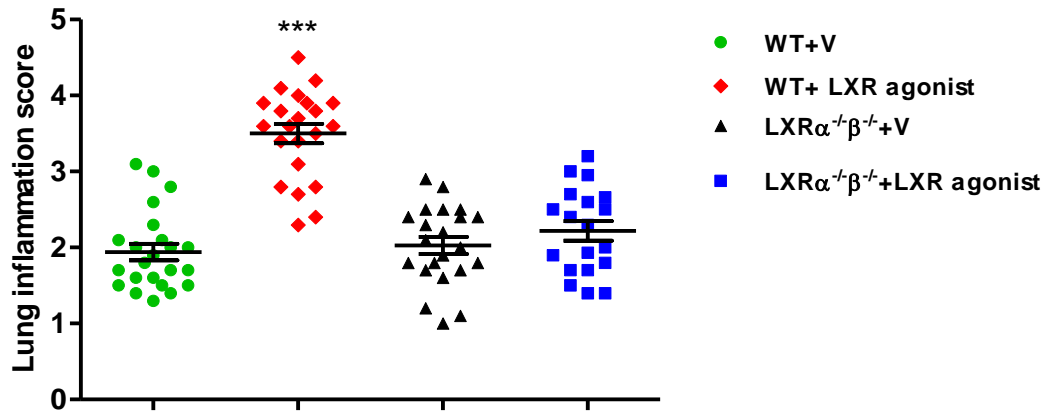


Figure 3.26 Lung inflammation score of WT and LXR $\alpha^{-}\beta^{-}$ mice given bleomycin and treated with LXR agonist or vehicle

Inflammation was assessed by a histological score (see Methods section 2.5.2). This demonstrated significantly higher inflammation in the WT mice group treated with LXR agonist compared with the other mice groups. One Way ANOVA; ***p<0.001; Mean \pm SEM; n=19-23 mice/group.

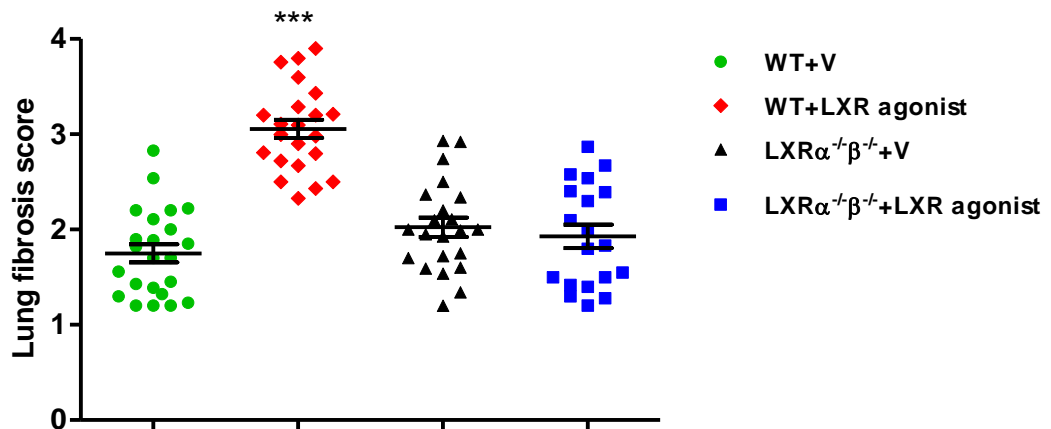


Figure 3.27 Lung fibrosis score of WT and LXR $\alpha^{-}\beta^{-}$ mice given bleomycin and treated with LXR agonist or vehicle

Fibrosis was assessed by histological scoring (see Methods section 2.5.2). This demonstrated significantly higher fibrosis in the WT mice treated with LXR agonist compared with the other groups. One Way ANOVA; ***p<0.001; Mean \pm SEM; n=19-23 mice/group.

LXR agonist increases the bleomycin-induced inflammatory cell numbers in the bronchoalveolar lavage fluid (BAL)

The BAL total cell count and differential profiles were made after processing the bronchoalveolar lavage fluid.

Total cell count:

Total BAL cell counts for bleomycin treated groups revealed significant differences between the groups. The total count was significantly higher in the WT mice treated with LXR agonist compared to the other experimental mice groups: WT mice treated with vehicle, $LXR\alpha^{-/-}\beta^{-/-}$ mice treated with vehicle, and $LXR\alpha^{-/-}\beta^{-/-}$ mice treated with LXR agonist ($p < 0.001$) (Figure 3.28).

The mean \pm Standard error of the mean of total BAL cell counts were as follows:

WT mice treated with LXR agonist	$1.68 \pm 0.21 \times 10^6$,
WT mice treated with vehicle	$0.88 \pm 0.19 \times 10^6$,
$LXR\alpha^{-/-}\beta^{-/-}$ mice treated with vehicle	$0.95 \pm 0.20 \times 10^6$,
$LXR\alpha^{-/-}\beta^{-/-}$ mice treated with LXR agonist	$1.01 \pm 0.22 \times 10^6$ (Figure 3.28).

There were no significant differences between these last three groups.

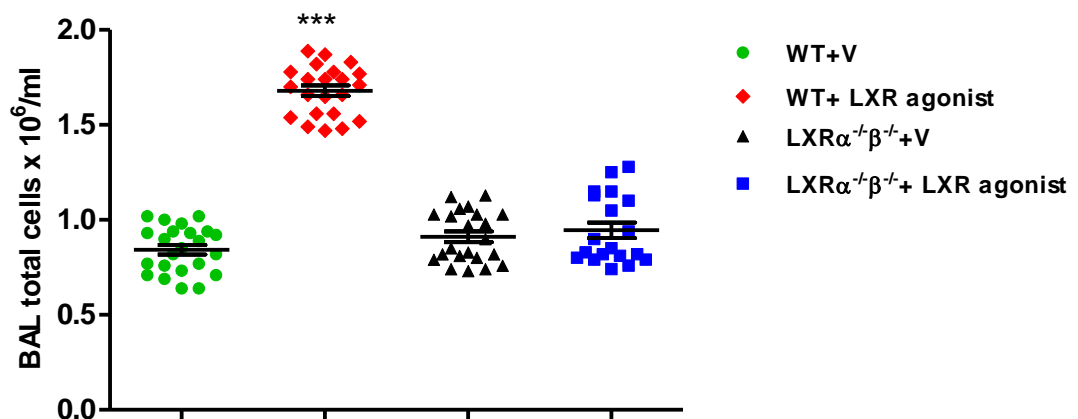


Figure 3.28 Total BAL cell count in the BAL of WT and $LXR\alpha^{-/-}\beta^{-/-}$ mice given bleomycin and treated with LXR agonist or vehicle

The total cell count for the inflammatory cells retrieved from bronchoalveolar lavage from the experimental mice demonstrated that the counts from WT mice treated with LXR agonist group was significantly higher compared with the WT mice treated with vehicle, $LXR\alpha^{-/-}\beta^{-/-}$ mice treated with vehicle, and $LXR\alpha^{-/-}\beta^{-/-}$ mice treated with LXR agonist. One Way ANOVA; *** $p < 0.001$; Mean \pm SEM; $n = 19-23$ mice/group.

The differential cell count profiles were made from the bronchoalveolar lavage fluid processed by cyto-centrifuge and H&E staining. The higher total cell count of the BAL was reflected in differences in the differential cell counts.

Macrophage cell count:

The macrophage proportions in the WT mice treated with LXR agonist showed the greatest increase which was significantly greater ($p < 0.001$) when compared with WT mice treated with vehicle, $LXR\alpha^{-/-}\beta^{-/-}$ mice treated with vehicle, and $LXR\alpha^{-/-}\beta^{-/-}$ mice treated with LXR agonist (Figure 3.29).

The mean \pm Standard deviation Standard error of the mean of macrophage cell counts were as follows:

WT mice treated with LXR agonist	$1.30 \pm 0.24 \times 10^6$,
WT mice treated with vehicle	$0.62 \pm 0.14 \times 10^6$,
$LXR\alpha^{-/-}\beta^{-/-}$ mice treated with vehicle	$0.68 \pm 0.20 \times 10^6$,
$LXR\alpha^{-/-}\beta^{-/-}$ mice treated with LXR agonist	$0.74 \pm 0.17 \times 10^6$ (Figure 3.29).

There were no significant differences between these last three groups.

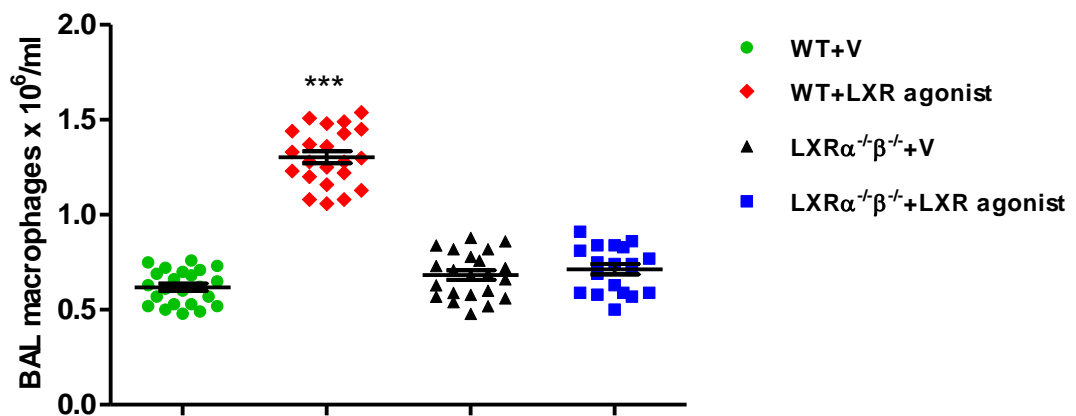


Figure 3.29 Macrophage cell count in the BAL of WT and $LXR\alpha^{-/-}\beta^{-/-}$ mice given bleomycin and treated with LXR agonist or vehicle

The macrophage cell count was significantly higher in the bronchoalveolar lavage fluid retrieved from the WT mice treated with LXR agonist compared to the WT mice treated with vehicle, $LXR\alpha^{-/-}\beta^{-/-}$ mice treated with vehicle, and $LXR\alpha^{-/-}\beta^{-/-}$ mice treated with LXR agonist. One Way ANOVA; *** $p < 0.001$; Mean \pm SEM; n=19-23 mice/group.

Lymphocyte cell count:

There were no significant differences in the lymphocyte count between WT mice treated with LXR agonist and both WT mice treated with vehicle and $LXR\alpha^{-/-}\beta^{-/-}$ treated with LXR agonist. However, this was a significantly lower ($p = 0.0017$) than the $LXR\alpha^{-/-}\beta^{-/-}$ treated with vehicle (Figure 3.30).

The mean \pm Standard error of the mean of lymphocyte cell counts were as follows:

WT mice treated with LXR agonist	$0.18 \pm 0.06 \times 10^6$,
WT mice treated with vehicle	$0.22 \pm 0.04 \times 10^6$,
LXR $\alpha^{-/-}\beta^{-/-}$ mice treated with vehicle	$0.23 \pm 0.82 \times 10^6$,
LXR $\alpha^{-/-}\beta^{-/-}$ mice treated with LXR agonist	$0.20 \pm 0.06 \times 10^6$ (Figure 3.30).

There were no significant differences between these last three groups.

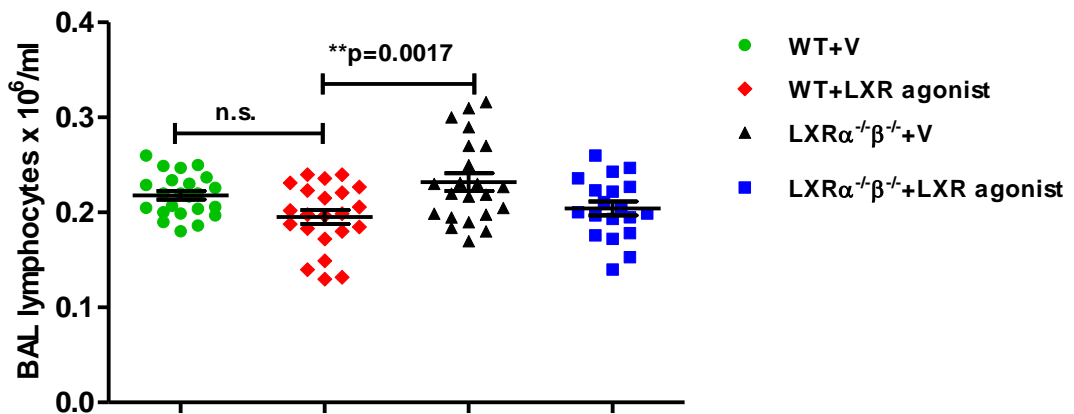


Figure 3.30 Lymphocyte cell count in the BAL of WT and LXR $\alpha^{-/-}\beta^{-/-}$ mice given bleomycin and treated with LXR agonist or vehicle
The lymphocyte cell count was not significantly different in the bronchoalveolar lavage fluid from the WT mice treated with LXR agonist compared to the WT mice treated with vehicle, and LXR $\alpha^{-/-}\beta^{-/-}$ mice treated with LXR agonist groups but it was significantly differ from LXR $\alpha^{-/-}\beta^{-/-}$ mice treated with vehicle. One Way ANOVA; n.s. $p>0.05$; ** $p<0.01$; Mean \pm SEM; n=19-23 mice/group.

Neutrophil cell count:

The neutrophil count for all the groups involved in the experiment showed no differences between groups. There were no significant differences between all experimental groups. The mean \pm Standard error of the mean of neutrophil cell counts were as follows:

WT mice treated with LXR agonist	$3.37 \pm 1.90 \times 10^4$,
WT mice treated with vehicle	$3.16 \pm 1.40 \times 10^4$,
LXR $\alpha^{-/-}\beta^{-/-}$ mice treated with vehicle	$3.64 \pm 1.36 \times 10^4$,
LXR $\alpha^{-/-}\beta^{-/-}$ mice treated with LXR agonist	$2.81 \pm 1.82 \times 10^4$ (Figure 3.31).

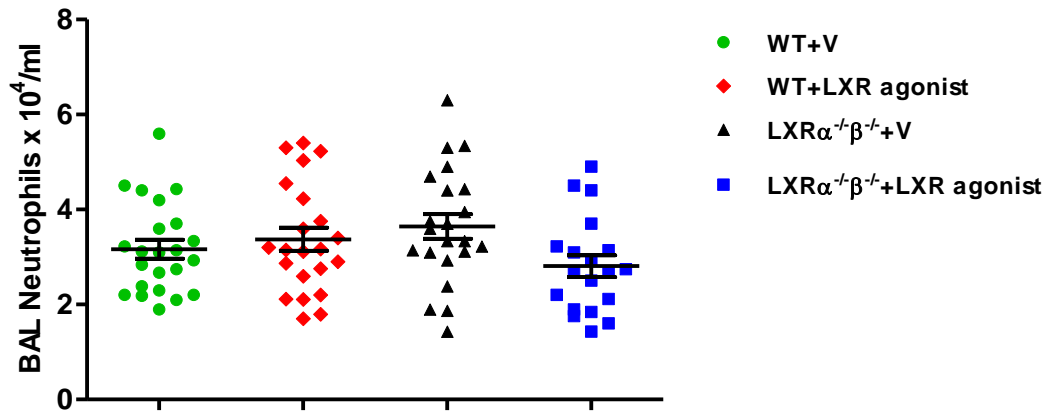


Figure 3.31 Neutrophil cell count in the BAL of WT and LXR $\alpha^{-/-}\beta^{-/+}$ mice given bleomycin and treated with LXR agonist or vehicle

The neutrophil cell count was not significantly different in the bronchoalveolar lavage fluid retrieved from the WT mice treated with LXR agonist compared to the other mice groups. One Way ANOVA; Mean \pm SEM; n=19-23 mice/group.

LXR agonist treatment increased the concentration of inflammatory and fibrotic mediators in the serum and BAL fluid of bleomycin treated mice.

A pragmatic range of cytokines, chemokines and growth factors relevant to the inflammatory and fibrotic responses was quantified in serum (Table 3.2) and in BAL fluid (Table 3.3) from the experimental groups of mice.

Serum mediators:

The concentrations of TNF α , IL-1 β , IL-2, IL-13, FGF basic, MCP-1, MIP-1 α and KC were increased in the WT mice treated with LXR agonist compared with the other groups (Table 3.2). The growth factors concentration in the serum of mice demonstrated a significant increase in TGF β 1 and bFGF in WT mice treated with LXR agonist group compared with the other groups. Chemokine results analysis demonstrated a significant increase in MCP-1, MIP-1 α , and KC. In the serum of WT mice treated with LXR agonist compared with the other groups.

Bronchoalveolar lavage fluid:

BAL analysis demonstrated a significant increased concentration of TGF β 1 and IL-1 β in the BAL of WT mice treated with LXR agonist compare to the other experimental groups (Table 3.3).

serum Mediators (pg/ml)	WT + V	WT + LXR agonist	LXR $\alpha^{-/-}\beta^{-/-}$ + V	LXR $\alpha^{-/-}\beta^{-/-}$ + LXR agonist	p value
Cytokines					
TNF α	23 (8-59)	85 ^{1,3} (52-127)	20 (17-44)	28 (16-69)	0.0495
IFN γ	9 (0-27)	0 (0-15)	34 (0-72)	0 (0-34)	0.5296
IL-1 α	0 (0-65)	24 (0-63)	80 (31-169)	0 (0-58)	0.1951
IL-1 β	42 (18-79)	90 ^{3,4} (53-164)	58 (27-109)	32 (24-52)	0.0156
IL-2	20 (7-43)	93 ^{1,3,4} (27-172)	23 (9-56)	28 (15-73)	0.0319
IL-4	13 (2-34)	0 (0-17)	39 (0-52)	0 (0-23)	0.1970
IL-5	16 (0-35)	19 (5-49)	94 ⁴ (21-172)	14 (6-27)	0.0703
IL-6	0 (0-27)	19 (0-44)	61 (18-128)	16 (7-40)	0.5959
IL-10	348 (95-680)	321 (203-526)	298 (145-502)	322 (114-577)	0.1290
IL-12	99 ³ (0-326)	67 ^{1,3,4} (15-168)	123 ⁴ (79-281)	107 (55-219)	0.0040
IL-13	7 ³ (3-15)	144 ^{1,3,4} (74-268)	18 ⁴ (0-43)	10 (0-31)	0.0047
IL-17	0 (0-6)	0 (0-0)	17 (0-48)	0 (0-0)	0.4505
Growth factors					
TGF β 1	74 ³ (38-122)	95 ^{1,3,4} (67-164)	63 (42-91)	69 (33-114)	0.0041
FGF basic	190 ³ (88-419)	2994 ^{1,3,4} (1373-6450)	140 (0-384)	158 (71-289)	0.0011
VEGF	16 (0-35)	21 (0-52)	19 (8-48)	13 (0-32)	0.0830
GM-CSF	0 (0-0)	0 (0-0)	13 (0-37)	0 (0-0)	0.0719
Chemokines					
MCP-1	28 (9-68)	84 ^{1,3,4} (57-136)	34 (0-75)	30 (16-53)	0.0138
MIP-1 α	29 (0-64)	43 ^{1,3,4} (11-99)	23 (9-45)	24 (0-56)	0.0311
KC	170 ⁴ (73-322)	956 ^{1,3,4} (215-1705)	157 (63-314)	203 (117-398)	0.0005
MIG	25 (0-57)	48 (22-93)	24 (17-38)	231 (35-515)	0.2815
IP-10	0 (0-24)	0 (0-19)	8 (0-26)	0 (0-41)	0.6288

Table 3.2 Inflammatory and fibrotic mediators in the serum of WT and LXR $\alpha^{-/-}\beta^{-/-}$ mice given bleomycin and treated with LXR agonist or vehicle

Inflammatory and fibrotic mediators exhibited a significantly higher concentration of TGF β 1, IL-13, IL-1 β , TNF α , IL-2, MCP-1, MIP-1 α , KC, and bFGF in the serum of the WT mice treated with LXR agonist than the WT mice treated with vehicle, LXR $\alpha^{-/-}\beta^{-/-}$ mice treated with vehicle, and LXR $\alpha^{-/-}\beta^{-/-}$ mice treated with LXR agonist groups. Significant reduction of IL-12 observed in the serum of the WT mice treated with LXR agonist than in the other groups. Median and interquartile range concentrations of each mediator were used to determine P-value for between category and between group differences; Kruskal-Wallis test; Mann-Whitney test respectively; *p<0.05; **p<0.01; ***p<0.001; groups n=19-23 mice/group.

BAL Mediators (pg/ml)	WT + V	WT + LXR agonist	LXR $\alpha^{-/-}\beta^{-/-}$ + V	LXR $\alpha^{-/-}\beta^{-/-}$ + LXR agonist	p value
Cytokines					
TNFα	46 (9-103)	49 (23-91)	42 (16-77)	40 (12-85)	0.0841
IFNγ	0 (0-0)	0 (0-0)	0 (0-0)	0 (0-0)	N.A.
IL-1α	0 (0-0)	0 (0-0)	0 (0-0)	0 (0-0)	N.A.
IL-1β	85 (53-147)	140 ^{1,3,4} (81-235)	97 (40-171)	91 (41-167)	0.0431
IL-2	36 (18-71)	29 (13-56)	31 (8-74)	38 (14-89)	0.1402
IL-4	0 (0-0)	0 (0-0)	0 (0-0)	0 (0-0)	N.A.
IL-5	10 (0-31)	8 (0-22)	11 (0-25)	11 (0-39)	0.5682
IL-6	0 (0-0)	0 (0-11)	33 (0-72)	0 (0-0)	0.4116
IL-10	387 (144-819)	349 (207-613)	416 (168-827)	425 (235-762)	0.1073
IL-12	80 (29-181)	102 (54-176)	91 (42-163)	63 (28-114)	0.0792
IL-13	0 (0-0)	0 (0-0)	0 (0-0)	0 (0-0)	N.A.
IL-17	0 (0-0)	0 (0-0)	0 (0-0)	0 (0-0)	N.A.
Growth factors					
TGFβ1	74 ³ (43-164)	143 ^{1,3,4} (62-349)	64 ⁴ (27-122)	72 (31-158)	0.0026
FGF basic	56 (18-131)	61 (27-119)	65 (15-122)	53 (32-98)	0.5984
VEGF	55 (27-136)	59 (18-110)	47 (12-94)	62 (20-124)	0.0922
GM-CSF	0 (0-0)	8 (0-36)	8 (0-25)	0 (0-0)	0.5319
Chemokines					
MCP-1	22 (7-46)	18 (11-34)	20 (6-42)	27 (15-49)	0.3631
MIP-1α	38 (21-69)	47 (16-105)	33 (18-74)	37 (7-81)	0.4227
KC	73 (34-138)	95 (39-167)	57 (33-106)	65 (22-139)	0.1035
MIG	0 (0-0)	0 (0-0)	0 (0-0)	0 (0-0)	N.A.
IP-10	0 (0-0)	0 (0-0)	0 (0-0)	0 (0-0)	N.A.

Table 3.3 Inflammatory and fibrotic mediators in the BAL of WT and LXR $\alpha^{-/-}\beta^{-/-}$ mice given bleomycin and treated with LXR agonist or vehicle
Inflammatory and fibrotic mediators exhibited a significant high production of TGF β 1 and IL-1 β in the BAL of the WT mice treated with LXR agonist than the WT mice treated with vehicle, LXR $\alpha^{-/-}\beta^{-/-}$ mice treated with vehicle, and LXR $\alpha^{-/-}\beta^{-/-}$ mice treated with LXR agonist groups. Median and interquartile range concentrations of each mediator were used to determine P-value for between category and between group differences; Kruskal-Wallis test; Mann-Whitney test respectively; *p<0.05; **p<0.01; *p<0.001; groups n=19-23 mice/group.**

LXR agonist increases bleomycin induced TGF β and collagen gene expression and collagen production in the murine lung.

TGF β expression:

Increased TGF beta and collagen gene expression is one of the characteristics of fibrosis. TGF- β 1 mRNA expression was determined in RNA extracted from the lung tissue of experimental groups of mice. This showed a significant ($p < 0.001$) increase among the WT mice treated with LXR agonist compared with the WT mice treated with vehicle, LXR $\alpha^{-/-}\beta^{-/-}$ mice treated with vehicle, and LXR $\alpha^{-/-}\beta^{-/-}$ mice treated with LXR agonist (Figure 3.32).

Collagen expression:

We demonstrated by using qPCR that treatment with LXR agonist increased the mRNA level of collagen type IA and collagen type IIIA expression (Figure 3.33). The Col IA mRNA expression in the WT mice treated with LXR agonist was upregulated significantly by approximately 2-fold compared to the other groups and Col IIIA mRNA expression increased by approximately 5-fold (Figure 3.33).

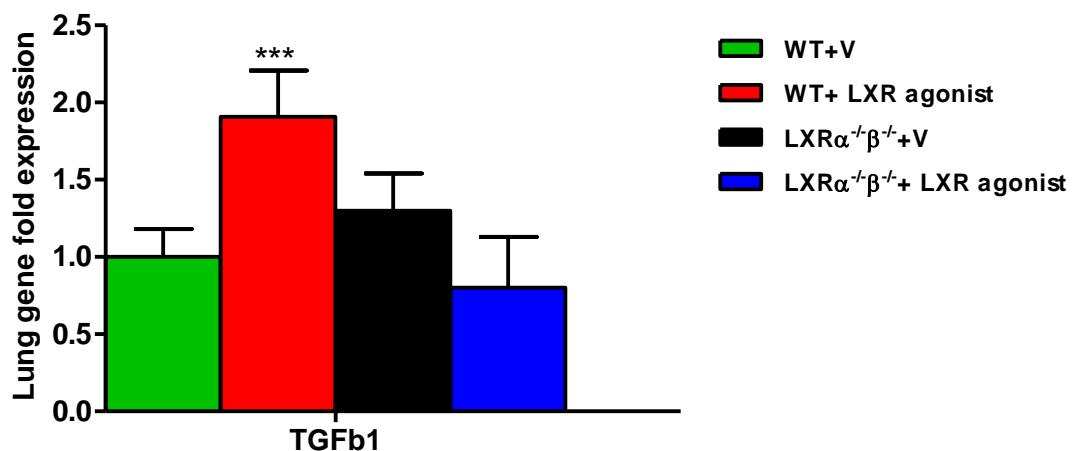


Figure 3.32 TGF β 1 gene expression in lung of WT and LXR $\alpha^{-/-}\beta^{-/-}$ mice given bleomycin and treated with LXR agonist or vehicle

TGF β 1 gene expression levels in the lungs of all groups of mice given bleomycin. TGF β 1 mRNA expression measured as fold-increase compared with control vehicle-treated mice was significantly higher in the lungs of WT mice treated with LXR agonist than the other groups. One Way ANOVA; *** $p < 0.001$; Mean \pm SEM; n=19-23 mice/group.

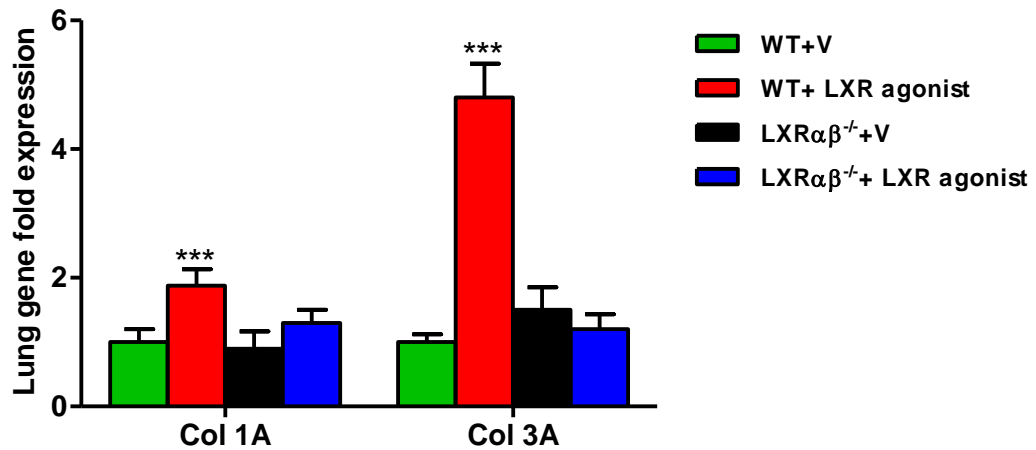


Figure 3.33 Collagen gene expression in lung of WT and LXR $\alpha^{-}\beta^{-}$ mice given bleomycin and treated with LXR agonist or vehicle

Collagen type IA and Col IIIA expression levels in the lungs of four groups of mice given bleomycin. Collagen IA and Col IIIA mRNA expression measured as fold-increase compared with control vehicle-treated mice was significantly higher in the lungs of WT mice treated with LXR agonist than the with the WT mice treated with vehicle, LXR $\alpha^{-}\beta^{-}$ mice treated with vehicle, and LXR $\alpha^{-}\beta^{-}$ mice treated with LXR agonist groups. One Way ANOVA; *** $p < 0.001$; Mean \pm SEM; $n = 19-23$ mice/group.

Collagen production:

The soluble collagen content of the lung was evaluated by using a Sirius-red binding assay as described in Materials and Methods (section 2.6). The assay is based on the binding of Sirius red to acid and pepsin-soluble collagen. This demonstrated a significant increase ($p < 0.001$) in lung collagen content in WT mice treated with LXR agonist compared with the WT mice treated with vehicle, LXR $\alpha^{-}\beta^{-}$ mice treated with vehicle, and LXR $\alpha^{-}\beta^{-}$ mice treated with LXR agonist (Figure 3.34). The mean \pm Standard error of the mean of lung soluble collagen content were as follows:

WT mice treated with LXR agonist	2.11 \pm 0.14 mg/ml,
WT mice treated with vehicle	1.73 \pm 0.11 mg/ml,
LXR $\alpha^{-}\beta^{-}$ mice treated with vehicle	1.83 \pm 0.17 mg/ml,
LXR $\alpha^{-}\beta^{-}$ mice treated with LXR agonist	1.78 \pm 0.13 mg/ml (Figure 3.34).

There were no significant differences between the last three groups.

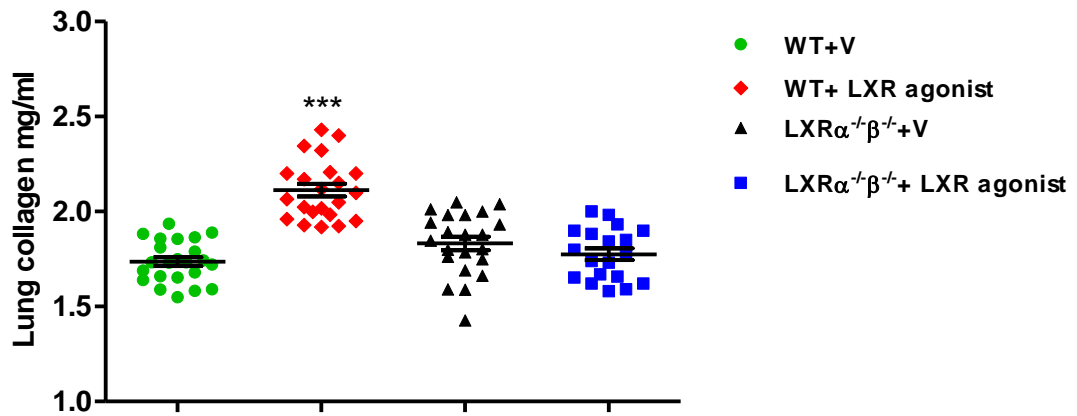


Figure 3.34 Soluble collagen content in lungs of WT and LXR $\alpha^{-}\beta^{-}$ mice given bleomycin and treated with LXR agonist or vehicle
Soluble collagen content level in the lungs of the WT mice treated with LXR agonist was significantly greater than the other experimental groups. One Way ANOVA; ***p<0.001; Mean \pm SEM; n=19-23 mice/group.

3.2.3.2 Mechanisms of LXR involvement in fibrosis

The likely main targets for LXR in the development of fibrosis are the fibroblast and the macrophage. In this section I will describe the expression pattern of phenotypic markers for classically activated macrophages (inducible nitric oxide synthase (iNOS2) and alternatively activated macrophages (chitinase-like lectin YM1, arginase type 2, IL-13 receptor), their changes associated with LXR activation and their relationship with fibrosis.

3.2.3.2.1 LXR modulation of macrophage phenotype

The inflammatory and fibrotic processes in mice given bleomycin and treated with LXR agonist was associated with significant increased expression of YM1, Arg 2, and IL-13R compared with the WT mice treated with vehicle, LXR $\alpha^{-}\beta^{-}$ mice treated with vehicle, and LXR $\alpha^{-}\beta^{-}$ mice treated with LXR agonist (Figure 3.35). Nitric oxide synthase 2 (NOS2) expressions was down-regulated in the WT mice treated with LXR agonist compare to the other groups (Figure 3.35).

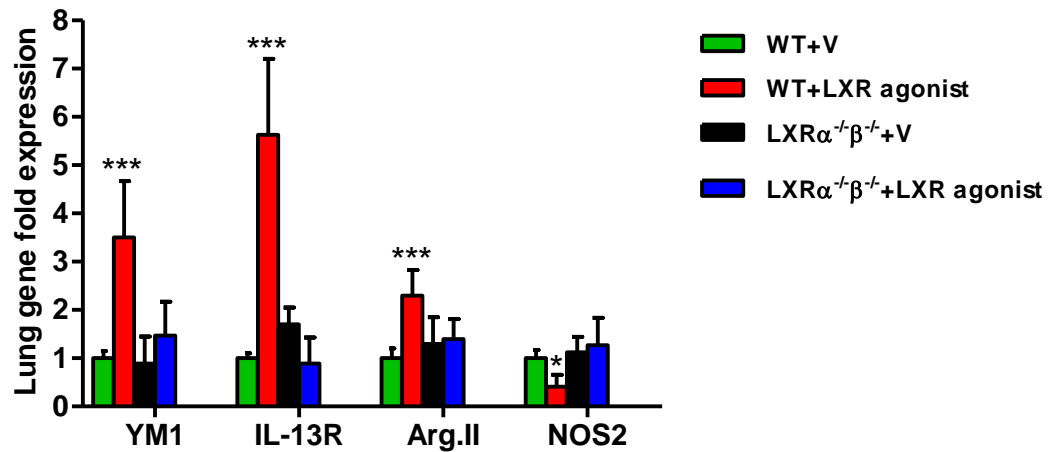


Figure 3.35 Expression levels of macrophage phenotype markers in the lungs of WT and LXR $\alpha^{-}\beta^{-}$ mice given bleomycin and treated with LXR agonist or vehicle. Expression levels of macrophage phenotype markers YM1, IL-13R, Arg 2 and NOS 2 in lungs of bleomycin treated mice. YM1, Arg 2, and IL-13R were significantly up-regulated in WT mice that received LXR agonist compared to the other groups. NOS2 was down-regulated significantly in WT mice given LXR agonist compared to the other groups. One Way ANOVA; * $p < 0.05$; *** $p < 0.001$; Mean \pm SEM; $n = 19-23$ mice/group.

3.2.3.2.2 LXR modulation of fibroblast function

The role of LXR agonist on fibroblast function was tested by using collagen gene expression in primary mouse fibroblasts lines derived from the lungs of bleomycin treated mice, and in human fibroblasts. The culture conditions were explained in Materials and Methods (section 2.9.3).

To explore the stimulation of fibroblasts, different concentrations of LXR agonist were used (0.125, 0.25 and 0.5 μ M) at different time points (6, 12 and 24 hours). The greatest increase in Col IA and Col IIIA mRNA expression in mouse lung fibroblast cultures was after 24 hours of stimulation using a dose of 0.5 μ M LXR agonist (Figure 3.36). The increase for Col IA mRNA was approximately 3-fold and for Col IIIA mRNA was approximately 5-fold in WT mouse lung fibroblasts stimulated with LXR agonist compared with WT mouse lung fibroblast stimulated with the vehicle. The increase was significantly higher ($p < 0.05$ and $p < 0.01$) respectively. There were no significant changes observed in the Col IA and Col IIIA mRNA expression of LXR $\alpha^{-}\beta^{-}$ mouse lung fibroblasts in culture (Figure 3.36).

Human fibroblasts exhibited the same pattern as the WT mouse lung fibroblast in their response to LXR agonist stimulation. Human primary fibroblast lines generated from human tendons were used (Kindly donated by Dr Neil Miller, Immunology, Glasgow University. Tissue obtained with ethics approval). Up-regulation of Col IA and Col IIIA mRNA expression for human fibroblast was less than of the mice lung fibroblast and it was 2-fold for Col IA mRNA and 2.5-fold for Col IIIA mRNA (Figure 3.37). Both human and mouse fibroblast tends to produce more collagen in response to stimulation with LXR agonist, and both Col IA and Col IIIA mRNA expression were higher.

Mouse fibroblast

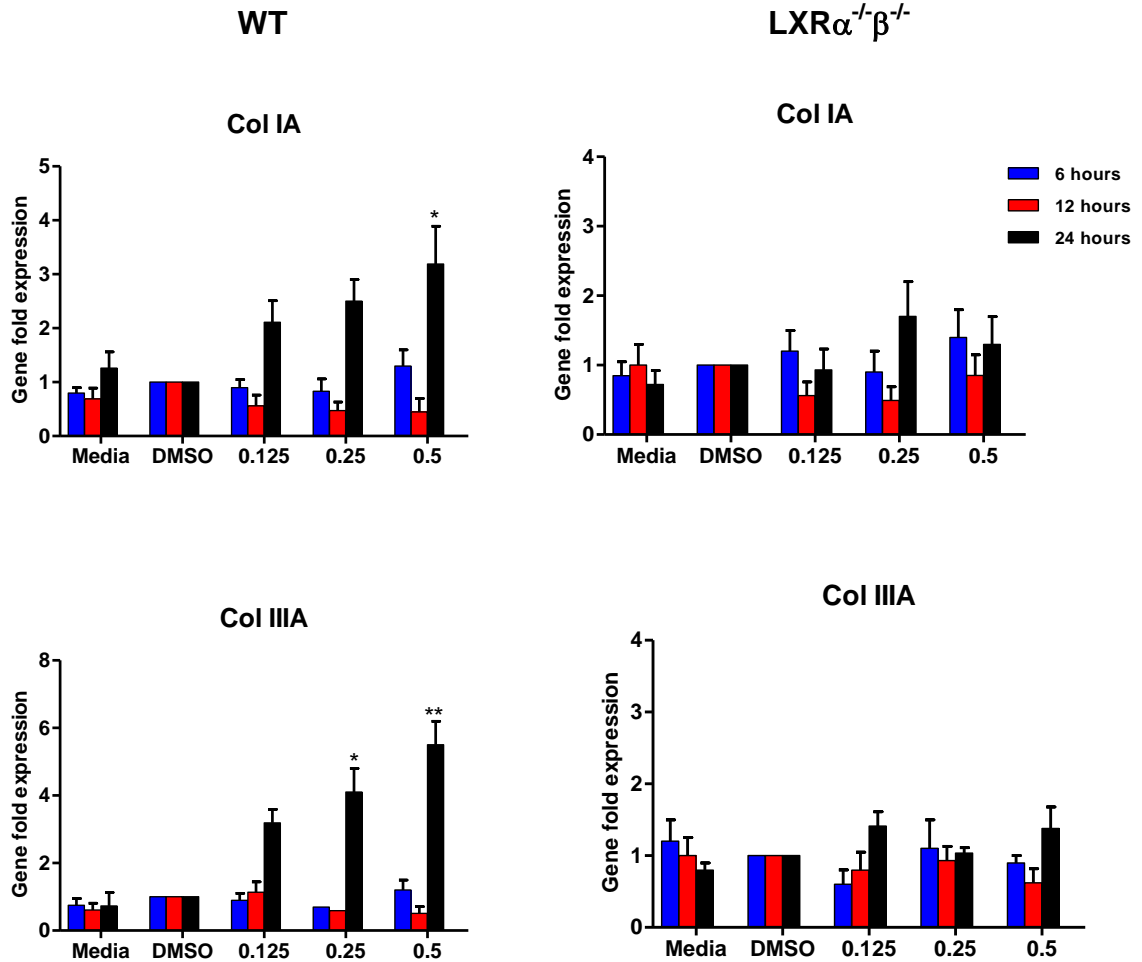


Figure 3.36 Collagen gene expression in primary mouse lung fibroblasts from WT and LXRα⁻β⁻ mice given bleomycin and treated with LXR agonist or vehicle
 Mouse lung fibroblasts were cultured with medium alone or different doses of LXR agonist or their excipient DMSO, for different incubation times. Increased mRNA expression for Col IA and Col IIIA was detected in WT mouse lung fibroblasts in response to stimulation with 0.5 μM LXR agonist at 24 hours. Student t-Test; * P < 0.05; ** P < 0.01; Mean ± SEM; n=3 independent experiment.

Human fibroblast

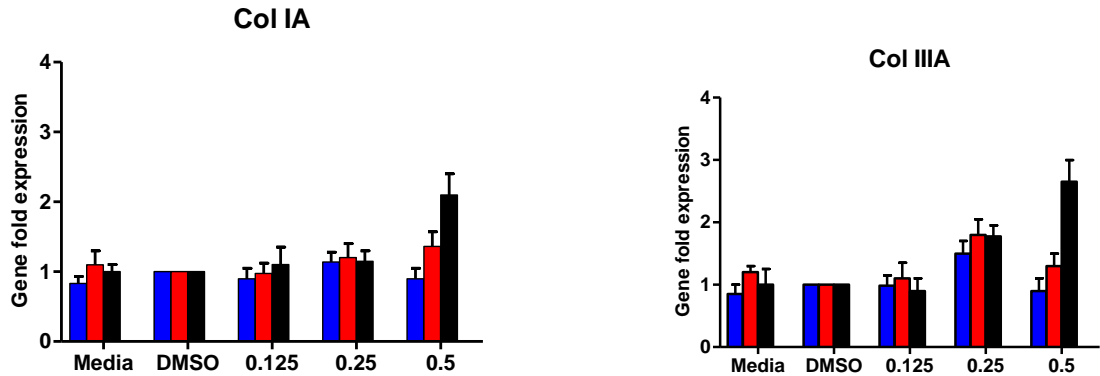


Figure 3.37 Collagen gene expression in primary human fibroblast treated with LXR agonist or vehicle

Human primary fibroblast cultured with medium alone or with alone or different doses of LXR agonist or their excipient DMSO for different incubation times. Collagen type IA and Col IIIA expression up-regulated in response to stimulation with LXR agonist. The up-regulation was higher at 24 hours with 0.5 μ M LXR agonist. Mean \pm SEM; n=3 independent experiment.

3.2.3.2.3 LXR directly targets collagen type I and III expression in murine fibroblast

Treatment with LXR agonist increased collagen gene expression and transcription in primary mouse fibroblasts as shown in Figure 4.36 above. To determine if the effect of LXR agonist on the expression of Col IA and Col IIIA mRNA required protein synthesis, the mouse primary fibroblasts were treated with cycloheximide; an inhibitor of translation. The cycloheximide was added at a concentration of 1 μ g/ml. for 24 hours as described in Materials and Methods (section 2.9.4).

The fibroblast stimulated with LXR agonist in presence of cycloheximide resulted in a significant up-regulation of Col IA and Col IIIA gene expression in comparison with the other experimental groups. There were no changes in the Col IA1 and Col IIIA gene expression in the fibroblast stimulated with DMSO and cycloheximide (Figure 3.38). This suggested that the function of LXR agonist on collagen gene expression did not require *de novo* protein synthesis and that this effect may have been directly on the promoter region of the collagen gene.

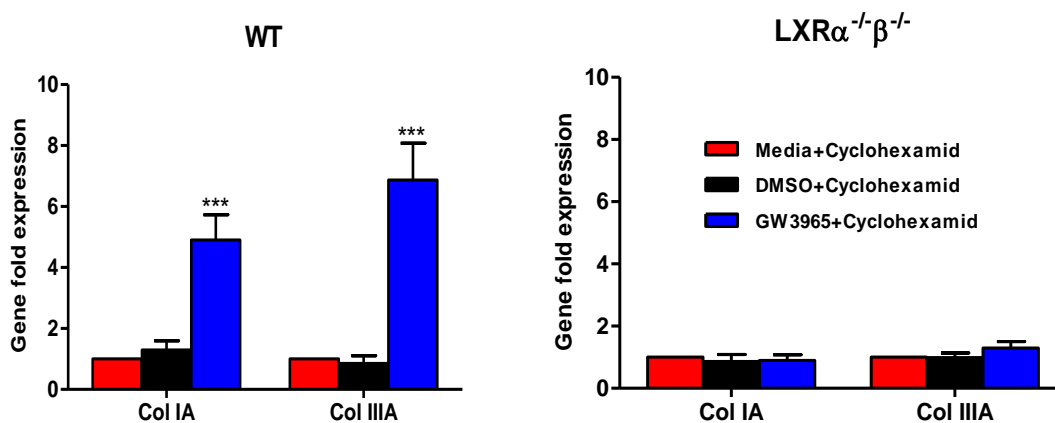


Figure 3.38 LXR agonist directly increased collagen gene expression in primary mouse lung fibroblasts

Primary mouse lung fibroblasts were cultured with medium, vehicle (DMSO) and LXR agonist (GW3965) in addition to cycloheximide. WT mice fibroblast exhibited a significant up-regulation in Col IA and Col IIIA expression under LXR agonist stimulation in comparison with cells incubated with medium or DMSO vehicle. No changes had been observed among the primary fibroblasts derived from LXRα^{-/-}β^{-/-} mice. One Way ANOVA; ***p<0.001; Mean ± SEM; n=3 independent experiment.

3.2.3.2.4 Activation of LXR directly targets the promoters of collagen types I and III in the murine fibroblast cell line T1317

To explore whether the increased Col IA and Col IIIA was a direct or indirect effect of LXR agonists, I tested the hypothesis that the collagen genes have response elements for LXR in their promoter regions. Since collagen is a major component in fibrosis, therefore, a luciferase reporter assay was used to determine the effect of LXR agonist on the promoters of collagen type IA1a, IA1b, IA1c, and IIIA1a. The details of this assay are described in the Material and methods section (2.10).

The cells activated with LXR agonist GW3965 showed increased relative luciferase activity for collagen type IA1b and IIIA1a in comparison with the cells stimulated with the excipient DMSO control (Figure 3.39). The assay efficiency was performed by observing the luciferase activity changes in control positive promoter plasmid PGL3 (+) and control negative promoter plasmid PGL3 (basic) samples (Figure 3.39).

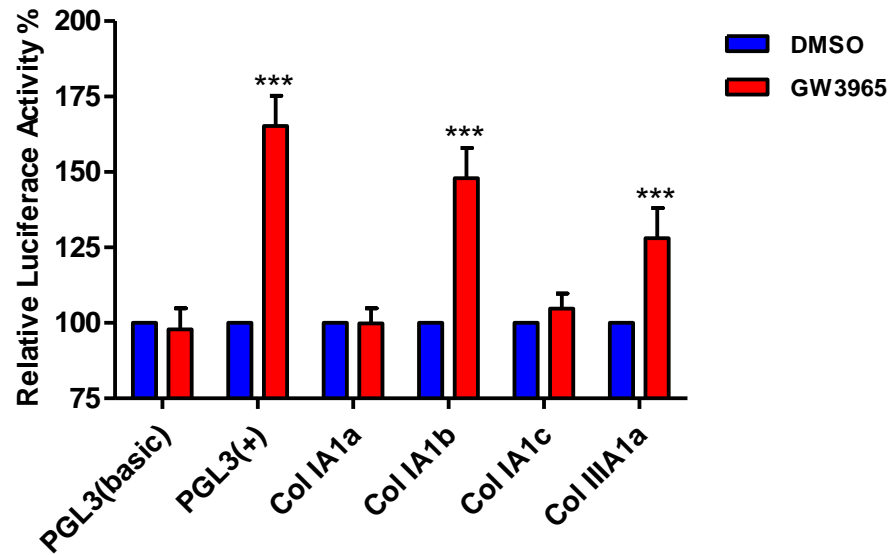


Figure 3.39 The effect of LXR agonist on luciferase activity indicating collagen gene expression in transfected mouse primary fibroblasts

The T1317 murine fibroblast cell line was transfected with collagen type IA1a, IA1b, IA1c, and IIIA1a then cultured with DMSO or LXR agonist. Collagen type IA1b and IIIA1a luciferase activity was increased in the cells activated with LXR agonist. One Way ANOVA; *** $p < 0.001$; Mean \pm SEM; $n = 3$ independent experiments.

3.2.4 Discussion and Conclusion

The aim of this results chapter was to provide evidence for a direct role for LXR activation in the inflammatory changes and tissue remodelling associated with bleomycin induced lung fibrosis. We demonstrated that activation of LXR by administration of the LXR agonist GW3965 lead to exacerbation in the inflammatory and fibrotic processes in mice given bleomycin. This was seen as increased loss of body weight, increased pathomorphological changes in the lung, increased number of inflammatory cells in the BAL, increased pro-inflammatory and pro-fibrotic mediators in the BAL and serum, and increased collagen expression and collagen content in the lung.

Having demonstrated that LXR agonist can exacerbate bleomycin induced lung fibrosis, the first consideration was the specificity of the response. To achieve this purpose a control murine bleomycin-induced pulmonary fibrosis model was tested using LXR $\alpha^{-/-}\beta^{-/-}$ mice. These mice responded to bleomycin with the same severity of pulmonary fibrosis as wild type mice, but was not exacerbated by agonist.

Monitoring of the body weight among these mice indicated a severe reduction in body weight in LXR $\alpha\beta$ wild type mice treated with LXR agonist than vehicle treated control mice or LXR $\alpha^{-/-}\beta^{-/-}$ mice (Figure 3.24). These results indicated a development of systemic inflammation which was exacerbated by activating the LXRs. This was accompanied by pathomorphological changes in the lungs. In the LXR agonist treated WT mice given bleomycin, severe inflammatory responses were observed accompanied by a high fibrosis score as an index of collagen deposition compared with LXR $\alpha^{-/-}\beta^{-/-}$.

Having shown that the exacerbation of inflammation and fibrosis was LXR-specific the next step was to interpret the mechanism as far as possible. Administration of LXR agonist stimulated a significant increase in the total number of inflammatory cells in the BAL; predominantly due to the proportion of macrophages and to a less extent to lymphocytes, that is BAL cell profile typical of bleomycin induced lung injury.

One potential mechanism of this pro-fibrotic effect was that LXR agonists can shift macrophage phenotype from an innate phenotype towards an alternatively activated M2 macrophage phenotype by up-regulation of expression of some anti-inflammatory genes such as Arginase 2 accompanied by suppression of expression of some pro-inflammatory genes such as inducible nitric oxide synthase (iNOS) [197]. Marathe and colleagues reported that *in vitro* activation of LXR in macrophage cell lines and in primary murine macrophages lead to up-regulation of Arginase 2 accompanied by down-regulation of iNOS and suggested that the mechanism of this reciprocal response was by antagonism of NF-kappa B activity [197]. The consequence of this alteration in the expression of Arginase 2 and iNOS led to shifting of inflammatory signalling within the macrophage. Expression of Arg 2 had been shown to have a selective effect on inflammatory pathways; this was determined by an absence of alteration on the

expression of other inflammatory mediators for example cyclooxygenase-2 (COX-2) and prostaglandin-E2 (PGE2). M2 macrophages had been demonstrated as major component in the wound healing process, Arginase characterised by its ability to inhibit nitrogen oxide (NO) production resulting in production of ornithine, a precursor of hydroxyproline and polyamines [43]. Recently a study demonstrated that Arginase 2 promotes macrophage pro-inflammatory responses in atherosclerosis and type II diabetes mellitus and this effect were mediated through the mitochondrial reactive oxygen species [29].

To help understand the mechanisms of the systemic and local lung inflammation the next step was to identify the pattern of inflammatory cytokines in serum and BAL fluid. There was a wide range of concentrations of mediators in the different categories of pro-inflammatory cytokines, chemokines and growth factors. In serum from mice given bleomycin and treated with LXR agonist, the concentrations of $\text{TNF}\alpha$, IL-1 β , IL-13, TGF β 1, FGF basic, MCP-1, MIP-1 α and KC were higher than in serum of the other experimental groups. Similarly, in the BAL fluid of mice given bleomycin and treated with LXR agonist, the concentration of TGF β 1 and IL-1 β were higher than in WT mice given bleomycin and both LXR $\alpha^{-/-}\beta^{-/-}$ groups (Table 3.2 and Table 3.3). The interpretation of the increase in these particular mediators indicates the presence of an active pro-inflammatory and pro-fibrotic process resulting from the activation of the LXRs, since the LXRs are ubiquitously distribution in the cells and tissues, therefore, activation of the receptor especially in the macrophages which is considered as a major source of pro-inflammatory and pro-fibrotic mediators lead to high production of these mediators. Higher concentration of the pro-inflammatory and pro-fibrotic mediators in the serum and BAL of LXR treated mice and increased recruitment of the inflammatory cells suggest an active inflammatory and fibrotic process manifested by high involvement of macrophage. High macrophage numbers with low lymphocytes and neutrophil number in the BAL had been in other studies using bleomycin-induced pulmonary fibrosis [192, 210].

Generally, serum and BAL mediator data supported a pro-inflammatory and pro-fibrotic role for LXRs. One of the mediator which is centrally important in the inflammatory and fibrotic processes, and was significantly increased in mice given bleomycin and treated with LXR agonist was TGF β 1. This is a powerful pro-fibrotic growth factor as shown by its ability to stimulate fibroblast collagen production and deposition [211]. There are three isoforms of TGF β with different gene expression levels during bleomycin-induced pulmonary fibrosis but they share the ability to stimulate fibroblast procollagen synthesis [212]. Interestingly, our data demonstrate a high concentration of Interleukin (IL)-13 in the serum and BAL of mice given bleomycin and treated with LXR agonist. IL-13 is associated with the induction of airway disease and considered as one of the most important mediators of tissue fibrosis [213]. It has fibrogenic effects mediated by TGF β 1 and is considered to be a strong activator and stimulator of TGF β 1 *in vivo* [214]. Lee and his colleagues showed that IL-13 was able selectively to stimulate TGF β 1 production in transgenic mice. In the present study, IL-13 and TGF β 1 together play a cooperative role in the initiation and progression of the inflammatory and fibrotic process in the lung. In addition, our analysis determined a high concentration of

interleukin 1 β and TNF α which are potent pro-inflammatory cytokines, and severe lung fibrosis is associated with high concentration of IL-1 β and TNF α [166].

Consistent with the high concentration of TGF β 1 in the serum and BAL, our results show greater up-regulation of TGF β 1 gene expression in the lungs of WT mice given bleomycin and treated with LXR agonist in comparison with the other experimental groups (Figure 3.32). There was increased collagen gene expression and enhancement of collagen synthesis. This consisted of an increase in the collagen type IA and IIIA gene expression. The WT mice given bleomycin and treated with LXR agonist exhibited significantly higher collagen type IA and IIIA gene expression than the other study groups. Shahzeidi et al 1993 [215] reported that the early collagen deposition is partially due to activation of interstitial fibroblasts which lead to up-regulation in the collagen type III gene expression in bleomycin induced murine pulmonary fibrosis. Collagen type IA is the most abundant form of collagen, the mRNA expression of procollagen type IA is markedly higher than the mRNA expression of procollagen type IIIA in the lung of mice given bleomycin [216]. In the present study, the greater relative increase of collagen gene expression during bleomycin-induced pulmonary fibrosis was that of collagen type IIIA, which was expressed at a higher level than collagen type IA. A study of the ratio of collagen type I to collagen type III in normal and fibrotic lungs observed changes from a typical normal ratio of 2:1 to a ratio of 4:1 in fibrotic lungs [217]. The differences between our results and the ratio above is that in my work I demonstrated the gene expression level while in the other study observed the collagen by using antibodies to human collagen types I, III. It is possible that not all gene expression necessarily was translated into protein, also the dynamic of collagen synthesis and degradation during fibrosis may affect each type of collagen differently.

Interrogating our data to interpret other possible mechanisms involved in the LXR-mediated exacerbation of fibrosis was an important goal. For example, in our *in vitro* work we showed significantly raised expression levels of collagen type IA and IIIA mRNA in human and mouse fibroblasts in response to LXR agonist stimulation (Figure 3.36 and Figure 3.37).

It was unknown whether the LXR agonist directly stimulated the expression of collagen or whether this was indirect through other mediators for example IL-13 and TGF β . To resolve this, investigations were carried out to determine if LXR agonist directly targeted collagen type 1 and 3 genes using mouse primary fibroblast lines generated from lung tissue of LXR α ^{-/-} β ^{-/-} and LXR $\alpha\beta$ wild type mice Materials and Methods (section 2.9.4). Cyclohexamide was used as an inhibitor of translation to establish if the effects required *de novo* protein synthesis. Our results demonstrated that the increased expression of collagen was not affected by cyclohexamide, therefore, this is preliminary data to suggest that LXR agonist directly targeted collagen type 1 and 3 expression conducted through the activation of LXRs. To extend this observation we generated a cell reporter system to demonstrate that the collagen genes have response elements for LXR in their

promoter regions. This is important new unpublished and extends the potential role of LXR function from initially a regulator of lipid metabolism, to a regulator of inflammation and now extended by our data to a regulator of remodelling.

Conclusion

The present work was established on the hypothesis that LXR agonist might be a mediator, and a suitable candidate for the treatment of pulmonary fibrosis. Several studies have shown that LXR agonists could play an anti-inflammatory role in the course of inflammation such as in atherosclerosis. We have determine that administration of LXR agonist to mice given bleomycin led to exacerbation of the inflammatory and in addition the fibrotic process which was seen as in pro-fibrotic mediators in the serum and BAL, increase in collagen expression and deposition in the lungs. These new findings will inform future therapy for chronic disease where collagen deposition is a life-limiting component.

Results 3.3 Index:

3.3 Requirement of LXR α and LXR β for fibrosis-enhancing effects of the LXR agonist

3.3.1 Introduction and Aims

3.3.2 LXR $\alpha^{-/-}$ and LXR $\beta^{-/-}$ mice

3.3.3 LXR activation had no effect on the augmentation of bleomycin-induced pulmonary fibrosis in single LXR $\alpha^{-/-}$ or LXR $\beta^{-/-}$ mice compared with wild-type mice

3.3.4 Discussion and Conclusion

3.3 Requirement of LXR α and LXR β for fibrosis-enhancing effects of the LXR agonist

3.3.1 Introduction and Aims

In Results Chapter 3.2 we demonstrated that wild-type mice given bleomycin had worsened inflammation and fibrosis when treated with the potent LXR agonist GW3965. This was not apparent in double LXR $\alpha\beta$ gene-deleted mice. The potential role of any separate effect or redundancy of each single LXR receptor in this process was investigated. The involvement of the different LXR α or LXR β receptor in the process of pulmonary fibrosis is an important consideration in this study. LXR α has been investigated widely in tissues and in immune cells, for example in the liver it enhances bile acid synthesis and excretion via ATP-binding cassette G5/G8 transporters resulting in inhibition of intracellular cholesterol deposition. Also, it can enhance cholesterol reverse transport in macrophages [218].

LXR β has importance in controlling lipid metabolism, for example mice with inactivated LXR β had pathological accumulation of sterols and lipids develop adult-onset motor neuron disease [219]. Generally, either of the two receptors tends to compensate for a deletion of the other. In some animal experimental models the two LXRs act independently; LXR α tends to be more important in the progression of atherosclerosis than LXR β and its deletion could not compensate in a murine model of atherosclerosis [220]. But activation of the LXR by using of a highly specific synthetic agonist showed an ability to compensate the physiological effect of LXR α deletion. Therefore, specific activation of LXR β has a beneficial effect as an anti-atherosclerotic intervention. In a selective knockout study of wild type, LXR $\alpha^{-/-}$ and LXR $\beta^{-/-}$ mice, gene expression analysis demonstrated differences between these groups; LXR $\beta^{-/-}$ tended to show stronger regulatory effects on genes coding for cytokines, whereas genes involved in carbohydrate metabolism tends to be more specific to LXR α regulation, and both LXR α and LXR β showed equivalent effects on genes belonging to lipid/cholesterol metabolism [221].

The link between a single LXR and fibrosis is undetermined, therefore, the primary aim of this work is to identify the relationship between activation of a single LXR α or LXR β and the development of fibrosis in murine bleomycin-induced pulmonary fibrosis model using LXR $\alpha^{-/-}$, LXR $\beta^{-/-}$, and LXR $\alpha\beta$ wild type mice.

Methods: Bleomycin-induced pulmonary fibrosis was carried out on male LXR $\alpha^{-/-}$, and LXR $\beta^{-/-}$ and LXR $\alpha\beta$ wild type mice. The mice were 10-12 weeks old and 22-25 grams weight and they were divided into groups as follows:

Animals were randomly allocated into 5 groups (n=22-23 mice in each):-

A- WT treated with vehicle (5% Cremophor in PBS as control),

B- LXR $\alpha^{-/-}$ treated with vehicle

C- LXR α ^{-/-} treated with LXR agonist

D- LXR β ^{-/-} treated with vehicle

E- LXR β ^{-/-} treated with LXR agonist

All mice were given bleomycin intranasally 0.06mg in 30 μ l PBS / animal. 3 days prior to the bleomycin challenge all mice received daily IP injection of vehicle (5% Cremophor v/v PBS) or LXR agonist GW3965 (30mg / kg dissolved in 5% Cremophor / PBS) according to the group. The injections continued daily until day 18 when all mice were culled

3.3.2 LXR α ^{-/-} and LXR β ^{-/-} mice

The LXR α ^{-/-} and LXR β ^{-/-} mice and wild type littermates on the C57BL/6 background were supplied by Lexicon Pharmaceuticals (TX, USA). These mice were already in use in our lab for other inflammatory models for example collagen induced arthritis and atherosclerosis [209].

3.3.3 LXR activation had no effect on the augmentation of bleomycin-induced pulmonary fibrosis in single LXR α ^{-/-} or LXR β ^{-/-} mice compared with wild-type mice

LXR agonist exhibited some effects on loss of body weight in bleomycin-induced pulmonary fibrosis initiated on single LXR α ^{-/-} or LXR β ^{-/-} mice compared with wild-type mice

The systemic inflammatory response to intra-nasal installation of bleomycin into murine lung was monitored by change in body weight (Figures 3.40). There were significant differences for change in body weight between the WT mice treated with vehicle and the rest of experimental group except LXR α ^{-/-} given LXR agonist and LXR β ^{-/-} given LXR agonist. The significant difference was with LXR α ^{-/-} mice given vehicle ($p < 0.001$) and LXR β ^{-/-} mice given vehicle ($p < 0.001$). The weight loss was most evident during the phase of acute inflammation which was up to 9 days after bleomycin installation in all experimental groups (Figure 3.40).

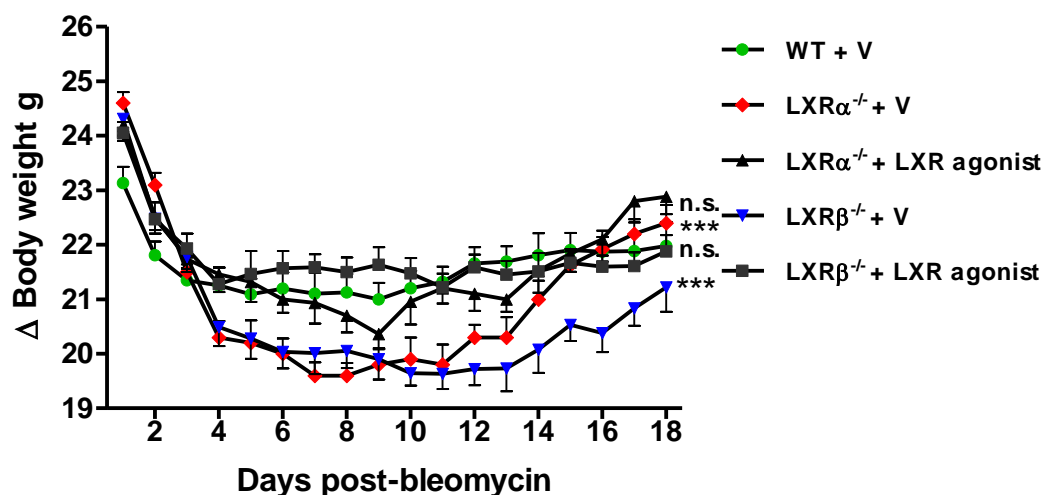


Figure 3.40 Daily body weight changes in WT, LXR $\alpha^{-/-}$ and LXR $\beta^{-/-}$ mice given bleomycin and treated with either LXR agonist or vehicle

The daily body weight changes in male C57BL/6, LXR $\alpha^{-/-}$ KO, and LXR $\beta^{-/-}$ KO mice (10-12 weeks old). All mice received bleomycin and were treated daily with IP injection of vehicle (5% Cremophor w/v PBS) or LXR agonist GW3965 (30mg / kg dissolved in 5% Cremophor / PBS). All the groups exhibited a decline in body weight. One Way ANOVA; n.s. $p > 0.05$; *** $p < 0.001$; Mean \pm SEM; $n = 22-23$ mice/group.

LXR agonist revealed no additional effect on lung histopathological inflammatory and fibrotic changes in bleomycin-induced pulmonary fibrosis in LXR $\alpha^{-/-}$ or LXR $\beta^{-/-}$ mice compared with wild type mice

Bleomycin installation is characterised by severe inflammatory and fibrotic morphological changes to the normal lung architecture (Figure 41 A and B). Sections stained with H&E revealed a similar infiltration of inflammatory cells, perivascular haemorrhage, and collapse of the alveoli as described above in Materials and Methods section (2.5.2). This was similar in all experimental groups (Figure 3.41 A), and quantified on (Figure 3.42).

Tissue collagen was demonstrated in all experimental groups by using Gomori's Trichrome staining. The active fibrotic process manifested by a collagen bundles and fibrotic foci were distributed mainly around the lung bronchioles and blood vessels in all mice groups irrespective of whether they received LXR agonist or vehicle. Typical images are shown in (Figure 3.41 B), and quantified on (Figure 3.43).

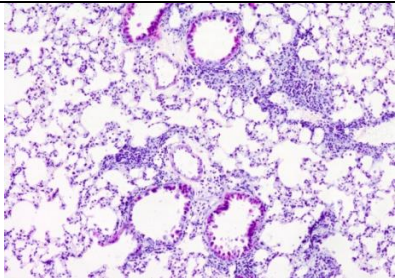
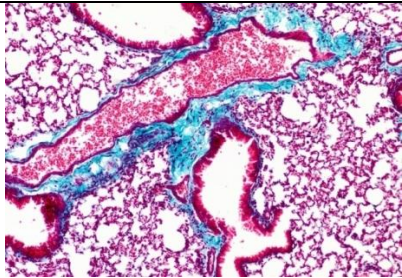
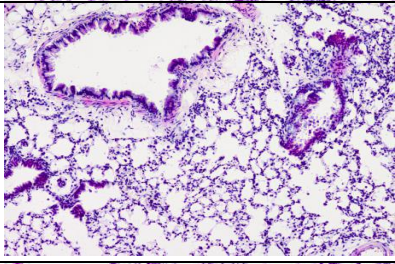
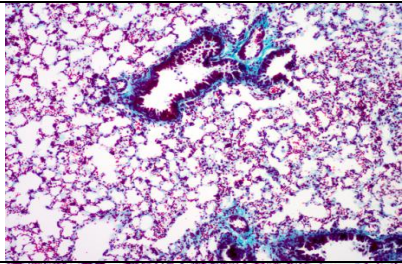
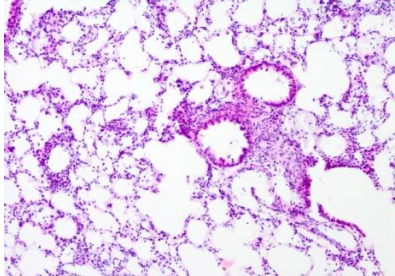
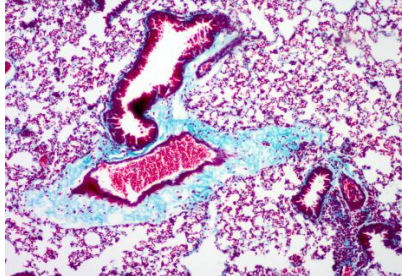
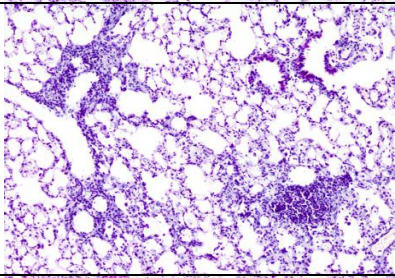
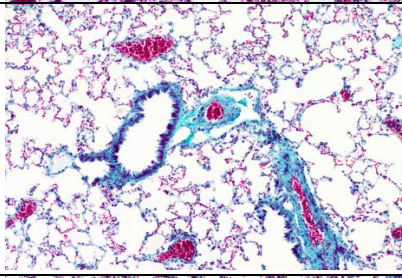
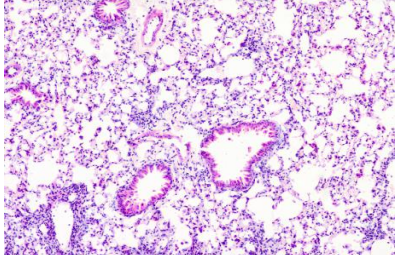
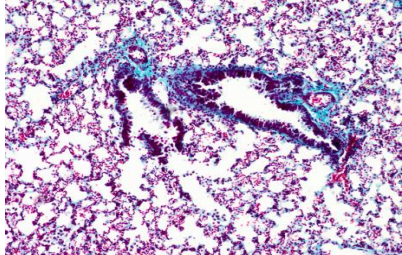
Group	A	B
	H&E	Trichrome
WT + Vehicle		
LXR α ^{-/-} + Vehicle		
LXR α ^{-/-} + LXR agonist		
LXR β ^{-/-} + Vehicle		
LXR β ^{-/-} + LXR agonist		

Figure 3.41 Histological inflammatory and fibrotic changes in the lung of the WT, LXR α ^{-/-} and LXR β ^{-/-} mice given bleomycin and treated with either LXR agonist or vehicle

(A) H&E staining: representative images of lung tissue sections are presented, showing morphological inflammatory changes in lung architecture after bleomycin installation. Severe inflammatory changes were demonstrated in all experimental mice groups in spite of they received daily injections of LXR agonist or vehicle. **(B) Gomori's Trichrome staining:** representative images of lung lobe sections are presented, showing extensive collagen deposition in the lung and large collagen patches around bronchioles, blood vessels and in the parenchyma. These fibrotic changes were similar in all mice groups. Sections were viewed under light microscopy (magnification x10).

Quantification of the extent of the inflammation and fibrosis was performed on the lung sections of the WT, $LXR\alpha^{-/-}$, and $LXR\beta^{-/-}$ mice. The lung tissue sections were labelled by an independent colleague who was unaware of the details of the experiment. The slides were then scored using an inflammation scoring scale described in Materials and Methods (section 2.5.2) by two independent observers thus the quantification for inflammation and fibrosis was performed blind to the origin of the samples. Scoring of H&E stained lung sections exhibited mild to moderate inflammation based on our inflammation scoring grade among all the experimental group; WT mice treated with vehicle, $LXR\alpha^{-/-}$ mice treated with vehicle, $LXR\alpha^{-/-}$ mice treated with LXR agonist, $LXR\beta^{-/-}$ mice treated with vehicle, and $LXR\beta^{-/-}$ mice treated with LXR agonist (Figure 3.42). There was no significant difference between these groups.

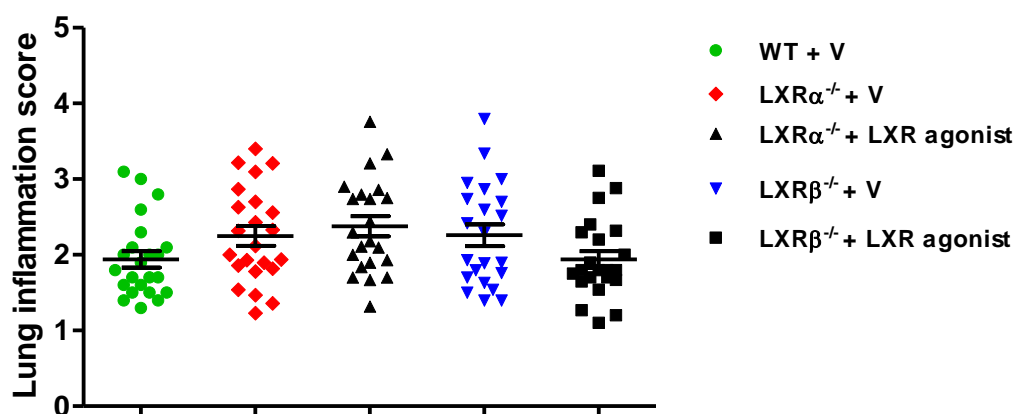


Figure 3.42 Lung inflammation score of the WT, $LXR\alpha^{-/-}$ and $LXR\beta^{-/-}$ mice given bleomycin and treated with either LXR agonist or vehicle
 Inflammation was assessed by histological score (see Materials and Methods section 2.5.2). There were no significantly differences in the inflammation score between all the experimental groups. One Way ANOVA; Mean \pm SEM; n=22-23 mice/group.

Quantification of fibrosis was performed for all lung tissue sections stained with Gomori's trichrome. Blind scoring of the fibrosis based on our scoring grades demonstrated mild fibrotic changes. The fibrosis pattern was similar among all the experimental groups given bleomycin followed by daily IP injection of LXR agonist or vehicle, WT mice treated with vehicle, $LXR\alpha^{-/-}$ mice treated with vehicle, $LXR\alpha^{-/-}$ mice treated with LXR agonist, $LXR\beta^{-/-}$ mice treated with vehicle, and $LXR\beta^{-/-}$ mice treated with LXR agonist (Figure 3.43). There was no significant difference between these groups.

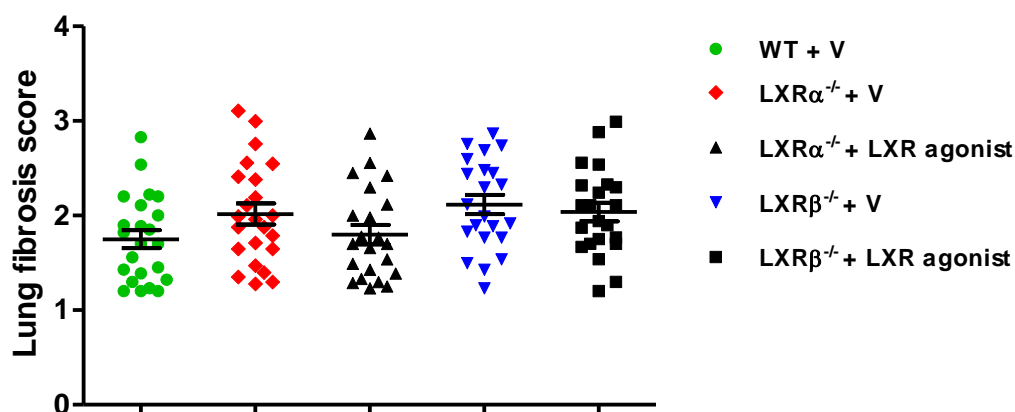


Figure 3.43 Lung fibrosis score of the WT, $LXR\alpha^{-/-}$ and $LXR\beta^{-/-}$ mice given bleomycin and treated with either LXR agonist or vehicle

Fibrosis was assessed by scoring (see materials and methods section 2.5.2). There was no significant differences between all mice experimental groups in spite of the received of either LXR agonist or vehicle. One Way ANOVA, Mean \pm SEM; n=22-23 mice/group.

LXR agonist revealed no additional effect on bronchoalveolar lavage fluid (BAL) cell counts in bleomycin-induced pulmonary fibrosis in $LXR\alpha^{-/-}$ or $LXR\beta^{-/-}$ mice compared with wild type mice

Total BAL cell count:

The BAL total cell count was performed for all experimental groups of mice (Figure 3.44). There were no significant differences between all bleomycin treated groups. The mean \pm Standard error of the mean of BAL total cell counts were as following:-

WT mice treated with vehicle	$0.88 \pm 0.19 \times 10^6$,
$LXR\alpha^{-/-}$ mice treated with vehicle	$0.82 \pm 0.18 \times 10^6$,
$LXR\alpha^{-/-}$ mice treated with LXR agonist	$0.89 \pm 0.23 \times 10^6$,
$LXR\beta^{-/-}$ mice treated with vehicle	$0.77 \pm 0.22 \times 10^6$,
$LXR\beta^{-/-}$ mice treated with LXR agonist	$0.87 \pm 0.26 \times 10^6$ (Figure 3.44).

There was no significant difference between these groups.

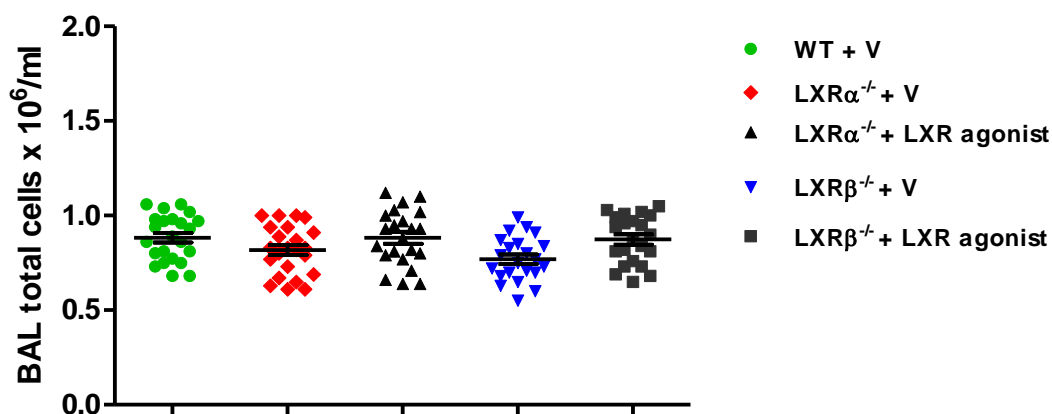


Figure 3.44 Total BAL cell count in the BAL of WT, LXR $\alpha^{-/-}$ and LXR $\beta^{-/-}$ mice given bleomycin and treated with either LXR agonist or vehicle

Total BAL cell count for the inflammatory cell retrieved from bronchoalveolar lavage of all the experimental mice demonstrated no significant differences between groups. One Way ANOVA, Mean \pm SEM; n=22-23 mice/group.

Differential BAL cell count:

The differential cell count profiles for BAL were performed to demonstrate the proportion of the inflammatory cells in the bronchoalveolar lavage fluid.

Macrophage cell count:

The macrophage cell count showed no significant differences between all the groups:

The mean \pm Standard error of the mean of BAL macrophage counts were as following:-

WT mice treated with vehicle	$0.62 \pm 0.14 \times 10^6$,
LXR $\alpha^{-/-}$ mice treated with vehicle	$0.61 \pm 0.21 \times 10^6$,
LXR $\alpha^{-/-}$ mice treated with LXR agonist	$0.67 \pm 0.20 \times 10^6$,
LXR $\beta^{-/-}$ mice treated with vehicle	$0.58 \pm 0.13 \times 10^6$,
LXR $\beta^{-/-}$ mice treated with LXR agonist	$0.63 \pm 0.17 \times 10^6$ (Figure 3.45).

There was no significant difference between these groups.

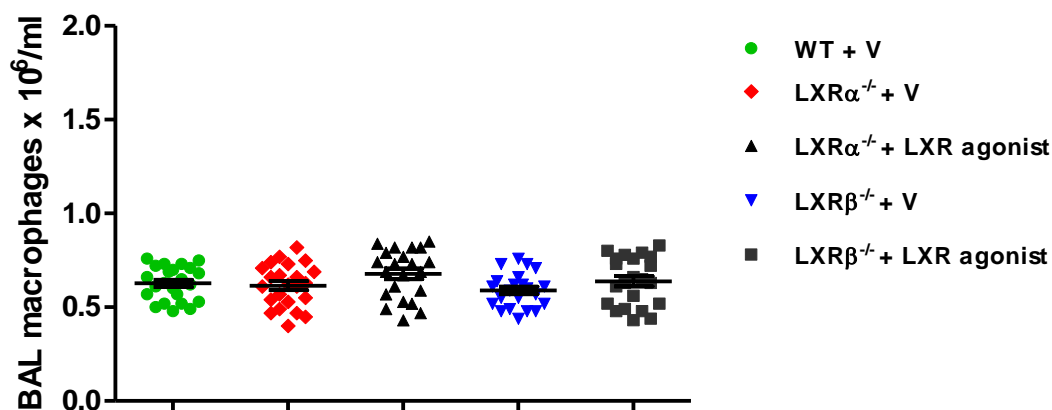


Figure 3. 45 Macrophage cell count in the BAL of WT, LXR $\alpha^{-/-}$ and LXR $\beta^{-/-}$ mice given bleomycin and treated with either LXR agonist or vehicle
The BAL macrophage cell count demonstrated no significant differences between the groups. One Way ANOVA, Mean \pm SEM; n=22-23 mice/group.

Lymphocyte cell count:

The lymphocyte cell count showed no significant differences between all the groups:

The mean \pm Standard error of the mean of BAL lymphocyte counts were as following:-

WT mice treated with vehicle	$0.22 \pm 0.04 \times 10^6$,
LXR $\alpha^{-/-}$ mice treated with vehicle	$0.19 \pm 0.05 \times 10^6$,
LXR $\alpha^{-/-}$ mice treated with LXR agonist	$0.20 \pm 0.04 \times 10^6$,
LXR $\beta^{-/-}$ mice treated with vehicle	$0.18 \pm 0.05 \times 10^6$,
LXR $\beta^{-/-}$ mice treated with LXR agonist	$0.21 \pm 0.06 \times 10^6$ (Figure 3.46).

There was no significant difference between these groups.

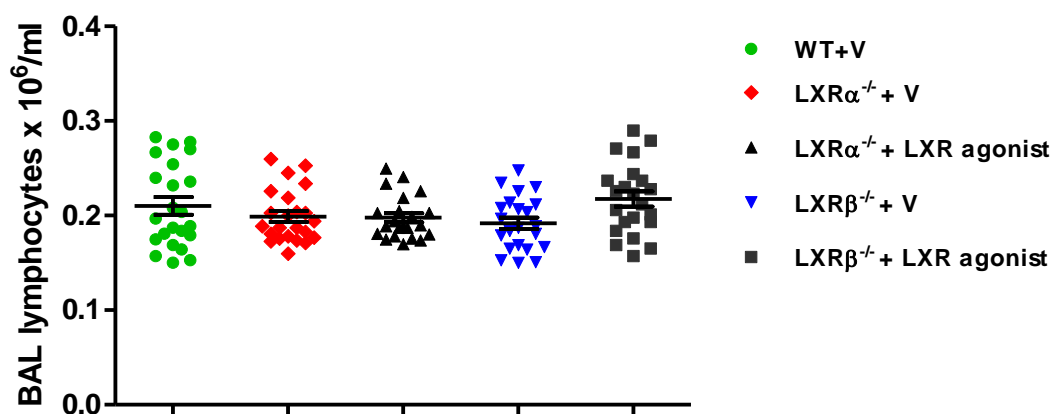


Figure 3.46 Lymphocyte cell count in the BAL of WT, $LXR\alpha^{-/-}$ and $LXR\beta^{-/-}$ mice given bleomycin and treated with either LXR agonist or vehicle. The BAL lymphocyte cell count demonstrated no significant differences between the groups. One Way ANOVA; Mean \pm SEM; n=22-23 mice/group.

LXR agonist treatment demonstrated no changes in concentration of inflammatory and fibrotic mediators in bleomycin-induced pulmonary fibrosis in $LXR\alpha^{-/-}$ and $LXR\beta^{-/-}$ mice compared with wild-type mice

A pragmatic range of cytokines, chemokines and growth factors relevant to the inflammatory and fibrotic responses was quantified in serum (Table 3.4) and in BAL fluid (Table 3.5) from the experimental groups of mice.

Serum and bronchoalveolar lavage (BAL) fluid mediators:

Serum and BAL analysis demonstrated no significant differences between the concentrations of any of the mediators in the serum or in the BAL of the WT mice treated with vehicle, $LXR\alpha^{-/-}$ mice treated with vehicle, $LXR\alpha^{-/-}$ mice treated with LXR agonist, $LXR\beta^{-/-}$ mice treated with vehicle, and $LXR\beta^{-/-}$ mice treated with LXR agonist (Tables 3.4 and 3.5).

serum Mediators (pg/ml)	LXR α ^{-/-} + V	LXR α ^{-/-} +LXR agonist	LXR β ^{-/-} + V	LXR β ^{-/-} +LXR agonist	p value
Cytokines					
TNFα	26 (3-47)	19 (0-53)	25 (11-65)	31 (8-71)	0.2683
IFNγ	0 (0-19)	0 (0-35)	29 (4-48)	0 (0-0)	0.5294
IL-1α	67 (8-105)	48 (17-81)	18 (0-42)	37 (19-69)	0.1733
IL-1β	69 (22-118)	63 (35-108)	55 (16-136)	58 (0-123)	0.3818
IL-2	17 (0-46)	24 (1-60)	27 (9-55)	23 (0-68)	0.3640
IL-4	0 (0-0)	3 (0-8)	19 (0-41)	8 (0-23)	0.4187
IL-5	22 (7-41)	0 (0-0)	13 (0-33)	12 (0-27)	0.1452
IL-6	5 (0-11)	8 (0-22)	23 (9-48)	43 (15-83)	0.0826
IL-10	349 (135-788)	364 (219-540)	338 (95-641)	371 (178-622)	0.2995
IL-12	115 (47-191)	141 (88-207)	124 (65-279)	136 (32-294)	0.1814
IL-13	18 (4-31)	25 (0-62)	23 (8-59)	17 (0-38)	0.3027
IL-17	0 (0-0)	0 (0-0)	2 (0-5)	0 (0-0)	0.6114
Growth factors					
TGFβ1	67 (34-105)	62 (25-123)	59 (19-117)	66 (28-131)	0.0975
FGF basic	213 (128-459)	175 (77-282)	162 (81-317)	181 (62-325)	0.1638
VEGF	20 (3-45)	12 (0-27)	17 (9-29)	21 (11-36)	0.2573
GM-CSF	2 (0-5)	0 (0-0)	0 (0-0)	5 (0-12)	0.4439
Chemokines					
MCP-1	22 (0-49)	35 (16-57)	29 (18-63)	31 (0-78)	0.2071
MIP-1α	24 (9-55)	21 (0-39)	19 (7-44)	26 (15-62)	0.1525
KC	183 (68-391)	211 (128-448)	177 (53-327)	195 (88-403)	0.8427
MIG	82 (36-145)	73 (0-121)	0 (0-0)	18 (10-32)	0.3108
IP-10	11 (0-29)	3 (0-7)	23 (6-44)	5 (0-12)	0.5969

Table 3.4 Inflammatory and fibrotic mediators in the serum of WT, LXR α ^{-/-} and LXR β ^{-/-} mice given bleomycin and treated with either LXR agonist or vehicle

There were no significant differences in concentrations of cytokines, chemokines, and growth factors in the serum of the LXR α ^{-/-} mice treated with vehicle, LXR α ^{-/-} mice treated with LXR agonist, LXR β ^{-/-} mice treated with vehicle, and LXR β ^{-/-} mice treated with LXR agonist treated. Median and interquartile range concentrations of each mediator were used to determine P-value for between category and between group differences; Kruskal-Wallis test; Mann-Whitney test respectively; n.s. p>0.05; n=22-23 mice/group

BAL Mediators (pg/ml)	LXR α ^{-/-} + V	LXR α ^{-/-} +LXR agonist	LXR β ^{-/-} + V	LXR β ^{-/-} +LXR agonist	p value
Cytokines					
TNF α	48 (17-93)	35 (9-61)	42 (26-79)	39 (12-74)	0.3274
IFN γ	3 (0-5)	0 (0-0)	0 (0-0)	0 (0-0)	0.5859
IL-1 α	0 (0-0)	0 (0-0)	0 (0-0)	0 (0-0)	N.A.
IL-1 β	108 (69-196)	81 (52-170)	94 (36-175)	83 (45-143)	0.1662
IL-2	24 (0-59)	32 (19-66)	29 (14-57)	25 (14-42)	0.3285
IL-4	0 (0-0)	0 (0-0)	3 (0-8)	0 (0-0)	0.6819
IL-5	5 (0-14)	2 (0-4)	16 (0-35)	0 (0-0)	0.2737
IL-6	0 (0-0)	0 (0-0)	33 (0-71)	0 (0-0)	0.5116
IL-10	427 (216-768)	291 (178-435)	352 (207-542)	376 (189-662)	0.0643
IL-12	73 (30-128)	85 (57-144)	77 (26-169)	114 (73-202)	0.1928
IL-13	0 (0-0)	0 (0-0)	2 (0-5)	0 (0-0)	0.5471
IL-17	0 (0-0)	0 (0-0)	0 (0-0)	0 (0-0)	N.A.
Growth factors					
TGF β 1	108 (39-235)	81 (47-159)	94 (56-182)	83 (42-177)	0.1531
FGF basic	62 (31-147)	46 (21-93)	54 (36-124)	52 (28-89)	0.2844
VEGF	66 (34-115)	36 (19-71)	49 (26-105)	42 (15-93)	0.2537
GM-CSF	0 (0-0)	0 (0-0)	0 (0-0)	0 (0-0)	N.A.
Chemokines					
MCP-1	26 (8-58)	23 (11-40)	17 (7-41)	29 (15-67)	0.1489
MIP-1 α	52 (31-99)	36 (14-78)	39 (20-71)	41 (18-82)	0.3185
KC	63 (35-118)	59 (27-102)	74 (41-132)	83 (52-140)	0.4629
MIG	0 (0-0)	1 (0-2)	0 (0-0)	0 (0-0)	0.6271
IP-10	0 (0-0)	0 (0-0)	0 (0-0)	0 (0-0)	N.A.

Table 3.5 Inflammatory and fibrotic mediators in the BAL of WT, LXR α ^{-/-} and LXR β ^{-/-} mice given bleomycin and treated with either LXR agonist or vehicle
There were no significant differences in concentrations of cytokines, chemokines, and growth factors in the BAL of the LXR α ^{-/-} mice treated with vehicle, LXR α ^{-/-} mice treated with LXR agonist, LXR β ^{-/-} mice treated with vehicle, and LXR β ^{-/-} mice treated with LXR agonist. Median and interquartile range concentrations of each mediator were used to determine P-value for between category and between group differences; Kruskal-Wallis test; Mann-Whitney test respectively; n.s. p>0.05; groups; n=22-23 mice/group

Administration of LXR agonist did not affect the expression of TGF β 1 and collagen 1 and 3 in bleomycin-induced lung fibrosis in single LXR $\alpha^{-/-}$ or LXR $\beta^{-/-}$ mice compared with wild-type mice

Lung tissue RNA was collected from all experimental groups of mice and analysed by qPCR to demonstrate the mRNA level of collagen type TGF β 1. No significant differences were measured between all groups (Figure 3.47). Similarly, collagen type IA and IIIA mRNA expression showed no significant differences between the groups (Figure 3.48).

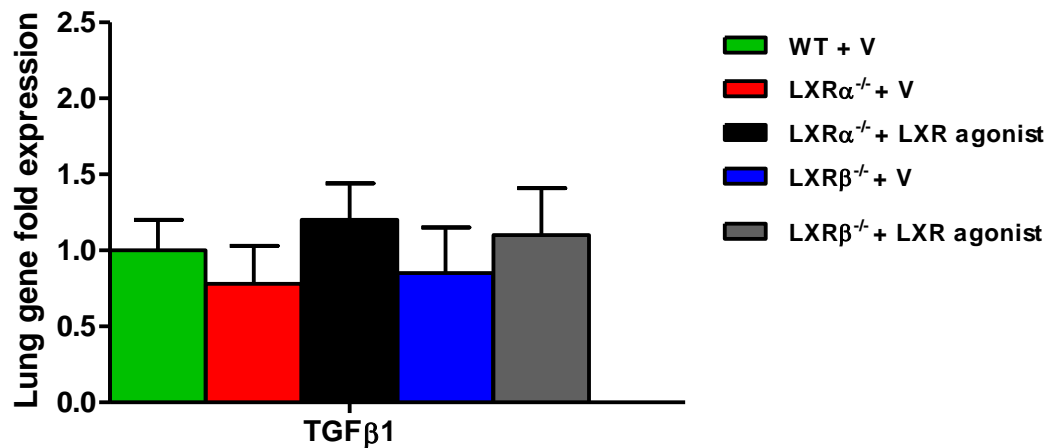


Figure 3.47 TGF β 1 gene expression in lungs of WT, LXR $\alpha^{-/-}$ and LXR $\beta^{-/-}$ mice given bleomycin and treated with either LXR agonist or vehicle
There were no differences in TGF β 1 expression levels between the groups. One Way ANOVA; Mean \pm SEM; n=22-23 mice/group.

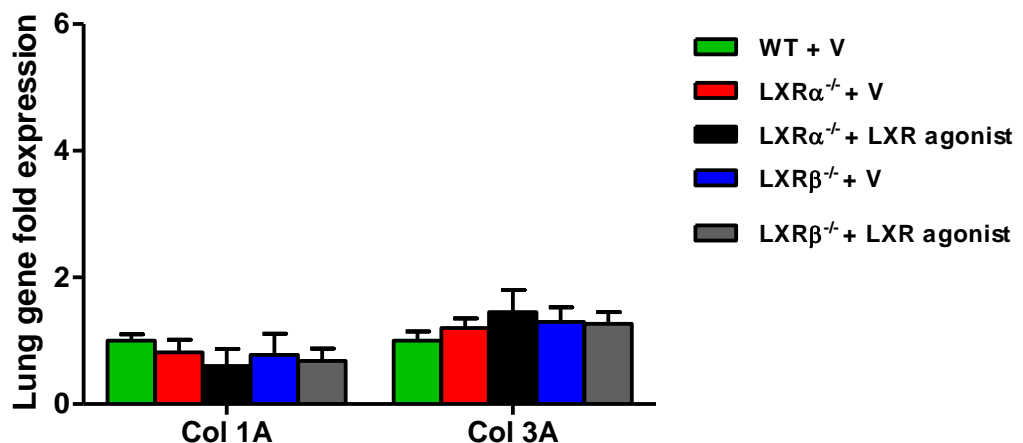


Figure 3.48 Collagen gene expression in lungs of WT, LXR $\alpha^{-/-}$ and LXR $\beta^{-/-}$ mice given bleomycin and treated with either LXR agonist or vehicle
There were no differences in collagen type IA1 and Col IIIA1 expression levels between the groups. One Way ANOVA; Mean \pm SEM; n=22-23 mice/group.

Administration of LXR agonist did not alter the lung collagen content in bleomycin induced lung fibrosis in single LXR α ^{-/-} or LXR β ^{-/-} mice compared with wild type mice.

Lung tissues were analysed for soluble collagen content. There was no significant difference between all experimental groups. The mean \pm Standard error of the mean of lung soluble collagen contents were as following:-

WT mice treated with vehicle	1.73 \pm 0.11 mg/ml,
LXR α ^{-/-} mice treated with vehicle	1.86 \pm 0.24mg/ml,
LXR α ^{-/-} mice treated with LXR agonist	1.72 \pm 0.20 mg/ml,
LXR β ^{-/-} mice treated with vehicle	1.67 \pm 0.22mg/ml,
LXR β ^{-/-} mice treated with LXR agonist	1.79 \pm 0.13mg/ml (Figure 3.49).

There was no significant difference between these groups.

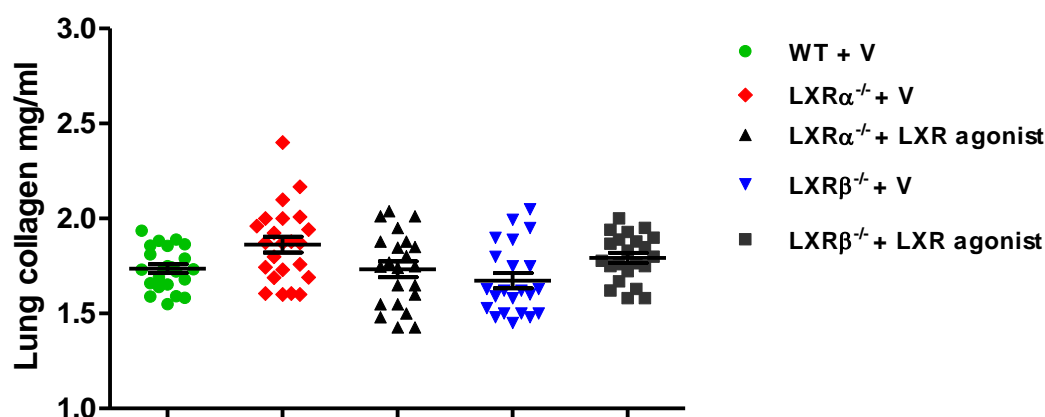


Figure 3.49 Soluble collagen content in lungs of WT, LXR α ^{-/-} and LXR β ^{-/-} mice given bleomycin and treated with either LXR agonist or vehicle
There were no significant differences of collagen content between the groups. One Way ANOVA; Mean \pm SEM; n=22-23 mice/group.

3.3.4 Discussion and Conclusion

The main aim of this experiment was to identify the potential individual roles of LXR α and LXR β in the inflammatory and fibrotic process associated with bleomycin-induced pulmonary fibrosis.

LXR α and LXR β have 77% amino acid sequence identity in both the DNA- and ligand-binding domains, therefore, it is highly likely that they recognise similar ligands and target DNA [222], for example the potent LXR agonist (GW3965) used in these experiments was able to activate both receptors. Therefore, we hypothesised that there is no difference between the presence of each receptor type on the subsequent extent of fibrosis.

We demonstrated that administration of LXR agonist 30 mg/kg into a single LXR $\alpha^{-/-}$ and LXR $\beta^{-/-}$ mice given bleomycin had no significant effect on the severity of the lung inflammation or fibrosis compared with vehicle. There was a significant difference in body weight among some groups LXR $\alpha^{-/-}$ mice treated with vehicle, and LXR $\beta^{-/-}$ mice treated with vehicle compared to wild type mice treated with vehicle (Figure 3.40). This suggested that there was an inflammation-related cachexia, however did not extend further to histological or inflammatory cellular involvement. It is possible that the loss of body weight in these circumstances related to metabolic changes which were beyond the scope of this thesis.

The activation of either LXR receptor was sufficient to circumvent the additional pro-fibrotic tendency of the double receptor knock-out mouse to bleomycin-induced fibrosis. The gene-deletion of either resulted in no significant differences in lung pathomorphology, lung collagen content and collagen gene type I, III and TGF β 1 expression.

Joseph and colleagues reported that LXR $\alpha^{-/-}$ mice were highly susceptible to infection with *Listeria monocytogenes*, but they found no changes from normal between LXR $\alpha^{-/-}$ and LXR $\beta^{-/-}$ mice and wild types in the serum inflammatory cytokines mediators [72]. This appeared to be in agreement with our results which showed no changes in the serum and BAL mediators between all experimental mice groups. It is possible that both LXR α and LXR β share a synergistic effect on the promoters of genes of inflammation and fibrosis. It is also possible that LXR α or LXR β may have different involvements, mainly in inflammation, but to have a detectable effect on bleomycin-induced pulmonary fibrosis both of the receptors were required. One of the suggestions is that LXR α or LXR β act in a cooperative pathway, therefore, deletion of both of them is needed for additional pro-inflammatory and pro-fibrotic changes, as detected by significant increases in the concentration of inflammatory and fibrotic mediators and associated processes.

Laffitte and colleagues reported that both oxysterols and synthetic ligands were able to regulate ApoE expression in peritoneal macrophages to different degrees [223]. They showed that ApoE expression was reduced in LXR $\alpha^{-/-}$ or LXR $\beta^{-/-}$ mice, and was abolished in LXR $\alpha^{-/-}$ $\beta^{-/-}$ mice. They also showed that any disruption of

both LXR α and LXR β in mice was characterised by a highly severe metabolic defect suggesting that both receptors have a degree of overlapping physiologic functions [223]. The results from my experiment were in contrast to those of Bradley et al [220]. They studied the contribution of both LXR isoforms to atherosclerosis [220]. Using the ApoE^{-/-} model of atherosclerosis they determined that deletion of LXR α on these mice correlated with a progressive atherosclerotic process, demonstrated by accumulation of cholesterol in the peripheral tissues and aortic root. Therefore, they suggested that LXR β is not sufficient to compensate for the absence of LXR α . However, using the high affinity LXRs agonist GW3965 that could bind with both receptor types, they were able to activate LXR β resulting in attenuation of the atherosclerosis.

It is possible that LXR α or LXR β may have different individual involvements in lipid metabolism and in inflammation, but that this does not extend to fibrosis. We found that to have a detectable change in bleomycin-induced pulmonary fibrosis both of the receptors were required. One of the suggestion is that LXR α or LXR β act in synergistic pathway, therefore, each one of them need the other for maximum activation which could be detected in form of significant differences certain levels of inflammatory and fibrotic process.

Conclusion

The purpose of this work was to understand the involvement of each of LXR α and LXR β receptor subtypes in the course bleomycin-induced pulmonary fibrosis. We have shown earlier that activation of both receptors in wild type mice led to exacerbation of inflammatory and fibrotic process. Interestingly, here we demonstrated that activation of either LXR receptor alone was not sufficient to have a significant effect on the inflammatory and fibrotic changes in the lung of mice given bleomycin, even in the presence of a highly potent LXR agonist (GW3965).

Results 3.4 Index:

3.4 Potential involvement of MicroRNA-155 in the development of pulmonary fibrosis

in a murine model

3.4.1 Introduction and Aims

3.4.2 MiR-155^{-/-} mice develop worse bleomycin-induced pulmonary fibrosis in comparison with miR-155 wild type mice

3.4.3 The macrophages in the miR-155^{-/-} mice had a different phenotype compared with the wild type littermates; both given bleomycin

3.4.4 Discussion and Conclusion

3.4 Potential involvement of MicroRNA-155 in the development of pulmonary fibrosis in a murine model

3.4.1 Introduction and Aims

Micro-RNA (miR) are small, evolutionary conserved, single-stranded, non-coding RNA molecule with 20- 22 nucleotide base pairs [76-78]. They have the ability to regulate mRNA translation resulting in fine tuning of the production of different molecules involved in the initiation or maintenance of inflammation in different diseases. For example, miR-155 is one of the most studied members of miR, and it has a regulatory role in certain inflammatory diseases such as collagen induced arthritis, lung fibrosis, and cardiovascular diseases [99, 104, 224]. Kurowska-Stolarska and colleagues demonstrated that miR-155^{-/-} mice were resistant to initiation of collagen induced arthritis model and this was characterised by inhibition of auto antibody response, antigen-specific Th17 cell, and suppression of articular inflammation [99]. In the first report describing the phenotype of a miR-deleted mouse Rodriguez and colleague described that deletion of miR155 was associated with an age-related increase in airway sub-epithelial collagen deposition [104]. Transfection of human primary lung fibroblast with miR-155 resulted in down-regulation of angiotensin II receptor (AT1R) which participates in blood and cardiovascular diseases indicating that miR-155 plays a protective role safeguarding against cardiovascular disease [224].

MiR-155 expression had been demonstrated in different cells including fibroblast and in different tissues such as epithelium, reproductive organs, central nervous system and haemopoietic tissue [225]. miR-155 has an important immune-regulatory ability for example, a study using miR-155^{-/-} mice has demonstrated that miR-155 was necessary for a normally functioning immune system [104]. Although this study also showed pathomorphological changes in the lung of miR-155^{-/-} mice, the direct functional role of miR-155 in bleomycin-induced pulmonary fibrosis still not defined.

We aimed to demonstrate the role of miR-155 in the course of pulmonary fibrosis in murine model of pulmonary fibrosis induced by bleomycin.

3.4.2 MiR-155^{-/-} mice develop worse bleomycin-induced pulmonary fibrosis in comparison with miR-155 wild type mice

The aim of this experiment was to investigate if there was a role for miR-155 in the pathogenesis of bleomycin-induced pulmonary fibroses in a murine model. The experiment consisted of using miR-155^{-/-} mice and miR-155 wild type littermates (10-12 weeks old and 22-25 grams weight). Mice were randomly allocated into 4 groups (n=7-14 mice per group) as following: -

A- WT mice given PBS (as control)

B- WT mice given bleomycin

C- MiR-155^{-/-} mice given PBS

D- MiR-155^{-/-} mice given bleomycin

All mice given either bleomycin intranasally at 0.06mg in 30 μ l PBS / mouse or 30 μ l PBS / mouse as a control according to the group classification. The animals were monitored for changes in body weight and survival until day 18 when all animal were culled.

Bleomycin treated miR-155^{-/-} mice exhibited a greater loss of body weight than miR-155 wild type mice.

An evaluation of systemic inflammatory response based on the loss of body weight was observed in the groups given bleomycin (Figure 3.50). A progressive reduction in body weight was observed primarily in the miR155^{-/-} group which was significantly greater than the control mice given PBS ($p < 0.001$ for each) and the wild-type miR155 mice ($p = 0.008$) given bleomycin (Figure 3.50).

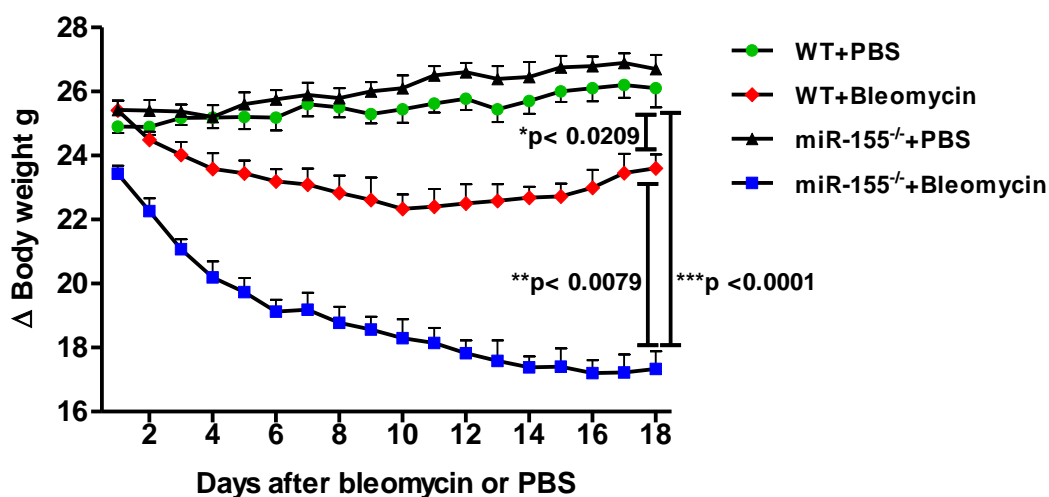


Figure 3.50 Daily body weights changes for miR-155^{-/-} and miR-155 wild type mice given PBS or bleomycin

10-12 week old male miR-155^{-/-} and WT mice were given either PBS or bleomycin. The groups of miR-155^{-/-} and WT mice given bleomycin lost significantly more body weight in comparison to mice given PBS ($p < 0.001$) and ($p = 0.0209$) respectively. The body weight loss revealed was significantly different between miR-155^{-/-} mice given bleomycin and WT mice given bleomycin ($p = 0.0079$). One Way ANOVA; * $P < 0.05$, ** $P < 0.01$, *** $P < 0.001$; Mean \pm SEM; $n = 7-14$ mice/group.

MiR-155^{-/-} mice given bleomycin had an increased in histopathological inflammatory and fibrotic changes in the lung compared with wild type littermates.

Mice given bleomycin had severe histopathological changes to the normal lung architecture as indentified by evaluation of inflammatory and fibrotic changes (Figure 3.51 A and B).

Lung sections stained with H&E from WT and miR-155^{-/-} mice given bleomycin revealed an infiltration of inflammatory cells, perivascular haemorrhage, and collapse of the alveoli as described in Materials and Methods (section 2.5.2). The inflammatory changes were more severe in the lungs of miR-155^{-/-} mice given bleomycin than in the WT mice given bleomycin ($p < 0.001$). No significant inflammatory changes were observed in the lung of WT and miR-155^{-/-} mice given PBS (Figure 3. 51 A).

Collagen deposition was observed in the lung tissue sections using Gomori's Trichrome stain. The collagen deposition was observed as bundles and fibrotic foci distributed mainly around the lung bronchioles and blood vessels. These collagen depositions were observed in WT and miR-155^{-/-} mice given bleomycin and tended to be more abundant in the lungs of miR-155^{-/-} mice group given bleomycin than WT mice group given bleomycin ($p = 0.0368$). No significant fibrotic changes were observed in the lungs of WT and miR-155^{-/-} mice given PBS (Figure 3.51 B).

Quantification of the extent of the inflammation and fibrosis was performed on the lung tissue sections of the WT and miR-155^{-/-} mice given either PBS or bleomycin. The sections were labelled by an independent colleague and the slides were then scored separately by two independent experienced observers unaware of the details of the experiment. Thus the quantification for inflammation and fibrosis was performed blind to the origin of the samples (Figure 3.52 and 3.53).

Scoring of H&E stained lung sections from WT mice given bleomycin revealed mild to moderate inflammation based on our inflammation scoring grade described in the Materials and Methods (section 2.5.2), while moderate to severe inflammation was recorded in miR155^{-/-} mice given bleomycin. WT and miR-155^{-/-} mice given PBS revealed no significant inflammation (Figure 3.52).

Quantifying the lung tissue fibrosis was carried out in a blinded manner by two independent observers. The mice groups given bleomycin were given a higher lung fibrosis score in comparison with the PBS treated groups ($p < 0.001$ for both), furthermore, the lung of the miR-155^{-/-} mice given bleomycin had a significantly higher fibrosis score than the WT mice given bleomycin ($p = 0.0368$) (Figure 3.53).

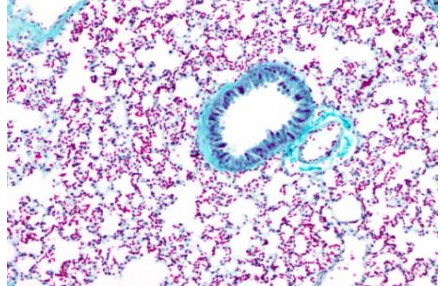
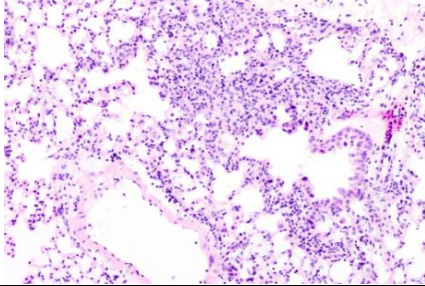
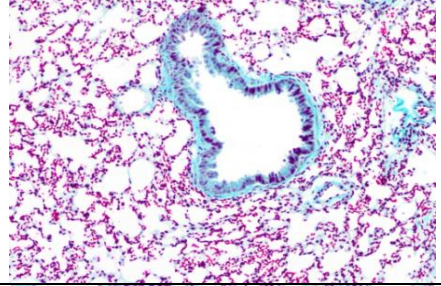
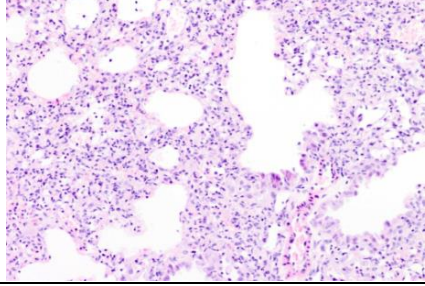
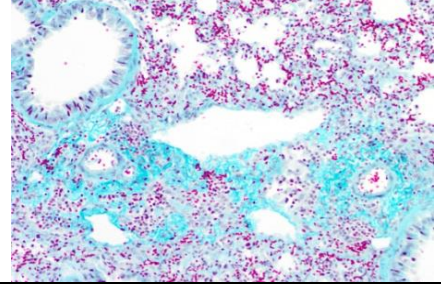
Group	A	B
	H&E	Trichrome
WT+PBS		
WT+ Bleomycin		
miR-155 ^{-/-} +PBS		
miR-155 ^{-/-} + Bleomycin		

Figure 3.51 Histological inflammatory and fibrotic changes in the lung of the lung of miR-155^{-/-} and miR-155 wild type mice given PBS or bleomycin
(A) Representative images of lung tissue sections showing morphological changes in lung architecture after PBS or bleomycin installation. H&E staining shows inflammatory changes in WT and miR-155^{-/-} mice given bleomycin, which were worse in the miR-155^{-/-} mice ($p < 0.037$). No inflammatory changes observed in the lung of WT and miR-155^{-/-} mice given PBS. **(B)** Gomori's Trichrome stain reveals large collagen patches around bronchioles, blood vessels and in the parenchyma. Extensive collagen deposition was seen in the lungs of WT and miR-155^{-/-} mice given bleomycin, with significantly higher deposition in the miR-155^{-/-} mice given bleomycin than WT mice given bleomycin. No significant fibrotic changes were observed in the lungs of WT and miR-155^{-/-} mice given PBS. Sections were viewed under light microscope (magnification x10).

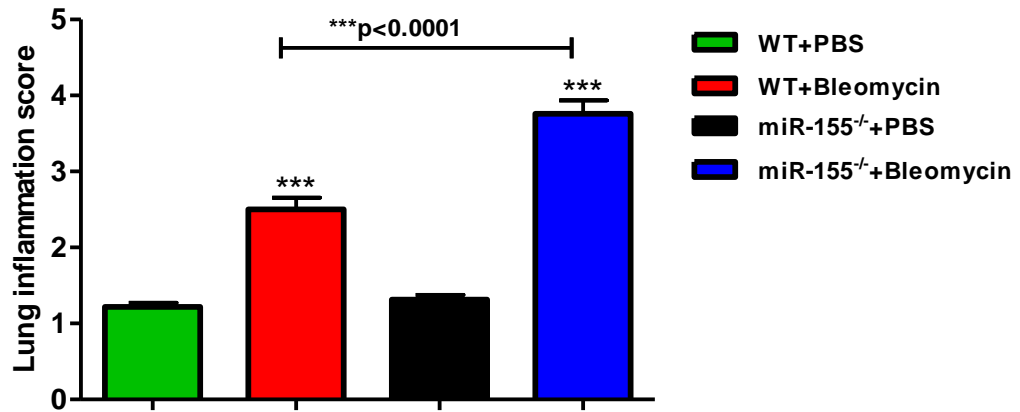


Figure 3.52 Lung inflammation score of the miR-155^{-/-} and miR-155 wild type mice given PBS or bleomycin

Inflammation was assessed by a histological score (see Materials and Methods section 2.5.2) demonstrating significantly higher inflammation in the WT and miR-155^{-/-} mice group given bleomycin in comparison with WT and miR-155^{-/-} mice given PBS. Also a significant higher inflammation score observed between miR-155^{-/-} and WT mice group given bleomycin. One Way ANOVA; *** p<0.001; Mean ± SEM; n = 7-14 mice/group.

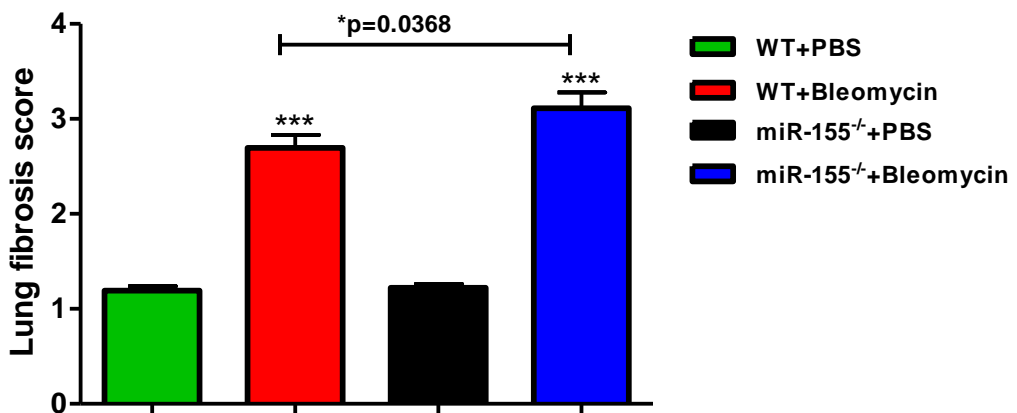


Figure 3.53 Lung fibrosis score of the miR-155^{-/-} and miR-155 wild type mice given PBS or bleomycin

Fibrosis was assessed by histological scoring (see Materials and Methods section 2.5.2). MiR-155^{-/-} and WT mice given bleomycin exhibited highly significant fibrosis in comparison with the groups given PBS. Also a significant higher fibrosis score observed between miR-155^{-/-} mice and WT group given bleomycin. One Way ANOVA; ***p<0.001; Mean ± SEM; n = 7-14 mice/group.

MiR-155^{-/-} mice given bleomycin have increased inflammatory cell numbers in the bronchoalveolar lavage fluid compared with wild type littermates

The BAL total and differential cell profiles were made after processing the bronchoalveolar lavage fluid. Administration of bleomycin to WT and miR-155^{-/-} mice lead to significant increase in the BAL total cell count in comparison with the WT and miR-155^{-/-} mice given PBS. The mean \pm Standard error of the mean of counts were as following:-

WT mice given bleomycin	1.31 \pm 0.17 x 10 ⁶ ;
MiR-155 ^{-/-} mice given bleomycin	7.33 \pm 1.06 x 10 ⁶ ;
WT mice given PBS	0.15 \pm 0.06 x 10 ⁶ ;
MiR-155 ^{-/-} mice given PBS	0.24 \pm 0.12 x 10 ⁶ (Figure 3.54).

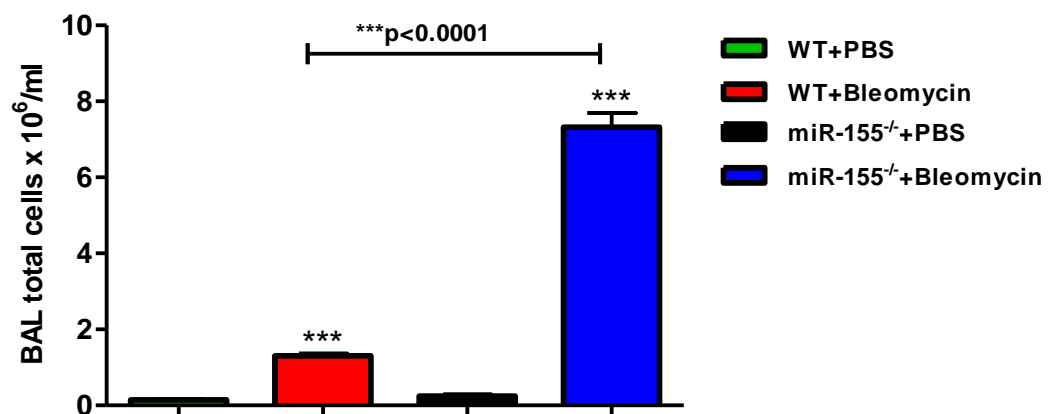


Figure 3.54 Total BAL cell count in the BAL of miR-155^{-/-} and miR-155 wild type mice given PBS or bleomycin

The counts from WT and miR-155^{-/-} mice given bleomycin were significantly higher than the WT and miR-155^{-/-} mice given PBS ($p < 0.001$). Also the count was significantly higher in miR-155^{-/-} mice compared with WT given bleomycin ($p < 0.001$). One Way ANOVA; *** $p < 0.001$; Mean \pm SEM; n = 7-14 mice/group.

The differential cell count profiles for the BAL were assessed after processing by cyto-centrifuge and H&E staining.

Macrophages:

The macrophages were found to be the greatest proportion of the BAL inflammatory cells. The macrophage count was significantly higher in the WT and miR-155^{-/-} mice given bleomycin compared with the WT and miR-155^{-/-} mice given PBS ($p < 0.001$ for each). The macrophage count was significantly greater in the miR155^{-/-} than the wild-type littermates given bleomycin ($p < 0.001$). The mean \pm Standard error of the mean of macrophage counts were as follows:

WT mice given bleomycin	$0.96 \pm 0.12 \times 10^6$,
MiR-155 ^{-/-} mice given bleomycin	$4.62 \pm 1.07 \times 10^6$,
WT mice given PBS	$0.13 \pm 0.05 \times 10^6$,
MiR-155 ^{-/-} mice given PBS	$0.17 \pm 0.12 \times 10^6$ (Figure 3.55).

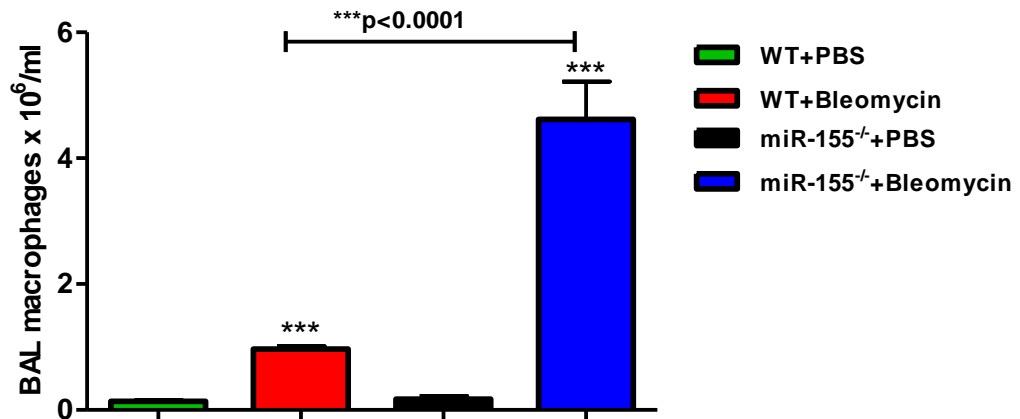


Figure 3.55 Macrophage cell count in the BAL of miR-155^{-/-} and miR-155 wild type mice given PBS or bleomycin

The macrophage cell count was significantly higher in the bronchoalveolar lavage fluid retrieved from the bleomycin treated groups compared to the PBS treated groups. Also the count was significantly higher in the miR-155^{-/-} mice than the WT; both given bleomycin. One Way ANOVA; ***p<0.001; Mean ± SEM; n = 7-14 mice/group.

Lymphocytes:

The lymphocyte count significantly increased in the BAL of the WT and miR-155^{-/-} mice given bleomycin groups compared with the PBS treated groups (p<0.01 and p<0.001 respectively). The lymphocyte count was significantly greater in the miR-155^{-/-} than the wild type littermates given bleomycin (p<0.001). The mean ± Standard error of the mean of lymphocyte counts were as follows:

WT mice given bleomycin	$24.78 \pm 19.6 \times 10^4$,
MiR-155 ^{-/-} mice given bleomycin	$237.56 \pm 73.75 \times 10^4$,
WT mice given PBS	$0.80 \pm 0.4 \times 10^4$,
MiR-155 ^{-/-} mice given PBS	$2.92 \pm 1.3 \times 10^4$ (Figure 3.56).

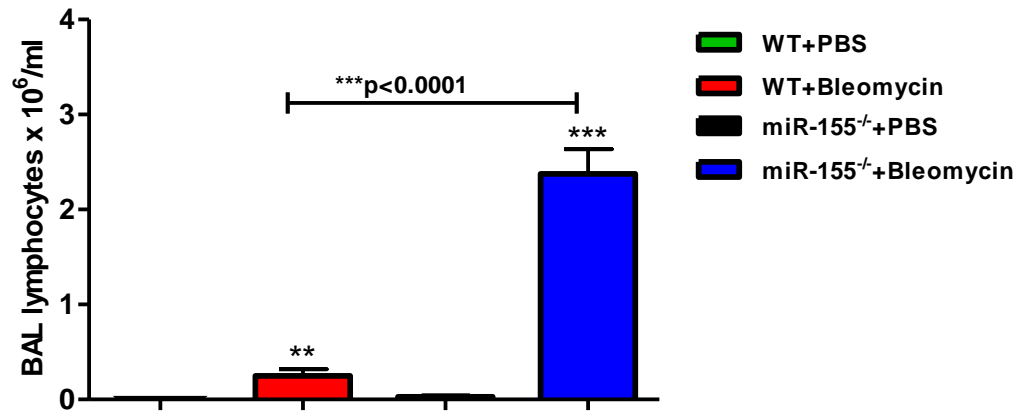


Figure 3.56 Lymphocyte cell count in the BAL of miR-155^{-/-} and miR-155 wild type mice given PBS or bleomycin

The BAL lymphocyte cell count was significantly greater in the bronchoalveolar lavage fluid from the WT and miR-155^{-/-} mice given bleomycin compared to the WT and miR-155^{-/-} mice given PBS ($p < 0.01$ and $p < 0.001$ respectively). Also the count was significant greater in the miR155^{-/-} group than the WT group; both given bleomycin. One Way ANOVA; ** $p < 0.01$; *** $p < 0.001$; Mean \pm SEM; $n = 7-14$ mice/group.

MiR-155^{-/-} mice given bleomycin had increased concentrations of inflammatory and fibrotic mediators in the serum and BAL fluid compared with wild-type littermates

A pragmatic range of cytokines, chemokines and growth factors relevant to the inflammatory and fibrotic responses was quantified in serum (Table 3.6) and in BAL fluid (Table 3.7) from the experimental groups of mice.

Serum mediators:

Serum analysis demonstrated a significant increased concentration of TGF β 1 in the serum of the miR-155^{-/-} and WT mice given bleomycin compared to miR-155^{-/-} and WT mice given PBS (Table 3.6). No significant differences in cytokines and chemokine concentration were demonstrated between all experimental groups.

Bronchoalveolar lavage fluid:

BAL analysis demonstrated a significant increased concentration of TGF β 1 in the BAL of the miR-155^{-/-} and WT mice given bleomycin compared to miR-155^{-/-} and WT mice given PBS. Also higher significant concentration of FGF basic in the BAL of miR-155^{-/-} mice given bleomycin compare to the other experimental groups (Table 3.7).

serum Mediators (pg/ml)	WT + PBS	WT + Bleomycin	miR-155 ^{-/-} + PBS	miR-155 ^{-/-} + Bleomycin	p value
Cytokines					
TNFα	0 (0-0)	0 (0-0)	0 (0-0)	0 (0-55)	0.1912
IFNγ	0 (0-0)	0 (0-0)	0 (0-53)	0 (0-43)	0.1338
IL-1α	0 (0-60)	0 (0-0)	0 (0-76)	0 (0-0)	0.3780
IL-1β	0 (0-12)	0 (0-12)	126 (0-12)	11 (0-22)	0.6899
IL-2	0 (0-0)	0 (0-0)	0 (0-0)	0 (0-0)	N.A.
IL-4	0 (0-0)	0 (0-0)	0 (0-135)	0 (0-197)	0.1645
IL-5	0 (0-0)	0 (0-0)	0 (0-0)	0 (0-31)	0.0576
IL-6	0 (0-0)	0 (0-0)	0 (0-0)	0 (0-0)	N.A.
IL-10	0 (0-0)	0 ^{3,4} (0-0)	60 (43-102)	74 (43-82)	0.0542
IL-12	2 (1-2)	2 (1-2)	2 (1-3)	1 (0-1)	0.1509
IL-13	0 (0-0)	0 (0-0)	0 (0-0)	0 (0-0)	N.A.
IL-17	0 (0-0)	0 (0-0)	0 (0-0)	0 (0-0)	N.A.
Growth factors					
TGFβ1	84 (65-96)	965 ^{1,3} (83-107)	80 (70-88)	98 ^{1,3} (91-108)	0.0001
FGF basic	152 (92-152)	94 (0-210)	129 (75-152)	114 (97-268)	0.5630
VEGF	22 ² (14-51)	13 (4-14)	14 (10-27)	13 (6-41)	0.1099
GM-CSF	0 (0-0)	0 (0-0)	0 (0-0)	0 (0-0)	N.A.
Chemokines					
MCP-1	0 (0-0)	0 (0-0)	0 (0-0)	0 (0-15)	0.0618
MIP-1α	110 (0-110)	44 (0-110)	110 (44-110)	110 (0-110)	0.3749
KC	37 (0-51)	0 ^{1,3} (0-0)	53 (0-111)	0 (0-21)	0.1479
MIG	0 (0-63)	2 (0-12)	0 (0-0)	0 (0-4)	0.3479
IP-10	12 (0-32)	0 (0-32) ³	32 (15-32)	7 (0-32)	0.1326

Table 3.6 Inflammatory and fibrotic mediators in the serum of miR-155^{-/-} and WT mice given PBS or bleomycin

Serum analysis exhibited a significantly higher concentration of TGF- β 1 in the serum of the miR-155^{-/-} and WT mice given bleomycin compared to miR-155^{-/-} and WT mice given PBS. Median and interquartile range concentrations of each mediator were used to determine P-value for between category and between group differences; Kruskal-Wallis test; Mann-Whitney test respectively; n.s. p>0.05; N.A.= no analysis was appropriate because all value were below assay detection limits; n=7-14 mice/group.

BAL Mediators (pg/ml)	WT + PBS	WT + Bleomycin	miR-155 ^{-/-} + PBS	miR-155 ^{-/-} + Bleomycin	p value
Cytokines					
TNF α	0 (0-55)	27 (0-55)	0 (0-55)	0 (0-55)	0.6349
IFN γ	0 (0-0)	0 (0-0)	0 (0-0)	0 (0-0)	N.A.
IL-1 α	0 (0-0)	0 (0-0)	0 (0-0)	0 (0-0)	N.A.
IL-1 β	0 (0-0)	0 (0-12)	0 (0-12)	0 (0-12)	0.8198
IL-2	0 (0-0)	0 (0-0)	0 (0-0)	0 (0-0)	N.A.
IL-4	0 (0-0)	0 (0-40)	0 (0-0)	0 (0-0)	0.5254
IL-5	0 (0-0)	0 (0-0)	0 (0-0)	0 (0-0)	N.A.
IL-6	0 (0-0)	0 (0-0)	0 (0-0)	0 (0-0)	N.A.
IL-10	102 (56-214)	91 (69-309)	75 (45-102)	64 (46-136)	0.3583
IL-12	0 (0-1)	0 (0-2)	0 (0-0)	1 (0-1)	0.1944
IL-13	0 (0-0)	0 (0-0)	0 (0-0)	0 (0-0)	N.A.
IL-17	0 (0-0)	0 (0-0)	0 (0-0)	0 (0-0)	N.A.
Growth factors					
TGF β 1	9 (0-6)	111 ^{1,3} (0-473)	21 (0-149)	208 ^{1, 2, 3} (0-823)	0.0010
FGF basic	27 (20-36)	22 (18-47)	21 (19-25)	39 ^{1, 2, 3} (33-87)	0.0170
VEGF	35 (16-102)	24 (13-51)	27(13-51)	16 ^{1,3} (7-27)	0.0872
GM-CSF	0 (0-0)	0 (0-0)	0(0-0)	0 (0-0)	N.A.
Chemokines					
MCP-1	0 (0-0)	0 (0-0)	0 (0-0)	0 (0-0)	0.5125
MIP-1 α	110 (44-110)	77 (44-110)	44 (11-110)	77 (0-110)	0.3724
KC	86 ³ (71-97)	65 (41-97)	45 (33-60)	78 (36-111)	0.2815
MIG	0 (0-0)	0 (0-3)	0 (0-0)	0 (0-6)	0.6110
IP-10	0 (0-0)	0 (0-32)	0 (0-32)	0 (0-32)	0.5306

Table 3.7 Inflammatory and fibrotic mediators in the BAL of miR-155^{-/-} and WT mice given PBS or bleomycin

BAL analysis exhibited a significantly higher concentration of TGF- β 1 in the BAL of the miR-155^{-/-} and WT mice given bleomycin compared to miR-155^{-/-} and WT mice given PBS. Also higher significant concentration of FGF basic in the BAL of miR-155^{-/-} given bleomycin compare to all experimental groups. Median and interquartile range concentrations of each mediator were used to determine P-value for between category and between group differences; Kruskal-Wallis test; Mann-Whitney test respectively; n.s. p>0.05; N.A.= no analysis was appropriate because all value were below assay detection limits; n=7-14 mice/group

MiR-155^{-/-} mice given bleomycin had increased TGF beta and collagen gene expression and transcription in the lung compared with wild-type littermates

Transcriptional analysis for TGFβ1 and collagen gene expression is performed on RNA extracted from lungs of mice in all groups. We used qPCR to demonstrate that miR-155^{-/-} and WT mice given bleomycin expressed a significantly higher mRNA level of TGFβ1 than their control group given PBS ($p < 0.001$ for each). An approximate 4-fold increase was demonstrated in WT mice given bleomycin and a 7-fold increase in miR-155^{-/-} mice (Figure 3.57). The increase in the miR-155^{-/-} compared with WT mice given bleomycin was significant ($p < 0.05$) (Figure 3.57).

The miR-155^{-/-} mice given bleomycin expressed a significantly higher mRNA level of collagen type IA and collagen type IIIA expression than WT mice given bleomycin, ($p < 0.05$ and $p < 0.05$) respectively (Figure 3.58).

The Col IA mRNA expression in the WT and miR155^{-/-} mice given bleomycin was significantly higher than in their PBS control groups ($p < 0.05$ and $p < 0.01$) respectively. Col IIIA mRNA expression followed the same pattern of Col IA, The expression was significantly higher in WT and miR155^{-/-} mice given bleomycin than PBS given groups, ($p < 0.001$) (Figure 3.58).

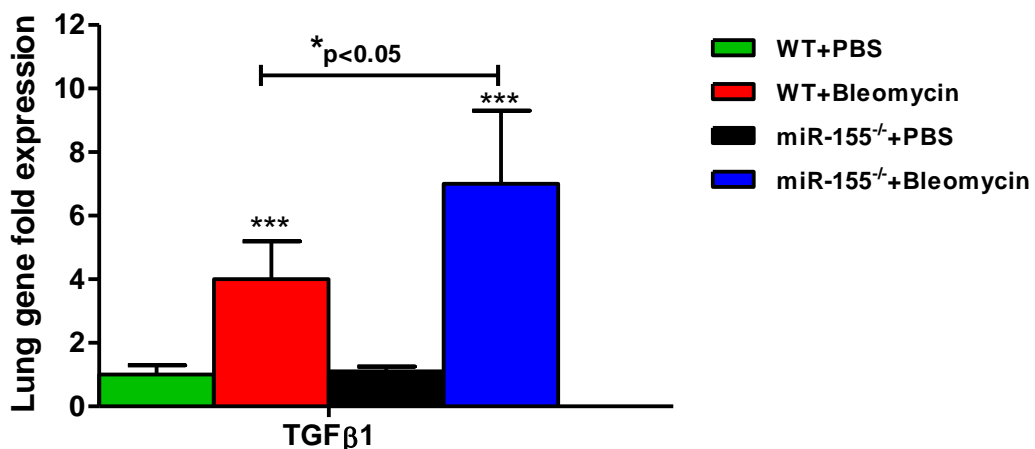


Figure 3.57 TGFβ1 gene expression in lungs of miR-155^{-/-} and WT mice given PBS or bleomycin

The measurement of TGFβ1 mRNA expression was calculated as fold-increase and showed a highly significant increase in miR155^{-/-} and WT mice given bleomycin in comparison with control PBS treated mice ($p < 0.001$ for each). There was a significant increase in the miR155^{-/-} compared with the WT littermates given bleomycin ($p < 0.05$). One Way ANOVA; * $p < 0.05$; *** $p < 0.001$; Mean \pm SEM; n = 7-14 mice/group.

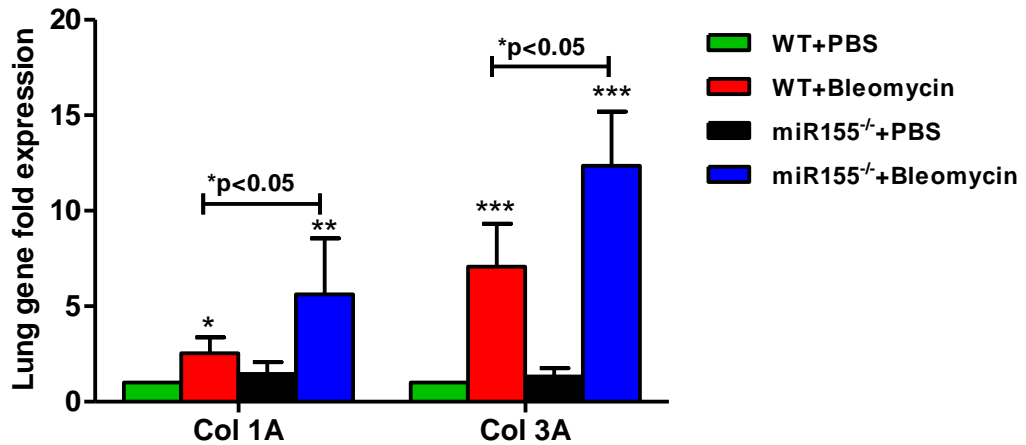


Figure 3.58 Collagen gene expression in lungs of miR-155^{-/-} and WT mice given PBS or bleomycin

Both collagen type IA and Col IIIA mRNA expression was measured as fold-increase compared with control PBS-treated mice. Both the miR-155^{-/-} and WT mice groups given bleomycin revealed a significant increase when compared with the groups given PBS. Expression levels were significantly higher in the lungs of miR-155^{-/-} mice given bleomycin than WT mice given bleomycin. No differences were observed in the PBS treated mice. One Way ANOVA; *p<0.05; **p<0.01; ***p<0.001; Mean ± SEM; n = 7-14 mice/group.

MiR-155^{-/-} mice given bleomycin had increased lung collagen compared with wild-type littermates

Lung tissue samples from the four experimental groups were used for measuring the content of soluble collagen by using a Sirius-red binding assay as described in Materials and Methods (section 2.5). The assay protocol is based on the binding of Sirius red to acid and pepsin-soluble collagen. This assay demonstrated a significant increase in lung collagen content in the bleomycin treated groups compared with the PBS groups (<0.001 for each) (Figure 3.59). There was a significantly higher collagen content in the miR-155^{-/-} mice than the WT given bleomycin, (p<0.01) (Figure 3.59).

The mean ± Standard error of the mean of values were:

WT mice given bleomycin	2.64 ± 0.25 mg/ml,
MiR-155 ^{-/-} mice given bleomycin	3.01 ± 0.33 mg/ml,
WT mice given PBS	2.04 ± 0.23 mg/ml,
MiR-155 ^{-/-} mice given PBS	2.18 ± 0.27 mg/ml (Figure 3.59).

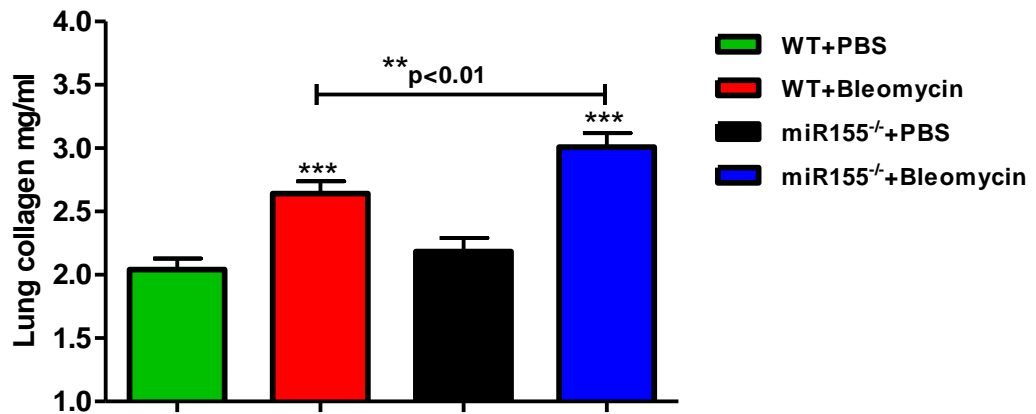


Figure 3.59 Soluble collagen content in lungs of miR-155^{-/-} and WT mice given PBS or bleomycin

Soluble collagen content level in the lungs of the WT and miR-155^{-/-} mice given bleomycin were significantly higher than PBS treated groups of mice. The miR-155^{-/-} mice had significantly higher collagen than the WT mice ($p < 0.01$); both given bleomycin. One Way ANOVA; ** $p < 0.01$; *** $p < 0.001$; Mean \pm SEM; n = 7-14 mice/group.

3.4.3 The macrophages in the miR-155^{-/-} mice had a different phenotype compared with the wild type littermates; both given bleomycin

Introduction and Aim:

The pathogenesis of the increased inflammation and remodelling in the miR155^{-/-} mice is unknown. Previous studies in lung fibrosis suggest an important role for lung macrophages. Therefore we investigated whether there was an effect of the deletion of miR-155 on the macrophage phenotype.

Method:

This was done by investigating the expression of the common phenotypic markers for the classically activated macrophages (inducible nitric oxide synthase (iNOS2) and comparing this with the alternatively-activated macrophages (chitinase-like lectin YM1, arginase type 2, IL-13 receptor). These changes were explored associated with the development of fibrosis in miR-155 WT and miR-155^{-/-} mice given bleomycin.

Studying the inflammatory and fibrotic processes comparing bleomycin or PBS treated mice; we studied the expression of macrophage phenotypic markers in RNA from lung tissue. We found a significantly upregulated expression of YM1, Arg 2, and IL-13R in miR-155^{-/-} mice given bleomycin compared with the PBS control, ($p < 0.01$, $p < 0.001$ and $p < 0.001$ respectively) (Figure 3.60). The WT mice given bleomycin demonstrated a significant up-regulated expression of YM1 and IL-13R compared with the PBS control, ($p < 0.05$ for each). Nitric oxide synthase 2

(NOS2) expression did not show any significant differences among all experimental groups (Figure 3.60).

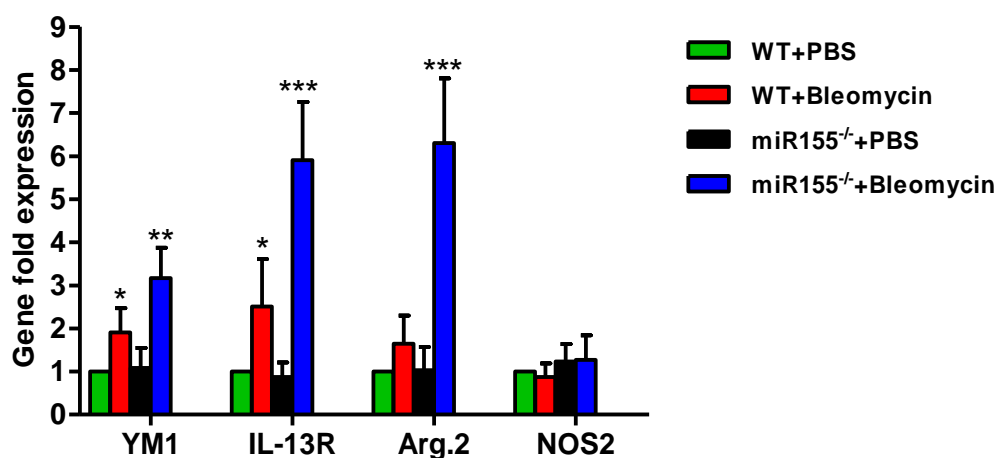


Figure 3.60 Expression levels of macrophage phenotype markers in the lungs of miR-155^{-/-} and WT mice given PBS or bleomycin
Expression levels of macrophage phenotype markers YM1, IL-13R, Arg 2 and NOS 2 in lungs of mice given bleomycin or PBS. YM1, Arg 2, and IL-13R were significantly upregulated in miR-155^{-/-} mice that given bleomycin compared with PBS treated groups. WT mice given bleomycin showed up-regulation in YM1 and IL-13R compared with PBS treated groups. No significant changes were found in NOS2 expression between all experimental groups. One Way ANOVA; *p<0.05; **p<0.01; ***p<0.001; Mean ± SEM; n = 7-14 mice/group.

3.4.4 Discussion and Conclusion

This second part of my thesis was to investigate and determine the possible mediators involved in the development of bleomycin-induced pulmonary fibrosis. The inspiration to study microRNA-155 came from several observations: The first report describing a miR gene deleted mouse was investigated using miR155 and part of this mouse phenotype was an age-related increase in airway sub-epithelial collagen deposition [104]. This observation was not further explained by the authors and to our knowledge this aspect has not been reported by others. The second observation was from our own pilot data from the Glasgow COPD and asthma dataset (Glasgow CAB study) that catalogued serum airway fluid and lung transcript biomarkers of disease. We found a decrease in BIC (miR155) expression in COPD that was significantly associated with carbon monoxide gas-transfer; indicating a possible involvement in restriction in gas exchange suggesting interstitial inflammation (unpublished data). The third factor was that we had the miR155^{-/-} mice available and we tested three models of lung disease; LPS-induced acute lung injury, antigen plus adjuvant- induced allergic airway inflammation, and bleomycin-induced lung fibrosis. Our pilot results showed that there was no clear phenotype in asthma or LPS-induced acute lung injury models but that the bleomycin lung fibrosis model was greatly exacerbated.

MiRNAs can act as regulators of mRNA translation. They exhibit this ability by coordinated regulation of multiple RNA targets often within the same molecular effector pathways. Using miR-155^{-/-} mice we determine a marked exacerbation in the development of pulmonary fibrosis, and these results provide new evidence of a possible involvement of a miR155 regulated pathway in the development of fibrosis. If we can identify these pathways we may reveal a new therapeutic approach for treating pulmonary fibrosis.

Administration of bleomycin to miR-155^{-/-} compared with WT mice showed significant exacerbation in the pulmonary fibrosis. This was reflected by significant inflammatory changes including reduction in body weight, and major pathomorphological changes in the lung. Pottier and colleagues, reported that administration of bleomycin to either sensitive C57BL/6 resulted in significant up-regulation in the lung miR-155 expression on comparison with bleomycin- resistant BALB/c mice or PBS treated mice [226]. Also miR-155^{-/-} mice had an age-related phenotype revealed as increased lung airway remodelling similar to lung fibrosis [104]. Our results showed that administration of bleomycin to miR-155^{-/-} mice had a significant detrimental effect on the body weight of these mice. This can be interpreted as being caused by cachexia related to an excessive systemic inflammatory process in these mice.

Further investigation of the lung of these mice demonstrated a severe histopathological changes occurring in the miR-155^{-/-} mice given bleomycin (Figure 3.51). Scoring of the lung sections revealed highly significant inflammatory and fibrotic change in the miR-155^{-/-} mice given bleomycin compared with wild type

mice given bleomycin or either mice types given PBS (Figure 3.52 and 3.53). Our results confirmed and extended the results of Rodriguez and colleagues, who showed that mice deficient for *bic/miR-155* were characterised by increased lung airway pathomorphological changes; with abnormal peribronchial collagen deposition, accompanied by augmentation of the subbronchiolar myofibroblasts. They suggested that the miR-155 deletion could result in a phenotype that is susceptible to fibrosis [104]. Our results were in contrast to those observation of Kurowska-Stolarska and colleagues, who showed that miR-155^{-/-} mice did not respond to administration of the antigen type II chicken collagen in a CIA model and there was no effect on articular inflammation and degradation of cartilage and bone which had seen in WT mice [99]. There was no excessive repair/fibrosis response in this model in miR-155^{-/-} mice because of the differences between animal models while CIA is resembling an autoimmune disease the bleomycin-induced lung fibrosis is resembling a wound healing disease.

miRNA-155 has an important role in regulation of the immune system, such as production of T cell–dependent antibody production by plasma cells, T helper cell differentiation and cytokine production [97]. Our results demonstrated an additional function role for miR155 in tissue inflammation and remodelling. We demonstrated a highly significant increase in the inflammatory cell numbers in the bronchoalveolar lavage of miR-155^{-/-} mice given bleomycin. These results were in agreement with Rodriguez and colleges, who revealed significant increase in the number of BAL leukocytes that accompanied the airway remodelling changes in aged *bic*-deficient mice [104]. The increased number of BAL macrophages and lymphocytes in the present study indicated an active inflammatory process; these cells can potentially participate in the initiation and maintenance of the inflammation through different pathways such as cytokine and chemokine production. The evidence for this was the significantly higher concentration of TGFβ1 and FGF basic in the serum and BAL of miR-155^{-/-} mice given bleomycin compared with WT mice or mice given control PBS instead of bleomycin.

The increased serum and BAL TGFβ was associated with a highly significant up-regulation of TGFβ1 gene expression in the lungs of the same miR-155^{-/-} mice given bleomycin compared with the other experimental group groups (Figure 3.57). The role of TGFβ in the process of fibrosis hasd been reported in different tissues such as lung, skin and joints. TGFβ1 receptor activation resulted in a strong downstream signalling pathway which maintains the fibro-proliferative process during the course of the disease [227]. The high TGFβ expression and concentration in miR-155^{-/-} mice given bleomycin in our study may be because the independent TGFβ production mechanism does not require direct regulation by miR-155, in more details; absence of miR-155 does not stop processes regulated by TGFβ. This is in disagreement with Kong and colleague who found that TGFβ can induce miR-155 expression and mediated through Smad4. Also knockdown of miR-155 in epithelial cells resulted in a suppression in the TGFβ-induced cell transition, migration and invasion [110]. Knockdown of miR-155 in their cells did

not stop cell migration and invasion induced by TGF β , this showed one of mediate mechanism of TGF β signalling through miR-155.

Our results demonstrated an enhanced fibrotic response in miR-155^{-/-} mice given bleomycin compared with WT mice as determined by the increased total lung collagen content (Figure 3.59) and increased deposition of collagen seen in the lung tissue histology (Figure 3.51). Fibroblast and myofibroblast are abundant in the fibrotic area and act as a major source of collagen production. Our results appear to be in agreement with the work of Sato and colleagues who studied the role of miR-155 in cell differentiation [228]. Their analysis of microarray result showed that the fibroblast-like cells treated with IL-4 induced cells with a more fibrogenic phenotype because of the reduction in the miR-155 expression.

A potential mechanism of miR-155 involvement in inflammation and apoptosis was suggested in one study that demonstrated an up-regulation of miR-155 expression by pro-inflammatory stimuli such as Toll-like receptor agonists in macrophages [101]. Koch and colleagues propose that miR-155 has antiapoptotic activity which increases macrophage resistance to apoptosis induced by DNA damage during bacterial infection [229], and the same mechanism may apply to bleomycin injury which is thought to be partly related to its ability to induce DNA damage.

Further analysis of my results determined a significantly increased expression of M2 macrophage phenotype markers YM1, IL-13R, and Arg 2 and reduction of M1 macrophage phenotype markers NOS 2 in lung tissues. Macrophages have an important involvement in the initiation and maintenance of inflammation and fibrosis. Human alveolar macrophages from idiopathic pulmonary fibrosis patients can be characterised by their ability to express different mediators involved in the fibrotic process such as IL-10, IL-13, and PDGF [157]. The up-regulation of Arg 2 expression observed in the lungs of miR-155^{-/-} mice given bleomycin were in agreement with Arranz and colleagues using Akt^{-/-} macrophages [230]. Akt is a family of three serine / threonine protein kinases that participate in cell survival, proliferation and differentiation. Arranz demonstrated that down-regulation of miR-155 in Akt2^{-/-} macrophages lead to up-regulation of C/EBP β , which is a target for mir-155 resulting in M2 macrophage polarization and the production of Arg1; which was restored by transfection of miR-155 into Akt2^{-/-} macrophages.

Conclusion

MiR-155 had been shown to have a potent involvement in the development of fibrosis in an experimental murine model. This suggests that miR-155 or the gene-products that miR-155 may regulate could be involved directly in pulmonary fibrosis and they may be potential target candidates for therapeutic strategies.

3.5 General discussion and conclusion

Recapitulation: The principal aim of this study was to investigate the potential regulatory role of the nuclear transcription factor LXR in pulmonary fibrosis. My initial approach was to search the literature for evidence of the possible involvement of LXR and found that it could function in murine models as either a positive immune-regulator such as in atherosclerosis or as a negative immune-regulator such as in collagen-induced arthritis. There was one unsubstantiated manuscript that suggested genes associated with the LXR pathway were significantly and specifically altered in IPF patients [207]. Therefore the role of LXR in remodelling is unresolved, but has research potential in IPF because the treatment options for this disease are limited. My working hypothesis for the study, therefore, was that LXR agonists have a beneficial effect on pulmonary fibrosis because of the established reputation of LXR as a functional anti-inflammatory regulator in atherosclerosis.

I designed experiments to demonstrate the effect of activation of LXR on the inflammatory and fibrotic process using a murine model of bleomycin-induced pulmonary fibrosis in order to identify potential mechanisms. I observed a pro-inflammatory and pro-fibrotic effect of LXR agonism; confirmed by significant exacerbation of the inflammatory and fibrotic processes in the lungs of mice treated with bleomycin that were given LXR agonist. This was reflected by an increased loss of body weight, increased proportions of BAL inflammatory cells and the identification of alternatively-activated macrophages, along with increased concentrations of pro-inflammatory and pro-fibrotic mediators that together suggested some potential pathways that might offer suggestion for therapeutic intervention. In summary, this study suggested a novel pro-inflammatory and pro-fibrotic role of LXRs activation that may affect the pathogenicity and progression of pulmonary fibrosis.

LXR is primarily considered as a regulator of lipid metabolism and therefore has only been studied in models of inflammatory diseases and has been studied in fewer chronic fibrotic conditions. My results show that LXR activation by GW3965 exacerbate the inflammatory and fibrotic process of bleomycin-induced lung fibrosis. This activity appears to be in contrast to reports which suggest an anti-inflammatory effect of LXR activation in atherosclerosis [58, 59, 69]. However, it is possible that the anti-inflammatory and repair processes are part of the same process of remodelling, and my results are consistent with a recent study which used a murine model of collagen-induced arthritis and demonstrated that activation of LXR with T1317 and GW3965 agonists resulted in exacerbation of the inflammatory response, with excessive cartilage destruction and remodelling [74].

Many studies have used the murine model of bleomycin-induced pulmonary fibrosis to study the inflammatory and fibrotic processes [182, 192, 200, 201]. In my study additional LXR agonism exacerbated the inflammation and fibrosis as shown by an additional loss of body weight, and higher concentrations of lung and serum pro-inflammatory and pro-fibrotic mediators.

Another important question was the requirement of bleomycin to see the effect of LXR agonist in WT mice treated with LXR agonist and why the effect did not appear in the control mice given PBS and treated with LXR agonist. A pro-inflammatory environment is the key characteristic of the pathogenesis of the different reactions to bleomycin. Human and animal studies had shown predominant pro-inflammatory cytokines in response to bleomycin administration into the lung [231, 232]. Challenging human and murine cells with bleomycin lead to the activation of transcription factors nuclear factor-kappa B (NF- κ B), activating transcription factor-2, and activator protein-1 [233, 234], and secretion of pro-inflammatory cytokines such as TNF- α , IL-1- β , MCP-1, and TGF- β [231, 235, 236]. Studies on THP-1 cells or macrophage-derived foam cells treated with TGF- β 1 revealed an up-regulation in LXR alpha mRNA expression and increased LXR α protein levels. These effects were confirmed by treating the cells with siRNA for LXR α which lead to down-regulation of LXR α protein expression by 84% [237]. A recent study showed cross-talk between TGF β and LXR signalling pathways and stimulation of cells with TGF β and LXR agonists had a synergistic effect increasing the expression of the LXR target gene ABCG1 [238]. Here, it is possible that the pro-inflammatory environment generated by administration of bleomycin was manifest by high TGF β level, which then lead to up-regulation of the expression of LXR α mRNA and protein. Higher level of LXR in WT mice given bleomycin and the presence of the highly potent LXR agonist will potentiate the LXR pathway resulting in exacerbation of the pulmonary fibrosis. This pro-inflammatory environment is not found in WT mice given PBS.

The role of LXR in inflammation can be demonstrated by its ability to regulate the expression of genes for certain pro-inflammatory mediators such as TNF α , IL-1, IL-6, cyclooxygenase (COX-2) and inducible nitric oxide synthase [68, 69]. Although not prominent, idiopathic pulmonary fibrosis (IPF) is characterised by an inflammatory response dominated by a lung infiltrate of macrophages with a phenotypic shift towards an alternatively activated (M2) macrophage phenotype that is associated with tissue remodelling and wound healing [156]. Consistent with this, my results showed that LXR agonism can modulate the macrophage phenotype by up-regulation the mRNA of genes associated with alternatively-activated macrophages (chitinase-like lectin YM-1, arginase type 2, and the IL-13 receptor) accompanied by down-regulation of inducible nitric oxide synthase 2 which is a biomarker of the classically-activated macrophages M1 phenotype in the lung tissue of bleomycin-treated mice. These data provide potential evidence for a direct effect of LXR agonism on macrophages exacerbating the bleomycin-induced pulmonary fibrosis.

Macrophages are considered to be the animportant source of the fibrogenic cytokines TGF β and IL-13. It had been shown that IL-13 was able to selectively stimulate TGF β 1 production in transgenic mice [214]. Activation of LXR in a macrophage cell line and in primary murine macrophages lead to up-regulation of anti-inflammatory gene expression including arginase 2, which was accompanied by down-regulation of the pro-inflammatory genes such as inducible nitric oxide

synthase (iNOS) and the suggested mechanism was by antagonism of NF-kappa B activity [197]. Together these observations plus the work presented in this thesis support that LXR agonism can drive the alveolar or lung macrophage phenotype towards an M2-type involved in remodelling.

In addition to the increased numbers of pro-fibrotic effect of M2 macrophages, the disease process was associated with an increased infiltrate of lymphocytes and neutrophils in the BAL and pathomorphological changes in the lung tissue sections. The over-riding increase in the number of macrophages could mask the recognition and contribution of these cells; therefore, further studies are required to illustrate how the LXR agonism may impact on each of these inflammatory cell types to identify their involvement in the development and maintenance of pulmonary fibrosis in murine models and in IPF patients.

The role of LXR in pulmonary fibrosis first attracted my attention because in preliminary studies we demonstrated that genes indicating activation of LXR were strongly expressed in blood monocytes of arthritis patients. We subsequently demonstrated in a murine model of collagen-induced arthritis that activation of LXR with T1317 and GW3965 agonists resulted in exacerbation of the inflammatory response, with excessive cartilage destruction and joint remodelling [74]. In addition, approximately 50% of rheumatoid arthritis patients will develop respiratory disease during their lifetime [239]. It is possible therefore that there is a common abnormality of inappropriate tissue repair. This suggests the involvement of fibroblasts. A number of studies have demonstrated that rheumatoid arthritis synovial fibroblasts (RASFs) show alterations in morphology and behaviour, including molecular changes in signalling cascades, apoptosis response and in the expression of adhesion molecules as well as matrix-degrading enzymes. They produce a wide range of cytokines, chemokines and matrix-degrading enzymes that mediate the interaction with neighbouring inflammatory and endothelial cells and are responsible for the progressive destruction of articular cartilage and bone. In this scenario, the production of cytokines and chemokines within the rheumatoid synovium would help to recruit T cells, macrophages and neutrophils, which, in turn, attract more inflammatory cells and, ultimately, enhance the activated state of the RASFs and of osteoclasts [240].

LXR are important in modulating fibroblast function. Fibrocytes are precursor fibroblasts that are characterised by their ability to produce proteins and glycoproteins such as collagen types I and III, vimentin and MMPs which participate in tissue remodelling and they also produce a wide range of cytokines. There are increased numbers of circulating fibrocytes in the peripheral blood of bleomycin-treated mice [146], and fibrocytes isolated from the wounds of animal models of wound-repair expressed mRNA for cytokines including IL-1 β , IL-10, TNF- α , MCP, MIP-1 α , MIP-1 β , MIP-2, PDGF-A, TGF- β 1, and Macrophage colony stimulating factor (M-CSF) [147]. It was important therefore to explore whether there were functional LXR in fibroblasts and whether activating these receptors initiated a fibrotic response for example increased production of collagen. These experiments are conveniently done using primary human and mouse fibroblast

lines *in vitro* or *in vivo* using genetically modified mice gene-deleted for LXR α and β (LXR $\alpha^{-/-}\beta^{-/-}$) and LXR $\alpha\beta$ sufficient wild-type littermates. These can be used to investigate the effects on the expression of collagen type I and collagen type III gene in response to LXR agonists. It has been reported that collagen production after bleomycin administration is partially due to activation of interstitial fibroblasts with predominant up-regulation of collagen type III gene expression [215]. I demonstrated that the collagen gene expression was directly associated with LXR activation by using primary fibroblast from the lungs of LXR $\alpha^{-/-}\beta^{-/-}$ and LXR $\alpha\beta$ wild-type mice. I was able to confirm that LXR agonism directly stimulated collagen gene expression by using a control step by the addition of cycloheximide, which is an inhibitor of translation, which blocked this effect.

I have shown that the up-regulation of collagen gene expression was mediated by the LXR agonist directly targeting the fibroblast LXRs. Using highly specific synthetic LXR agonist have been proven a potent systemic activation for LXR stimulation in comparison with the physiological ligands which show a divers in their ability depending on the location and their type [31]. Presence of more than one physiological ligand in the body and presence of different concentration across body tissues may affect the degree of activation of LXRs. Therefore, in our study we used a high potent synthetic LXR agonist (GW3965) which shown high-affinity binding and activation. Further studies required to determine the different types of physiological endogenous ligand which may be involve in the pro-inflammatory and pro-fibrotic process. This may include identification and classification of different type of cholesterol and oxysterols which may have the ability to activation of LXRs, also identification the concentration in different tissues such as in blood, serum or organs such as lung of the IPF patients. This will facilitate the understanding of the all possible endogenous factors that may involve in the exacerbation in the inflammation and fibrosis.

Having demonstrated that GW3965 had a direct on human and mouse primary fibroblast, my next aim was to determine if the Col IA and Col IIIA genes have response elements for LXR in their promoter regions. This was carried out by performing a luciferase reporter assay which demonstrated that activation of LXR directly promotes collagen types 1 and 3 in mouse fibroblast cell line T1317. A study had been conducted on mesangial cells treated with the LXR agonist showed that activation of LXR α with TO901317 synthetic agonist resulted in an a significantly increases production of collagen IV. To confirm this effect cells were transfected with siRNAs of LXR α and cultured with TO901317, a reduction in the level of LXR α protein to 70% and mRNA of LXR α to 76% had been demonstrated. The expressions of collagen IV were decreased in protein level to 28% and mRNA level to 80% [241]. My collagen promoter data came in parallel to the above mentioned study and we determined that both Col IA and Col IIIA genes have response elements for LXR in their promoter regions.

My *in vivo* results have demonstrated an increased production of pro-inflammatory and pro-fibrotic cytokines such as TGF β , TNF α , IL-13 and FGF basic in response

to bleomycin along with LXR-agonists. This can also increase collagen production. It had been reported that TGF β is able to bind the human collagen type 1A2 promoter and activate Smad signalling in human skin fibroblasts [242]. It is now accepted that pathology associated with metabolic disease and chronic inflammatory diseases may cooperate to promote a state of generally enhanced inflammation. As well as understanding a role of LXRs in inflammation this study was also initiated in an attempt to understand how altered lipid metabolism may drive pulmonary fibrosis pathology. I hypothesise that cholesterol degradation within the periphery to form oxysterols could drive the development of pulmonary fibrosis pathology by activation of LXRs. Indeed, my results which suggest a pro-inflammatory and pro-fibrotic effect of LXR activation support this hypothesis. However, although my studies, as with other reports in the literature using GW3965 or T1317, are informative of LXR activation they may not faithfully represent the action of specific endogenous oxysterol species upon the activation of LXRs. Synthetic LXR agonists induce activation of LXRs systemically whereas endogenous agonists are restricted to particular anatomical locations and indeed different oxysterols are recognised to differentially activate or inhibit LXRs [31].

Another important part of my work was to understand the specific involvement of each of the LXR α and LXR β isoforms in pulmonary fibrosis. Their different function was investigated in lipid metabolic disease models such as atherosclerosis but not yet in fibrotic diseases. A murine model of atherosclerosis using ApoE^{-/-} mice demonstrated that the absence of LXR α was strongly associated with severe atherosclerosis; characterised by the accumulation of cholesterol in peripheral tissues and in the aortic root; and this effect could not be compensated by an intact LXR β [220]. However, the highly potent LXR agonist GW3965 was able to activate LXR β resulting in attenuation of the atherosclerosis, suggesting that the different strengths of the ligand binding might modulate function. In my bleomycin induced lung fibrosis model, neither LXR α nor LXR β could compensate for the absence of each other, even using the highly specific LXR agonist GW3965. The reasons for this are unclear but may be because LXR α or LXR β work in a cooperative pathway.. Understanding the individual roles of LXR α and LXR β is important to understanding how lipid metabolism may impact upon inflammation and fibrosis and for the design of future therapeutics; For example it is recognised that agonists designed specifically towards the activation of LXR β are more favourable than dual LXR α /LXR β agonists for the treatment of atherosclerosis [220, 243]. Furthermore, deletion of LXR α or LXR β is protective against the pro-inflammatory and pro-fibrotic effects mediated by administration of GW3965 in a murine bleomycin-induced pulmonary fibrosis and suggests that cooperation between the LXR isoforms is necessary to drive the inflammation and fibrosis. The separate role of LXR α and LXR β in inflammation and fibrosis still unknown. Interestingly these observations have considerable implications for the development of LXR agonists as future therapy in which LXR agonists are already been in use in pre-clinical trials for the treatment of atherosclerosis [244, 245]. To validate our findings, further studies are required to test for the individual effects of each receptor in other fibrotic models.

A related research topic was to explore the possible involvement of microRNA-155 as a regulator for mRNA translation in lung fibrosis. The miR-155 gene-deleted

mouse was one of the first models of induced microRNA deficiency. The mice developed immune deficiency primarily of B-cell and innate immunity, however, with aging the mice developed mild lung fibrosis. It had been shown in our lab that miR-155 is upregulated in rheumatoid arthritis synovial macrophages associated with the development of autoimmunity and joint inflammation [99]. It is possible that preclinical arthritis may be associated with lung changes such as bronchial wall thickening. This was an important consideration for the clinical relevance of my findings because clinical targeting of the LXRs may be of benefit but may also be a risk because the receptors are ubiquitous and because these receptors are likely involved in more than one physiological function, therefore, targeting of the outcome of the LXRs agonism at post-transcriptional level may be an ideal option and this may be performed through miR-155.

To better understand the contribution of the miR-155 in the regulation pathway of pulmonary fibrosis, a bleomycin pulmonary fibrosis model was established using miR-155^{-/-} and miR-155 wild type mice. This demonstrated that the absence of miR-155 led to exacerbation in the pulmonary fibrosis associated with bleomycin administration. The mechanism of this is unknown. Therefore, we studied the lung cytology and histology. This bleomycin model demonstrated a shift toward alternative activation of lung lavage macrophages. There is supporting literature showing that transfection of lung fibroblasts with a synthetic miR-155 resulted in modulating of translation of genes involved with cell movement, cell death and cell-to-cell signalling. The authors concluded that transfection of fibroblasts with miR-155 could promote apoptosis and reduce cell migration [226]. This might explain why fibrosis is more evident in miR-155^{-/-} mice; the greater migratory ability with decreased apoptosis, along with excessive production of pro-inflammatory and pro-fibrotic cytokines especially TGF β can drive the fibroblast to produce excessive collagen in the lung of these mice when given bleomycin. These results are in agreement with work on mice deficient for bic/miR-155, that showed lung airway pathomorphological changes; an increased peribronchial collagen deposition and large number of sub-bronchiolar myofibroblasts [104]. Further work needs to be done to determine whether the complete absence or low level of the miR-155 in fibroblast may lead to the similar results.

TGF β plays an important role in wound healing. It directly targets fibroblasts and stimulates collagen production. Previous work demonstrated a positive inter-relationship between miR-155 and TGF β in that TGF β was able to induce miR-155 expression through Smad4, and knockdown of miR-155 in epithelial cells resulted in the suppression of TGF β -induced cell migration invasion [110]. It is likely that the high production of TGF β in miR-155^{-/-} mice is because of the independent TGF β production mechanism which does not require direct regulation by miR-155. Further experiments are required to identify the tentative relationship between miR-155 and TGF β , this may include *in vitro* work at a transcriptional level in the presence or absence of each component.

The work on this thesis prompted some pilot experiments to investigate whether there was a direct relationship between LXR and miR-155. Using luciferase assays we demonstrated that LXR alpha mRNA is a direct target of miR-155. Moreover, a highly significant up-regulation of the expression of LXR alpha was demonstrated in the lungs of miR-155^{-/-} mice that were further increased in mice given bleomycin. In parallel experiments we demonstrated that administration of LXR agonist to WT mice lead to an increase in the LXR expression. Thus there is an important LXR-miR-155 axis that appears to modulate fibrosis. This is a novel concept that will direct new thinking into disease pathogenesis of IPF and perhaps improved therapeutic options for this devastating disease.

Conclusion

My results demonstrate that both LXR and miR-155 have an important impact on murine bleomycin-induced pulmonary fibrosis. MiR-155 may have an important role in lung homeostasis, possibly by fine tuning levels of LXR α resulting in a prevention of excessive remodelling. This may be envisaged as the possibility that miR-155 may act as a master switch determining the degree and duration of inflammation and the initiation of remodelling.

My results showed that administration of exogenous synthetic LXR agonist GW3965 induced activation of LXRs systemically. Whereas in the body there are different endogenous agonists, it is possible that these endogenous physiological LXR ligands which are restricted to particular anatomical locations with different ability to recognise and activate or inhibit LXRs, therefore, further studies are required to determine how specific oxysterols exert their pro-inflammatory effects. Determining which species of oxysterols are present in the serum and BAL of IPF patients and if concentrations of these are altered relative to healthy controls is also important for understanding whether LXRs have a pathological role in IPF.

Further work is required to determine the nature and diversity in the pro or anti-inflammatory and pro or anti-fibrotic responses of the LXR in different disease models since the LXR activation shows diverse effects across a wide range of disease models. Studies are needed to investigate the control of the inflammatory and fibrotic responses at the level of LXR activation because targeting the LXR *in vivo* is of potential risk because of the involvement of these receptors in many physiological processes.

Finally, improved understanding of LXR in this context, perhaps with improved understanding of the role of miR155 may therefore be of considerable clinical importance.

VIII References

1. Francis, G.A., et al., *Nuclear receptors and the control of metabolism*. Annu Rev Physiol, 2003. **65**: p. 261-311.
2. Lopez-Velazquez, J.A., et al., *Nuclear receptors in nonalcoholic Fatty liver disease*. J Lipids, 2012. **2012**: p. 139875.
3. Zhang, Z., et al., *Genomic analysis of the nuclear receptor family: new insights into structure, regulation, and evolution from the rat genome*. Genome Res, 2004. **14**(4): p. 580-90.
4. Szanto, A., et al., *Retinoid X receptors: X-ploring their (patho)physiological functions*. Cell Death Differ, 2004. **11 Suppl 2**: p. S126-43.
5. Novac, N. and T. Heinzl, *Nuclear receptors: overview and classification*. Curr Drug Targets Inflamm Allergy, 2004. **3**(4): p. 335-46.
6. Horie-Inoue, K., et al., *Identification of novel steroid target genes through the combination of bioinformatics and functional analysis of hormone response elements*. Biochem Biophys Res Commun, 2006. **339**(1): p. 99-106.
7. Nuclear Receptors Nomenclature, C., *A unified nomenclature system for the nuclear receptor superfamily*. Cell, 1999. **97**(2): p. 161-3.
8. Sonoda, J., L. Pei, and R.M. Evans, *Nuclear receptors: decoding metabolic disease*. FEBS Lett, 2008. **582**(1): p. 2-9.
9. Germain, P., et al., *Overview of nomenclature of nuclear receptors*. Pharmacol Rev, 2006. **58**(4): p. 685-704.
10. Mangelsdorf, D.J., et al., *The nuclear receptor superfamily: the second decade*. Cell, 1995. **83**(6): p. 835-9.
11. Moore, J.T., J.L. Collins, and K.H. Pearce, *The nuclear receptor superfamily and drug discovery*. ChemMedChem, 2006. **1**(5): p. 504-23.
12. Warnmark, A., et al., *Activation functions 1 and 2 of nuclear receptors: molecular strategies for transcriptional activation*. Mol Endocrinol, 2003. **17**(10): p. 1901-9.
13. Apfel, R., et al., *A novel orphan receptor specific for a subset of thyroid hormone-responsive elements and its interaction with the retinoid/thyroid hormone receptor subfamily*. Mol Cell Biol, 1994. **14**(10): p. 7025-35.
14. Baranowski, M., *Biological role of liver X receptors*. J Physiol Pharmacol, 2008. **59 Suppl 7**: p. 31-55.
15. Ulven, S.M., et al., *LXR is crucial in lipid metabolism*. Prostaglandins Leukot Essent Fatty Acids, 2005. **73**(1): p. 59-63.
16. Wojcicka, G., et al., *Liver X receptors (LXRs). Part I: structure, function, regulation of activity, and role in lipid metabolism*. Postepy Hig Med Dosw (Online), 2007. **61**: p. 736-59.
17. Willy, P.J., et al., *LXR, a nuclear receptor that defines a distinct retinoid response pathway*. Genes Dev, 1995. **9**(9): p. 1033-45.
18. Hong, C., et al., *Constitutive activation of LXR in macrophages regulates metabolic and inflammatory gene expression: identification of ARL7 as a direct target*. J Lipid Res, 2011. **52**(3): p. 531-9.
19. Geyeregger, R., et al., *Liver X receptors regulate dendritic cell phenotype and function through blocked induction of the actin-bundling protein fascin*. Blood, 2007. **109**(10): p. 4288-95.
20. Walcher, D., et al., *LXR activation reduces proinflammatory cytokine expression in human CD4-positive lymphocytes*. Arterioscler Thromb Vasc Biol, 2006. **26**(5): p. 1022-8.

21. Song, C., et al., *Ubiquitous receptor: a receptor that modulates gene activation by retinoic acid and thyroid hormone receptors*. Proc Natl Acad Sci U S A, 1994. **91**(23): p. 10809-13.
22. Repa, J.J. and D.J. Mangelsdorf, *The role of orphan nuclear receptors in the regulation of cholesterol homeostasis*. Annu Rev Cell Dev Biol, 2000. **16**: p. 459-81.
23. Janowski, B.A., et al., *An oxysterol signalling pathway mediated by the nuclear receptor LXR alpha*. Nature, 1996. **383**(6602): p. 728-31.
24. Jusakul, A., et al., *Mechanisms of oxysterol-induced carcinogenesis*. Lipids Health Dis, 2011. **10**: p. 44.
25. Gupta, S., W.M. Pandak, and P.B. Hylemon, *LXR alpha is the dominant regulator of CYP7A1 transcription*. Biochem Biophys Res Commun, 2002. **293**(1): p. 338-43.
26. Repa, J.J., J.M. Dietschy, and S.D. Turley, *Inhibition of cholesterol absorption by SCH 58053 in the mouse is not mediated via changes in the expression of mRNA for ABCA1, ABCG5, or ABCG8 in the enterocyte*. J Lipid Res, 2002. **43**(11): p. 1864-74.
27. Fontaine, C., et al., *Liver X receptor activation potentiates the lipopolysaccharide response in human macrophages*. Circ Res, 2007. **101**(1): p. 40-9.
28. Torra, I.P., et al., *Phosphorylation of liver X receptor alpha selectively regulates target gene expression in macrophages*. Mol Cell Biol, 2008. **28**(8): p. 2626-36.
29. Oram, J.F. and R.M. Lawn, *ABCA1. The gatekeeper for eliminating excess tissue cholesterol*. J Lipid Res, 2001. **42**(8): p. 1173-9.
30. Zarubica, A., D. Trompier, and G. Chimini, *ABCA1, from pathology to membrane function*. Pflugers Arch, 2007. **453**(5): p. 569-79.
31. Janowski, B.A., et al., *Structural requirements of ligands for the oxysterol liver X receptors LXRA and LXRbeta*. Proc Natl Acad Sci U S A, 1999. **96**(1): p. 266-71.
32. Song, C., R.A. Hiipakka, and S. Liao, *Selective activation of liver X receptor alpha by 6alpha-hydroxy bile acids and analogs*. Steroids, 2000. **65**(8): p. 423-7.
33. Zierler, K., *Whole body glucose metabolism*. Am J Physiol, 1999. **276**(3 Pt 1): p. E409-26.
34. Mitro, N., et al., *The nuclear receptor LXR is a glucose sensor*. Nature, 2007. **445**(7124): p. 219-23.
35. Motoshima, K., et al., *Separation of alpha-glucosidase-inhibitory and liver X receptor-antagonistic activities of phenethylphenyl phthalimide analogs and generation of LXRA-selective antagonists*. Bioorg Med Chem, 2009. **17**(14): p. 5001-14.
36. Molteni, V., et al., *N-Acylthiadiazolines, a new class of liver X receptor agonists with selectivity for LXRbeta*. J Med Chem, 2007. **50**(17): p. 4255-9.
37. Plat, J., J.A. Nichols, and R.P. Mensink, *Plant sterols and stanols: effects on mixed micellar composition and LXR (target gene) activation*. J Lipid Res, 2005. **46**(11): p. 2468-76.
38. Lee, S., et al., *Activating signal cointegrator-2 is an essential adaptor to recruit histone H3 lysine 4 methyltransferases MLL3 and MLL4 to the liver X receptors*. Mol Endocrinol, 2008. **22**(6): p. 1312-9.
39. Stenson, B.M., et al., *Activation of liver X receptor regulates substrate oxidation in white adipocytes*. Endocrinology, 2009. **150**(9): p. 4104-13.

40. Repa, J.J., et al., *Regulation of absorption and ABC1-mediated efflux of cholesterol by RXR heterodimers*. Science, 2000. **289**(5484): p. 1524-9.
41. Collins, J.L., et al., *Identification of a nonsteroidal liver X receptor agonist through parallel array synthesis of tertiary amines*. J Med Chem, 2002. **45**(10): p. 1963-6.
42. Reschly, E.J., et al., *Ligand specificity and evolution of liver X receptors*. J Steroid Biochem Mol Biol, 2008. **110**(1-2): p. 83-94.
43. Chinetti, G., et al., *PPAR-alpha and PPAR-gamma activators induce cholesterol removal from human macrophage foam cells through stimulation of the ABCA1 pathway*. Nat Med, 2001. **7**(1): p. 53-8.
44. Tobin, K.A., et al., *Cross-talk between fatty acid and cholesterol metabolism mediated by liver X receptor-alpha*. Mol Endocrinol, 2000. **14**(5): p. 741-52.
45. Prufer, K. and J. Boudreaux, *Nuclear localization of liver X receptor alpha and beta is differentially regulated*. J Cell Biochem, 2007. **100**(1): p. 69-85.
46. Alberti, S., K.R. Steffensen, and J.A. Gustafsson, *Structural characterisation of the mouse nuclear oxysterol receptor genes LXRAalpha and LXRBeta*. Gene, 2000. **243**(1-2): p. 93-103.
47. Hashimoto, K., et al., *Liver X receptor-alpha gene expression is positively regulated by thyroid hormone*. Endocrinology, 2007. **148**(10): p. 4667-75.
48. Lundholm, L., et al., *Gene expression profiling identifies liver X receptor alpha as an estrogen-regulated gene in mouse adipose tissue*. J Mol Endocrinol, 2004. **32**(3): p. 879-92.
49. Laffitte, B.A., et al., *Autoregulation of the human liver X receptor alpha promoter*. Mol Cell Biol, 2001. **21**(22): p. 7558-68.
50. Kohro, T., et al., *Genomic structure and mapping of human orphan receptor LXR alpha: upregulation of LXRA mRNA during monocyte to macrophage differentiation*. J Atheroscler Thromb, 2000. **7**(3): p. 145-51.
51. Li, Y., et al., *Induction of human liver X receptor alpha gene expression via an autoregulatory loop mechanism*. Mol Endocrinol, 2002. **16**(3): p. 506-14.
52. Zelcer, N. and P. Tontonoz, *Liver X receptors as integrators of metabolic and inflammatory signaling*. J Clin Invest, 2006. **116**(3): p. 607-14.
53. Juvet, L.K., et al., *On the role of liver X receptors in lipid accumulation in adipocytes*. Mol Endocrinol, 2003. **17**(2): p. 172-82.
54. Seo, J.B., et al., *Activated liver X receptors stimulate adipocyte differentiation through induction of peroxisome proliferator-activated receptor gamma expression*. Mol Cell Biol, 2004. **24**(8): p. 3430-44.
55. Hotamisligil, G.S., *Inflammation and metabolic disorders*. Nature, 2006. **444**(7121): p. 860-7.
56. Marathe, C., et al., *Preserved glucose tolerance in high-fat-fed C57BL/6 mice transplanted with PPARgamma^{-/-}, PPARdelta^{-/-}, PPARgammadelta^{-/-}, or LXRAalphabeta^{-/-} bone marrow*. J Lipid Res, 2009. **50**(2): p. 214-24.
57. Weisberg, S.P., et al., *Obesity is associated with macrophage accumulation in adipose tissue*. J Clin Invest, 2003. **112**(12): p. 1796-808.
58. McLaren, J.E., et al., *Cytokines, macrophage lipid metabolism and foam cells: implications for cardiovascular disease therapy*. Prog Lipid Res, 2011. **50**(4): p. 331-47.
59. Venkateswaran, A., et al., *Control of cellular cholesterol efflux by the nuclear oxysterol receptor LXR alpha*. Proc Natl Acad Sci U S A, 2000. **97**(22): p. 12097-102.
60. Claudel, T., et al., *Reduction of atherosclerosis in apolipoprotein E knockout mice by activation of the retinoid X receptor*. Proc Natl Acad Sci U S A, 2001. **98**(5): p. 2610-5.

61. Peet, D.J., B.A. Janowski, and D.J. Mangelsdorf, *The LXRs: a new class of oxysterol receptors*. *Curr Opin Genet Dev*, 1998. **8**(5): p. 571-5.
62. Dai, X., et al., *Effect of T0901317 on hepatic proinflammatory gene expression in apoE^{-/-} mice fed a high-fat/high-cholesterol diet*. *Inflammation*, 2007. **30**(3-4): p. 105-17.
63. Bueno, C., et al., *Liver X receptors inhibit human monocyte-derived macrophage foam cell formation by inhibiting fluid-phase pinocytosis of LDL*. *J Lipid Res*, 2007. **48**(11): p. 2411-8.
64. Zhao, J.F., et al., *Molecular mechanism of curcumin on the suppression of cholesterol accumulation in macrophage foam cells and atherosclerosis*. *Mol Nutr Food Res*, 2012. **56**(5): p. 691-701.
65. Honzumi, S., et al., *Synthetic LXR agonist inhibits the development of atherosclerosis in New Zealand White rabbits*. *Biochim Biophys Acta*, 2011. **1811**(12): p. 1136-45.
66. Schultz, J.R., et al., *Role of LXRs in control of lipogenesis*. *Genes Dev*, 2000. **14**(22): p. 2831-8.
67. Smoak, K., et al., *Effects of liver X receptor agonist treatment on pulmonary inflammation and host defense*. *J Immunol*, 2008. **180**(5): p. 3305-12.
68. Joseph, S.B., et al., *Reciprocal regulation of inflammation and lipid metabolism by liver X receptors*. *Nat Med*, 2003. **9**(2): p. 213-9.
69. Cui, W., et al., *Liver X receptor activation attenuates inflammatory response and protects cholinergic neurons in APP/PS1 transgenic mice*. *Neuroscience*, 2012. **210**: p. 200-10.
70. Gupta, D.S., et al., *Psoriasis: crucial role of LXR-alpha RNomics*. *Genes Immun*, 2010. **11**(1): p. 37-44.
71. Bensinger, S.J., et al., *LXR signaling couples sterol metabolism to proliferation in the acquired immune response*. *Cell*, 2008. **134**(1): p. 97-111.
72. Joseph, S.B., et al., *LXR-dependent gene expression is important for macrophage survival and the innate immune response*. *Cell*, 2004. **119**(2): p. 299-309.
73. Lu, B., et al., *Type II nuclear hormone receptors, coactivator, and target gene repression in adipose tissue in the acute-phase response*. *J Lipid Res*, 2006. **47**(10): p. 2179-90.
74. Asquith, D.L., et al., *Liver X receptor agonism promotes articular inflammation in murine collagen-induced arthritis*. *Arthritis Rheum*, 2009. **60**(9): p. 2655-65.
75. Beaven, S.W., et al., *Liver X receptor signaling is a determinant of stellate cell activation and susceptibility to fibrotic liver disease*. *Gastroenterology*, 2011. **140**(3): p. 1052-62.
76. Bartel, D.P., *MicroRNAs: target recognition and regulatory functions*. *Cell*, 2009. **136**(2): p. 215-33.
77. Farh, K.K., et al., *The widespread impact of mammalian MicroRNAs on mRNA repression and evolution*. *Science*, 2005. **310**(5755): p. 1817-21.
78. Pillai, R.S., S.N. Bhattacharyya, and W. Filipowicz, *Repression of protein synthesis by miRNAs: how many mechanisms?* *Trends Cell Biol*, 2007. **17**(3): p. 118-26.
79. Lee, R.C., R.L. Feinbaum, and V. Ambros, *The C. elegans heterochronic gene lin-4 encodes small RNAs with antisense complementarity to lin-14*. *Cell*, 1993. **75**(5): p. 843-54.
80. Griffiths-Jones, S., *miRBase: microRNA sequences and annotation*. *Curr Protoc Bioinformatics*, 2010. **Chapter 12**: p. Unit 12 9 1-10.

81. Friedman, R.C., et al., *Most mammalian mRNAs are conserved targets of microRNAs*. Genome Res, 2009. **19**(1): p. 92-105.
82. Brodersen, P. and O. Voinnet, *Revisiting the principles of microRNA target recognition and mode of action*. Nat Rev Mol Cell Biol, 2009. **10**(2): p. 141-8.
83. Houbaviy, H.B., M.F. Murray, and P.A. Sharp, *Embryonic stem cell-specific MicroRNAs*. Dev Cell, 2003. **5**(2): p. 351-8.
84. Chen, C.Z., et al., *Regulation of immune responses and tolerance: the microRNA perspective*. Immunol Rev, 2013. **253**(1): p. 112-28.
85. O'Connell, R.M., et al., *Physiological and pathological roles for microRNAs in the immune system*. Nat Rev Immunol, 2010. **10**(2): p. 111-22.
86. Lee, Y., et al., *MicroRNA maturation: stepwise processing and subcellular localization*. EMBO J, 2002. **21**(17): p. 4663-70.
87. Li, X., et al., *MicroRNA expression profiles in differentiated thyroid cancer, a review*. Int J Clin Exp Med, 2013. **6**(1): p. 74-80.
88. Guo, H., et al., *Mammalian microRNAs predominantly act to decrease target mRNA levels*. Nature, 2010. **466**(7308): p. 835-40.
89. Lewis, B.P., C.B. Burge, and D.P. Bartel, *Conserved seed pairing, often flanked by adenosines, indicates that thousands of human genes are microRNA targets*. Cell, 2005. **120**(1): p. 15-20.
90. Chen, W.J., et al., *The magic and mystery of microRNA-27 in atherosclerosis*. Atherosclerosis, 2012. **222**(2): p. 314-23.
91. Metzler, M., et al., *High expression of precursor microRNA-155/BIC RNA in children with Burkitt lymphoma*. Genes Chromosomes Cancer, 2004. **39**(2): p. 167-9.
92. Tam, W., D. Ben-Yehuda, and W.S. Hayward, *bic, a novel gene activated by proviral insertions in avian leukosis virus-induced lymphomas, is likely to function through its noncoding RNA*. Mol Cell Biol, 1997. **17**(3): p. 1490-502.
93. Clurman, B.E. and W.S. Hayward, *Multiple proto-oncogene activations in avian leukosis virus-induced lymphomas: evidence for stage-specific events*. Mol Cell Biol, 1989. **9**(6): p. 2657-64.
94. Czyzyk-Krzeska, M.F. and X. Zhang, *MiR-155 at the heart of oncogenic pathways*. Oncogene, 2013.
95. Tam, W., *Identification and characterization of human BIC, a gene on chromosome 21 that encodes a noncoding RNA*. Gene, 2001. **274**(1-2): p. 157-67.
96. Moffett, H.F. and C.D. Novina, *A small RNA makes a Bic difference*. Genome Biol, 2007. **8**(7): p. 221.
97. Thai, T.H., et al., *Regulation of the germinal center response by microRNA-155*. Science, 2007. **316**(5824): p. 604-8.
98. O'Connell, R.M., et al., *Inositol phosphatase SHIP1 is a primary target of miR-155*. Proc Natl Acad Sci U S A, 2009. **106**(17): p. 7113-8.
99. Kurowska-Stolarska, M., et al., *MicroRNA-155 as a proinflammatory regulator in clinical and experimental arthritis*. Proc Natl Acad Sci U S A, 2011. **108**(27): p. 11193-8.
100. Bazzoni, F., et al., *Induction and regulatory function of miR-9 in human monocytes and neutrophils exposed to proinflammatory signals*. Proc Natl Acad Sci U S A, 2009. **106**(13): p. 5282-7.
101. O'Connell, R.M., et al., *MicroRNA-155 is induced during the macrophage inflammatory response*. Proc Natl Acad Sci U S A, 2007. **104**(5): p. 1604-9.
102. Ceppi, M., et al., *MicroRNA-155 modulates the interleukin-1 signaling pathway in activated human monocyte-derived dendritic cells*. Proc Natl Acad Sci U S A, 2009. **106**(8): p. 2735-40.

103. Vigorito, E., et al., *microRNA-155 regulates the generation of immunoglobulin class-switched plasma cells*. *Immunity*, 2007. **27**(6): p. 847-59.
104. Rodriguez, A., et al., *Requirement of bic/microRNA-155 for normal immune function*. *Science*, 2007. **316**(5824): p. 608-11.
105. Stahl, H.F., et al., *miR-155 inhibition sensitizes CD4+ Th cells for TREG mediated suppression*. *PLoS One*, 2009. **4**(9): p. e7158.
106. Kong, W., et al., *MicroRNA-155 regulates cell survival, growth, and chemosensitivity by targeting FOXO3a in breast cancer*. *J Biol Chem*, 2010. **285**(23): p. 17869-79.
107. Kluiver, J., et al., *BIC and miR-155 are highly expressed in Hodgkin, primary mediastinal and diffuse large B cell lymphomas*. *J Pathol*, 2005. **207**(2): p. 243-9.
108. Costinean, S., et al., *Pre-B cell proliferation and lymphoblastic leukemia/high-grade lymphoma in E(mu)-miR155 transgenic mice*. *Proc Natl Acad Sci U S A*, 2006. **103**(18): p. 7024-9.
109. Chen, J., B.C. Wang, and J.H. Tang, *Clinical significance of microRNA-155 expression in human breast cancer*. *J Surg Oncol*, 2012. **106**(3): p. 260-6.
110. Kong, W., et al., *MicroRNA-155 is regulated by the transforming growth factor beta/Smad pathway and contributes to epithelial cell plasticity by targeting RhoA*. *Mol Cell Biol*, 2008. **28**(22): p. 6773-84.
111. Dempsey, O.J., *Clinical review: idiopathic pulmonary fibrosis--past, present and future*. *Respir Med*, 2006. **100**(11): p. 1871-85.
112. Dempsey, O.J., et al., *Idiopathic pulmonary fibrosis: an update*. *QJM*, 2006. **99**(10): p. 643-54.
113. Sime, P.J. and K.M. O'Reilly, *Fibrosis of the lung and other tissues: new concepts in pathogenesis and treatment*. *Clin Immunol*, 2001. **99**(3): p. 308-19.
114. Raghu, G., et al., *An official ATS/ERS/JRS/ALAT statement: idiopathic pulmonary fibrosis: evidence-based guidelines for diagnosis and management*. *Am J Respir Crit Care Med*, 2011. **183**(6): p. 788-824.
115. King, T.E., Jr., A. Pardo, and M. Selman, *Idiopathic pulmonary fibrosis*. *Lancet*, 2011. **378**(9807): p. 1949-61.
116. King, T.E., Jr., et al., *Predicting survival in idiopathic pulmonary fibrosis: scoring system and survival model*. *Am J Respir Crit Care Med*, 2001. **164**(7): p. 1171-81.
117. Navaratnam, V., et al., *The rising incidence of idiopathic pulmonary fibrosis in the U.K*. *Thorax*, 2011. **66**(6): p. 462-7.
118. Olson, A.L., et al., *Mortality from pulmonary fibrosis increased in the United States from 1992 to 2003*. *Am J Respir Crit Care Med*, 2007. **176**(3): p. 277-84.
119. Meltzer, E.B. and P.W. Noble, *Idiopathic pulmonary fibrosis*. *Orphanet J Rare Dis*, 2008. **3**: p. 8.
120. Martinez, F.J., et al., *The clinical course of patients with idiopathic pulmonary fibrosis*. *Ann Intern Med*, 2005. **142**(12 Pt 1): p. 963-7.
121. Panos, R.J., et al., *Clinical deterioration in patients with idiopathic pulmonary fibrosis: causes and assessment*. *Am J Med*, 1990. **88**(4): p. 396-404.
122. Oh, C.K., L.A. Murray, and N.A. Molfino, *Smoking and idiopathic pulmonary fibrosis*. *Pulm Med*, 2012. **2012**: p. 808260.

123. Katzenstein, A.L. and J.L. Myers, *Idiopathic pulmonary fibrosis: clinical relevance of pathologic classification*. Am J Respir Crit Care Med, 1998. **157**(4 Pt 1): p. 1301-15.
124. Baumgartner, K.B., et al., *Cigarette smoking: a risk factor for idiopathic pulmonary fibrosis*. Am J Respir Crit Care Med, 1997. **155**(1): p. 242-8.
125. Antoniou, K.M., et al., *Idiopathic pulmonary fibrosis: outcome in relation to smoking status*. Am J Respir Crit Care Med, 2008. **177**(2): p. 190-4.
126. Kinnula, V.L., et al., *Oxidative stress in pulmonary fibrosis: a possible role for redox modulatory therapy*. Am J Respir Crit Care Med, 2005. **172**(4): p. 417-22.
127. Steele, M.P. and K.K. Brown, *Genetic predisposition to respiratory diseases: infiltrative lung diseases*. Respiration, 2007. **74**(6): p. 601-8.
128. Boucher, R.C., *Idiopathic pulmonary fibrosis--a sticky business*. N Engl J Med, 2011. **364**(16): p. 1560-1.
129. Xaubet, A., et al., *A haplotype of cyclooxygenase-2 gene is associated with idiopathic pulmonary fibrosis*. Sarcoidosis Vasc Diffuse Lung Dis, 2010. **27**(2): p. 121-30.
130. Gross, T.J. and G.W. Hunninghake, *Idiopathic pulmonary fibrosis*. N Engl J Med, 2001. **345**(7): p. 517-25.
131. Tang, Y.W., et al., *Herpesvirus DNA is consistently detected in lungs of patients with idiopathic pulmonary fibrosis*. J Clin Microbiol, 2003. **41**(6): p. 2633-40.
132. Hubbard, R., et al., *Occupational exposure to metal or wood dust and aetiology of cryptogenic fibrosing alveolitis*. Lancet, 1996. **347**(8997): p. 284-9.
133. Kitamura, H., et al., *Inhalation of inorganic particles as a risk factor for idiopathic pulmonary fibrosis--elemental microanalysis of pulmonary lymph nodes obtained at autopsy cases*. Pathol Res Pract, 2007. **203**(8): p. 575-85.
134. Wynn, T.A., *Integrating mechanisms of pulmonary fibrosis*. J Exp Med, 2011. **208**(7): p. 1339-50.
135. Mahendran, S. and T. Sethi, *Treatments in idiopathic pulmonary fibrosis: time for a more targeted approach?* QJM, 2012.
136. Checa, M., et al., *MMP-1 polymorphisms and the risk of idiopathic pulmonary fibrosis*. Hum Genet, 2008. **124**(5): p. 465-72.
137. Yao, H.W., et al., *TGF-beta1 induces alveolar epithelial to mesenchymal transition in vitro*. Life Sci, 2004. **76**(1): p. 29-37.
138. Charbeneau, R.P. and M. Peters-Golden, *Eicosanoids: mediators and therapeutic targets in fibrotic lung disease*. Clin Sci (Lond), 2005. **108**(6): p. 479-91.
139. Gunther, A., et al., *Unravelling the progressive pathophysiology of idiopathic pulmonary fibrosis*. Eur Respir Rev, 2012. **21**(124): p. 152-60.
140. Chen, C.Z. and M. Raghunath, *Focus on collagen: in vitro systems to study fibrogenesis and antifibrosis state of the art*. Fibrogenesis Tissue Repair, 2009. **2**: p. 7.
141. Madri, J.A. and H. Furthmayr, *Collagen polymorphism in the lung. An immunochemical study of pulmonary fibrosis*. Hum Pathol, 1980. **11**(4): p. 353-66.
142. Cutroneo, K.R., et al., *Therapies for bleomycin induced lung fibrosis through regulation of TGF-beta1 induced collagen gene expression*. J Cell Physiol, 2007. **211**(3): p. 585-9.

143. Kasuga, I., et al., *Clinical evaluation of serum type IV collagen 7S in idiopathic pulmonary fibrosis*. *Respirology*, 1996. **1**(4): p. 277-81.
144. Nath, R.K., et al., *Treatment with antisense oligonucleotide reduces the expression of type I collagen in a human-skin organ-wound model: implications for antifibrotic gene therapy*. *Ann Plast Surg*, 2007. **59**(6): p. 699-706.
145. Strieter, R.M., et al., *The role of circulating mesenchymal progenitor cells, fibrocytes, in promoting pulmonary fibrosis*. *Trans Am Clin Climatol Assoc*, 2009. **120**: p. 49-59.
146. Xu, J., et al., *Use of senescence-accelerated mouse model in bleomycin-induced lung injury suggests that bone marrow-derived cells can alter the outcome of lung injury in aged mice*. *J Gerontol A Biol Sci Med Sci*, 2009. **64**(7): p. 731-9.
147. Chesney, J., et al., *Regulated production of type I collagen and inflammatory cytokines by peripheral blood fibrocytes*. *J Immunol*, 1998. **160**(1): p. 419-25.
148. Visscher, D.W. and J.L. Myers, *Histologic spectrum of idiopathic interstitial pneumonias*. *Proc Am Thorac Soc*, 2006. **3**(4): p. 322-9.
149. Yang, S., et al., *miR-31 is a negative regulator of fibrogenesis and pulmonary fibrosis*. *FASEB J*, 2012. **26**(9): p. 3790-9.
150. Mason, R.J., et al., *NHLBI Workshop Summary. Pharmacological therapy for idiopathic pulmonary fibrosis. Past, present, and future*. *Am J Respir Crit Care Med*, 1999. **160**(5 Pt 1): p. 1771-7.
151. Desmouliere, A., C. Chaponnier, and G. Gabbiani, *Tissue repair, contraction, and the myofibroblast*. *Wound Repair Regen*, 2005. **13**(1): p. 7-12.
152. Wynn, T.A., *Cellular and molecular mechanisms of fibrosis*. *J Pathol*, 2008. **214**(2): p. 199-210.
153. Phan, S.H., *The myofibroblast in pulmonary fibrosis*. *Chest*, 2002. **122**(6 Suppl): p. 286S-289S.
154. Nakagome, K., et al., *In vivo IL-10 gene delivery attenuates bleomycin induced pulmonary fibrosis by inhibiting the production and activation of TGF-beta in the lung*. *Thorax*, 2006. **61**(10): p. 886-94.
155. Drakopanagiotakis, F., et al., *Decreased apoptotic rate of alveolar macrophages of patients with idiopathic pulmonary fibrosis*. *Pulm Med*, 2012. **2012**: p. 981730.
156. Diaz, K.T., et al., *Delivery and safety of inhaled interferon-gamma in idiopathic pulmonary fibrosis*. *J Aerosol Med Pulm Drug Deliv*, 2012. **25**(2): p. 79-87.
157. Pechkovsky, D.V., et al., *Alternatively activated alveolar macrophages in pulmonary fibrosis-mediator production and intracellular signal transduction*. *Clin Immunol*, 2010. **137**(1): p. 89-101.
158. Strieter, R.M., *What differentiates normal lung repair and fibrosis? Inflammation, resolution of repair, and fibrosis*. *Proc Am Thorac Soc*, 2008. **5**(3): p. 305-10.
159. Luzina, I.G., et al., *Roles of T lymphocytes in pulmonary fibrosis*. *J Leukoc Biol*, 2008. **83**(2): p. 237-44.
160. Gilani, S.R., et al., *CD28 down-regulation on circulating CD4 T-cells is associated with poor prognoses of patients with idiopathic pulmonary fibrosis*. *PLoS One*, 2010. **5**(1): p. e8959.

161. Kotsianidis, I., et al., *Global impairment of CD4+CD25+FOXP3+ regulatory T cells in idiopathic pulmonary fibrosis*. Am J Respir Crit Care Med, 2009. **179**(12): p. 1121-30.
162. Marchal-Somme, J., et al., *Dendritic cells accumulate in human fibrotic interstitial lung disease*. Am J Respir Crit Care Med, 2007. **176**(10): p. 1007-14.
163. Kinder, B.W., et al., *Baseline BAL neutrophilia predicts early mortality in idiopathic pulmonary fibrosis*. Chest, 2008. **133**(1): p. 226-32.
164. Cha, S.I., et al., *Lung mast cell density defines a subpopulation of patients with idiopathic pulmonary fibrosis*. Histopathology, 2012. **61**(1): p. 98-106.
165. Mori, H., et al., *Bleomycin-induced pulmonary fibrosis in genetically mast cell-deficient WBB6F1-W/W^v mice and mechanism of the suppressive effect of tranilast, an antiallergic drug inhibiting mediator release from mast cells, on fibrosis*. Int Arch Allergy Appl Immunol, 1991. **95**(2-3): p. 195-201.
166. Kolb, M., et al., *Transient expression of IL-1beta induces acute lung injury and chronic repair leading to pulmonary fibrosis*. J Clin Invest, 2001. **107**(12): p. 1529-36.
167. Kuroki, M., et al., *Repression of bleomycin-induced pneumopathy by TNF*. J Immunol, 2003. **170**(1): p. 567-74.
168. Agostini, C. and C. Gurrieri, *Chemokine/cytokine cocktail in idiopathic pulmonary fibrosis*. Proc Am Thorac Soc, 2006. **3**(4): p. 357-63.
169. Yokoyama, A., et al., *Prognostic value of circulating KL-6 in idiopathic pulmonary fibrosis*. Respirology, 2006. **11**(2): p. 164-8.
170. Kadota, J., et al., *High plasma concentrations of osteopontin in patients with interstitial pneumonia*. Respir Med, 2005. **99**(1): p. 111-7.
171. Rosas, I.O., et al., *MMP1 and MMP7 as potential peripheral blood biomarkers in idiopathic pulmonary fibrosis*. PLoS Med, 2008. **5**(4): p. e93.
172. Walter, N., H.R. Collard, and T.E. King, Jr., *Current perspectives on the treatment of idiopathic pulmonary fibrosis*. Proc Am Thorac Soc, 2006. **3**(4): p. 330-8.
173. Demedts, M., et al., *High-dose acetylcysteine in idiopathic pulmonary fibrosis*. N Engl J Med, 2005. **353**(21): p. 2229-42.
174. Taniguchi, H., et al., *Pirfenidone in idiopathic pulmonary fibrosis*. Eur Respir J, 2010. **35**(4): p. 821-9.
175. Mackinnon, A.C., et al., *Regulation of transforming growth factor-beta1-driven lung fibrosis by galectin-3*. Am J Respir Crit Care Med, 2012. **185**(5): p. 537-46.
176. Park, S.H., et al., *Increased endothelin-1 in bleomycin-induced pulmonary fibrosis and the effect of an endothelin receptor antagonist*. Am J Respir Crit Care Med, 1997. **156**(2 Pt 1): p. 600-8.
177. King, T.E., Jr., et al., *BUILD-3: a randomized, controlled trial of bosentan in idiopathic pulmonary fibrosis*. Am J Respir Crit Care Med, 2011. **184**(1): p. 92-9.
178. Bradley, B., et al., *Interstitial lung disease guideline: the British Thoracic Society in collaboration with the Thoracic Society of Australia and New Zealand and the Irish Thoracic Society*. Thorax, 2008. **63** Suppl 5: p. v1-58.
179. Moore, B.B. and C.M. Hogaboam, *Murine models of pulmonary fibrosis*. Am J Physiol Lung Cell Mol Physiol, 2008. **294**(2): p. L152-60.
180. Meadors, M., J. Floyd, and M.C. Perry, *Pulmonary toxicity of chemotherapy*. Semin Oncol, 2006. **33**(1): p. 98-105.
181. O'Sullivan, J.M., et al., *Predicting the risk of bleomycin lung toxicity in patients with germ-cell tumours*. Ann Oncol, 2003. **14**(1): p. 91-6.

182. Gharaee-Kermani, M., M. Ullenbruch, and S.H. Phan, *Animal models of pulmonary fibrosis*. Methods Mol Med, 2005. **117**: p. 251-9.
183. Roberts, S.N., et al., *A novel model for human interstitial lung disease: haptan-driven lung fibrosis in rodents*. J Pathol, 1995. **176**(3): p. 309-18.
184. Lardot, C.G., et al., *Role of urokinase in the fibrogenic response of the lung to mineral particles*. Am J Respir Crit Care Med, 1998. **157**(2): p. 617-28.
185. Davis, G.S., K.O. Leslie, and D.R. Hemenway, *Silicosis in mice: effects of dose, time, and genetic strain*. J Environ Pathol Toxicol Oncol, 1998. **17**(2): p. 81-97.
186. Johnston, C.J., et al., *Radiation-induced pulmonary fibrosis: examination of chemokine and chemokine receptor families*. Radiat Res, 2002. **157**(3): p. 256-65.
187. Sharplin, J. and A.J. Franko, *A quantitative histological study of strain-dependent differences in the effects of irradiation on mouse lung during the early phase*. Radiat Res, 1989. **119**(1): p. 1-14.
188. Rube, C.E., et al., *Dose-dependent induction of transforming growth factor beta (TGF-beta) in the lung tissue of fibrosis-prone mice after thoracic irradiation*. Int J Radiat Oncol Biol Phys, 2000. **47**(4): p. 1033-42.
189. Collard, H.R., et al., *Acute exacerbations of idiopathic pulmonary fibrosis*. Am J Respir Crit Care Med, 2007. **176**(7): p. 636-43.
190. Sime, P.J., et al., *Adenovector-mediated gene transfer of active transforming growth factor-beta1 induces prolonged severe fibrosis in rat lung*. J Clin Invest, 1997. **100**(4): p. 768-76.
191. Phillips, R.J., et al., *Circulating fibrocytes traffic to the lungs in response to CXCL12 and mediate fibrosis*. J Clin Invest, 2004. **114**(3): p. 438-46.
192. Izbiccki, G., et al., *Time course of bleomycin-induced lung fibrosis*. Int J Exp Pathol, 2002. **83**(3): p. 111-9.
193. Adamson, I.Y. and D.H. Bowden, *The pathogenesis of bleomycin-induced pulmonary fibrosis in mice*. Am J Pathol, 1974. **77**(2): p. 185-97.
194. Russo, R.C., et al., *Role of the chemokine receptor CXCR2 in bleomycin-induced pulmonary inflammation and fibrosis*. Am J Respir Cell Mol Biol, 2009. **40**(4): p. 410-21.
195. Tangirala, R.K., et al., *Identification of macrophage liver X receptors as inhibitors of atherosclerosis*. Proc Natl Acad Sci U S A, 2002. **99**(18): p. 11896-901.
196. Chawla, A., et al., *A PPAR gamma-LXR-ABCA1 pathway in macrophages is involved in cholesterol efflux and atherogenesis*. Mol Cell, 2001. **7**(1): p. 161-71.
197. Marathe, C., et al., *The arginase II gene is an anti-inflammatory target of liver X receptor in macrophages*. J Biol Chem, 2006. **281**(43): p. 32197-206.
198. Chua, F., J. Gauldie, and G.J. Laurent, *Pulmonary fibrosis: searching for model answers*. Am J Respir Cell Mol Biol, 2005. **33**(1): p. 9-13.
199. Moeller, A., et al., *The bleomycin animal model: a useful tool to investigate treatment options for idiopathic pulmonary fibrosis?* Int J Biochem Cell Biol, 2008. **40**(3): p. 362-82.
200. Chaudhary, N.I., A. Schnapp, and J.E. Park, *Pharmacologic differentiation of inflammation and fibrosis in the rat bleomycin model*. Am J Respir Crit Care Med, 2006. **173**(7): p. 769-76.
201. Zhang, W., et al., *[A rat model of pulmonary fibrosis induced by infusing bleomycin quickly through tracheal intubation]*. Zhong Xi Yi Jie He Xue Bao, 2008. **6**(1): p. 60-7.

202. Oury, T.D., et al., *Attenuation of bleomycin-induced pulmonary fibrosis by a catalytic antioxidant metalloporphyrin*. *Am J Respir Cell Mol Biol*, 2001. **25**(2): p. 164-9.
203. Murray, L.A., et al., *Serum amyloid P therapeutically attenuates murine bleomycin-induced pulmonary fibrosis via its effects on macrophages*. *PLoS One*, 2010. **5**(3): p. e9683.
204. Todd, N.W., I.G. Luzina, and S.P. Atamas, *Molecular and cellular mechanisms of pulmonary fibrosis*. *Fibrogenesis Tissue Repair*, 2012. **5**(1): p. 11.
205. Komura, K., et al., *CD19 regulates the development of bleomycin-induced pulmonary fibrosis in a mouse model*. *Arthritis Rheum*, 2008. **58**(11): p. 3574-84.
206. Jung, U.J., et al., *n-3 fatty acids ameliorate hepatic steatosis and dysfunction after LXR agonist ingestion in mice*. *Biochim Biophys Acta*, 2011. **1811**(9): p. 491-7.
207. Hsu, E., et al., *Lung tissues in patients with systemic sclerosis have gene expression patterns unique to pulmonary fibrosis and pulmonary hypertension*. *Arthritis Rheum*, 2011. **63**(3): p. 783-94.
208. Kurup, V.P., M.C. Zacharisen, and J.N. Fink, *Hypersensitivity pneumonitis*. *Indian J Chest Dis Allied Sci*, 2006. **48**(2): p. 115-28.
209. Asquith, D.L., et al., *Simultaneous activation of the liver X receptors (LXRalpha and LXRBeta) drives murine collagen-induced arthritis disease pathology*. *Ann Rheum Dis*, 2011. **70**(12): p. 2225-8.
210. Smith, R.E., et al., *Production and function of murine macrophage inflammatory protein-1 alpha in bleomycin-induced lung injury*. *J Immunol*, 1994. **153**(10): p. 4704-12.
211. Leask, A. and D.J. Abraham, *TGF-beta signaling and the fibrotic response*. *FASEB J*, 2004. **18**(7): p. 816-27.
212. Coker, R.K., et al., *Transforming growth factors-beta 1, -beta 2, and -beta 3 stimulate fibroblast procollagen production in vitro but are differentially expressed during bleomycin-induced lung fibrosis*. *Am J Pathol*, 1997. **150**(3): p. 981-91.
213. Kaviratne, M., et al., *IL-13 activates a mechanism of tissue fibrosis that is completely TGF-beta independent*. *J Immunol*, 2004. **173**(6): p. 4020-9.
214. Lee, C.G., et al., *Interleukin-13 induces tissue fibrosis by selectively stimulating and activating transforming growth factor beta(1)*. *J Exp Med*, 2001. **194**(6): p. 809-21.
215. Shahzeidi, S., et al., *Enhanced type III collagen gene expression during bleomycin induced lung fibrosis*. *Thorax*, 1993. **48**(6): p. 622-8.
216. Swiderski, R.E., et al., *Differential expression of extracellular matrix remodeling genes in a murine model of bleomycin-induced pulmonary fibrosis*. *Am J Pathol*, 1998. **152**(3): p. 821-8.
217. Raghu, G., et al., *Extracellular matrix in normal and fibrotic human lungs*. *Am Rev Respir Dis*, 1985. **131**(2): p. 281-9.
218. Gabbi, C., M. Warner, and J.A. Gustafsson, *Minireview: liver X receptor beta: emerging roles in physiology and diseases*. *Mol Endocrinol*, 2009. **23**(2): p. 129-36.
219. Andersson, S., et al., *Inactivation of liver X receptor beta leads to adult-onset motor neuron degeneration in male mice*. *Proc Natl Acad Sci U S A*, 2005. **102**(10): p. 3857-62.

220. Bradley, M.N., et al., *Ligand activation of LXR beta reverses atherosclerosis and cellular cholesterol overload in mice lacking LXR alpha and apoE*. J Clin Invest, 2007. **117**(8): p. 2337-46.
221. Laurencikiene, J. and M. Ryden, *Liver X receptors and fat cell metabolism*. Int J Obes (Lond), 2012. **36**(12): p. 1494-502.
222. Huie, T.J., M. Moss, and S.K. Frankel, *What can biomarkers tell us about the pathogenesis of acute exacerbations of idiopathic pulmonary fibrosis?* Am J Physiol Lung Cell Mol Physiol, 2010. **299**(1): p. L1-2.
223. Lazor, R., A. Bonetti, and L.P. Nicod, *[Acute exacerbations of idiopathic pulmonary fibrosis]*. Rev Med Suisse, 2010. **6**(272): p. 2228-30, 2232.
224. Martin, M.M., et al., *MicroRNA-155 regulates human angiotensin II type 1 receptor expression in fibroblasts*. J Biol Chem, 2006. **281**(27): p. 18277-84.
225. Landgraf, P., et al., *A mammalian microRNA expression atlas based on small RNA library sequencing*. Cell, 2007. **129**(7): p. 1401-14.
226. Pottier, N., et al., *Identification of keratinocyte growth factor as a target of microRNA-155 in lung fibroblasts: implication in epithelial-mesenchymal interactions*. PLoS One, 2009. **4**(8): p. e6718.
227. Warburton, D., W. Shi, and B. Xu, *TGF-beta-Smad3 signaling in emphysema and pulmonary fibrosis: an epigenetic aberration of normal development?* Am J Physiol Lung Cell Mol Physiol, 2013. **304**(2): p. L83-5.
228. Sato, T., et al., *IL-4 induces differentiation of human embryonic stem cells into fibrogenic fibroblast-like cells*. J Allergy Clin Immunol, 2011. **127**(6): p. 1595-603 e9.
229. Koch, M., et al., *Induction of microRNA-155 is TLR- and type IV secretion system-dependent in macrophages and inhibits DNA-damage induced apoptosis*. Proc Natl Acad Sci U S A, 2012. **109**(19): p. E1153-62.
230. Arranz, A., et al., *Akt1 and Akt2 protein kinases differentially contribute to macrophage polarization*. Proc Natl Acad Sci U S A, 2012. **109**(24): p. 9517-22.
231. Scheule, R.K., et al., *Bleomycin stimulation of cytokine secretion by the human alveolar macrophage*. Am J Physiol, 1992. **262**(4 Pt 1): p. L386-91.
232. Ortiz, L.A., et al., *Expression of TNF and the necessity of TNF receptors in bleomycin-induced lung injury in mice*. Exp Lung Res, 1998. **24**(6): p. 721-43.
233. Zhang, X.Y., et al., *Antisense oligonucleotides to NF-kappaB improve survival in bleomycin-induced pneumopathy of the mouse*. Am J Respir Crit Care Med, 2000. **162**(4 Pt 1): p. 1561-8.
234. Day, R.M., et al., *Bleomycin upregulates gene expression of angiotensin-converting enzyme via mitogen-activated protein kinase and early growth response 1 transcription factor*. Am J Respir Cell Mol Biol, 2001. **25**(5): p. 613-9.
235. Phan, S.H., et al., *Stimulation of rat endothelial cell transforming growth factor-beta production by bleomycin*. J Clin Invest, 1991. **87**(1): p. 148-54.
236. Huang, W., et al., *Combined SP-A-bleomycin effect on cytokines by THP-1 cells: impact of surfactant lipids on this effect*. Am J Physiol Lung Cell Mol Physiol, 2002. **283**(1): p. L94-L102.
237. Hu, Y.W., et al., *TGF-beta1 up-regulates expression of ABCA1, ABCG1 and SR-BI through liver X receptor alpha signaling pathway in THP-1 macrophage-derived foam cells*. J Atheroscler Thromb, 2010. **17**(5): p. 493-502.

238. Antonson, P., et al., *RAP250 is a coactivator in the transforming growth factor beta signaling pathway that interacts with Smad2 and Smad3*. J Biol Chem, 2008. **283**(14): p. 8995-9001.
239. Hamblin, M.J. and M.R. Horton, *Rheumatoid arthritis-associated interstitial lung disease: diagnostic dilemma*. Pulm Med, 2011. **2011**: p. 872120.
240. Huber, L.C., et al., *Synovial fibroblasts: key players in rheumatoid arthritis*. Rheumatology (Oxford), 2006. **45**(6): p. 669-75.
241. Chin, H. J., et al., *Over-expression of Liver X Receptor- α (LXR α) by TO901317 Exaggerated the Production of Mesangial Matrix*. Korean J Nephrol, 2010. **29**(4): p. 189-97.
242. Chen, S.J., et al., *Stimulation of type I collagen transcription in human skin fibroblasts by TGF- β : involvement of Smad 3*. J Invest Dermatol, 1999. **112**(1): p. 49-57.
243. Quinet, E.M., et al., *Liver X receptor (LXR)-beta regulation in LXRalpha-deficient mice: implications for therapeutic targeting*. Mol Pharmacol, 2006. **70**(4): p. 1340-9.
244. Katz, A., et al., *Safety, pharmacokinetics, and pharmacodynamics of single doses of LXR-623, a novel liver X-receptor agonist, in healthy participants*. J Clin Pharmacol, 2009. **49**(6): p. 643-9.
245. DiBlasio-Smith, E.A., et al., *Discovery and implementation of transcriptional biomarkers of synthetic LXR agonists in peripheral blood cells*. J Transl Med, 2008. **6**: p. 59.

IX Publications

1- The liver X receptor pathway is highly upregulated in rheumatoid arthritis synovial macrophages and potentiates TLR-driven cytokine release.